TECHNISCHE UNIVERSITÄT MÜNCHEN

Wissenschaftszentrum Weihenstephan für Ernährung, Landnutzung und Umwelt

Lehrstuhl für Technische Mikrobiologie

# Stress-induced phenotypic and proteomic plasticity of *Lactobacillus paracasei* subsp. *paracasei* F19

Ann-Sophie Schott

Vollständiger Abdruck der von der Fakultät Wissenschaftszentrum Weihenstephan für Ernährung, Landnutzung und Umwelt der Technischen Universität München zur Erlangung des akademischen Grades eines

Doktors der Naturwissenschaften

genehmigten Dissertation.

| | | |
|---|---|---|
| Vorsitzender: | | Prof. Dr. S. Scherer |
| Prüfer der Dissertation: | 1. | Prof. Dr. R. F. Vogel |
| | 2. | Prof. Dr. W. Liebl |

Die Dissertation wurde am 28.08.2018 bei der Technischen Universität München eingereicht und durch die Fakultät Wissenschaftszentrum Weihenstephan für Ernährung, Landnutzung und Umwelt am 10.01.2019 angenommen.

Remember to look up at the stars and not down at your feet. Try to make sense of what you see and wonder about what makes the universe exist. Be curious. And however difficult life may seem, there is always something you can do and succeed at.
(Stephen Hawkins)

# Vorwort | Forword

Die vorliegende Arbeit ist Teil eines Verbundprojektes, das aus dem BMEL-Förderprogramm des Bundesamtes für Landwirtschaft und Ernährung (BLE) hervorgegangen ist und vom Bundesministerium für Ernährung und Landwirtschaft (BLE 2817400111) gefördert wurde.

Teilergebnisse der vorliegenden Arbeit wurden vorab in Fachzeitschriften veröffentlicht. Siehe Kapitel 12 „List of Publications and Student Theses“.

# Danksagung | Acknowledgement

Keiner schreibt eine Dissertation allein. Und nun - nach fünf Jahren mit Höhen und Tiefen - möchte ich allen herzlichen Dank sagen, die meinen Weg begleitet und diesen unvergesslich für mich gemacht haben.

Als erstes gebührt mein Dank meinem Doktorvater Prof. Dr. Rudi Vogel, der diese Arbeit erst ermöglicht hat. Neben der Bereitstellung des Themas, der Organisation der Finanzierung und der umfassenden Unterstützung, möchte ich mich bei dir für dein entgegengebrachtes Vertrauen bedanken. Ich erinnere mich noch heute an mein Vorstellungsgespräch in deinem Büro in der alten Brennerei als wäre es gestern gewesen. Dies war der Beginn zu fünf ganz besonderen Jahren.

Des Weiteren gilt mein Dank Prof. Dr. Wolfgang Liebl, der sich bereit erklärt hat diese Arbeit als Zweitprüfer zu begutachten und Prof. Dr. Siegfried Scherer für die Übernahme als Prüfungsvorsitzender.

Ich danke meinen Projektpartnern Dr. Simon Bauer und Prof. Dr.-Ing. Ulrich Kulozik für die fachübergreifenden Diskussionen und die konstruktive Zusammenarbeit. Ein großer Dank gilt zudem dem Lehrstuhl für Proteomik und Bioanalytik unter der Leitung von Prof. Dr. Bernhard Küster und der OmicScouts GmbH. Allen voran Dr. Hannes Hahne, ohne dessen Zeit, Geduld, fachliche Unterstützung und Bereitstellung des experimentellen Equipments Teile dieser Arbeit niemals machbar gewesen wären.

Ein großes Dankeschön geht ferner an Dr. Andreas Geißler und Dr. Jürgen Behr, die mir tatkräftig zur Seite standen als es darum ging, die schiere Masse an Proteomdaten mittels Bioinformatik zu bändigen.

Außerdem möchte ich mich bei meiner Bachelorstudentin Franzi, sowie bei meinen Forschungspraktikantinnen Jennifer und Melanie für die tatkräftige Unterstützung und die erbrachten Ergebnisse, welche in diese Arbeit eingeflossen sind, bedanken.

Prof. Dr. Matthias Ehrmann und Prof. Dr. Ludwig Niessen danke ich für die fachliche Unterstützung, Angela Seppeur für die verlässliche Abwicklung aller administrativer Angelegenheiten und die vielen sonnigen Grüße, Maggie Schreiber, Andrea Pape, Sabine Forster, Moni Engel für ihre Unterstützung und Hilfe im Laboralltag. Danke für eine stets freundschaftliche, entspannte und unterstützende Atmosphäre am Lehrstuhl für Technische Mikrobiologie Weihenstephan.

Ganz besonders möchte ich mich bei allen anderen Kollegen des TMW Lehrstuhls bedanken, die meine Zeit in Freising zu einer ganz besonderen und für mich prägenden gemacht haben. Allen voran meinem Büro mit Andi, Linda und Tukta. Ihr seid mir sehr ans Herz gewachsen und ich werde die lustigen, herzlichen und vertrauten Gespräche

vermissen. Danke für offene Arme, Schultern zum Anlehnen, Ohren zum Zuhören. Weiterhin danke ich Alex, Jonas, Krissy, Andrea, Lara, Jule, Meike, Lisa, Marion, Vroni, Thomas, Tomas und Dominik für unterhaltsame Mittagspausen, für Ausflüge in den Zoo und ins Freisinger Nachtleben, für „Perfekte Dinner“, für schöne Radtouren, Bergabenteuer, Bootstouren.... Die Liste scheint endlos. Ich könnte ewig so weitermachen.

Außerdem möchte ich mich bei meinen Freunden und Handballern für die oftmals fehlende Zeit entschuldigen und mich für euer Verständnis bedanken. Im Besonderen danke ich Sophie für ihre Unterstützung jeglicher Art, für ihre Freundschaft und für das Bekanntmachen mit der bayrischen Kultur, welche mir als „pälser Määd“ doch recht unbekannt war.

Zum Schluss möchte ich mich bei meiner Familie und insbesondere bei meinen Eltern und meinem Bruder bedanken. Für Liebe, Geborgenheit, Ehrlichkeit, Vertrauen und die unendliche Geduld. Ihr habt mich den gesamten Weg über unterstützt, mir in jeglicher Hinsicht den Rücken freigehalten, mich immer aufgebaut und euch mit mir gefreut.

Danke.

# Table of Contents

# List of Tables

# List of Figures

## List of Figures

## List of Figures

# Abbreviations

| | |
|---|---|
| °C | Degree celsius |
| 2D | Two dimensional |
| aa | Amino acid |
| ADP | Adenosine diphosphate |
| ATP | Adenosine triphosphate |
| *B.* | *Bifidobacterium* |
| *C.* | *Carnobacterium* |
| CID | Collision-induced dissociation |
| DDA | Data dependent acquisition |
| DNA | Deoxyribonucleic acid |
| e.g. | Latin *exempli gratia* (for example) |
| *et al.* | Latin *et alii* (and others) |
| FAO | Food and Agriculture Organization |
| FDR | False discovery rate |
| HCD | Higher energy C-trap dissociation |
| HPLC | High performance liquied chromatography |
| hSAX | Hydrophilic strong anion exchange |
| kcal | Kilo calorie |
| kDa | (Kilo-)Dalton |
| KEGG | Kyoto Encyclopedia of Genes and Genomes |

**Abbreviations**

| | |
|---|---|
| kg | Kilogram |
| kj | Kilo joule |
| *L.* | *Lactococcus* |
| *Lb.* | *Lactobacillus* |
| LC | Liquid chromatography |
| LC-MS/MS | Liquid chromatography coupled to tandem mass spectrometry |
| *Leuc.* | *Leuconostoc* |
| m/z | Mass-to-charge ratio |
| MALDI | Matrix-assisted laser desorption/ionization |
| mRNA | Messenger ribonucleic acid |
| MS | Mass spectrometer |
| MS | Mass spectrometry |
| MS/MS | Tandem mass spectrometry |
| MS1 | Precursor mass spectrum |
| MS2 | Fragment mass spectrum |
| NAD(P) | Nicotinamide adenine dinucleotide (phosphate |
| nESI | (Nano-)Electrospray ionization |
| *O.* | *Oenococcus* |
| *P.* | *Pediococcus* |
| ppm | Parts per million |
| PSM | Peptide spectrum match |
| PTM | Post-translational modification |
| RNA | Ribonucleic acid |

| | |
|---|---|
| RP | Reversed phase |
| *S.* | *Streptococcus* |
| SAX | Strong anion exchange |
| SCX | Strong cation exchange |
| subsp. | subsp. |
| *T.* | *Tetragenococcus* |
| TMT | Tandem mass tag |
| TMW | Technische Mikrobiologie Weihenstephan (strain collection) |
| TOF | Time-of-flight |
| tRNA | Transfer ribonucleic acid |
| v/v | Volume per volume |
| *W.* | *Weissella* |
| w/v | Weight per volume |
| WHO | World Health Organization |

# 1 Introduction

## 1.1 Dairy sector

### 1.1.1 Dairy industry

Due to the increased health awareness in developed economies, the demand for high-quality and nutritionally valuable foods has been growing steadily for several years. The consequences are the ever-growing demand for organically produced foods, the increased need of nutritional advice or the increased consumption of foods with health benefits.

By far the greatest added value for companies and consumer appreciation is achieved with milk and its fermented products (dairy products) due to their health promoting properties and nutrient deliveries. Milk is one of the most valuable agricultural commodities worldwide. It is produced and consumed basically in all the world's countries (Figure 1) and, in most of them, it ranks among the top five agricultural commodities in both quantity and value term [1].

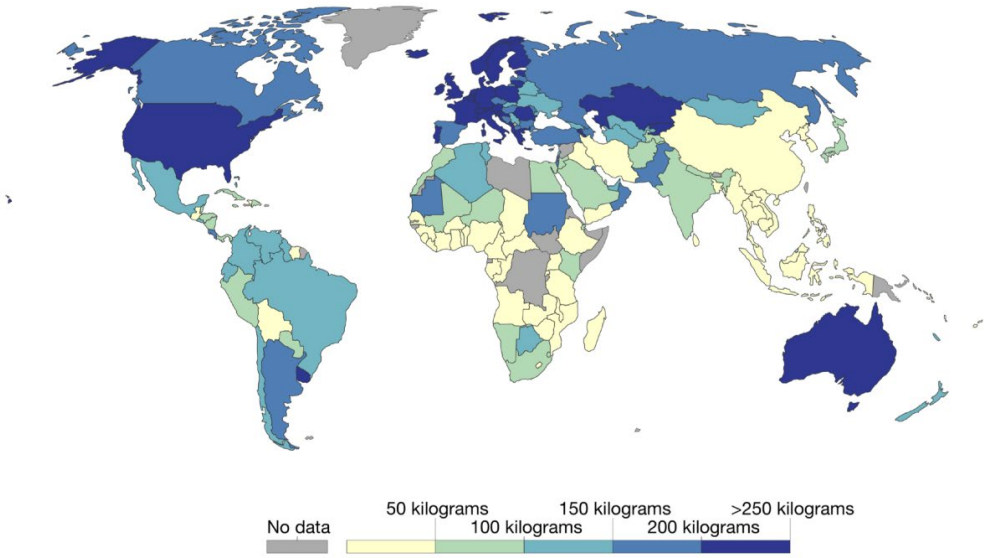


Figure 1: Worldwide average per capita milk consumption in year 2013, measured in kg per person per year (https://ourworldindata.org/). This includes the milk equivalents of dairy products made from milk ingredients but excludes butter. Data is based on per capita food supply at the consumer level but does not account for food waste at the consumer lever.

Since the beginning of the FAO[1]'s recording in 1961, the world average per capita milk consumption increased from 75.55 kg per person per year to 90 kg per person per year in 2013 (Figure 2) [1]. According to the FAO, per capita consumption of dairy products is projected to increase by 0.8 % and 1.7 % per year in developing countries and between 0.5 % and 1.1 % in developed economies in the next 10 years [2].

[1] The Food and Agriculture Organization (FAO) of the United Nations is a specialized agency that leads international efforts to defeat hunger. The FAO was founded in 1945 and is headquarterd in Rome, Italy (http://www.fao.org).

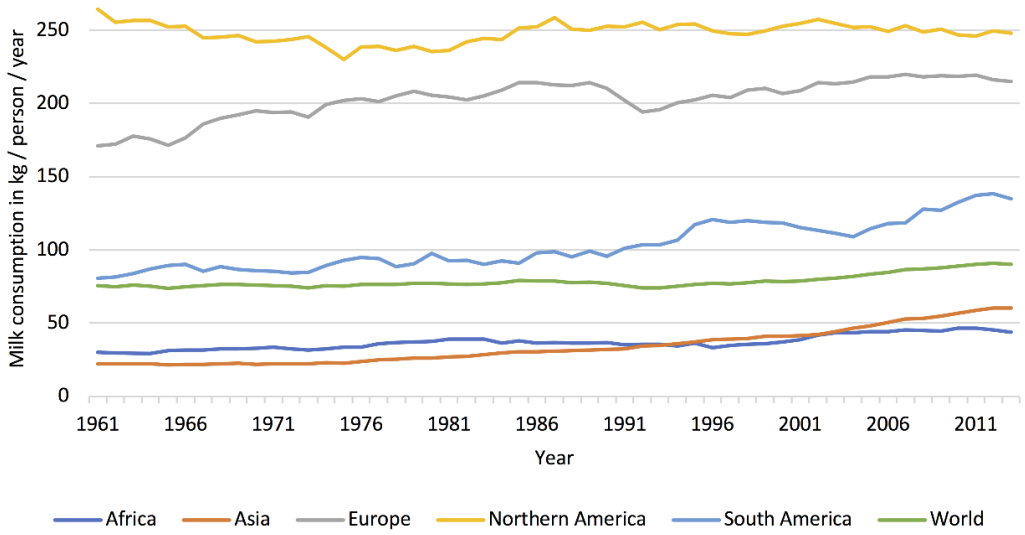


Figure 2: Global per capita milk consumption from 1961-2013.

As a result, the global milk production has increased almost annually. In 2013, with a total production of 770 billion liters valued at USD 328 billion, milk ranked third by production tonnage and was the top agricultural commodity in value terms worldwide. The global milk production is further projected to increase by 177 million tons by 2025, at an average growth rate of 1.8 % per annum in the next 10 years indicating a fast growing dairy sector. However, the dairy sector is heterogeneous as the world milk production derives from various dairy animals like cattle, buffaloes, goats, sheep and camels [2].

### 1.1.2 Dairy products

Milk and dairy products are nutrient-dense foods supplying energy and significant amounts of macro- and micronutrients including minerals/trace elements and vitamins making dairy products essential in terms of nutrition and health (Table 1).

## Introduction

Table 1: Nutrition facts of 100 ml cow milk (whole) [3].

| Nutrients | Amount[2] / 100 ml | NRV (%)[3] |
|---|---|---|
| Calories (kcal/kj) | 64/267 | |
| Water | 87.2 g | |
| Carbohydrates | 4.5 g | |
| Proteins | 3.3 g | |
| Fats | 3.5 g | |
| **Minerals / Trace elements** | | |
| Calcium | 120 mg | 15.0 |
| Phosphate | 92 mg | 13.1 |
| Magnesium | 12 mg | 3.2 |
| Zinc | 400 µg | 4.0 |
| Iodine | 3.3 µg | 2.2 |
| Fluoride | 17 µg | 0.5 |
| **Vitamins** | | |
| Vitamin A | 31 µg | 3.9 |
| Vitamin B2 (riboflavin) | 180 µg | 12.9 |
| Vitamin B12 (cobalamin) | 0.4 µg | 16.0 |
| Vitamin D | 0.06 µg | 1.2 |
| Vitamin B9 (folic acid) | 5 µg | 2.5 |

Milk consists of high-quality protein, easily digestible fat and well-usable carbohydrates in the form of milk sugar. About 3.3 % of the milk is milk protein consisting of 80 % casein and 20 % of whey. The various caseins ($\alpha$-, $\beta$- and $\chi$-casein) form sub-micelles that are cemented via calcium-phosphate complexes to larger aggregates (micelles). The content of milk fat varies depending on the dairy animal and contributes to the appearance, texture, flavor and satiability of dairy foods. Milk contains several different carbohydrates including lactose, glucose, galactose and other oligosaccharides, whereby lactose is the principal one.

[2] Amount varies depending on dairy animal and its' consumed food.
[3] Nutrient Reference values: A set of nutritional recommendations, based on Regulation (EU) No 1169/2011, used to assess the health status of populations and individuals.

In the dairy industry the use of starter cultures for the production of dairy products is most widespread and developed. Dairy products, including butter, sour milk products, yoghurt products, kefir products and cheese, are manufactured by adding starter cultures to the milk. Due to the consumers' demand for foods with sensory and health promoting properties, dairy products have been additionally upgraded with probiotics[4] (see section 9) of high cell concentration over the past few years resulting in an increased preparation and use of cultures showing double-digit growth rates [8].

[4] According to the World Health Organization's (WHO) in 2001 probiotics are "live microorganisms that, when administered in adequate amounts, confer a health benefit on the host." Although this definition is widely adopted, European national regulatory authorities forbid the use of the word "probiotic" since it embeds non-validated health claim. Until lately, European Food Safety Authority (EFSA) rejected all submitted health claims for probiotics. Scientific requirements have to be considered in the context of each application [7]

## 1.2 Starter cultures

### 1.2.1 Starter cultures in the food industry

Starter cultures are defined as a microbial preparation of high cell density of at least one microorganism that is directly added to raw material in order to produce a fermented food by accelerating and steering its fermentation process. Lactic acid bacteria (LAB), predominantly the genus of *Lactobacillus,* and bifidobacteria play a major role in these processes.

Starter cultures improve the quality and functionality of fermented foods as they enhance shelf life and microbial safety, improve texture and contribute to the pleasant sensory profile of the end product [9]. By adding them to the raw material, they cause rapid acidification while producing organic acids, such as lactic acid from lactose resulting in a consequent pH reduction. Also, the production of acetic acids, ethanol, aroma compounds, bacteriocins, exopolysaccharides and several enzymes are of importance.

Starter cultures have a long history of application and consumption in the production of many different fermented foods and beverages, ranging from fermented meats/vegetables/cereals (sausages/pickles/sourdough) to alcoholic beverages (wine) to dairy products [10-13]. In the past, the earliest production of fermented foods was based on spontaneous fermentation due to the development of the microflora naturally present in the raw material. Thus, the successful fermentation and the quality of the end product depend on the microbial load and spectrum of the raw material. Over time, spontaneous fermentation was optimized through back-slopping, a procedure in which a small quantity of a previously performed successful fermentation product is used to inoculate raw material. Today, the large-scale production of fermented foods and beverages relies on the use of starter cultures in concentrated forms for direct inoculation into the food matrix (Direct-to-Vat-Set cultures, DVS culture [14]). By doing so a high degree of control over the fermentation process and standardization of the end product has been enabled while spontaneous fermentations are avoided [15, 16].

Consequently, starter cultures have to be reliable in terms of quality. Therefore, they are produced and distributed by specialized companies granting their “biological activity”: bacterial viability, physiological state and property, ability to acidify a certain medium, enzymatic activity resulting in the production of aroma and thickening agent, absence of germs, resistance towards bacteriophages and storage stability [17-19]. Hence, the production of starter cultures requires manufacture and preservation techniques that maximize their biological activity in order to ensure a successful fermentation process and survival in the human gastro intestinal (GI) tract.

### 1.2.2 Starter cultures in the dairy industry

In the dairy industry, starter cultures have to fulfill many tasks, whereby essential ones are:

- **acidification** of the milk by LAB which causes the release of calcium and phosphate from casein micelles (until pH 5.2 – 5.3). It is accompanied by the destabilization of the colloidal dissolved micelles leading to precipitated/agglomerated casein (sour milk products, yoghurt products, cheese), as well as the protection against microbial spoilage and pathogens,
- **hole formation** ($CO_2$ development) in cheese products from citrate by homo- and heterofermentative LAB and/or hexoses by heterofermentative LAB,
- **aroma formation** by LAB in butter and some cheeses (formation of diacetyl) or yoghurt (formation of acetaldehyde) or by proteolytic and lipolytic molds.

However, different LAB and bifidobacteria are used as starter cultures in the dairy industry, since particular starter cultures crucially affect the consistency and flavor of the end product and are specifically isolated and bred for this purpose. Just as there is a wide variety of them, there is a wide variety of different dairy products. (Table 2).

Table 2: Starter cultures for the production of sour milk and yoghurt products [8].

| Dairy product | Starter culture[5] | Maturation Temperature / Time |
|---|---|---|
| **Yoghurt** | *S. thermophilus*<br>*Lb. delbrueckii* subsp. *bulgaricus* | 42-45°C/3h |
| **Yoghurt, mild**<br>**(ex. organic yoghurt)** | *S. thermophilus*<br>*Lb. acidophilus* | 41°C/3-4h or /16-19h |
| **Yoghurt, mild**<br>**(ex. Biogarde®)** | *S. thermophilus*<br>*Lb. acidophilus*<br>*B. bifidum* | 41°C/14-16h |
| **Junket, sour cream butter, buttermilk** | *L. lactis* susp. *cremoris, L. lactis*<br>*L. lactis* subsp. *diacetylactis* and/or *Leuconostoc mesenteroides* susp. *cremoris* | 22-30°C/16-20h |
| **Junket on fruits** | *Lb. acidophilus*<br>*B. bifidum*<br>*S. thermophilus* | 41°C/3-4h |
| **Sour cream** | *Lb. acidophilus* | 26-32°C/8-14h |
| **Junket** | *Lb. acidophilus*<br>*B. bifidum*<br>*S. thermophilus*<br>*L. lactis, L. lactis* subsp. *cremoris* | 28°C/16h |
| **Acidophilus-milk** | *Lb. acidophilus* | 41°C/4h or 14h |
| **Kefir** | Kefir: yeasts, *Lactobacillus* species, mesophilic lactic acid streptococci | 20-22°C/10-24h |
| **Kumys (Kumis)** | Yeasts<br>*Lb. delbrueckii* subsp. *bulgaricus* | 26-30°C/30-48h |

[5] *Lb. = Lactobacillus, S. = Streptococcus, B. = Bifidobacterium, L. = Lactococcus*

## 1.3 Probiotics

### 1.3.1 Definition and application

The natural habitat of lactic acid bacteria varies from plants to animals and humans, including the oral, genital and gastrointestinal (GI) tracts. As described above, LAB are predominantly used as starter cultures in the fermentation of foods. Recently, specific strains have been associated with health-promoting effects in humans, whereby strains of the genera *Lactobacillus* and *Bifidobacterium* are most representatives (Table 3). These strains are called probiotics defined by the Food and Agriculture Organization of the United Nations World Health Organization as “live microorganisms which when administered in adequate amounts confer a health benefit on the host” [20].

Table 3: Most important representatives of probiotics [21].

| Microorganisms considered as probiotics | |
|---|---|
| *Lactobacillus* species | *Bifidobacterium* species |
| *Lb. acidophilus* | *B. adolescentis* |
| *Lb. casei* | *B. animalis* |
| *Lb. crispatus* | *B. bifidum* |
| *Lb. gallinarum* | *B. breve* |
| *Lb. gasseri* | *B. infantis* |
| *Lb. johnsonii* | *B. longum* |
| *Lb. paracasei* | |
| *Lb. plantarum* | |
| *Lb. reuteri* | |
| *Lb. rhamnosus* | |
| Other lactic acid bacteria | Non lactic acid bacteria |
| *Enterococcus faecalis* | *Bacillus cereus va. to yoi* |
| *E. faecium* | *Escherichia coli strain nissle* |
| *Lactococcus lactis* | *Propionibacterium freudenreichii* |
| *Leuconostoc mesenteroides* | *Saccharomyces cerevisiae* |
| *Pediococcus acidilactici* | *S. boulardii* |
| *Sporollactobacillus inulinus* | |
| *Streptococcus thermophilus* | |

The reason for applying probiotics involves the restoration of the microbial balance in the gastrointestinal tract [22-24]. More than 500 different bacterial species live in the adult GI tract [23-25], of which some are considered beneficial to the human host, while others are pathogenic. Although an adequate balance of gut flora is generally maintained, antibiotics, immunosuppressive medications, surgery, and irradiation can cause an increase in the pathogenic bacteria and interfere with this homeostasis.

Essential qualifications for the use of a microorganism as a probiotic includes a number of certain characteristics:

- the biosafety (strains should have GRAS-status)
- the survivability and the preservation of the desired activity in the application form (fermented product, pure culture, etc.)
- a high resistance to the juices of the digestive tract (e.g., survive acid and bile degradation)
- the ability to colonize and to reproduce the intestinal tract over an extended period of time

Moreover, probiotic strains must be able to attach and to adhere to the intestinal epithelium, and to stabilize the balance of the gut flora [26-28].

Some of the beneficial health benefits of probiotics have been validated, while other applications have been supported by limited evidence. However, diseases associated with the GI tract have been a common target of probiotics, mainly because of their ability to restore gut flora. The strongest evidence for the use of probiotics lies in the treatment of certain diarrheal diseases. Clinical studies have also supported the role of probiotics in the treatment of pouchitis [25-27]. Data on the efficacy of probiotics in antibiotic-associated diarrhea (AAD) and travelers' diarrhea [26, 27] are inconsistent. Although the results of clinical trial are contradictory, probiotic therapy may also be beneficial in the treatment of ulcerative colitis (UC), Crohn's disease, irritable bowel syndrome (IBS) and *Helicobacter pylori* infections [22, 25, 29, 30]. Besides, probiotics have also been shown to decrease the symptoms of lactose intolerance [28, 30-32].

### 1.3.2 Pharmacology

Several health effects are associated with the application of probiotics. While some of these indications are well documented, probiotics are often used to treat conditions for which data regarding the efficacy of probiotics are lacking or contradictory [27, 33, 34]. Moreover, the exact mechanisms of action of probiotics are not known, several have been suggested:

*Lactobacillus* and *Bifidobacterium* species produce lactic acid, acetic acid, and propionic acid. These acids lower the intestinal pH and suppress the growth of various pathogenic bacteria, thereby reestablishing the balance of the gut flora [23, 24].

Another mechanism of bacterial interference involves the production of various substances, such as organic acids, hydrogen peroxide, bacteriocins, and biosurfactants, which are toxic to pathogens [24, 29, 35]. Probiotic *Lactobacillus* species strain GG has been shown to secrete a low-molecular-weight compound inhibiting a broad spectrum of gram-positive, gram-negative, and anaerobic bacteria [36].

Probiotics also decrease colonization of pathogenic organisms in the urinary and intestinal tracts by competitively blocking their adhesion to the epithelium [29]. Lactobacilli have been shown to inhibit the attachment of *Escherichia coli*, *Klebsiella pneumoniae*, and *Pseudomonas aeruginosa* to uroepithelial cells and intestinal epithelial cells [37, 38]. This inhibition may occur as lactobacilli raise steric hindrance and increase intestinal mucins, high- molecular-weight glycoproteins produced by epithelial cells, resulting in the formation of a protective barrier. Furthermore, lactobacilli strengthen the gut mucosal barrier by stabilizing tight junctions between epithelial cells and decreasing intestinal permeability [24].

Another suggested mechanism of probiotic action involves immunomodulation. Animal studies have shown that some probiotic strains augment the immune response by stimulating the phagocytic activity of lymphocytes and macrophages [39]. Probiotics also increase immunoglobulin A (IgA) and stimulate cytokine production by mononuclear cells [30, 39].

## 1.4 *Lb. paracasei* subsp. *paracasei* F19

Probiotic *Lb. paracasei* subsp. *paracasei* F19 (isogenic with strain *Lb. paracasei* subsp. *paracasei* TMW 1.1434), which belongs to the genus of *Lactobacillus*, is a gram positive, rod shaped, facultatively heterofermentative LAB. According to its phylogenetic relationship, F19 is affiliated to the *Lb. casei - Pediococcus* group. As heterofermentative LAB, it ferments hexoses almost exclusively to lactic acid via the Embden-Meyerhof-Parnas (EMP) pathway. It poses both aldolase and phosphoketolase and therefore not only ferment hexoses but also pentoses (and often gluconate). In the presence of glucose the enzymes of the phosphogluconate pathway are repressed [13].

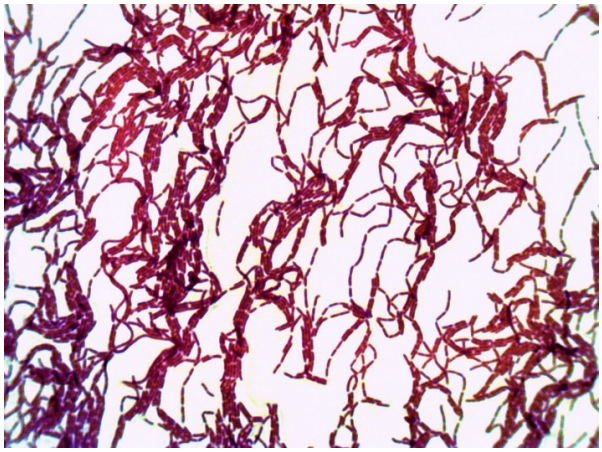

Figure 3: Microscopy image of *Lb. paracasei* subsp. *paracasei* F19.

*Lb. paracasei* subsp. *paracasei* F19 occurs naturally in foods and humans and has been isolated from cheese and humans, e.g. from healthy human colonic mucosa layer of patients [40, 41]. In the food industry, F19 has been used as starter culture or probiotic in several food and dietary supplements. F19 is supplied as freeze-dried concentrate (Hoersholm, Denmark, www.chr-hansen.com/F19), and obtains a higher stability and survival rate compared to other LAB, if it is subjected to low-temperature vacuum-drying rather than freeze-drying [42].

F19 enhances the stability, viscosity and sensoric properties of yoghurt products with and without fruit preparations and flavors [43]. Since 1995, F19 is the flagship starter culture in the yoghurt “Arla Cultura” by Arla Foods.

Human feeding trials showed F19’s potential to survive gastric transit, to persist in the colonic environment of humans and to colonize the human intestinal tract. Particularly, F19 tolerated the acidic environment in the stomach (pH 2.5, 1 h), survived the exposure to bile (20 %, 2 h), bacteriocins production and proteolytic activity [44]. F19 is further able to bind gastric and bovine mucin, collagen I and III and fibronectin and to transcribe NF-κB[6] to the nucleus of macrophages [45]. Due to the absence of delirious effects during the human feeding trials and its potential immunomodulatory effects, F19 has been suggested as safe for use as a human probiotic [41].

[6] NF-κB (nuclear factor kappa-light-chain-enhancer of activated B cells) is a protein complex that controls transcription of DNA, cytokine production and cell survival. It plays a role in regulating the immune response to infections.

## 1.5 Starter cultures and probiotics and their confrontation with stresses

Starter cultures and probiotics are confronted with various stresses during industrial processes and consumption resulting in losses of fitness and survival along with losses of probiotic activity / performance. The current industrial starter and probiotic culture production utilizes freeze-drying as the state-of-the-art preservation process of LAB. However, freeze-drying is lengthy, energy intensive and comes with a loss of living cells of up to 99 % [46, 47]. This loss of viability is caused by unfavorable environmental conditions which LAB encounter upon starter culture production. There are drying, temperature and pressure stress, as well as osmotic, oxidative and starvation stress [19, 48]. Additionally, during food fermentation and transit through the GI tract, starter and probiotic cultures are again confronted with extreme values of pH, temperature, aridity and osmotic stress, which negatively affect their survival by disturbing cellular viability [49, 50].

## 1.6 Stress responses in LAB

This chapter presents responses of LAB to stresses, which are typically present during industrial production and transit through the GI tract. A stress response is defined as the response of a microorganism to major environmental changes such as temperature or pH shifts. Changes of transcription rates, translation products and/or metabolism are some of the mechanisms how cells react to what is called a stimulus.

Microorganisms are equipped with a widely spread regulatory network of stress response mechanisms to maintain cellular viability [51]. Van de Guchte *et al.* [19], Papadimitriou *et al*. [48] and Vinusha *et al.* [52] review about stress responses in LAB. Responses to acid, heat and cold stress have been studied intensively, while stresses that have been investigated to less extent and considered as physiological irrelevant to the lifestyle of LAB are alkaline stress and pressure stress. A common way of stress protection is the development of adaptive responses to an induced stress, which to some extent, are reflected in the proteome of bacteria [53-56]. Besides, adaptive responses often induce cross tolerances leading to a significantly increased stress tolerance level and survival rate [57-60]. However, it seems that general stress responses are rare and the stress-specific response varies among the species or even strains [19].

### 1.6.1 Drying stress response

Drying stress is a central stress that is associated with the technological production of starter cultures. In the current industrial standard, commercially produced starter

cultures[7] are mainly preserved by drying, which is regarded as the state-of-the-art process in the preservation of perishable material [61, 62].

During drying, water is removed around the cells and results in the concentration of solutes providing an osmotic stress. As water is removed, oxygen reacts with the cells causing an oxidative stress. Starvation stress is also imposed on the cells, since nutrients are no longer readily available. These stresses affect starter cultures when they are preserved for distribution or used in the final product. Additionally, starter cultures are confronted with temperature stress from very high (up to 200 °C) during spray-drying to very low (down to -196 °C) during freeze-drying.

In order to enhance survival of dried starter cultures, most of the investigations have focused on influencing the drying process. Compatible solutes like betaine, carnitine, and trehalose were found to improve survival during freeze- and air-drying, the most frequently used drying processes during starter culture production [42, 63-65]. However, only very few investigations examined the protein expression under drying stress [66, 67]. Flessa *et al*. [66] investigated drying stress responses of *Shigella* and *Salmonella* on proteome level. In both, stress proteins (DnaK, GroEL, sigma factor $\sigma^B$), membrane proteins (outer membrane proteins) and proteins of energy pathways (nitrate reductase, glyceraldehyde-3-phosphate dehydrogenase, pyruvate kinase II) were induced during drying.

As drying stress amalgamates various different stress conditions (see above), cross protection against other stresses appears frequently. During desiccation, the bacterial membrane is the main target of drying stress. It undergoes a phase transition from liquid-crystalline to gel, analogously to the temperature and pressure stress response. This phase transition leads to decreased membrane fluidity and a compromised cellular integrity. Basic cell processes like ribosomal function, protein folding and enzymatic activity are affected [68]. When dried cells are rehydrated and change back to their initial phase, membrane leakages occur and solutes are released in the extracellular environment [69] – see sections 1.6.5 ‘Pressure stress response’ and 1.6.7 ‘Temperature stress response’. In case of drying stress, membrane leakages can be prevented by the addition of trehalose [69]. In addition, dehydrated cells are also confronted with osmotic and oxidative stress [68]. An increase in the environmental osmolarity (hyperosmotic stress) leads in the efflux of water causing a detrimental loss of cell turgor pressure, a change in the intracellular solute concentration and cell volume, which affect cell viability. As during osmotic stress, stress proteins (GroES, GroEL, HtrA) are induced and

[7] Commercial starter cultures are ready-mixed-starters that are used for direct inoculation of the raw material (DVS).

compatible solutes (betaine, carnitine, trehalose) are accumulated (section 1.6.2 'Osmotic stress response') [70-72]. Further, LAB use enzymes (NADH oxidase, NADH peroxidase, SOD) or nonenzymatic compounds ($Mn^2$, ascorbate, tocopherols, glutathione) to reduce or eliminate the deleterious effects of oxygen radicals (section 1.6.3 and 'Oxidative stress response') [19, 70, 73].

### 1.6.2 Osmotic stress response

In order to be metabolically active, the intracellular conditions of the bacterial cell must remain relatively constant with regard to ionic composition, pH and metabolite levels [74]. Furthermore, the maintenance of constant positive turgor is generally considered as the driving force for cell expansion, growth and division. As the cytoplasmic membrane of bacteria is permeable to water, but forms an effective barrier for most solutes, a change in the osmolality of the environment could rapidly compromise essential cell functions.

Thus, bacteria need to adapt to environmental changes in order to survive. In general, they adapt by regulating the presence of compatible solutes (osmoprotectants), to balance the difference between intracellular and extracellular osmolarities. Osmoprotectants can be classified in three groups: betaines and associated molecules, sugars and polyols, and amino acids. While under hyperosmotic conditions osmoprotectants are either accumulated by uptake or by synthesis, they are released (or degraded) under hypoosmotic conditions. Beside their role in the osmotic balance, osmoprotectants can also stabilize enzymes and thus also provide protection against other unfavorable environmental conditions such as high temperature, freeze-thawing and drying [75-77].

LAB are exposed to osmotic stress in the food industry when quantities of salt or sugar are added to the product. However, they are limited in the synthesis of osmoprotectants [76] and thus primarily rely on the uptake of such compounds from the culture medium. The process of the rapid response to changing osmotic conditions is best known for the LAB *Lactobacillus plantarum* and *Lactococcus lactis*. Under high-osmolality conditions, growth is much more inhibited by KCl and NaCl than by equiosmolar concentrations of sucrose or lactose. Sucrose and lactose cause only a temporary osmotic stress since the internal and external sugar concentrations equilibrate quickly as a result of sugar uptake. Salt stress (KCl and NaCl), instead, can have a stimulating effect on the accumulation of glycine-betaine in the cytoplasm of LAB [78-81]. Glaasker *et al.* showed that in high-osmolality medium enriched with KCl, *Lb. plantarum* accumulates the amino acids glutamate and proline in the cells [82]. They also observed that when glycine-betaine is provided in the medium, *Lb. plantarum*, like many other LAB [83], preferentially accumulate glycine-betaine over glutamate and proline. While the uptake of proline and

glycine-betaine using osmodependent transport systems is activated by an osmotic upshift, no activation of glutamate uptake was observed in *Lb. plantarum* [82]. In contrast to the osmotic upshift, the osmotic downshift results in a rapid efflux of a limited number of compatible solutes such as proline, glycine-betaine and glutamate. Thereby, a separate system, probably a mechanosensitive channel protein, mediates the efflux of glycine-betaine [82].

Glycine-betaine generally augment osmotolerance in several LAB, such as *Lb. plantarum*, *Lb. acidophilus* and *L. lactis* [78, 79, 82, 84, 85]. Therefore, LAB have evolved highly efficient osmodependent transport systems that are dedicated to its uptake. Knowledge reported in literature mainly refers to the accumulation of glycine-betaine in *Lb. plantarum* and *L. lactis*. In *Lb. plantarum*, the accumulation of glycine-betaine is mediated with high affinity by a single semiconstitutive ATP-dependent uptake system QacT. QacT also mediates the accumulation of carnitine (high affinity) and proline (low affinity) [78]. In *L. lactis*, glycine-betaine uptake is subject to a two-step osmoregulation composed of gene expression of a transport system and transport activity [84-86]. Glycine-betaine uptake is controlled by the *opu/bus* operon [87] which encodes the transporter OpuA/BusA that belongs to the ATP-binding cassette (ABC) transporter superfamily. The ABC transporter OpuA/BusA utilizes two ATP molecules per translocated molecule of glycine betaine [88]. Beside its role in osmoregulation, the transporter can also function as osmosensor. At this, a change in intracellular ionic strength serves as a primary signal of osmotic stress, which is transmitted via its effect on interactions between membrane lipids and the protein to the transporter [89]. The change in membrane fatty acid composition observed after growth in high osmolality media can affect transport activity [90].

Moreover, largely the same proteins were induced after salt and heat stress in *L. lactis* [59]. Among these proteins are the general stress proteins GroES, GroEL and DnaK. Other proteins influenced in osmotic stress resistance are membrane proteins like OpuA as well as two other membrane-associated proteins, the intracellular protease FtsH [91] and the extracellular housekeeping protease HtrA [92]. Furthermore, growth medium was found to affect exopolysaccharide [93] and bacteriocin [94] production in *L. lactis*.

### 1.6.3 Oxidative stress response

LAB that are associated with food are facultative anaerobic microorganisms. In order to regenerate $NAD^+$ from NADH, which is formed during glycolysis, they commonly reduce the produced pyruvate to lactate. However, they do not require oxygen for growth and in fact, oxygen is generally associated with negative effects in LAB. The toxicity of oxygen is usually attributed to reactive oxygen species (ROS) such as $O_2^-$ (superoxide) and $OH^\bullet$

(hydroxyl radical). These ROS attack proteins, lipids and nucleic acids and are therefore the major causes of aging and cell death. Prokaryotes and eukaryotes have developed various ways to cope with oxygen toxicity by preventing the formation of these ROS (i), by eliminating them by enzymatic degradation or scavenging (ii), by rendering their possible targets less vulnerable (iii), or by repairing the damaged caused (iv). In case of the food-associated LAB, knowledge about the present resistance mechanisms is incomplete, but has been emerging in the past years. Representative resistance mechanisms have been described in different LAB, but these mechanisms differ between species and even between strains (with respect to the presence of enzymatic and scavenging activities). An overview of common mechanisms is presented below. Apart from the toxic effects of oxygen, aeration induces important changes in the sugar metabolism of LAB. Thus, the redox balance plays an important role in pyruvate metabolism [95, 96].

*Reducing intracellular environment*

Reducing the intracellular environment is of great importance for normal aerobic growth. Therefore, cells require one of two partially overlapping disulfide-reducing pathways, the thioredoxin with thioredoxin reductase (*trxB*) or the glutathione/glutaredoxin pathway with glutathione reductase (*gshR*) [97-99]. Another way to reduce the intracellular environment is the implication of an L-cystine uptake system in the resistance to oxidative stress [100]. Thereby, cysteine is intracellularly broken down to produce the reducing free sulfhydryl compound thiocysteine. Since this sulfhydryl compound is subsequently exported, the underlying mechanisms of cell-protection against internal or external oxidizing agents remain unclear.

*Prevention of ROS formation*

The formation of ROS can be limited by the elimination of free oxygen. One way to do so under oxidative stress is to increase the activity of the oxygen consuming fatty acid desaturase system, which serve to reduce free radical damage to the cell. As a result of the increased activity, the fatty acid composition in the cell membrane can change [101].

*Elimination of ROS*

Other main players in LAB that help to counteract the deleterious effects of oxidative stress are NADH oxidase/NADH peroxidase (i), superoxide dismutase (SOD) (ii), cytochrome d oxidase (iii), catalase in the presence of necessary cofactors (iv), and non-enzymatic dismutation of $H_2O_2$ by $Mn^{2+}$(v).

NADH oxidase/NADH peroxidase: The most conserved oxidative resistance mechanism in LAB results from the coupling of NADH oxidase and NADH peroxidase [102]. Oxygen

is initially used for the oxidation of NADH to $NAD^+$ via the NADH oxidase, a reaction that produces $H_2O_2$. As $H_2O_2$ itself is toxic to the cells, it is further reduced to water by the NADH peroxidase. If the activity of the NADH peroxidase is rather low, the detoxification of $H_2O_2$ is incomplete. It was recently proposed that metabolically synthetized pyruvate reacts nonenzymatically with residual $H_2O_2$ to produce water [103].

SOD: Another key player in resistance to oxidative stress is SOD, which eliminates superoxide anion radicals ($O_2^-$) in a reaction that produces $H_2O_2$ [104]. It is induced under aeration but is also transcribed at low pH. Bacteria possess different types of SOD enzymes depending on the bivalent metal cofactor with which the enzyme is coupled, i.e., $Fe^{2+}$, $Mn^{2+}$, and/or $Cu^{2+}$-$Zn^{2+}$. LAB produce mainly $Mn^{2+}$-binding SODs [104]. A study of an *Lc. lactis* sod mutant clearly revealed that SOD protects against superoxide anion radicals [104]. The least oxygen-tolerant lactobacilli *Lb. bulgaricus* and *Lb. acidophilus* do not contain high levels of Mn nor a superoxide dismutase [105].

Cytochrome d oxidase: Several LAB species possess genes that code for a respiratory electron transport chain, although they are having a fermentative metabolism [106]. They harbor the *cydABCD* operon, which encodes a heme-dependent cytochrome *bd* oxidase with the capacity to generate PMF. At this, the LAB can engage in respiratory metabolism when quinone and heme is present in the environment [107].

Catalase in the presence of necessary cofactors: An alternative strategy to counteract superoxide anion radicals is by the production of high levels of intracellular glutathione [108], or by the transcription of catalases (when grown in a medium containing heme) or pseudocatalases (non-heme catalase) to detoxify $H_2O_2$ [109]. If a catalase is not present to render the $H_2O_2$ harmless, the detoxification of $H_2O_2$ is incomplete [96, 110, 111]. A true catalase, encoded by the *katA* gene, is found in *Lactobacillus sakei* [112] and is induced by aeration or addition of $H_2O_2$ [113]. A Mn-containing pseudocatalase can be found in *Lb. plantarum* ATCC14431 [114, 115].

Non-enzymatic dismutation of $H_2O_2$ by $Mn^{2+}$: Moreover, in some LAB (*Lb. plantarum*, *Lb. casei*, *Lb. fermentum* and *Leuconostoc mesenteroides*) high concentrations of Mn can serve as an efficient scavenger of $O_2^-$ and thereby compensate the lack of a superoxide dismutase [105]. *L. lactis* additionally obtains a SOD, which is encoded by the *sodA* gene.

*Repair of oxidative damage*

The ultimate mechanism of resistance against oxidative and other stresses is its damage repair. Thereby, the *recA* gene product, which has a direct role in DNA repair or a regulatory role on other genes required for the repair of oxygen damage, could alleviate oxidative stress [116]. However, general stress resistance mechanisms such as a

decreased intracellular phosphate concentration as internal stress signal elicit stress response conferring protection to multiple stress conditions including oxidative stress [117].

### 1.6.4 pH stress response

The growth of LAB is characterized by the production of acidic fermentation products that accumulate in the extracellular environment and thus create an environment of low pH. Although most of the LAB are neutrophils (optimal growth at pH 5-9), these bacteria can encounter an acidic environment, even in the stomach after consumption, and survive the passage through the GI tract.

*Acid stress*

The effect of acid stress on the bacterial physiology has been explored in many studies. It is known that acids passively diffuse through the cell membrane and dissociate into protons and charged derivatives in the cytoplasm. The intracellular accumulation of protons lowers the internal pH ($pH_{in}$) and thus affects the transmembrane $\Delta$pH that contributes to the proton motif force (pmf). The pmf is used in numerous transmembrane transports as an energy source. The internal acidification further reduces the activity of acid-sensitive enzymes and damages proteins and DNA. Furthermore, the accumulation of anionic moiety may result in chelating interactions with essential elements and thus has a detrimental effect on the cellular physiology [118].

The acid tolerance (AT) increases in LAB in at least two distinct physiological states. First, during exponential growth an adaptive response can be induced by incubation at non-lethal acidic pH and is referred to L-ATR [119]. L-ATR is possessed by most of the LAB and improves the bacterial survival under lethal acid stress [117, 120-124]. The induction of L-ATR can also protect LAB from other stresses such as heat, osmotic or oxidative stress. Second, AT increases after entry in the stationary phase as a result of the induced general stress response (GSR) [119].

Altogether, the LAB acid responses are processes that involve a variety of mechanisms (Figure 4) and the synthesis of a variety of proteins such as the major heat-shock proteins DnaK and GroL [125]. Striking resistance mechanisms addressing the negative effects of the acid stress are the ATP dependent expulsion of protons out of the cell in order to maintain pH gradient ($\Delta$pH) [126] (i), the increased $H^+$-ATPase activity as a consequence of upregulated $F_0F_1$-ATPase or complexes thereof to maintain $\Delta$pH [125, 127-129] (ii), the exchange of $K^+$ for $H^+$ using cation transport ATPases (e.g. $K^+$-ATPase) for the conversion of transmembrane potential ($\Psi$) into transmembrane $\Delta$pH which contributes to pH homoeostasis [130, 131] (iii), the production of basic compounds

(arginine deiminase[8] and urease[9]) to maintain pH homeostasis (iv), the repair of acid-induced damaged proteins by upregulating heat-shock chaperones such as DnaK and GroEL [125] (v) and the repair of DNA damage using an acid-inducible RecA-independent DNA repair system and Uvr system [134-136] (vi).


Figure 4: Striking resistance mechanisms addressing the negative effects of the acid stress in LAB.

[8] Arginine deiminase of the ADI deiminase pathway catalyzes together with ornithine carbamoyltransferase and carbamate kinase the conversion of arginine into ornithine, ammonia, carbon dioxide and ATP. The resulting NH3 reacts with H+ and alkalizes the environment and the generated ATP can enable extrusion of cytoplasmic protons by the F0F1-ATPase [132].

[9] Urease catalyzes the hydrolysis of urea to CO2 and ammonia that alkalizes the pH [133].

*Alkaline stress*

The acid stress response of LAB and underlying mechanisms have been intensively examined. In contrast, alkaline stress is considered as not relevant to the lifestyle of LAB and thus has been rarely investigated. Very few studies examined the response of LAB to alkaline environments. LAB that are capable of growing at pH values of > 9.5 (alkali-tolerant or alkaliphilic) are among others *Enterococcus hirae* (formerly *Streptococcus faecalis*) [137] and *Pediococcus urinaeequi* [138]. Regulation of the cytoplasmic or $pH_{in}$ is a fundamental requirement for their survival and viability. There are five mechanisms facilitating their survival and growth under alkaline conditions (Figure 5) [139-145].


Figure 5: Striking mechanisms addressing the negative effects of the alkaline stress in LAB for facilitating survival and growth.

The adaptation and the response to alkaline stress have also been reported for *E. faecalis* ATCC 19433$^T$, in which DnaK and GroEL were also induced [146].

### 1.6.5 Pressure stress response

High hydrostatic pressure is normally applied as a non-thermal inactivation method for food preservations [147-149], since it reduces undesirable chemical changes of food components [150]. During this preservation method, bacteria in food encounter severe stress and are consequently inactivated. At this, long-term application of high hydrostatic pressure results in higher microbial inactivation levels compared to a short-term pressure application [151, 152]. Several hundred MPa (up to 1000 MPa) are generally required for the inactivation of mesophilic gram-positive bacteria such as LAB. Thereby, the inactivation at high pressure is dependent on pressure level and duration, as well as several factors like pH, osmolarity and temperature etc. [153-155]. Bacteria can survive below 200 MPa and are capable to grow up to 50 MPa (mesophilic) [156-159]. Deep sea

bacteria even show optimal growth rates up to 94 MPa (piezophiles or piezo-tolerant) [159, 160].

The effects of high pressure on cells of mesophilic bacteria and their biological systems are multilateral. High pressure causes protein denaturation as it affects weak chemical bonds such as hydrophobic or ionic interactions. While the primary structure of proteins is preserved during high pressure treatment [161], secondary structures (mainly hydrogen bonds) and tertiary structures (mainly hydrophobic and ionic interactions) are influenced. Depending on the pressure level, this leads to irreversible protein denaturation [162]. Further, ribosomes become unstable and disintegrate in their subunits during high pressure treatment. As a consequence, transcription and translation processes are inhibited [163-165]. High pressure also influences the cell membrane by causing phase transitions leading to a less fluid cell membrane, which is similar to the effects caused by drying and temperature stress (section 1.6.1 and 1.6.7). While piezophilic bacteria increase actively the ratio of unsaturated to saturated fatty acids in order to maintain their membrane fluidity under high pressure [156, 166-171], a pressure dependent regulation of the membrane fluidity in mesophilic bacteria such as LAB has not been found, although it is known to play a role [172]. Phase transitions cause damages to the cell membrane resulting in membrane leakages followed by the release of RNA and intracellular proteins into the environment and in the complete lysis of the cell [173, 174]. Further, the cell is not able to maintain the osmotic potential required for energy production leading either directly to the cell death or increases its' sensitivity to otherwise tolerable environmental conditions. Sublethal stresses such as heat, cold, low pH or osmotic stress hence kill the pressure damaged cells [175-180]. Under high pressure, metabolic activities, such as the maltose metabolism of *Lb. sanfranciscensis,* are negatively affected [181]. Further, $F_1F_0$-ATPase, a transmembrane protein for energy production, is inhibited in *E. coli* and *Lb. plantarum*, while $H^+$-ATPase is inhibited in *S. cerevisiae* [178, 182, 183]. Morphological alterations occur also under high pressure stress like the formation of filaments in *E. coli* [184-187] as well as in *L. lactis* [158]. In both bacteria, cell division is inhibited as the FtsZ ring, a GTP cleaving protein necessary in the early proliferation phase for fragmentation, is repressed by high pressure [188-190].

While the use of high pressure for preservation has already been described by Certes in 1884 [191], only a few investigations have examined the protein expression under high pressure stress. Proteome [187, 192-196] and transcription [197] studies revealed that the pressure stress response varies and depends on pressure level and duration, on specie and strain and on environmental conditions. Cross tolerances are observed in LAB, like *Lb. rhamnosus* and *Lb. sanfranciscensis*, between high pressure and cold,

heat, osmotic or oxidative stress [194-196, 198-201]. There is in increased expression of the major heat-shock proteins DnaK, GroES and GroEL [187, 202] and of typical cold-shock proteins [203].

### 1.6.6 Starvation stress response

Bacteria spend most of their time in stationary nutrient-starved phase with limited access to nutrients. Entry into stationary phase and thus growth arrest, can be provoked by numerous stress conditions such as cold, heat, osmotic, oxidative or acid stress, or starvation. Nutrient starvation is the most common one as bacterial growth itself contributes to nutrient limitations in the growth medium leading to starvation for one or several compounds. Moreover, other stress conditions can indirectly provoke starvation or energy depletion, independent of the extracellular amount of the substrate [204, 205]. This starvation or energy depletion can be detrimental for long-term cell viability. Nonetheless, bacteria including LAB are well adapted to survive long-term starvation and have developed several different strategies such as the accumulation of alternative energy sources or the modification of the cell morphology [206-210]. However, as LAB make up a heterogeneous group of bacteria growing in different media, they do not encounter identical starvation conditions and thus have developed various starvation surviving mechanisms.

Starvation responses in LAB are best-studied for responses to three types of limiting compounds:

- phosphate starvation, which can be detrimental for both energy supply and DNA/RNA synthesis,
- nitrogen (amino acids) starvation, which primarily results in the limitation of protein synthesis and
- carbohydrate (sugar) starvation leading to cell energy depletion

This study focuses on glucose starvation. For some LAB, it is known that particularly glucose starvation induces an increased resistance to several other stress conditions (heat, oxidative, ethanol, acid and osmotic stress) [57, 209]. Heat, acid and bile stress resistance were also increased for lactose-starved *Lb. bulgaricus* (Chervaux *et al.* unpublished data). Some of the glucose-starvation induced proteins were characterized [211] whereby the majority of them are involved in carbon metabolism (triose phosphate isomerase, a putative dihydroxy-acetone kinase, the Gls24 protein which is probably involved in the regulation of pyruvate metabolism). Other identified proteins (carbamate kinase, a putative glycine cleavage system and L-serine dehydratase) are related to amino acid catabolism. Only one characterized glucose starvation-induced protein, a

manganese superoxide dismutase, could play a direct role in protection against oxidative stress. However, it is unclear whether starvation-induced proteins are generally involved in the modulation of LAB's metabolism.

Most LAB have the capacity to maintain an active metabolic state in order to survive in the stationary phase. This survival capacity is based on the accumulation of energetic polymeric compounds preventing energy depletion at the entry into stationary phase. LAB use mainly the arginine catabolism, particularly glycolytic capacity (conversion of glucose to pyruvate or lactate) [204, 207] and amino acid catabolism [206, 212, 213], for energy production. Polyphosphate accumulation is observed [214], as polyphosphate represents a high energy source that is convertible to ATP or promote the degradation of ribosomal proteins [215, 216]. Other energy sources are glycogen and trehalose, whereby the accumulation of the two and polyphosphate has not been observed in LAB.

A popular way of bacteria to survive stationary phase is the development of a general stress-resistant state by the synthesis of general stress proteins (GSP) [217-219]. The expression of the majority of GSP is regulated by the alternative sigma factor $\sigma^B$, which is activated by distinct pathways depending on the stress conditions [220]. Thus, some of the GSP in bacteria are involved in their survival during stationary phase and some have a protective role against potential environmental stress. In LAB, GSPs are commonly induced by more than one stress, but only a few proteins are common to all stress. However, no $\sigma^B$ homologue has so far been found for LAB. Some studies indicate potential pathways for general stress response regulation and particularly for induction during amino acids starvation. Amino acid starvation has been shown to induce the stringent response (SR) in several LAB [221-223] and other bacteria of the order *Bacillales* [224], *Enterobacterales* [225] and *Actinomycetales* [226]. The SR is characterized by the accumulation of guanine nucleotides (ppGpp) synthesized by *relA* (ppGpp synthetase). ppGpp is involved in the control of many stress induced genes and is considered as a major signal involved in saving the cells' energy [227]. In *L. lactis*, the synthesis of ppGpp plays a role in acid-stress resistance [117] and, more generally, pools of guanine and phosphate have been implicated in stress response in lactococci [116, 117]. Moreover, SR in *S. pyogenes* strongly supports its survival under nutritional stress conditions [228].

Starvation-induced mechanisms in LAB are different to those of the well-studied bacterial models *E. coli* and *B. subtilis*. The striking difference includes the absence of an $\sigma^B$ homologoue. Thus, the regulation of the starvation-induced GSP remains unclear for LAB, but unknown regulation mechanisms compensate for the absence of an $\sigma^B$ homologoue. Further, proteome studies revealed that only a small overlap exists

between stress-specific and starvation regulons and that general stress proteins are rare.

### 1.6.7 Temperature stress response

LAB are primarily mesophilic, rarely thermophilic, with respect to their optimal growth temperature. However, during industrial processes, such as frozen storage of starter cultures, low temperature fermentation during cheese ripening and refrigerated storage of fermented products, LAB are exposed to temperatures far below their optimal growth temperature.

*Cold stress*

When cells are exposed to a temperature downshift they perform physiological changes like a decrease in membrane fluidity and a stabilization of secondary structures of RNA and DNA leading to a reduced efficiency of translation, transcription and DNA replication. In order to overcome these effects, microorganisms have developed a transient adaptive response, the cold-shock response, during which a number of cold-induced proteins (CIPs) are synthesized (Figure 6). CIPs maintain membrane fluidity by increasing the proportion of shorter and/or unsaturated fatty acids in the lipids (i), DNA super-coiling by reducing the negative supercoiling (ii) and transcription and translation needed for cellular adaptation to low temperature (iii) [229].

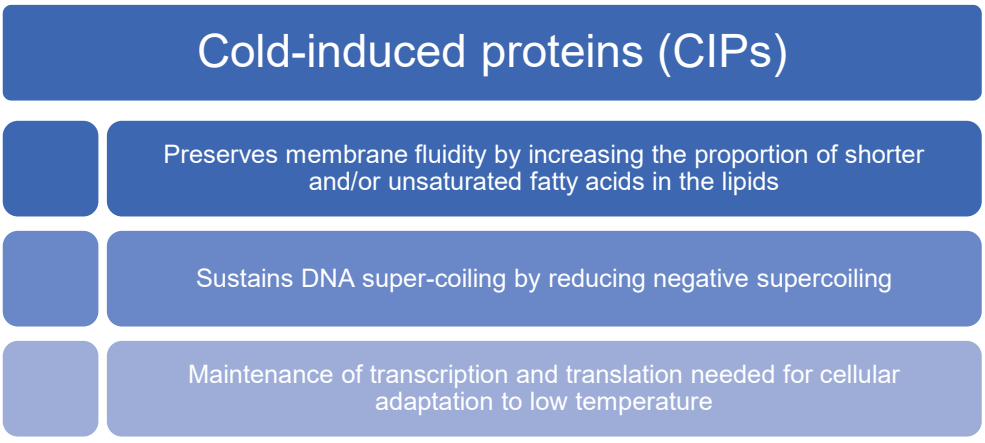


Figure 6: Role and functions of cold-induced proteins (CIPs) in microorganisms [229].

Most strongly induced CIPs include a family of proteins of low-molecular weight (~7.5 kDa), termed cold-shock proteins (CSP) [230]. CSP have a high degree of sequence identity (> 45 %) and orthologs have been found in both gram-positive and gram-negative bacteria [230]. Cold induced CSP have an unusually long 5' untranslated region (5'-UTR) which can play a role in mRNA stability and translation efficiency [231-233]. Cold induction of CSP is complex and is controlled mainly by post-transcriptional modification [232, 234-236] as single deletions of *csp* resulted in increased levels of the

remaining CSPs and thus compensated the loss of each other [237-239]. CSPs are β-barrel proteins with two RNA-binding motifs, able to bind to single-stranded DNA and to RNA with little specificity and to destabilize secondary RNA structures [240-243]. By doing so, CSPs have been proposed to act as RNA chaperones supporting transcription and translation at low temperature by preventing formation of mRNA secondary structures [240, 241].

*Heat stress*

In contrast to temperature downshifts, the major problem encountered by cells at high temperature is the denaturation of proteins and their subsequent aggregation [244]. Additionally, destabilization of macromolecules such as ribosomes and RNA and alterations of membrane fluidity were also described [245-247]. The heat-shock (HS) response is best-studied for the gram-positive model organisms *E. coli* and *B. subtilis*. HS response of LAB is similar (*L. lactis*, [59, 248, 249]; *Leuconostoc mesenteroides*, [250]; *E. faecalis*, [251]; *O. oeni*, [252]; *Lb. bulgaricus*, [253]). In gram-positive bacteria, HS inducible genes are classified according to their regulators. Genes of class I are regulated by the HrcA repressor that binds to the palindromic operator sequence CIRCE (controlling inverted repeat of chaperone expression) [254]. Class II consists of genes that are controlled by the sigma factor $\sigma^B$ (section 1.6.6) governing the expression of a large set of genes involved in the general stress resistance [255, 256]. While class III genes are controlled by the class three stress gene repressor CtsR which binds to a specific direct repeat, the CtsR-box [257], the regulation of heat-shock genes of class IV remains unclear.

Studies of LAB HS responses revealed variable numbers of induced proteins: 34 in *E. faecalis* [251], 40 in *S. mutans* [258] and 17 in *L. lactis* [59]. These HS proteins are among others well conserved chaperones (DnaK, DnaJ, GrpE, GroES and GroEL) and proteases (Clp, HtrA, FtsH). As already mentioned in section 1.6.1 (‘Drying stress response’) 1.6.2 (‘Osmotic stress response’), 1.6.4 (‘pH stress response’) and 1.6.5 (‘Pressure stress response’), a subset of heat-shock proteins (HSP) (DnaK, GroES, GroEL) is also induced by other environmental stresses indicating to be general stress proteins. In *L. lactis*, 12 proteins of HS stimulon are induced after salt stress (NaCl) [59]. The overlap of heat-shock and osmotic stress responses also exist in *S. mutans* as 21 HSP are expressed during osmotic stress.

## 1.7 Phenotypic and proteomic plasticity

Ever since the first appearance of life, environmental changes have occurred in the lifespan of an individual organism. However, organisms have lived, developed, and evolved in these changing environments. In evolutionary biology, the ability of populations to adapt to a particular habitat/environment is a key topic, since the exploitation of new niches plays a key role in the speciation process [259-261]. At this, organisms either become extinct or extirpated or use three main evolutionary strategies in order to survive in heterogeneous habitats (Figure 7) [262, 263]. They migrate or shift their current distributional range (i), adapt through a change in genetic composition of the population (ii) or become phenotypically plastic (iii).

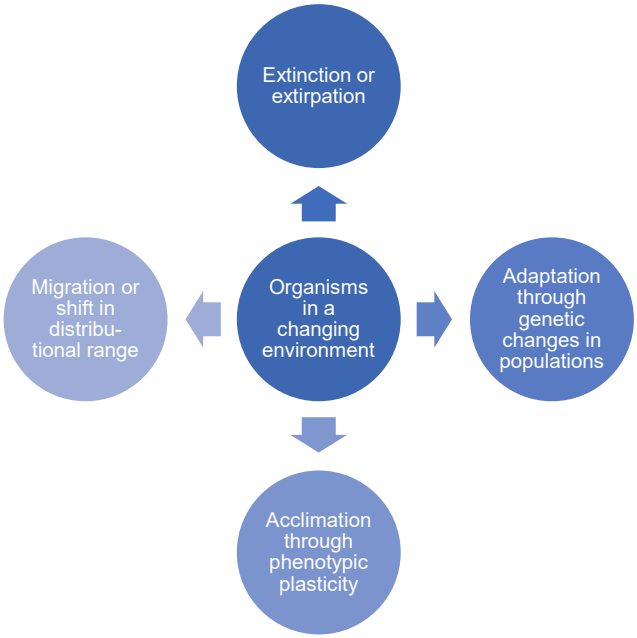


Figure 7: Four outcomes for an organism in a changing environment [262].

Genetic changes and phenotypic plasticity are the most promising outcomes that can prevent local extinction. As the rapid rate of environmental changes will diminish the chances of observing the evolution of adaptive heritable traits through classical Darwinian selection (evolutionary adaptation), at least in species with long generation time [264], acclimation through phenotypic plasticity is consequently of crucial importance for the fate of organisms in a changing environment [265]. Phenotypic plasticity is defined as 'the property of individual genotypes to produce different phenotypes when exposed to different environmental conditions' [266, 267]. Phenotypic plasticity also includes the ability of an individual organism to change its phenotypic state or activity (e.g. its metabolism) in response to variations in environmental conditions/stresses [261].

At this, the subset of transcribed genes in an organism is a dynamic and plastic link between the genome, the proteome, and the cellular phenotype [268]. The understanding of the phenotype formation requires the investigation of all steps from gene regulation to their final products at the proteomic level [269, 270]. In general, among the most powerful tools for investigating the mechanisms of environmental stressors are omics methods [271, 272], which are applied for the large-scale study of genomes, transcriptomes, proteomes, and metabolomes. Compared to transcriptomics, proteomics is closer to physiology - since the proteome, unlike the transcriptome, directly influences the phenotype - and provides a better understanding of the regulation of gene expression [273]. Pan *et al.* have argued that the cellular phenotype should be assessed by quantitative proteomics [274]. Moreover, effects on fitness, the ability of an organism to survive and reproduce, are ultimately crucial to an organism in a stressful situation. During adaptation of an organism to a new environmental situation, natural selection acts directly at the phenotypic level to select individuals with the highest fitness [275, 276]. At the biochemical level, fitness is primarily a consequence of the proteins' ability to function properly under normal or stressful conditions [269]. The abundance of mRNA provides little information on fitness and cannot substitute for proteins in detailing functional analyses of candidate genes [269].

Consequently, proteomics is the most appropriate approach to discover cellular stress response mechanisms and links the genotype to the phenotype. As a bridge between genotype and organismic/cellular phenotype, the proteome could also describe protein expression patterns across a range of environments. Hence, Bedon *et al*. introduced the term "proteomic plasticity" to describe the protein expression patterns of two ecophysiologically contrasted genotypes of *Eucalyptus* trees under osmotic stress [277]. They could highlight adaptive mechanisms to water deficit specific to each genotype. Proteomic plasticity has also been reported to occur in the parasitic nematode worm *Heligmosomoides polygyrus bakeri* [278] and in the marine snail *Littorina saxatilis* [279, 280].

## 1.8 Mass-spectrometry based proteomics

The proteome is defined as the full complement of proteins, which is present in a biological system at any given point in time. As such, the proteome is not static but the protein abundance, its post-translational modifications, their structure and interactions are dynamically regulated in response to a variety of external and internal stimuli. Proteomics, the large-scale study of the proteome, complements genomic and transcriptomic approaches, but is unique in the sense that it enables the direct analysis of the executing molecules within a cell and is in turn capable of providing a different level of biological insight and understanding [272].

### 1.8.1 Bottom-up proteomics

Bottom-up (or shotgun) proteomics is the most frequently used proteomics approach to identify and quantify proteins derived from complex biological samples and is based on the measurement of peptides instead of full length proteins (top-down proteomics) [281, 282]. Shotgun approaches are less time consuming and therefore suited for comprehensive proteomic analysis of large-scale studies. Figure 8 shows a standard shotgun proteomics workflow.

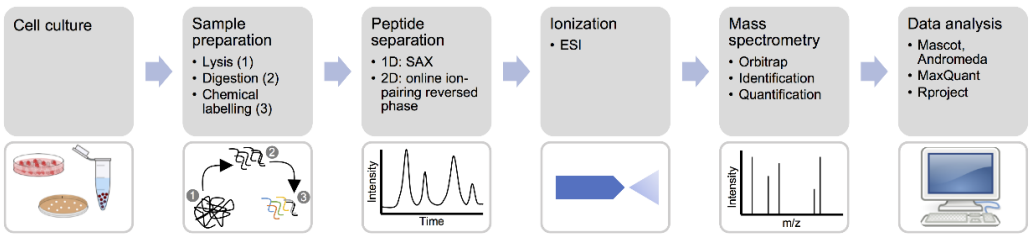


Figure 8: Standard bottom-up proteomics workflow (adapted from [282]).

According to this workflow, proteins are first extracted from cells or tissue, either by physical disruption or solution-based lysis conditions. Next, the proteins are digested to peptides by treatment with a proteolytic enzyme [283-285]. Typically, this is accomplished by the enzyme trypsin, which introduces a proteolytic cleavage C-terminal to arginines and lysines [282]. Subsequently, sample complexity is reduced by chromatographic peptide separation prior to mass spectrometric analysis (high-resolution peptide separation; one or two dimensional). Common setups separate tryptic peptides by an on-line ion-pairing reversed-phase liquid chromatography (LC) system [272, 286, 287]. Hereby, the separation power is generated by interactions of nonpolar side chains of peptides with the nonpolar stationary phase (C18). Upon elution with

increasing concentrations of organic solvent (e.g. acetonitrile), peptides are separated according to hydrophobicity, influenced by the size and polarity of peptides. With coupling of the on-line ion-pairing reversed-phase LC system to the MS (online-coupling), peptides are directly ionized after LC separation and enter the mass spectrometer subsequently which measures the mass-to-charge (m/z) ratio and intensity of each peptide. Thereafter, data analysis identifies and quantifies peptides and proteins present in the sample.

According to sample type and experimental strategy, the standard workflow can be modified regarding different fractionation/separation steps. For deep proteome coverage, two-dimensional separation techniques are used (high-resolution peptide separation). An additional first dimension (often offline) should apply an orthogonal peptide fractionation principle to the second peptide separation dimension using ion pairing reversed phase chromatography. Common techniques include strong anion exchange chromatography (SAX) [286, 288] or strong cation exchange chromatography (SCX) [289] and separate peptides according to their charge.

The following paragraphs provide a more detailed introduction into the relevant techniques applied in the respective workflow steps.

### 1.8.2 Mass spectrometry

Simplified, a mass spectrometer can be described as a balance, which measures the molecular weight of the respective analyte as a m/z ratio [290]. It utilizes the fundamental principle that charges can be manipulated by electromagnetic fields in the gas phase by assessing the influence of electromagnetic forces on ions with differing mass. A mass spectrometer roughly consists of three modules: an ion source where analyte molecules are charged and transferred into the gas phase, a mass analyzer where ions are separated based on their m/z ratio and a detection system which measures the resulting ion current.

Due to technological development, a variety of different ionization systems (e.g. electrospray, matrix-assisted laser desorption) and mass analyzers (e.g. ion traps, time-of-flight analyzers, orbitraps) have been generated. In this study, a hybrid ion trap mass spectrometer, namely the Q Exactive HF (Figure 9) [291, 292], was used. An overview of its underlying technology is presented hereafter.

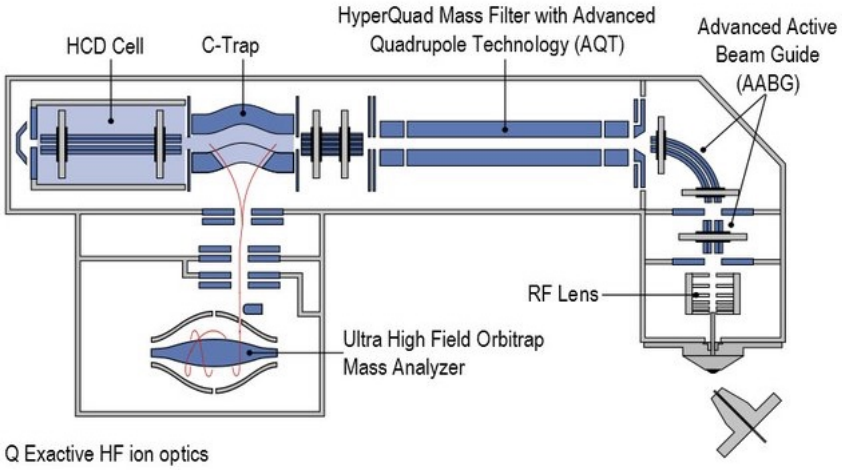


Figure 9: Schematic overview of the Q Exactive HF. Peptides are ionized via electrospray, enter the mass spectrometer, and droplets and uncharged species are removed in the Advanced Active Beam Guide (injection flatapole and bent flatapole). Peptides are collected in the segmented quadrupole mass filter (HyperQuad Mass Filter with Advanced Quadrupole Technologey (AGT)) and further transferred to the C-trap. Peptides are injected into the orbitrap mass analyzer (Ultra High Field Orbitrap Mass Analyzer) where m/z ratios are determined (MS1). Selected peptides are fragmented in the HCD collision cell and fragments are subjected to the orbitrap mass analyzer again (MS2). Figure from Thermo Fisher Scientific.

Ionization of the peptides is accomplished by electrospray ionization (ESI), a soft ionization technique [293-295]. Since ESI enables the ionization from liquid phase and the efficient, robust and automated online-coupling to peptide separation, it is the most prevalent ionization technique in modern mass spectrometry. As the peptides elute in a volatile solvent from the nanoLC [296], they pass a thin capillary to which an electric potential is applied. Once the solvent reaches the tip of the capillary, charges are electrophoretically separated and, if the electrostatic potential is greater than the surface tension, a Taylor cone forms at the end of the capillary emitting a continuous liquid jet towards the counter electrode. During this process, the liquid jet becomes unstable and bursts into a spray of multiply charged droplets, which contain the dissolved peptide molecules. As the droplets continue to migrate through the electrostatic field, the liquid evaporates while the surface charge increases. When the Raleigh limit is reached, the repulsion of like-charges induces the uneven fission of droplets into nano-droplets in a process called Coulomb explosion. The newly created droplets again undergo desolvation and Coulomb fission. As the mobile phase evaporates leading to droplet fission, charged species are finally released.

Ionized peptides enter the mass spectrometer through a transfer tube to an RF-lens and then via an injection flatapole into a bent flatapole, both part of the Advanced Active Beam Guide (AABG). In the AABG solvent droplets are ejected and other neutral species

are removed. After collisional cooling in the bent flatapole, peptides are transmitted via a lens into a segmented quadrupole mass filter (HyperQuad Mass Filter with Advanced Quadrupole Technology) where a defined precursor peptide ion is isolated and collected [292]. Peptides are further transferred into the C-trap which focuses the ions for subsequent injection into the high resolution orbitrap mass analyzer [297-299]. The orbitrap mass analyzer consists of an outer barrel-shaped and a central spindle-shaped electrode generating an electromagnetic field when voltage is applied. This electromagnetic field traps the injected peptides by oscillation of the charged species around the z-axis as well as radial movement around the central spindle electrode [300]. Dependent on their m/z ratio, charged species adapt stable trajectories with certain oscillation frequencies. The movement of charged species around the central electrode within the applied electromagnetic field leads to transients that are recorded in image current and are subsequently translated (de-convoluted) by fast Fourier Transformation from the time domain into the m/z domain to generate a mass spectrum [297, 301].

In tandem mass spectrometry, the arrangement of multiple consecutive scan and selection events with intermediate fragmentation is enabled [302]. Two different types of mass spectra are acquired: MS1 spectra of intact peptides eluted at the same time from the LC column and MS2 spectra of peptide fragments of selected precursors [282]. A MS1 spectrum, where the m/z and intensities of intact peptide precursors are recorded, is followed by isolation and fragmentation of a selected precursor in the higher-energy collisional dissociation (HCD) cell. Depending on the fragmentation techniques, different ions are generated by different breakpoints within the amino acid chain. HCD fragmentation leads to breakage between the carbonyl C=O and the nitrogen N-H of the peptide bonds, which connect the single amino acids [303]. This generates characteristic b- (charge retained at N-terminus) and y- ion series (charge retained at C-terminus) [303]. After fragmentation of a selected precursor, generated fragment ions are then subjected to the C-trap and fragment masses are again read out in the orbitrap mass analyzer generating a MS2 spectrum. Combined information about accurate precursor and fragment ion masses enables determination of the peptide sequence.

Data-dependent acquisition (DDA) is a widely used, automated and real-time strategy to decide on which precursor to pick for fragmentation. In DDA, the mass spectrometer alternates between MS1 and MS2 spectra and picks a predefined number of peptide precursors for subsequent fragmentation based on their abundance in the preceding MS1 spectrum [304, 305].

### 1.8.3 Protein identification and quantification

As described, the sequence of peptides is derived from fragment ion spectra generated by tandem mass spectrometry (MS2 spectra). Typically, peptide identification relies on an approach referred to as “database searching” in which measured fragment ion masses are compared to theoretically calculated ones [305]. Therefore, a theoretical search space is generated by a proteolytic *in silico* digest of proteins collected in a database in order to yield theoretical tryptic peptides. This list of potentially present peptides is then filtered for the list of experimentally measured and charge state-deconvoluted peptide precursor masses. Subsequently, spectra of *in silico* tryptic peptides are predicted and compared with the acquired MS2 fragment spectra. A score, which is based on metrics such as number and type of matching fragments or fragment and precursor mass deviation, is derived in order to probabilistically describe the quality and similarity of how well the predicted and the experimental spectra fit to each other. Usually the match between the experimental spectrum and the highest-scoring peptide is referred to as a peptide-spectrum-match (PSM). However, given the sheer number of spectra acquired in each shotgun experiment and the size of the *in silico* search space, the occurrence of false peptide assignments (false positive spectrum matches) is a common shortcoming of database searching algorithms. In order to ensure that the PSMs are reliable, decoy searches are performed allowing the determination of a false discovery rate (FDR), and hence a score cutoff to filter the outcome for high confidence identifications [306-308]. Briefly, a decoy database containing reversed versions of the *in silico* generated tryptic peptides is derived and experimental spectra are searched not only against the specified database, but also against this decoy database [309-312]. Any true matches from the decoy database are not expected and are wrong by definition. It can be expected that the number of matches that are found in the decoy database are equal to the wrongly assigned matches in the “target” database. Scoring spectra against both search spaces enables the calculation of a FDR reflecting the ration of decoy and target hits and thus the tolerated number of false positive assignments in the target space. The limitation of this peptide identification strategy is the requirement for a comprehensive and well-curated sequence database for proteome experiments limiting the approach to sequenced organisms. For the purpose of peptide identification, numerous search engines, such as Mascot or Andromeda (MaxQuant) [306, 313-315], were developed. If the identified peptide is present in several related proteins or protein isoforms (referred to as razor peptides in MaxQuant), an unambiguous assignment of peptides to one particular protein is often not possible. Hence, proteomic experiments often report protein groups of related proteins if no unique peptide was found allowing the unambiguous assignment to a single protein.

Besides the qualitative information if a protein is present in a sample or not, it is often of interest how proteins change in abundance over time or how a certain stimulus influences the proteome abundance in cells or tissues [316, 317]. Quantification by mass spectrometry relies on the fact that the triggered response by the analyte in the mass detector is proportionate to its abundance. Absolute and relative quantification approaches can be distinguished. The exact concentration and copy number of a given peptide or protein present in a biological sample is determined by absolute quantification, relative changes are quantified by relative quantification. There are several different relative quantification strategies that are based on either label-free or label-based quantification techniques. In label-based quantification techniques, stable isotopes or chemical tags are introduced and enable the mass-encode multiplexing of peptides from different samples. The resulting mass increment of the labeled over the non-labeled version is resolved by the mass analyzer and is used for relative quantification within the same spectrum. Chemical labeling is one of the most common and powerful relative quantification strategies and it is used in this study. In chemical labeling, primary amine targeting tags are attached via succinimide chemistry. Due to their isobaric nature (of same nominal mass), differently labeled species cannot be distinguished in MS1 scans. However, during fragmentation they lose isotopically encoded reporter ions which are detected on the low mass region of the MS2 spectrum (MS2-based quantification) and can be used for relative quantification. The most widely used approaches make use of tandem mass tags (TMT) that are composed of an amine-reactive NHS-ester group, a spacer arm and a mass reporter containing stable isotopes [318].

# 2 Hypothesis and objectives

Lactic acid bacteria (LAB) are widely used as starter and probiotic cultures in the manufacture of foods, e.g. for the production of dairy products, or as probiotics with health-promoting effects. However, during industrial processes and consumption, these cultures are confronted with various stresses resulting in an almost complete loss of fitness and living cells [19, 46-50]. Hence, a high number of additional fermentation batches with expensive substrates are required in order to yield high quantities of viable cultures. An increase in the proportion of viable cells would result in a reduction of the necessary fermentation batches. The dairy industry is consequently anxious for a resource-saving production of effective cultures. Optimal survival of LAB would contribute to the culture's industrial performance and health-promoting properties. To prevent the loss of fitness and living cells during industrial processes and consumption, stress responses need to be analyzed. Many previous studies emphasized the importance of understanding stress response mechanisms in order to avoid detrimental damage to the cells and in order to optimize fermentation processes, and to improve storage and conservation of the products. However, stress response mechanisms, which are based on differentially expressed proteins, are plastic and dynamically regulated depending on induced stress, strain and even species. Prior research has shown that stress induces the development of adaptive responses to an induced stress or cross resistances to another stress resulting in increased stress tolerance level and survival rate. The detailed analysis and comparison of stress responses in LAB induced by several different stresses have not yet been fully elucidated.

**General working hypothesis:**

- Stresses induce changes in the proteome of LAB which can be exploited to enhance cellular fitness, viability and probiotic activity / performance of LAB.

**Hypotheses:**

- Stress response mechanisms are dynamically regulated in LAB depending on the induced stress.
- Stress induces phenotypic and proteomic plasticity in prokaryotic LAB.
- Pretreatment with sublethal stresses induce adaptive responses and cross-tolerances.
- Adaptive responses and cross-tolerances result in increased survival and performance of a strain in the preparation process and in the intestinal tract.
- Adaptive responses and cross-tolerances affect the expression of proteins related to the probiotic performance of a strain.

- *Lb. paracasei* subsp. *paracasei* F19 represents an appropriate model organism for this study.

**General objectives:**

- characterizing underlying stress responses that are frequently present during industrial processes and consumption of starter cultures by using *Lb. paracasei* subsp. *paracasei* F19
- evaluating underlying stress responses towards cellular fitness, viability and probiotic activity/performance of probiotic *Lb. paracasei* subsp. *paracasei* F19

**Detailed objectives:**

- establishing a procedure for the selection of stress conditions that have comparable sublethal influence on *Lb. paracasei* subsp. *paracasei* F19's physiology
- selecting comparable sublethal stress conditions for the analysis of bacterial stress responses utilizing the established procedure
- establishing an experimental strategy for the investigation of bacterial stress responses on basis of genomics and quantitative proteomics
- obtaining the complete genome sequence of F19 as reference genome during database searching
- analyzing and identifying proteomic stress responses of F19 based on the identification of differentially expressed proteins using the established experimental strategy
- comparing stress responses in order to identify similarities and possible cross-protections among them
- determining an optimal pretreatment of F19 with sublethal stresses in order to induce adaptive responses towards drying (optimal preconditioning)
- evaluating the effect of optimal preconditioning regarding survival of F19
- demonstrating phenotypic and proteomic plasticity in prokaryotic cells
- evaluating data towards changes in survival rates and predicted changes towards probiotic activity/performance of F19

# 3 Material and Methods

## 3.1 Material

### 3.1.1 Devices, chemicals and consumables

For devices chemicals and consumables, see Supporting Part I.

### 3.1.2 R packages

Most data were evaluated and visualized using Excel (Microsoft, Redmond, USA) and R Software (Version 3.3.2, http://www.r-project.org/). Table 4 lists the R packages used and their purpose.

Table 4: Overview of R packages used. Package and functions are given together with the purpose.

| Package | Functions used | Purpose / Usage |
|---|---|---|
| adegenet | find.clusters, dapc, scatter.dapc | Discriminant analysis of principle components (Jombart and Ahmed, 2011) |
| DESeq | CountDataSet | Differential expression analysis for sequence count data (Anders and Huber, 2010) |
| grofit | grofit, grofit.control | Fitting biological growth curves with R (Kahm et al., 2010) |
| gplots | heatmap.2, hclust | Cluster analysis – creation of heatmaps including dendrogram based on hierarchical clustering (Warnes, 2015) |
| pheatmap | pheatmap | A function to draw clustered heatmaps where one has better control over some graphical parameters such as cell size, etc. (Kolde, 2015) |
| PTXQC | Automated pipeline | PTXQC: Quality Report Generation for MaxQuant Results (Bielow, 2017) |
| stats | fisher.test | Statistical significance test for the analysis of contingency tables; testing the null of independence of rows and columns in a contingency table with fixed marginal (R Core Tea, 2012) |

### 3.1.3 Microorganism and growth media

*Lactobacillus (Lb.) paracasei* subsp. *paracasei* TMW 1.1434 (isogenic with strain F19 from Chr. Hansen A/S, Hørsholm, Denmark) was cultivated using Spicher agar and broth, a modified MRS medium [319]. The term Spicher[1] will subsequently refer to the medium described in Table 5 with a pH of 5.4, if not otherwise indicated.

Table 5: Composition of Spicher[1]. Compounds (chemicals) are listed together with the corresponding supplier and, if available, the purity grade. Concentrations are given in g/l.

| Compound | Supplier and grade | Concentration (g/l) |
|---|---|---|
| Agar for solid media | BD biosciences, Heidelberg, Germany; European agar | 15 |
| Di-ammonium hydrogen citrate | Carl Roth, Karlsruhe, Germany; ≥ 98 % | 5 |
| $FeSO_4$ * 7 $H_20$ | Sigma-Aldrich, Steinheim, Germany; ≥ 99 % | 0.05 |
| $K_2HPO_4$* 3 $H_20$ | Carl Roth, Karlsruhe, Germany; ≥ 99 % | 2.5 |
| $KH_2PO_4$ | Carl Roth, Karlsruhe, Germany; ≥ 99 % | 2.5 |
| L-Cysteine-HCl | Carl Roth, Karlsruhe, Germany; ≥ 98.5 % | 0.5 |
| Meat extract | Merck Millipore, Darmstadt, Germany; for microbiology | 2 |
| $MgSO_4$ * 7 $H_20$ | Merck Millipore, Darmstadt, Germany | 0.2 |
| $MnSO_4$ * $H_20$ | Carl Roth, Karlsruhe, Germany; ≥ 99 % | 0.075 |
| Peptone from casein | Merck Millipore, Darmstadt, Germany; for microbiology | 10 |
| Sodium acetate trihydrate | Carl Roth, Karlsruhe, Germany; ≥ 99.5 % | 5 |

| | | |
|---|---|---|
| Sodium gluconate | Carl Roth, Karlsruhe, Germany; ≥ 99 % | 2 |
| Tween 80 | Gerbu, Heidelberg, Germany; purified | 1 |
| Yeast extract | Carl Roth, Karlsruhe, Germany; for bacteriology | 7 |
| D-Glucose | Merck Millipore, Darmstadt, Germany; ≥ 99.5 % | 7 |
| D-Maltose | Merck Millipore, Darmstadt, Germany; ≥ 98 % | 14 |

Modifications of Spicher[1], regarding growth challenge experiments, are mentioned in the particular sections. In order to obtain sterility, all media were autoclaved at 121 °C for 20 min. Temperature sensitive components were sterile filtrated (pore size 0.2 µm) and added after autoclaving. Sugars were separately autoclaved to avoid Maillard reactions. The pH of the media was adjusted with 2 to 6 M HCl or NaOH.

### 3.1.4 Medium additives

Table 6 lists relevant additives used for different experiments.

Table 6: Relevant medium additives. Additives are listed with purity grade and supplier of the respective chemical.

| Additive | Grade | Supplier |
|---|---|---|
| D-Lactose (lac) | ≥ 98 % | Gerbu, Heidelberg, Germany |
| D-Sucrose (suc) | ≥ 99 % | Gerbu, Heidelberg, Germany |
| Hydrochloric acid solution (HCl) | 37 % | Carl Roth, Karlsruhe, Germany |
| Hydrogen peroxide ($H_2O_2$) | ≥ 30 % | Merck Millipore, Darmstadt, Germany |
| Potassium chloride (KCl) | ≥ 99.5 % | Carl Roth, Karlsruhe, Germany |
| Potassium hydroxide (NaOH) | 50 % | Merck Millipore, Darmstadt, Germany |
| Sodium chloride (NaCl) | ≥ 99.5 % | Carl Roth, Karlsruhe, Germany |

### 3.1.5 Culture conditions and standard preculture

Unless otherwise declared, TMW 1.1434 was anaerobically incubated in Spicher[1] at 37 °C. In order to achieve anaerobic conditions, reaction tubes were maximally filled, microtiter plates were overlaid with paraffin oil and agar plates were incubated using the Anaerocult® C System (both Merck Millipore, Darmstadt, Germany).

TMW 1.1434 was streaked out on Spicher[1] agar and incubated until single colonies were visible. A single colony was analyzed using Matrix-assisted-Laser-Desorption-Ionization-Time-Of-Flight Mass Spectrometry (MALDI-TOF MS, section 3.2.4) in order to test whether the indicated specie of the isolate was correct. Past specie confirmation, TMW 1.1434 was sub-cultured in triplicates on Spicher[1] plates and anaerobically incubated at 37 °C. A single colony was then transferred into 50 ml Spicher[1], followed by incubation at 37 °C. For storage, a sufficient amount of cells was harvested by centrifugation, suspended in Spicher[1] with a final glycerol concentration of 45 % (Gerbu, Heidelberg, Germany) and stored at -80 °C. From glycerol culture, TMW 1.1434 was reconstituted for usage by streaking out on Spicher[1] agar.

Standard preculture: Unless otherwise declared, Spicher[1] liquid preculture was used in order to obtain cell suspensions for all kind of experiments. Therefore, 2 ml Spicher[1] was inoculated with a single colony (= biological replicate) and incubated for 24 h at 37 °C to stationary phase. These precultures will consequently be stated as standard precultures.

## 3.2 Methods

### 3.2.1 Experimental strategy for the analysis of stress proteins using genomics and quantitative proteomics

The efficient analysis of bacterial stress responses was enabled applying a straightforward experimental strategy based on genomics and quantitative proteomics using chemical labeling (Figure 10).

Bacterial stress responses of the strain *Lb. paracasei* subsp. *paracasei* TMW 1.1434 were investigated accompanied by the identification of differentially expressed (DE) proteins. Stress treatments were prepared in biological triplicates based on identified stress conditions (section 3.2.3) [320], cell lysis was carried out and whole-cell protein extracts were subjected to proteolytic digestion with trypsin (subsection 3.2.6.1). Peptide samples were labelled with isobaric tandem mass tags (TMT) (subsection 3.2.6.2), sample complexity reduced and TMT ratio distortion alleviated using offline pre-fractionation with hSAX liquid chromatography (subsection 3.2.6.3). Full in-depth proteome analysis was performed with LC-MS/MS (subsection 3.2.6.4). For protein identification and quantification, tandem mass spectra were processed with MaxQuant, searched against a protein sequence database based on the whole genome of *Lb. paracasei* susp. *paracasei* TMW 1.1434 (subsection 3.2.6.5). Statistical analysis of proteomic data was performed in R (subsection 3.2.6.6). Thereby, quality control and quality analysis of MaxQuant output was conducted using the automated R-based QC pipeline Protemics Quality Control (‘PTXQC’ package). For generating the whole genome sequence for quantitative proteomics, see section 3.2.2.

Each trial of this work was performed at least using three independent biological replicates (n = 3).

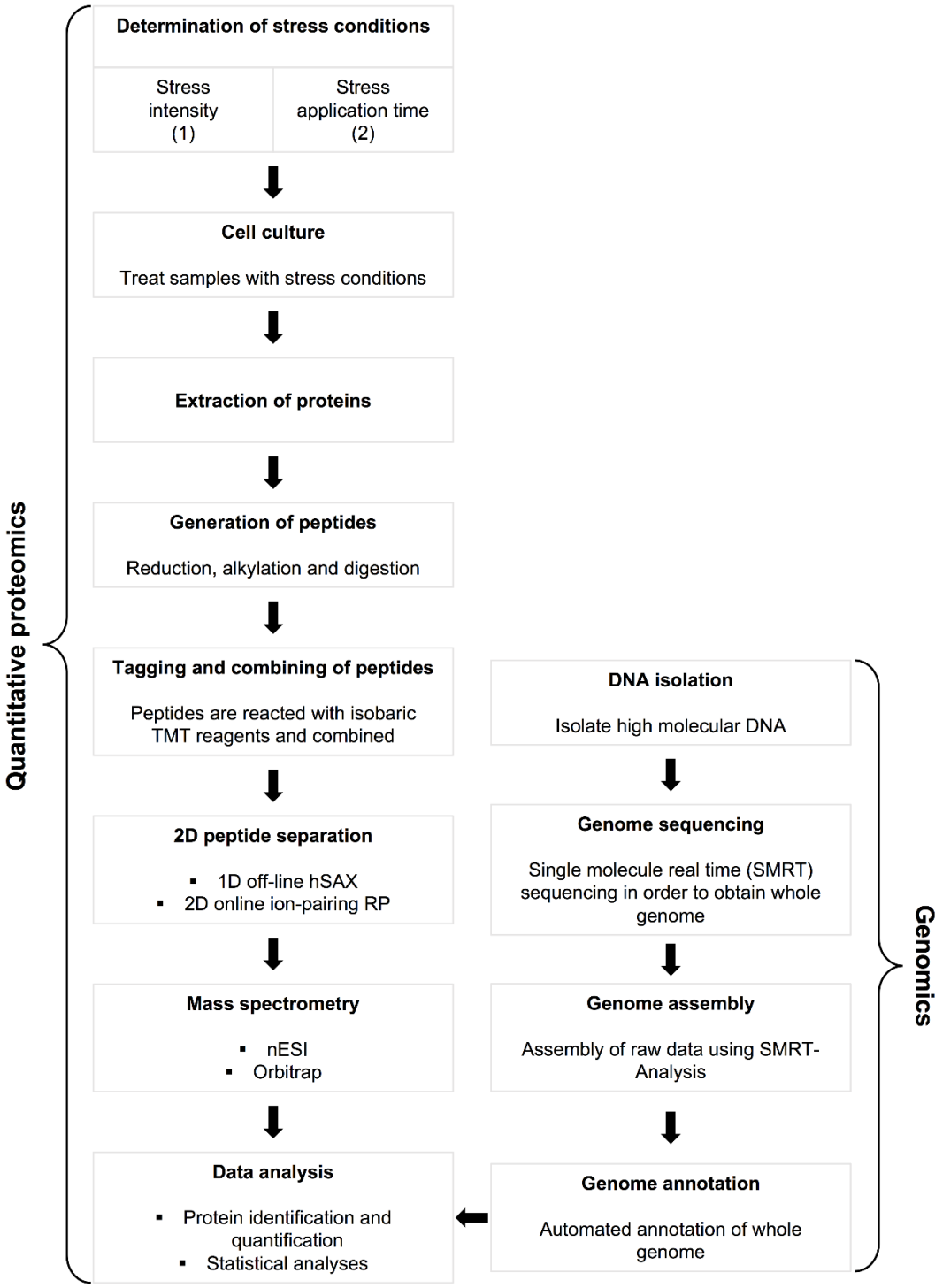


Figure 10: Experimental strategy for the efficient analysis of bacterial stress responses based on genomics and quantitative proteomics using chemical labeling. Note, the analysis of bacterial stress responses is accompanied by the identification of differentially expressed proteins.

### 3.2.2 Establishing a genome for proteomics

In order to have a high quality genome for *in silico* protein prediction and for the consequent mapping of MS data, a complete genome sequence was determined.

#### 3.2.2.1 Isolation of total bacterial DNA

High molecular weight DNA of TMW 1.1434 was isolated using the Genomic-tip 100/G kit (Qiagen, Venlo, Netherlands) according to the manufacture with modifications. Cell lysis was performed with exponentially grown cells and was adapted with respect to lysis time. An exceeded lysis time (16 h maximum) was sufficient for obtaining a clear lysate.

#### 3.2.2.2 Agarose gel electrophoresis

Quantity and quality of isolated DNA was checked using agarose gel electrophoresis (Thermo Fisher Scientific). Nucleic acids were separated based on their size using 1 % gels (agarose in 0.5 x TBE-buffer) and separation was accomplished while applying an electric tension of 100 V in 0.5 x TBE (using an Electrophoresis Power Supply EPS 300, Pharmacia Biotech, Uppsala, Sweden). According to requirements, a 6x Loading Dye and different GeneRuler DNA Ladders (Lambda DNA/EcoRI plus HindIII ladder, 1 Kb Plus DNA Ladder, Thermo Fisher Scientific, Waltham, USA) were used. Visualization was accomplished using dimidium bromide and an UVT-28 M transilluminator (Herolab, Wiesloch, Germany). Pictures were taken with a CCD camera.

#### 3.2.2.3 Genome sequencing

Isolated, high molecular weight DNA was sequenced at GATC Biotech (Konstanz, Germany) via SMRT sequencing [321, 322]. Employing P4-C2 chemistry, a single library was prepared with an insert size of 8 to 12 kb, and more than 200 Mb of raw data were generated from a single SMRT cell.

#### 3.2.2.4 Genome assembly

Assemblage of raw data was performed via SMRT-Analysis software (Version 2.2.0 p2, Pacific Biosciences, Menlo Park, USA), using several Hierarchical Genome Assembly Process (HGAP2/3) protocols [323], which allow the complete shotgun assembly of bacterial sized genomes. Quality of assemblies were checked focusing on several quality criteria, such as subread N50, mean read score, pre-assembly yield, number of contigs, contig N50, coverage and average consensus concordance.

Manual curation of assemblies was mainly executed as recommended and described by PacBio online (https://github.com/PacificBiosciences/Bioinformatics-Training/wiki/Finishing-Bacterial-Genomes). Assembly, which was obtained from the assembly process using the RS_HGAP_Assembly_3 protocol, was stated as polished

assembly (fasta), whereas the assembly obtained from RS_HGAP_Assembly_2 protocol was stated as draft assembly and served as control for the polished assembly. Furthermore, a correct genome assembly was checked with BridgeMapper (RS_BridgeMapper) which is also implemented in SMART-Analysis.

By the implementation of BioPerl (http://www.bioperl.org/) and the Bio::SeqIO system, the polished assembly was split into contigs. Redundancy of contigs were tested using NCBI BLAST [324, 325] and checked for overlapping ends via the dot plot tool of Gepard software [326] and via SMRT-View 2.30 (Pacific Biosciences, Menlo Park, USA) focusing on the mapping quality (polished), since a decrease also indicated overlapping ends. Furthermore, the overlapping ends were examined for conspicuous coverage behavior with SMRT-View 2.30.

Contigs, being redundant or covered by another contig (non-sense), were discarded, while all other contigs with existing overlapping ends were circularized. Circularization of contigs were achieved by the introduction of an *in silico* break into the contig followed by the circularization itself with minimus2 (AMOS, http://amos.sourceforge.net). Subsequently, proper circularization of the resulting contigs were checked using Gepard. In order to confirm that 100 % of the initial sequence information was retained, all circularized contigs were tested using Gepard and NCBI BLAST versus the original contigs.

Subsequently, all circularized contigs, as well as those where circularization was not possible, were merged and were provided as a reference in the resequencing job by SMRT-Analysis using RS-Resequencing_1 protocol. Resequencing was repeated until an average reference consensus accordance of 100 % was accomplished. Quality criteria mentioned above were checked for each resequencing job and finally the consensus sequence of the genome from the last resequencing job was downloaded and stored as fasta-file. This genome fasta file served as input for all consequent genome analysis applications, including submission and annotation.

#### 3.2.2.5 Genome annotation and submission - RAST

Bacterial genome annotation was achieved by submitting the genome to the automated web-based tool RAST (Rapid Annotations using Subsystems Technology) using default settings: classic RAST, RAST as gene caller, automatically fix errors, backfill gaps [327-329]. RAST identifies open reading frames (orf) and uses the subsystems in the SEED database to provide a rapid annotation of the assembly. RAST additionally provides metabolic reconstruction and gene function of the bacterial genome. RAST annotation was completed using RAST2BADGE in order to become ‘human-readable’ and

informative [330]. No manual curation was performed. Single annotations were checked using NCBI blastp [324, 325] in cases of relevance for specific analyses.

#### 3.2.2.6 Genome annotation and submission – NCBI

Bacterial genome annotation was also conducted by submitting the genome to the NCBI Prokaryotic Genome Annotation Pipeline (https://www.ncbi.nlm.nih.gov/genome/annotation_prok/) [331]. NCBI Prokaryotic Genome Annotation Pipeline combines ab initio gene prediction algorithms with homology based methods. Protein-coding genes and other functional genome units such as structural RNAs, tRNAs, small RNAs, pseudogenes, control regions, direct and inverted repeats, insertion sequences, transposons, and other mobile elements are predicted and the genome annotated. Locus tags and protein IDs are automatically provided. Genome was submitted to GenBank as described online in detail (https://www.ncbi.nlm.nih.gov/genbank/genomesubmit/) [332, 333].

#### 3.2.2.7 Genomic properties

General genomic properties (size and nucleotide composition, GC content, coding density etc.) were extracted using in-house Bash tools and biotools for comparative microbial genomics (CMG biotools) [334]. Subcellular localization of proteins was predicted utilizing the tool PSORTb (Version 3.0.2, http://www.psort.org/psortb/) [335-337].

#### 3.2.2.8 Subcellular localization prediction, functional analysis and metabolic reconstruction

Subcellular localization of proteins was predicted utilizing the tool PSORTb (Version 3.0.2, http://www.psort.org/psortb/) [332, 333].

Functional analysis and metabolic reconstruction of the genome were performed including the annotation of biological functions, the functional classification and the metabolic potential.

Annotation of biological functions was accomplished using SEED categorization based on RAST and the SEED subsystem analysis (Subsystem and FIGfams Technology) [327, 329]. The SEED subsystem analysis enables the assignment of predicted genes to a hierarchical three-level categorization system (category, subcategory, subsystem), whereby they can be assigned to several subsystems.

Metabolic potential was analyzed using the Kyoto Encyclopedia of Genes and Genomes (KEGG) mapper [338-340] and checked by NCBI BLASTp analysis [324, 325]. KEGG links the genome to metabolic pathways (metabolic reconstruction) using EC numbers.

Resulting metabolic networks were exported and visualized using the KEGG mapper [340, 341].

### 3.2.3 Selection of stress conditions

#### 3.2.3.1 Procedure

In order to investigate and compare several proteomic stress responses evoked by different stressors, stress conditions need to be determined having comparable sublethal influence on the microorganism's physiology. Therefore, stress conditions were specified as the combination of a stress intensity tolerance (subsection 3.2.3.3) and a stress application time tolerance (subsection 3.2.3.4) of *Lb. paracasei* subsp. *paracasei* TMW 1.1434, as previously described by Schott et al. [320] and Schurr et al. [342].

For the purpose of stress intensity tolerance determination, growth challenge experiments with TMW 1.1434 under various different stress qualities were performed and inhibitory concentration (IC) identified. In case of high hydrostatic pressure (HHP) stress, the experimental approach was not applicable. As long-term application of high hydrostatic pressure is not feasible, high hydrostatic pressure was applied in this study as short-term pressure shock having mild sublethal pressure stress conditions. A mild sublethal pressure condition (MSPC) was identified that can be analogously used to IC (subsection 3.2.3.3). Subsequently, for the determination of the stress application time tolerance, IC and MSPC were exploited, kinetics of stress responses profiled using MALDI-TOF MS and stress application time determined ($T_{max}$) (subsection 3.2.3.4).

#### 3.2.3.2 Stress media

Stress media for the determination of the stress conditions was prepared on the basis of Spicher[1] and are listed in Table 7. Medium additives of the respective stress compound/parameter are listed in Table 6.

Table 7: Stress applied in growth challenge experiments. The aimed stress quality, the used basic medium and the stress compound/parameter are listed with the tested intensity range for the respective compound/parameter. Regarding high hydrostatic pressure (HHP) stress, a recovery phase in Spicher[1] was attached (*) and is yet, for simplification, further discussed as stress quality. In order to simulate the drying process during starter culture preparation, drying stress (°) was prepared according to Flessa [66].

| Stress quality | Basic medium / condition | Compound / Parameter (Additive X) | Concentration / Intensity range |
|---|---|---|---|
| **Acid stress** | Spicher[1] | pH adjusted with HCl | pH 3 - 6 |
| **Alkaline stress** | Spicher[1] | pH adjusted with NaOH | pH 6 - 10 |
| **Cold stress** | Spicher[1] | Incubation at low temperature | 5 - 30 °C |
| **Lack of glucose** | Spicher[1] | Spicher[1] without10 glucose | 0 - 100 % of Spicher[1] |
| **Heat stress** | Spicher[1] | Incubation at high temperature | 30 - 60 °C |
| **Osmotic stress** | Spicher[1] | KCl | 0 - 2 M |
| **Osmotic stress** | Spicher[1] | NaCl | 0 - 2 M |
| **Osmotic stress** | Spicher[1] | lac | 0 - 0.6 M |
| **Osmotic stress** | Spicher[1] | suc | 0 - 5.8 M |
| **Oxidative stress** | Spicher[1] | $H_2O_2$ | 0 - 2 mM |
| **HHP stress*** | IPB, 37 °C | HHP treatment with attached recovery phase* in Spicher[1] | 0 - 400 MPa (50 MPa steps); 0 - 600 s; 0- 240* min (30 min steps) |
| **Drying stress°** | Ultra pure water | Exposed to drying at room temperature | 0 – 120 min° (30 min steps) |

### 3.2.3.3 Determination of stress intensity tolerances

#### 3.2.3.3.1 Methods to determine bacterial growth and cell count

*Total count - Turbidity test*

The total bacterial population in a sample is estimated by applying the physical method of turbidity measurement.

Cell suspensions start to get turbid at concentrations of $10^7$ cells/ml. This turbidity (= optical density, OD) is caused by the absorbance, reflection and scattering of light by cells and can be measured using a photometer. Within a specific measurement range

(usually OD < 0.4), the cell density of vegetative growing cells is proportional to the measured absorbance [343]. Samples approaching this critical OD require a dilution prior measurement.

In this study, growth in the presence of stress, with exceptions, was primarily detected by turbidity measuring the OD at λ = 600 nm. Growth curves were ascertained by utilizing a spectrophotometer Novaspec II (Pharmacia Biotech, Uppsala, Sweden) or a Tecan Sunrise Plate Reader (Männedorf, Switzerland).

*Viable count - Plate count test*

The number of viable counts of a bacterial population in a sample is estimated by applying the biological method of plate counting.

A viable count assumes that a visible colony will develop from each organism. However, bacteria are rarely separated entirely from their fellows and are often clumped together in large numbers. Therefore, a single colony could develop from one organism or from hundreds or even thousands of organisms. Thus, each colony developing is assumed to have grown from one viable unit, which may be one organism. Viable counts are usually given as numbers of colony-forming units (CFU).

In this study, 0.8 ml of cells were diluted with $TS^+$ buffer (14 g/l triptone, 8.5 g/l NaCl, 0.1 ml/l antifoam B) 1:1 and plated on Spicher[1] agar. Incubation was performed at 37 °C for 48 h and CFU were counted.

Details regarding procedure and subsequent analysis can be found in subsection 3.2.3.3.

#### 3.2.3.3.2 Growth under stress

Growth challenge experiments were performed using a standard preculture. Stress was applied in form of stress media (Table 7, subsection ‘Stress qualities’) or high hydrostatic pressure (subsection ‘High hydrostatic pressure’). Bacterial growth and cell count were determined using turbidity and plate count tests. Turbidity tests for total cell count (subsection 3.2.3.3.1) were respectively conducted for pH, osmotic, oxidative and temperature stress (referred to ‘stress qualities’ in the following) and ICs identified (subsection 3.2.3.3.3).The turbidity test is not applicable for growth challenge experiments under high hydrostatic pressure stress due to experimental limitations. Thus, HHP growth challenge experiments were performed using plate count tests for viable cell count (subsection 3.2.3.3.1) and MSPC identified, which can be analogously used to IC (subsection 3.2.3.3.3).

*Stress qualities*

Growth challenge experiments were carried out in batch culture at an initial pH of 5.4 and turbidity tests were performed to determine bacterial growth under stress. Note that in case of pH stress, the initial pH relies on the applied stress intensity and thus media.

Growth challenge experiments were generally performed in microtiter plates filled with stress media. At this, an intensity gradient based on gradient steps of the stress compound/parameter was prepared using a pipette robot, RoboSeq® 4204S (MWG Biotech AG, Ebersberg, Germany). This pipette robot filled each well with a final volume of 200 µl. A gradient from 0 % of the maximum concentration of the additive X (Spicher[1], control) to 100 %, in 10 % steps, was created. Tested stress media including compounds/parameter and the respective minimal/maximal concentration/intensity are listed in Table 7.

Standard preculture was harvested by centrifugation, washed twice with phosphate buffer (0.1 M $K_2HPO_4/KH_2PO_4$ with 0.1 M NaCl; pH 7.0) and suspended in Spicher[1] to an $OD_{600}$ of 3. Wells were inoculated with 20 µl of this cell suspension to an initial $OD_{600}$ of 0.3 and overlaid with 75 µl of paraffin oil. Bacterial cell growth at 37 °C was measured at λ = 600 nm to stationary phase using an automated microtiter plate reader (Tecan Sunrise Plate Reader, Männerdorf, Switzerland).

However, due to experimental limitations, growth challenge experiments applying temperature stress was carried out in reaction tubes. Standard preculture was harvested, washed and suspended as described above. 9 ml Spicher[1] were inoculated with 1 ml of this cell suspension to an initial $OD_{600}$ of 0.3 and incubated at intended temperatures in 5 °C temperature steps (Table 7). Growth was monitored at λ = 600 nm to stationary phase via spectrophotometer (Novaspec II, Amersham Biosciences, Freiburg, Germany). The test was as well performed in control condition (basic Spicher[1], 37 °C).

For details regarding the statistical analysis of growth parameters of the obtained growth curves, see subsection 3.2.3.3.3.

*High hydrostatic pressure stress*

HHP stress growth challenge experiments were performed in cryovials in a dual vessel high pressure unit (TMW-RB; Knam Schneidetechnik, Germany), as described by Lenz et al. [344, 345].

Mild sublethal pressure stress conditions are defined as one log reduction of colony forming units (CFU) which are achieved by the combination of a target pressure level with a target pressure holding time. In order to identify MSPC, HHP stress growth challenge experiments were executed varying in pressure level and pressure holding

time. At first, HHP treatments were performed at different pressure levels in order to identify the target pressure level. Cells were pressure treated at 37 °C for 60 s at various pressure levels (50-400 MPa, 50 MPa steps), CFU were determined and the target pressure level identified. Subsequently, the target pressure level was exploited and implemented in following HHP treatments, in which pressure holding time was varied. At this, cells were pressure treated at 37 °C for various pressure holding times (1-600 s) at the target pressure level, CFU were determined and the target pressure holding time identified. Tested compounds/parameter and the respective minimal/maximal concentration/intensity are listed and marked (*) in Table 7.

HHP treatment: A standard preculture was harvested by centrifugation, washed twice with phosphate buffer (0.1 M $K_2HPO_4/KH_2PO_4$ with 0.15 M NaCl; pH 7.0) and suspended in Spicher[1] to an $OD_{600}$ of 3, respectively. 9 ml Spicher[1] were inoculated with 1 ml of this cell suspension to an initial $OD_{600}$ of 0.3 and again incubated at 37 °C until stationary phase, in order to obtain high cell concentration. Afterwards, cells were harvested by centrifugation and suspended in 50 mM imidazole phosphate buffer (IPB; 50 mM potassium dihydrogen phosphate, 50 mM disodium hydrogen phosphate dihydrate, 50 mM imidazole, pH 7). Control sample was taken prior to HHP treatments. CFU of untreated and pressure treated cells were determined (3.2.3.3.1), statistically analyzed and MSPC identified (3.2.3.3.3).

#### 3.2.3.3.3 Analysis of growth challenge experiments

*Growth curve analysis*

Raw data based on $OD_{600}$ (growth curves) were evaluated using groFit ('grofit' package) for R which provides the calculation of several growth parameters including the duration of the lag phase (λ), the integral area, the maximal reached optical density ($OD_{max}$) and the maximum specific growth rate ($\mu_{max}$) [346]. Most important parameters, such as $OD_{max}$, λ and $\mu_{max}$ were extracted, whereby normalization for comparison was conducted for the last two. The effects of stress (quality and intensity) on growth were determined by comparing $\mu_{max}$ of control conditions with $\mu_{max}$ in the presence of stress. For all stress qualities, respectively, this was achieved by providing a dose response curve, which plots $\mu_{max}$, in control condition and in the presence of stress, versus the stress intensity. Using the dose response curve, the half maximal effective concentration (EC50), which refers to an intensity/concentration of a compound/parameter where 50 % of $\mu_{max}$ of control condition is achieved, was calculated. Exploiting EC50, the inhibitory concentration (IC) is identified by choosing the intensity/concentration that is closest to EC50 (less than or equal in response), in respect to $OD_{max}$ and λ. IC was cross-checked

with the definition of SSC by Sanders et al. who described them as the reduction of the growth rate $\mu_{stress}$ to one tenth of the maximal growth rate $\mu_{max}$ [347].

*CFU determination*

Raw data based on CFU was evaluated using SigmaPlot (Systat Software, San Jose, USA) and visualized using Microsoft Excel (Microsoft, Redmond, USA).

At first, dependent variable significance of sample/groups (pressure level or pressure holding time) was checked using ANOVA, followed by the calculation of differences (similarities) between sample/groups using the Tukey Honest Significance Difference (HSD) correction in order to proof statistical significance (p-value < 0.05).

Target pressure values (target pressure level and target pressure holding time) were determined by choosing HHP conditions displaying a significant reduction of 0.5- 1 log10(CFU/ml), respectively.

#### 3.2.3.4 Determination of stress application time tolerances

##### 3.2.3.4.1 Proteomic-based approach for profiling stress responses

The stress application time tolerance was determined while investigating kinetics of stress responses. Stress response were profiled using MALDI-TOF MS, which enables the examination of stress responses on proteome level focusing on low molecular weight (lmw) proteins in a range of 2 kDa to 20 kDa (section 3.2.4).

In order to determine stress application time tolerances, cells were subjected to previously identified stress intensity tolerances (subsection 3.2.3.3), respectively, with varying application times. Identified stress intensity tolerances, on basis of SSC and MSPC, are listed in Table 14.

The sample preparation is described in the following. A standard preculture was harvested by centrifugation, washed twice with phosphate buffer (0.1 M $K_2HPO_4/KH_2PO_4$ with 0.15 M NaCl; pH 7.0) and suspended in Spicher[1] to an $OD_{600}$ of 3, respectively. 9 ml Spicher[1] were inoculated with 1 ml of this cell suspension to an initial $OD_{600}$ of 0.3, and incubated in control condition (basic Spicher[1], 37 °C) to mid exponential phase. Control sample was taken prior subjection to stress intensity tolerances. Subsequently, with the exception of HHP treatment, cells were harvested and suspended in 9 ml IC media (Table 14). Unless otherwise stated, stress sampling was conducted regularly every 30 min over a period of 2 h incubation period. HHP treatment was carried out as described in subsection 3.2.3.3.3.Cells were HHP treated using the identified MSPC at 37°C. After HHP treatment, pressure treated cells were transferred in Spicher[1] for recovery. Stress sampling was done regularly every 30 min during a 4 h recovery period.

Additionally, drying stress was investigated. Since the approach for determining stress intensity tolerance was not applicable, drying stress was applied according to Flessa with minor modifications [66]. Therefore, a standard preculture was harvested, washed twice with phosphate buffer and suspended in Spicher[1] to an $OD_{600}$ of 3, as described above. Cells were incubated in control condition (basic Spicher[1], 37 °C) to mid exponential phase, harvested again and suspended in water. Prior subjection to drying stress, control sample was taken. Subsequently, 30 µl of cell suspension was spot inoculated onto 20 mm x 20 mm glass coverslips (Sigma-Aldrich), which were stored under a biological hood with the fan running at 24 °C ±1 °C for up to 2 h. Stress sampling was done regularly every 30 min during a 2 h drying period. Control and stress samples were placed into 50 ml reaction tubes and suspended in 10 ml of ethanol (70 v/v %), respectively. Cells were detached from the glass coverslips by sonication (5 min; Bandelin electronic GmbH & Co. KG, Berlin, Germany).

Obtained control and stress samples were analyzed using MALDI-TOF MS protein profiling (section 3.2.4).

### 3.2.4 MALDI-TOF MS

#### 3.2.4.1 Sample preparation

Two different sample preparation methods were applied, as described by Kern et al. [348], and are specified below.

For species identification, the direct transfer method utilizing cell smear (CS) was sufficient. Therefore, single colonies were picked from agar plates and the cell material was evenly smeared directly onto a stainless steel target (Bruker Daltonics, Bremen, Germany). The sample position (= spot) was overlaid with HCCA matrix solution (Bruker Daltonics, Bremen, Germany) and samples were air dried prior measurement.

For stress response profiling, high quality mass spectra were required and the plain cell extraction (CE) method was carried out. Therefore, gathered samples were harvested by centrifugation and supernatant was disposed. Inactivation of cells was achieved by resuspending in 1 ml ethanol (70 v/v %) and proteins extracted adding formic acid, water and acetonitrile (HPLC grade; 35:15:50, v/v %). 1 µl of the extract was transferred onto the target, spots were overlaid with HCCA matrix solution and samples were air dried prior measurement.

#### 3.2.4.2 MALDI-TOF MS analysis

Mass spectra were obtained by a Microflex LT MALDI-TOF mass spectrometer (Bruker Daltonics, Bremen, Germany) which was equipped with a nitrogen laser (lambda = 337 nm) operating with a linear positive ion detection mode under Biotyper Automation

Control 2.0 (Bruker Daltonics, Bremen, Germany). If not stated otherwise, the mass spectra (in a range from mass range 2,000-20,000 Da) of 400 laser shots was accumulated to create sum spectra. A bacterial standard was obtained from Bruker Daltonics (Bremen, Germany) and used for external mass calibration [348].

Species identification is described in subsection 3.2.4.3, while processing of stress response profiles can be obtained from subsection 3.2.4.4.

#### 3.2.4.3 Species identification

Species identification was performed using the MALDI-Biotyper 3 (Bruker Daltonics, Bremen, Germany) featuring a database of microbial reference spectra provided by the manufacturer. Each isolate, obtained either by CS or by CE method, was checked for correct species assignment before cryo conservation and after reconstitution from cryo cultures.

#### 3.2.4.4 Data export and processing

MALDI-TOF mass spectra of stress responses were exported and processed according to Kern et al. [349].

Briefly, raw data were exported with FlexAnalysis 3.3 (Bruker Daltonics, Bremen, Germany). Peak processing, detection and alignment were performed as described by Mantini et al. [350] with a limit of distance tolerance set to 600 ppm for alignment and clustering of peaks. Peaks were processed using a MASCAP [350] based software utilizing GNU octave (www.octave.org) [351, 352]. For this purpose, MALDI-TOF mass spectra were checked for differences with a minimum accepted peak detection rate of 0.4, excluding all peaks absent in 60 % of the analyzed spectra. Lowest accepted peak intensity was set to 50 % of a respective peak's average and a limit of 20 % standard deviation was defined for signal intensity. Peaks were picked showing the highest intensity among their nearest points. Subsequently, processed spectra (protein expression profiles) were analyzed using cluster analysis and discriminant analysis of principle components, and stress application time tolerances determined (subsection 3.2.4.5).

#### 3.2.4.5 Bioinformatic data analyses

Statistical data analyses of proteomic data were carried out using the 'adegenet' package for R software (Version 3.3.2, http://www.r-project.org/).

#### 3.2.4.6 Cluster analysis

Peak-based cluster analysis was carried out to investigate kinetics of stress responses, to determine a specific time point when the expression of lmw stress proteins reached

its maximum ($T_{Max}$), and thus to identify stress application time tolerances. For this purpose, hierarchical cluster analysis was performed using the function 'hclust' ('adegenet' package). A heat map with dendrogram was created, first calculating the distance matrix, using the method 'manhattan_bc', and then using the function 'hclust' combined with the cluster method 'complete linkage' for plotting.

### 3.2.5 Stress treatment

Stress treatments were carried out as described by Schott et al. [320].

A standard preculture was harvested by centrifugation, washed twice with phosphate buffer (0.1 M $K_2HPO_4$/$KH_2PO_4$ with 0.15 M NaCl; pH 7.0) and suspended in Spicher[1] to a final volume of 50 ml, respectively. Cell suspension was incubated in control condition (basic Spicher[1], 37 °C) to mid exponential phase. Prior stress treatment, a control sample was taken. Subsequently, cell suspension was harvested and subjected to stress treatment based on identified stress conditions. The control (untreated) and stress (treated) samples were prepared in biological triplicates and applied to sample preparation for proteomic analysis.

### 3.2.6 Mass spectrometry-based proteomics

#### 3.2.6.1 Sample preparation

Cell samples for proteomic analysis were washed twice in TBS buffer (50 mM Tris, 150 mM NaCl, pH 7.5), reconstituted in lysis buffer (8 M urea, 50 mM TEAB, 1x protease inhibitor SigmaFast) and mechanically disrupted by passing them three times through a French Press at 275 MPa (HTU DIGI-F-Press, Modell F-013, G. Heinemann Ultraschall- und Labortechnik, Schwäbisch Gmünd, Germany). Total protein concentration of the whole cell lysate was determined using the Bradford method (Bio-Rad Protein Assay, Bio-Rad Laboratories GmbH, Munich, Germany). 200 µg of protein from the whole cell lysate were used for in-solution digestion. Protein was reduced with 1 M DTT (1:100 v/v, final concentration 10 mM DTT) at 56 °C for 45 min and subsequently alkylated with iodoacetamide (1:10 v/v, final concentration 50 mM IAA) at room temperature for 60 min. Reduced protein was digested overnight at 37 °C using 2 µg trypsin. Digested peptides were desalted according to the manufacturer's instructions by $C_{18}$ solid phase extraction using stop and go extraction tips ($C_{18}$-Stage Tips) [353]. Lately, the samples were frozen at -80°C and dried completely in a speed vac.

#### 3.2.6.2 Chemical labeling for MS2-based quantification

Lyophilized peptides (200 µg) were reconstituted in 50 mM TEAB to a concentration of 1.25 µg/µl peptide. Further, to allow accurate quantification of differences in abundance

levels between different treatments, appropriate amounts of each peptide sample (including biological triplicates) was pooled to a peptide mix that served as internal standard (IS).

Internal standard and peptide samples were chemically labelled with the TMT10plex™ Isobaric Label Reagent Set according to the instructions of the supplier (Thermo Fisher Scientific). Briefly, TMT stock was prepared by adding 25.6 µl anhydrous ACN to 0.5 mg TMT. Labeling was carried out by adding 10 µl TMT stock solution to 50 µg of peptide followed by the incubation for 1 hour at 20 °C. The labeling reaction was quenched with the addition of 4 µl of 5 % hydroxylamine (final concentration ~0.2 %) and the subsequent incubation for 15 min at 20 °C. The TMT labeling pattern is presented in Table 8.

Table 8: TMT labeling pattern of all samples with respect to TMT tag and LC-MS/MS mixture for quantitative proteomics. Samples are named according to applied stress treatment, whereby stress IDs can be found in Table 1. Biological triplicates are displayed in consecutive numbering (_1 - _3). Further internal standards (IS) are presented. TMT-labeled samples are combined by row to five LC-MS/MS mixtures (#1-#5).

| | | **TMT10™-Label Reagent** | | | | | | | | | |
|---|---|---|---|---|---|---|---|---|---|---|---|
| | | **126** | **127N** | **127C** | **128N** | **128C** | **129N** | **129C** | **130N** | **130C** | **131** |
| **LC-MS/MS mixture** | #1 | IS | IS | contr_1 | glu10_1 | 15C_1 | 45C_1 | D_1 | pH4_1 | pH9_1 | HHP_1 |
| | #2 | IS | IS | H2O2_1 | NaCl_1 | KCl_1 | lac_1 | suc_1 | contr_2 | glu10_2 | 15C_2 |
| | #3 | IS | IS | 45C_2 | D_2 | pH4_2 | pH9_2 | HHP_2 | H2O2_2 | NaCl_2 | KCl_2 |
| | #4 | IS | IS | lac_2 | suc_2 | contr_3 | glu10_3 | 15C_3 | 45C_3 | D_3 | pH4_3 |
| | #5 | IS | IS | pH9_3 | HHP_3 | H2O2_3 | NaCl_3 | KCl_3 | lac_3 | suc_3 | blank |

For correcting potential sample loss and varying labeling efficiency, a labeling test was carried out by measuring defined mixtures by LC-MS/MS (LC-MMS/MS mixtures), as indicated in Table 8. Samples were then mixed in equimolar ratios according to TMT labeling pattern for proteomic analysis, again desalted using $C_{18}$-Stage Tips and reconstituted in 50 µl 5 mM Tris-HCl (pH 8.5; hSAX solvent A) prior to fist dimension peptide separation.

#### 3.2.6.3 First dimension peptide separation (hSAX)

First dimension peptide separation was performed at the institute of Proteomics and Bioanalytics (Technische Universität München, Freising, Germany) using offline liquid chromatography.

For full proteome analysis, peptide separation based on hydrophilic strong anion exchange (hSAX) was performed using a Dionex Ultimate 3000 LC system (Thermo Scientific, Bremen, Germany) which was equipped with an IonPac AG24 guard column (2 mm I.D. x 50 mm, Thermo Fisher Scientific) and an IonPac AS24 SAX-column (2 mm I.D. x 250 mm, Thermo Fisher Scientific). The system was operating at 25 °C with a flow rate of 250 µl/min and an initial equilibration step with 100 % hSAX solvent A (5 mM Tris-HCl, pH 8.5) followed by elution with a linear 24 min gradient up to 25 % hSAX solvent B (5 mM Tris-HCl pH 8.5, 1 M NaCl). hSAX solvent B was increased to 100 % in 13 min and held constant for 4 min. Subsequently, a switch to 100 % hSAX solvent A in 1 min was followed by column re-equilibration with 100 % hSAX solvent A for 10 min. 24 fractions were collected starting from 2 min to 40 min, desalted using $C_{18}$-Stage Tips, and reconstituted in 20 µl 0.1 % formic acid (FA) prior liquid chromatography tandem mass spectrometry (LC-MS/MS) analysis.

#### 3.2.6.4 LC-nESI-MS/MS

The analysis of full proteome fractions was performed at the institute of Proteomics and Bioanalytics (Technische Universität München, Freising, Germany).

Detailed LC-MS/MS parameters can be found in Table 9.

Briefly, LC-MS/MS analysis was carried out by coupling an UltiMate 3000 nano LC system (Thermo Scientific, Bremen, Germany) to a Q Exactive HF (Thermo Scientific, Bremen, Germany). Online second dimension peptide separation was conducted applying nanoflow ion-pairing reversed-phase (RPIP) chromatography. Peptides were transported to a trap column (100 µm I.D. x 2 cm, ReproSil-Pur C18-AQ, 5 µm, Dr. Maisch, Ammerbuch, Germany) for 10 min at a flow rate of 5 µl/min in loading solvent (0.1 % FA in HPLC grade water). For separation, peptides were then transferred and loaded onto an analytical column (75 µm I.D. x 40 cm, ReproSil-Pur C18-AQ, 3 µm, Dr. Maisch, Ammerbuch, Germany) using a 120 min gradient at a flow rate of 300 nl/min (solvent A: 0.1 % FA, 5 % DMSO in HPLC grade water; solvent B: 0.1 % FA, 5 % DMSO in ACN) (0 min: 2 % B; 11 min: 4 % B; 112 min: 32 % B; 114 min: 80 % B; 118 min: 2 % B). The ionization of the resulting peptides was conducted at a capillary temperature of 275 °C using 2.2 kV ion spray voltage. The mass spectrometer operated in data dependent acquisition mode, automatically switching between MS1 and MS2. Full scan MS1 spectra (360-1300 m/z) were acquired in the Orbitrap for a maximum ion

injection time of 50 ms at 60,000 resolution and an automatic gain control (AGC) target value of 3e6. Up to 25 precursor ions were allowed to be selected for fragmentation, whereby isolation window was set to 1.3 m/z, normalized collision energy (NCE) to 33 % and the underfill ratio to 1 % with a dynamic exclusion of 20 s. MS2 spectra (200-2000 m/z) were acquired in the Orbitrap mass analyzer at a resolution of 30,000 and an AGC target value of 2e5 with a maximum ion injection time of 57 ms.

Table 9: MS parameters.

| **MS parameters** | | **Full Proteome**<br>**Q Exactive HF** |
|---|---|---|
| **Ionization** | Spray Voltage | 2.2 kV |
| | Capillary Temperature | 275 °C |
| **Global Settings** | Method duration | 120 min |
| **General Full MS / dd-MS2 (TOPN)** | Runtime | 10 to 120 min |
| | Default charge state | 2 |
| **Full MS** | Resolution | 60,000 |
| | AGC target | 3.00E+06 |
| | Maximum injection time (IT) | 50 ms |
| | Scan range | 360 to 1300 m/z |
| **dd-MS2 / dd-SIM** | Resolution | 30,000 |
| | AGC target | 2.0E+05 |
| | Maximum IT | 57 ms |
| | Loop count | 25 |
| | MSX count | 1 |
| | TopN | 25 |
| | Isolation window | 1.3 m/z |

| | | |
|---|---|---|
| | Isolation offset | 0.0 m/z |
| | Fragmentation | HCD |
| | Scan range | 200 to 2000 m/z |
| | Fixed first mass | 120.0 m/z |
| | NCE / stepped NCE | 33% |
| **dd Settings** | Underfill ratio | 1.0% |
| | Intensity threshold | 3.5E+04 |
| | Exclude isotopes | on |
| | Dynamic exclusion | 20.0 s |
| **LC system** | Type | UltiMate 3000 nano LC system |
| | HPLC solvent A | 0.1 % FA, 5 % DMSO in dd$H_2O$ |
| | HPLC solvent B | 0.1 % FA, 5 % DMSO in ACN |
| | Gradient length | 120 min |
| | Gradient | 0 min: 2 % B; 11 min: 4 % B; 112 min: 32 % B; 114 min: 80 % B; 118 min: 2 % B |

#### 3.2.6.5 Peptide and protein identification and quantification

For protein identification and quantification, raw files (MS/MS data) were analyzed at the Bavarian Center for Biomolecular Mass Spectrometry (Technische Universität München, Freising, Germany) using MaxQuant (Version 1.5.5.2, http://www.coxdocs.org/doku.php?id=:maxquant:start) and the integrated search engine Andromeda. Raw files of full proteome fractions were searched against the strain-specific database composed of the *in silico* proteome of *Lb. paracasei* susp. *paracasei* TMW 1.1434 (2938 entries) and common contaminant proteins. Carbamidomethylate cysteine was set as fixed modifications, and oxidation of methionine was allowed as variable modification with maximal 5 modifications per peptide. Proteolytic enzyme was set to trypsin/P with cleavage after proline to account for quantification, whereby two missed cleavage sites were allowed. Minimum peptide length was set to seven amino acids. Quantification was performed on reporter ion MS2 using the isobaric label set

TMT10plex with a reporter mass tolerance of 0.01 Da. The mass tolerance was set to 4.5 ppm for precursor ions and to 20 ppm for fragment ions. For peptide and protein identification, peptide spectrum matches (PSM) FDR, protein False Discovery Rate (FDR) and site decoy fraction filtering were set to 1 %, 5 % and 1 %, respectively. The minimum number of total peptides a protein group should have to be considered as identified is adjusted to one. Further, second peptides, Match-between-runs (MBR) with a match time window of 0.7 min and an alignment time window of 20 min and dependent peptides with FDR of 1 % and mass tolerance (mass bin size) of 0.0065 Da were enabled. For protein quantification, minimum ratio count for protein quantification was set to one, unique and razor peptides were used for quantification, whereby unmodified and modified peptides (oxidized methionine) were used for quantification.

Data were further processed using Microsoft Excel and the R statistical programming environment (see below).

#### 3.2.6.6 Bioinformatic data analyses and visualization

Statistical data analyses of proteomic data were carried out using R software (Version 3.3.2, http://www.r-project.org/) and Excel (Microsoft, Redmond, USA).

Quality control (QC) and quality analysis of MaxQuant output was conducted using the automated R-based QC pipeline Proteomics Quality Control (‘PTXQC’ package) [354]. PTXQC analyzes measurement bias, consistency and error by creating a QC report containing a set of QC metrics that are augmented with automated scoring functions. The automated scores are summarized in an overview heatmap providing a quality rating of the MaxQuant output ranging from “fail” over “under performing” to “best”. PTXQC was executed, whereby PTXQC settings can be found in Table 10.

Table 10: PTXQC settings.

| PTXQC settings | |
|---|---|
| **Parameters** | enabled |
| **Summary** | enabled |
| **IDRate: Thresh_bad_num** | 20 |
| **IDRate: Thresh_great_num** | 35 |
| **ProteinGroups** | enabled |
| **RatioPlot: LabelIncThresh_num** | 4 |
| **RatioPlot: IntensityThreshLog2_num** | 25 |
| **Evidence** | enabled |
| **ProteinCountThresh_num** | 500 |
| **IntensityThreshLog2_num** | 25 |
| **PeptideCountThresh_num** | 1500 |
| **SpecialContaminants** | no |
| **MQpar_MatchingTimeWindow_num** | 1 |
| **MatchBetweenRuns_wA** | auto |
| **MQpar_firstSearchTol_num** | 20 |
| **firstSearch_outOfCalWarnSD_num** | 2 |
| **MQpar_mainSearchTol_num** | .na |
| **MsMs** | enabled |
| **MsMsScans** | enabled |
| **IonInjectionThresh_num** | 57 |

An automatic analysis of the proteomic data was achieved applying a self-constructed bioinformatic R script using various R packages. The R script is provided in Supplementary Part I (I.2.1) and is subsequently described in detail. Proteomic data, on the basis of identified protein groups and respective reporter intensities (RI), were filtered, whereby contaminants, reverse and only identified by site proteins were excluded. Further, proteins with at least seven missing RI values across all samples were excluded from analysis. To reduce technical and experimental variations, normalization to the internal standard was conducted across all TMT channels and across all TMT experiments using Microsoft Excel, followed by normalization using the function 'CountDataSet' ('DESeq' package) [353]. Subsequently, proteomic data was log2-transformed. Since the data were log- normally distributed, we used MANOVA for checking dependent variable significance of quantified proteins. Tukey Honest Significance Difference (HSD) correction was performed to proof statistical significance over the groups (p-value < 0.05) followed by the calculation of Log2FoldChange (FC) of proteins in any condition. Proteins displaying large magnitude changes within a defined cutoff (allocated in the 5 % bottom and top edge of the extreme) were classified as differentially expressed proteins and visualized in volcano plots ('gplot' package).

Fisher's exact test, which uses the analysis of contingency table, was performed applying the function 'fisher.test' ('stats' package) in order to assess the influence of stress on protein expression. Thereby, the null hypothesis of independence is tested for two nominal variables (expressed and differentially expressed proteins). Resulting p-values < 0.05 indicate the rejection of the null hypothesis and thus indicate significant difference.

Hierarchical cluster analysis was performed using the function 'heatmap.2' ('gplot' package) in order to detect stress response similarities. Thereby, a heat map with dendrogram was created, first calculating the Minkowski distance of a matrix and then using the function 'hclust' combined with the cluster method 'average' for plotting.

Protein expression analysis was computed based on the calculation of clustered heat maps using the function 'pheatmap' ('pheatmap' package). First, cluster analysis was performed calculating the Euclidean distance and then using the function 'hclust' combined with the cluster method 'complete' for plotting.

Proteomic distribution of differentially expressed proteins was visualized using BLAST ring image generator (BRIG) [355]. Further, visualization of shared differentially expressed proteins was achieved in venn diagrams using VennMaster (Version 0.38.2, http://sysbio.uni-ulm.de/?Software:VennMaster).

# 4 Results

## 4.1 Genomics

### 4.1.1 Genome sequencing

Whole genome sequencing of *Lactobacillus paracasei* subsp. *paracasei* F19 was performed. The genome was sequenced using SMRT sequencing [321, 322] assembled via SMRT-Analysis (Pacific Biosciences, Menlo Park, USA) and annotated with RAST and NCBI annotation pipeline, as described in section 3.2.2. The genome could be assembled to complete status, resulting in a chromosome and one plasmid. No manual curation was performed. The important statistics of the sequenced genome are listed in Table 11.

Note that in this study the annotation of genes and their gene products are based on the NCBI annotation pipeline, while RAST annotation was exploited for their functional analysis using SEED subsystem analysis.

Table 11: Genome statistics of sequenced strain. Listed properties are: BioProject and the respective BioSample, accession numbers for all contigs, coverage (= average coverage of assemblies), contigs (= chromosome plus plasmids), PEG (= protein encoding genes based on NCBI annotation).

| Specie | Strain | BioProject | BioSample | NCBI accession | Coverage | Size (Mbp) | Contigs | GC content (%) | PEG (NCBI) |
|---|---|---|---|---|---|---|---|---|---|
| *Lactobacillus paracasei* | TMW 1.1434 (F19) | PRJNA327719 | SAMN05356834 | CP016355-CP016356 | 253 | 3.2 | 2 | 46.4 | 2938 |

### 4.1.2 Genome analysis

The genome of *Lactobacillus paracasei* subsp. *paracasei* F19 including general genomic properties, functional analysis and metabolic reconstruction was analyzed. The whole genome analysis section orients itself on the genome analysis of beer-spoiling lactic acid bacteria by Geißler (2016).

In a first subsection, general genomic properties are described with respect to parameters such as genome size, GC content or the number of rRNA operons and subcellular localization prediction.

In a second subsection, the functional analysis is provided. The SEED subsystem analysis enables the assignment of predicted genes to a hierarchical three-level categorization system ranging from category (Nucleosides and Nucleotides), subcategory (Pyrimidines) to subsystem (De Novo Pyrimidine Synthesis). It enables a global and functional view on the genome, as all genes are assigned to comprehensible, functional categories.

Functional analysis: SEED subsystem was performed, total count of a given category and the respective proportion in relation to total assignments/genome size calculated. The proportion (coverage) of genes assigned to the respective SEED category will be mentioned in the corresponding sections. Consider that in case of the SEED subsystem analysis a gene can be assigned to several subsystems and that generally only about 40 to 50 % of all genes are assigned to a category. The functional analysis of the genome is described in detail in the following subsections.

Note that the following sections are based on *in silico* prediction and that this fact will not stressed repeatedly by using terminology such as “*in silico*” or “predicted” etc.

#### 4.1.2.1 General genomic properties

The complete genome of *Lb. paracasei* subsp. *paracasei* F19 was obtained in this study, whereby the newly sequenced genome could be assembled to one chromosome and one plasmid. The chromosome sizes 3.1 Mbp with a consistent GC content of 46.4 %, whereas the plasmid accounts for 106,416 bp and a GC content of 44.1 %. In total, 2,938 open reading frames (ORFs) based on NCBI annotation were found, resulting in a coding density of about 84 %. Further, 15 complete rRNA operons, 59 tRNAs and two pseudo-tRNAs were found to be encoded. In Figure 11, the predicted subcellular localization of F19 proteins in respect to chromosome and plasmid encoded genes are illustrated.

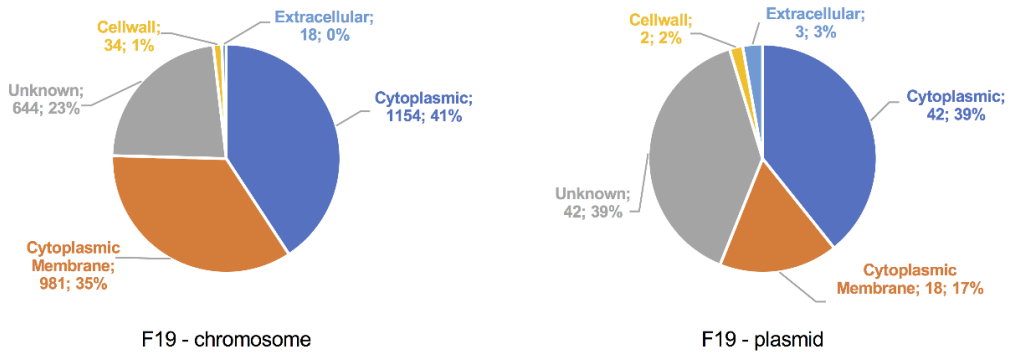


Figure 11: Subcellular localization of *Lb. paracasei* subsp. *paracasei* F19 proteins in numbers and %. Distribution is shown for chromosomally (left) and plasmid (right) encoded genes.

### 4.1.2.2 Functional genomic analysis

In total, 40.0 % of the found ORFs could be assigned to SEED categories and the corresponding classification system. Out of the unassigned ORFs, 586 were annotated as hypothetical proteins. The functional analysis displayed a conserved pattern for the whole genome. Thereby, most genes were assigned to categories related to carbohydrate, protein (translation and transcription) and amino acid metabolism, followed by genes associated with cell wall, capsule and nucleosides, nucleotide metabolism (Figure 12).

Note that categories with an overall proportion of less than or equal to 3 % within the genome were summarized and will further refer to the term “Other SEED categories”. An exception was made for the SEED category “Stress Response” (2.7 %).

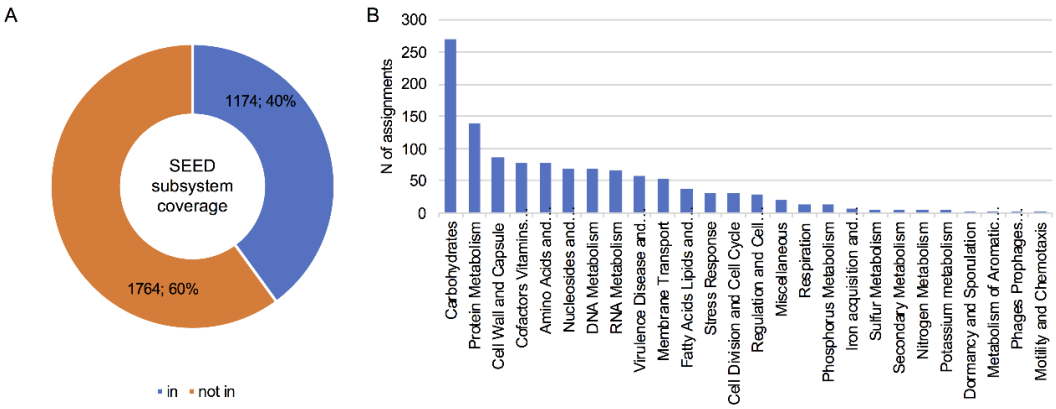


Figure 12: Functional analysis of *Lb. paracasei* subsp. *paracasei* F19. SEED subsystem coverage (A) of the genome is displayed. Further, number (N) of assigned proteins are shown with respect to functional SEED category (B).

SEED categories of the whole genome were broken down with respect to those subcategories making up less than or equal to 10 % within these categories. Relative proportions and absolute numbers of the respective category are listed in Table 12.

Table 12: SEED subsystem analysis of the whole genome. SEED categories are listed in descending order, according their overall proportion within the genome. SEED subcategories making up the majority within these categories are displayed, together with their number (N) and proportion (%) within the respective category.

| SEED category | SEED subcategory | N in category | % of category |
|---|---|---|---|
| **Carbohydrates** | Di- and oligosaccharides | 87 | 33.2 % |
| | Central carbohydrate metabolism | 64 | 24.4 % |
| | Monosaccharides | 49 | 18.7 % |
| | Sugar alcohols | 27 | 10.3 % |
| **Protein Metabolism** | Protein biosynthesis | 104 | 74.8 % |
| | Protein degradation | 20 | 14.4 % |
| **Cell Wall and Capsule** | Capsular and extracellular polysaccharides | 37 | 42.5 % |
| | Cell Wall and Capsule - no subcategory | 29 | 33.3 % |
| | Gram-Positive cell wall components | 21 | 24.1 % |
| **Cofactors Vitamins Prosthetic Groups Pigments** | Folate and pterines | 20 | 26.0 % |
| | Cofactors Vitamins Prosthetic Groups Pigments - no subcategory | 11 | 14.3 % |
| | NAD and NADP | 11 | 14.3 % |
| | Riboflavin FMN FAD | 10 | 13.0 % |
| **Amino Acids and Derivatives** | Histidine Biosynthesis | 12 | 15.6 % |
| | Lysine Biosynthesis DAP Pathway GJO scratch | 10 | 13.0 % |
| | Methionine Degradation | 10 | 13.0 % |
| | Glutamine Glutamate Aspartate and Asparagine Biosynthesis | 8 | 10.4 % |
| | Polyamine Metabolism | 8 | 10.4 % |
| **Nucleosides and Nucleotides** | Purines | 28 | 41.2 % |
| | Pyrimidines | 23 | 33.8 % |
| | Nucleosides and Nucleotides - no subcategory | 12 | 17.6 % |

| | | | |
|---|---|---|---|
| **DNA Metabolism** | DNA repair | 49 | 72.1 % |
| | CRISPs | 9 | 13.2 % |
| **RNA Metabolism** | RNA processing and modification | 54 | 80.6 % |
| | Transcription | 13 | 19.4 % |
| **Virulence, Disease and Defense (VDD)** | Resistance to antibiotics and toxic compounds | 35 | 60.3 % |
| | Invasion and intracellular resistance | 15 | 25.9 % |
| | Bacteriocins ribosomally synthesized antibacterial peptides | 6 | 10.3 % |
| **Membrane Transport** | ABC transporters | 26 | 48.1 % |
| | Membrane Transport - no subcategory | 13 | 24.1 % |
| | Cation transporters | 7 | 13.0 % |
| | Protein translocation across cytoplasmic membrane | 7 | 13.0 % |
| **Fatty Acids Lipids and Isoprenoids** | Phospholipids | 16 | 42.1 % |
| | Fatty acids | 13 | 34.2 % |
| | Isoprenoids | 9 | 23.7 % |
| **Stress Response** | Oxidative stress | 14 | 43.8 % |
| | Osmotic stress | 13 | 40.6 % |

Additionally, functional analysis was broken down with respect to chromosome and plasmid. A SEED subsystem coverage of 40.8 % and of 17.8 % was observed for chromosome and plasmid, respectively. Most plasmid encoded genes were associated to categories related to carbohydrate metabolism and VDD, while a few could be assigned to categories related to cell division and cycle, amino acid and derivatives, and DNA metabolism. The complete lists of found ORFs assigned to a SEED category with respect to chromosome and plasmid are provided in Supplementary Part II (I.1.1.1.).

## 4.2 Selection of comparable stress conditions

This chapter corresponds to a previous publication by Schott *et al*., which is entitled: “MALDI-TOF Mass Spectrometry Enables a Comprehensive and Fast Analysis of Dynamics and Qualities of Stress Responses of Lactobacillus paracasei subsp. paracasei F19” [320].

Stress responses of microorganisms alter depending on the induced stress, intensity and application time. To enable the comparison of several stress responses evoked by different stressors, stress conditions need to be determined having comparable influence on the microorganism’s physiology. Therefore, stress conditions of different stress qualities were specified as the combination of stress intensity tolerance with stress application time tolerance, respectively.

For illustration of the selection process of comparable stress conditions consisting of the determination of stress intensity and stress application time tolerances, potassium chloride stress is depicted.

### 4.2.1 Determination of stress intensity tolerances

Growth challenge experiments under various different stress qualities were performed in order to determine the stress intensity tolerance of *Lb. paracasei* subsp. *paracasei* F19.

For this purpose, turbidity test for total cell count and plate count test for viable cell count were conducted. Turbidity tests were done for the following stress qualities: pH stress, osmotic stress, oxidative stress and temperature stress. While the plate count test was performed for HHP stress. Subsequently, SSCs and MSPC were identified, respectively.

#### 4.2.1.1 Sublethal stress conditions

Growth behavior was checked for ten different stress qualities (acid and alkaline stress, cold and heat stress, glucose limitation, oxidative stress induced by $H_2O_2$, osmotic stress induced by KCl, NaCl, lac and suc) in batch culture at an initial pH of 5.4 with varying intensities, while applying turbidity measurements (section 3.2.3). Note that in case of pH stress, the initial pH varied with the applied stress intensity.

Growth was measured photometrically at 600 nm for 24 h. More than 2,880 growth curves were generated and raw data evaluated using groFit. The most affected growth parameters lag phase (λ), maximal reached optical density ($OD_{max}$) and maximum specific growth rate ($\mu_{max}$) were extracted for comparison and statistical analysis. Consider that normalization was conducted for the calculation of $\mu_{max}$ and λ.

In general, all or single growth parameters were affected by stresses and varied depending on stress intensity. Thereby, parameters were less influenced at low stress intensities for any stress (Table 13).

Table 13: Extracted growth parameters. The maximum specific growth rate ($\mu_{max}$), the duration of the lag phase λ and the maximum turbidity ($OD_{max}$) were listed for all growth data obtained in average ± standard deviation. This table represents the growth parameters of *Lb. paracasei* subsp. *paracasei* grown in Spicher[1] and under various stress qualities. Note that normalization was conducted for the calculation of $\mu_{max}$ and λ. NA = not available.

| | concentration/intensity | $\mu_{max}$ | | λ | | $OD_{max}$ | |
|---|---|---|---|---|---|---|---|
| **pH stress** | 3.0 | 3.0 | ± 0.01 | 0.01 | ± 1.74 | 0.26 | ± 0.01 |
| | 3.5 | 3.5 | ± 0.02 | 0.00 | ± 1.28 | 0.77 | ± 0.01 |
| | 4.0 | 4.0 | ± 0.07 | 0.00 | ± 1.52 | 1.18 | ± 0.00 |
| | 4.5 | 4.5 | ± 0.12 | 0.00 | ± 1.42 | 1.27 | ± 0.00 |
| | 5.0 | 5.0 | ± 0.17 | 0.00 | ± 1.24 | 1.12 | ± 0.01 |
| | 5.8 | 5.8 | ± 0.20 | 0.00 | ± 0.97 | 1.15 | ± 0.01 |
| | 6.0 | 6.0 | ± 0.21 | 0.00 | ± 0.96 | 1.16 | ± 0.01 |
| | 7.0 | 7.0 | ± 0.23 | 0.00 | ± 0.64 | 1.26 | ± 0.01 |
| | 8.0 | 8.0 | ± 0.25 | 0.00 | ± 0.75 | 1.31 | ± 0.01 |
| | 9.0 | 9.0 | ± 0.20 | 0.00 | ± 2.38 | 1.13 | ± 0.02 |
| | 10.0 | 10.0 | ± 0.01 | 0.02 | ± 17.77 | NA | NA |
| **Temperature stress (°C)** | 5 | NA | NA | NA | NA | NA | NA |
| | 10 | NA | NA | NA | NA | NA | NA |
| | 15 | 0.02 | ± 0.01 | 10.79 | ± 0.57 | NA | NA |
| | 20 | 0.08 | ± 0.00 | 3.72 | ± 0.11 | 1.23 | ± 0.00 |
| | 25 | 0.11 | ± 0.00 | 1.22 | ± 0.08 | 1.41 | ± 0.00 |

| | | | | | | | |
|---|---|---|---|---|---|---|---|
| | 30 | 0.13 | ± 0.00 | 2.02 | ± 0.10 | 1.21 | ± 0.04 |
| | 35 | 0.09 | ± 0.00 | 1.58 | ± 0.08 | 0.82 | ± 0.04 |
| | 37 | 0.13 | ± 0.00 | 9.16 | ± 0.05 | 1.07 | ± 0.01 |
| | 40 | 0.16 | ± 0.13 | 0.88 | ± 1.17 | 0.71 | ± 0.03 |
| | 42 | 0.08 | ± 0.01 | -0.34 | ± 0.15 | 0.73 | ± 0.00 |
| | 45 | 0.05 | ± 0.01 | -0.91 | ± 0.28 | 0.68 | ± 0.00 |
| | 50 | NA | NA | NA | NA | NA | NA |
| **Lack of glucose (Spicher[1] v/v %)** | 100 | 0.24 | ± 0.00 | 0.76 | ± 0.03 | 1.42 | ± 0.00 |
| | 90 | 0.24 | ± 0.00 | 1.01 | ± 0.04 | 1.12 | ± 0.01 |
| | 80 | 0.23 | ± 0.00 | 0.89 | ± 0.04 | 1.37 | ± 0.00 |
| | 70 | 0.23 | ± 0.00 | 1.10 | ± 0.04 | 0.97 | ± 0.01 |
| | 60 | 0.22 | ± 0.00 | 1.05 | ± 0.06 | 0.93 | ± 0.01 |
| | 50 | 0.19 | ± 0.01 | 0.75 | ± 0.07 | 0.86 | ± 0.01 |
| | 40 | 0.18 | ± 0.01 | 0.88 | ± 0.11 | 0.78 | ± 0.01 |
| | 30 | 0.14 | ± 0.00 | 0.62 | ± 0.14 | 0.73 | ± 0.01 |
| | 20 | 0.10 | ± 0.00 | 0.54 | ± 0.06 | 0.94 | ± 0.00 |
| | 10 | 0.05 | ± 0.00 | 0.77 | ± 0.10 | 0.70 | ± 0.00 |
| | 0 | 0.01 | ± 0.00 | 2.93 | ± 0.26 | 0.41 | ± 0.00 |
| **Osmotic stress - KCl (M)** | 0.00 | 0.20 | ± 0.00 | 1.19 | ± 0.03 | 1.86 | ± 0.00 |
| | 0.20 | 0.18 | ± 0.00 | 0.74 | ± 0.04 | 1.50 | ± 0.00 |

| | | | | | | | |
|---|---|---|---|---|---|---|---|
| | 0.40 | 0.17 | ± 0.00 | 0.88 | ± 0.03 | 1.36 | ± 0.00 |
| | 0.60 | 0.16 | ± 0.00 | 1.15 | ± 0.03 | 1.25 | ± 0.00 |
| | 0.80 | 0.12 | ± 0.00 | 1.45 | ± 0.07 | 0.67 | ± 0.01 |
| | 1.00 | 0.10 | ± 0.00 | 1.41 | ± 0.04 | 0.51 | ± 0.01 |
| | 1.20 | 0.06 | ± 0.00 | 1.83 | ± 0.06 | 0.47 | ± 0.00 |
| | 1.40 | 0.03 | ± 0.00 | 1.56 | ± 0.08 | 0.34 | ± 0.00 |
| | 1.60 | 0.01 | ± 0.00 | NA | NA | 0.17 | ± 0.01 |
| | 1.80 | 0.04 | ± 0.15 | 1.80 | ± 0.28 | 0.07 | ± 0.01 |
| | 2.00 | 0.04 | ± 0.15 | 1.09 | ± 0.27 | 0.06 | ± 0.00 |
| **Osmotic stress - NaCl (M)** | 0.00 | 0.24 | ± 0.00 | 0.85 | ± 0.03 | 1.43 | ± 0.00 |
| | 0.20 | 0.19 | ± 0.00 | 0.96 | ± 0.04 | 1.33 | ± 0.00 |
| | 0.40 | 0.18 | ± 0.00 | 1.06 | ± 0.03 | 1.21 | ± 0.00 |
| | 0.60 | 0.17 | ± 0.00 | 1.30 | ± 0.05 | 1.18 | ± 0.00 |
| | 0.80 | 0.15 | ± 0.00 | 1.89 | ± 0.05 | 1.22 | ± 0.00 |
| | 1.00 | 0.11 | ± 0.00 | 2.25 | ± 0.08 | 1.12 | ± 0.00 |
| | 1.20 | 0.07 | ± 0.00 | 2.40 | ± 0.06 | 1.00 | ± 0.00 |
| | 1.40 | 0.04 | ± 0.00 | 2.31 | ± 0.11 | 0.77 | ± 0.01 |
| | 1.60 | 0.01 | ± 0.00 | 0.22 | ± 0.29 | 0.81 | ± 0.09 |
| | 1.80 | 0.01 | ± 0.01 | -0.82 | ± 0.44 | 0.23 | ± 0.00 |
| | 2.00 | 0.02 | ± 0.06 | 0.42 | ± 0.33 | 0.21 | ± 0.00 |

| | | | | | | | |
|---|---|---|---|---|---|---|---|
| **Osmotic stress - lac (M)** | 0.00 | 0.20 | ± 0.00 | 1.19 | ± 0.03 | 1.86 | ± 0.00 |
| | 0.20 | 0.18 | ± 0.00 | 0.74 | ± 0.04 | 1.50 | ± 0.00 |
| | 0.40 | 0.17 | ± 0.00 | 0.88 | ± 0.03 | 1.36 | ± 0.00 |
| | 0.60 | 0.16 | ± 0.00 | 1.15 | ± 0.03 | 1.25 | ± 0.00 |
| | 0.80 | 0.12 | ± 0.00 | 1.45 | ± 0.07 | 0.67 | ± 0.01 |
| | 1.00 | 0.10 | ± 0.00 | 1.41 | ± 0.04 | 0.51 | ± 0.01 |
| | 1.20 | 0.06 | ± 0.00 | 1.83 | ± 0.06 | 0.47 | ± 0.00 |
| | 1.40 | 0.03 | ± 0.00 | 1.56 | ± 0.08 | 0.34 | ± 0.00 |
| | 1.60 | 0.01 | ± 0.00 | NA | NA | 0.17 | ± 0.01 |
| | 1.80 | 0.04 | ± 0.15 | 1.80 | ± 0.28 | 0.07 | ± 0.01 |
| | 2.00 | 0.04 | ± 0.15 | 1.09 | ± 0.27 | 0.06 | ± 0.00 |
| **Osmotic stress - suc (M)** | 0.00 | 0.22 | ± 0.00 | 0.87 | ± 0.03 | 1.42 | ± 0.00 |
| | 0.58 | 0.13 | ± 0.00 | 1.11 | ± 0.13 | 1.23 | ± 0.04 |
| | 1.15 | 0.11 | ± 0.00 | 2.70 | ± 0.23 | 0.89 | ± 0.03 |
| | 1.73 | 0.08 | ± 0.00 | 4.29 | ± 0.21 | 1.16 | ± 0.01 |
| | 2.30 | 0.05 | ± 0.00 | 6.46 | ± 0.27 | 0.92 | ± 0.02 |
| | 2.88 | 0.03 | ± 0.00 | 8.44 | ± 0.24 | 0.57 | ± 0.04 |
| | 3.46 | 0.01 | ± 0.00 | 7.61 | ± 0.72 | 0.24 | ± 0.13 |
| | 4.03 | 0.00 | ± 0.03 | 5.89 | ± 13.39 | NA | NA |
| | 4.61 | NA | NA | NA | NA | NA | NA |

| | | | | | | | |
|---|---|---|---|---|---|---|---|
| | 5.18 | NA | NA | NA | NA | NA | NA |
| | 5.76 | NA | NA | NA | NA | NA | NA |
| **Oxidative stress - $H_2O_2$ (mM)** | 0.00 | 0.18 | ± 0.00 | 0.73 | ± 0.02 | 0.96 | ± 0.01 |
| | 0.20 | 0.20 | ± 0.00 | 1.31 | ± 0.02 | 1.05 | ± 0.01 |
| | 0.40 | 0.19 | ± 0.00 | 1.42 | ± 0.02 | 1.06 | ± 0.01 |
| | 0.60 | 0.20 | ± 0.00 | 1.81 | ± 0.04 | 1.06 | ± 0.01 |
| | 0.80 | 0.18 | ± 0.00 | 2.37 | ± 0.03 | 1.03 | ± 0.01 |
| | 1.00 | 0.14 | ± 0.00 | 3.03 | ± 0.04 | 1.23 | ± 0.00 |
| | 1.20 | 0.10 | ± 0.00 | 5.40 | ± 0.05 | 1.12 | ± 0.01 |
| | 1.40 | 0.08 | ± 0.00 | 8.67 | ± 0.13 | 0.88 | ± 0.07 |
| | 1.60 | 0.10 | ± 0.01 | 16.55 | ± 0.87 | NA | NA |
| | 1.80 | 0.03 | ± 0.01 | 16.16 | ± 0.18 | NA | NA |
| | 2.00 | 0.01 | ± 1.17 | 21.23 | ± 12.79 | NA | NA |

In the following, the growth curve analysis of single stress qualities is presented (Figure 13). The determination of stress intensity tolerance on basis of estimated growth parameters is illustrated by the example of potassium chloride stress. The growth curve analyses from nine more stress qualities were performed analogously, and the corresponding data and figures can be obtained from Supplementary Part II (II.1.2.1.).

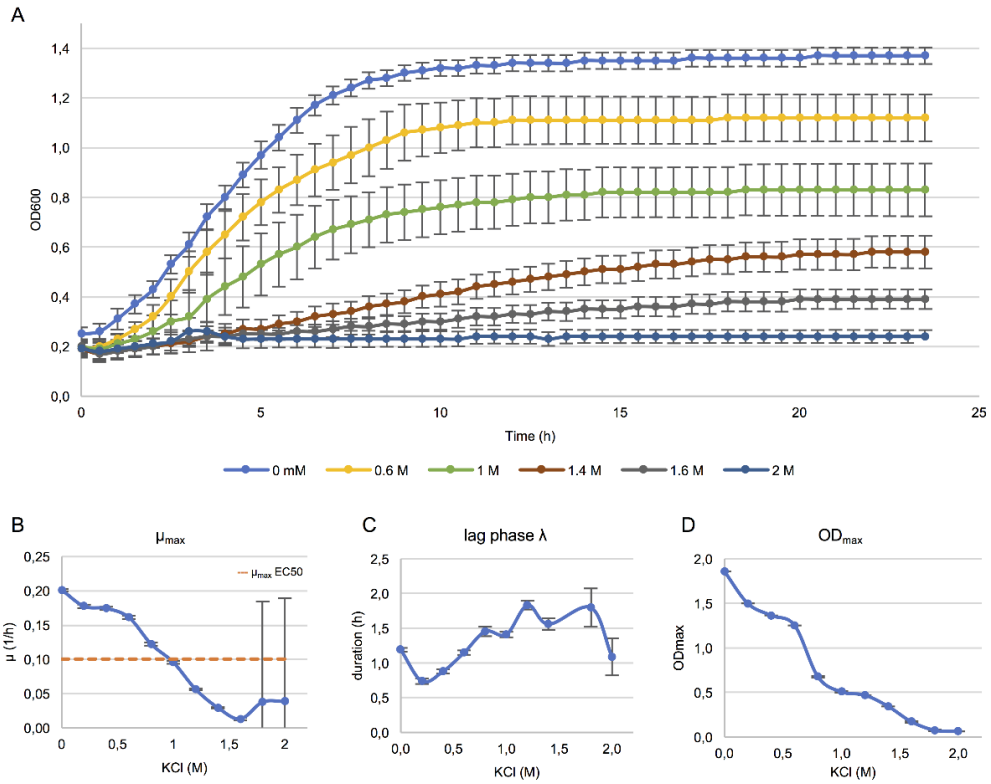


Figure 13: Growth curve analysis of *Lb. paracasei* subsp. *paracasei* F19 grown in increasing potassium chloride (KCl) concentration. Growth curves are illustrated for some selected concentrations. (A). Growth parameters maximum specific growth rate ($\mu_{max}$), duration of lag phase λ and maximum turbidity ($OD_{max}$) were extracted for all growth data obtained and plotted against the KCl concentration (B, C, D) $\mu_{max}$ and $OD_{max}$ were affected by the induced stress and λ remained more or less constant. EC50 was estimated based on the calculation of $\mu_{max}$ EC50 (- - -) (B). Note that normalization was conducted for the calculation of $\mu_{max}$ and λ.

In the absence of potassium chloride (KCl), referring to control condition, F19 entered the exponential phase after approximately an hour incubation (λ = 1.19) and reached $\mu_{max}$ of 0.2 in mid exponential phase. After 10 h growth in Spicher[1], cells of F19 passed into stationary phase with an $OD_{max}$ of 1.86. Overall, $\mu_{max}$ and $OD_{max}$ were affected by an increase of the potassium chloride concentration. With increasing content, $\mu_{max}$ and $OD_{max}$ were decreasing to 0.04 and 0.06, respectively, while λ remained more or less constant (Table 13).

At the end, a dose response curve was provided for all stress qualities, respectively, and the half effective concentration (EC50) along with the inhibitory concentration (IC) were

identified (Figure 13B, Table 13). Exploiting the identified IC, sublethal stress condition and thus stress intensity tolerance was estimated for all stress qualities (Table 14), respectively. Regarding the presented example of potassium chloride stress, IC was identified at 1 M KCl.

Table 14: Identified inhibitory concentrations (IC) of *Lb. paracasei* subsp. *paracasei* F19. The IC with the corresponding maximal specific growth rate ($\mu_{max}$ IC) and the maximal specific growth rate of the half effective concentration ($\mu_{max}$ EC50) were listed for various stress qualities in average ± standard deviation. Note that EC50 refers to an intensity/concentration of a compound/parameter where 50 % of $\mu_{max}$ of control condition was achieved, and thus $\mu_{max}$ EC50 is based on calculation.

| Stress | IC | $\mu_{max}$ IC | | $\mu_{max}$ EC50 |
|---|---|---|---|---|
| **pH stress** | 4 | 0.07 | ± 0.10 | 0.10 |
| | 9 | 0.20 | ± 0.10 | 0.10 |
| **Temperature stress (°C)** | 15 | 0.02 | ± 0.07 | 0.07 |
| | 45 | 0.05 | ± 0.07 | 0.07 |
| **Lack of glucose (Spicher[1] v/v %)** | 10 | 0.05 | ± 0.12 | 0.12 |
| **Osmotic stress - KCl (M)** | 1 | 0.10 | ± 0.10 | 0.10 |
| **Osmotic stress - NaCl (M)** | 1 | 0.11 | ± 0.03 | 0.12 |
| **Osmotic stress - lac (M)** | 0.32 | 0.10 | ± 0.03 | 0.10 |
| **Osmotic stress - suc (M)** | 1.15 | 0.11 | ± 0.03 | 0.11 |
| **Oxidative stress - $H_2O_2$ (mM)** | 1.40 | 0.08 | ± 0.09 | 0.09 |

#### 4.2.1.2 Mild sublethal pressure condition

Growth challenge experiments under HHP stress were investigated varying in pressure level and pressure holding time while applying plate count tests. HHP treatment was performed at 37 °C and CFU of *Lb. paracasei* subsp. *paracasei* F19 determined. Raw data were evaluated applying ANOVA and Tukey HSD correction for comparison and statistical analysis (subsection 3.2.3.3.3).

First, HHP treatment was performed at varying pressure levels with a constant pressure holding time of 60 s, respectively. A significant reduction of CFU was determined after the HHP treatment at 300 MPa. Although with increasing pressure level, CFU after the

pressure treatment at 250 MPa and 400 MPa were comparable (Figure 14A). Thus, a target pressure level was manually defined at a pressure of 350 MPa, and subsequently exploited for the determination of the target pressure holding time.

For the purpose of target pressure holding time determination, HHP treatments were performed at varying pressure holding times with the previously defined target pressure level (350 MPa), respectively. With increasing pressure holding time, CFUs were decreasing. A significant reduction of CFUs was determined after the HHP treatment for 600 s. Thus, the target pressure holding time was defined for 600 s (Figure 14B).

In consequence, the mild sublethal pressure condition was determined at 350 MPa and 600 s.

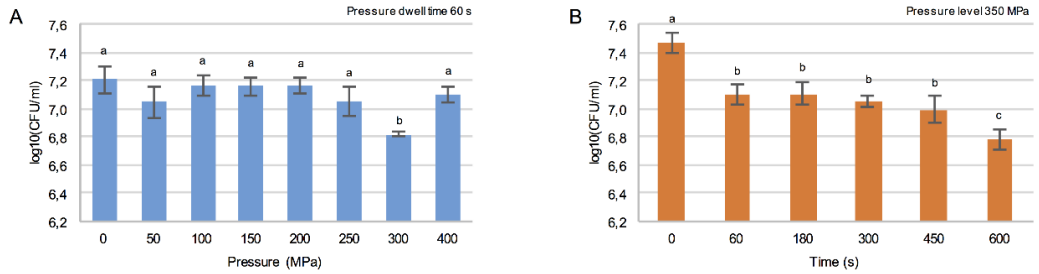


Figure 14: High hydrostatic pressure (HHP) treatments and survivors of *Lb. paracasei* subsp. *paracasei* F19. Survivors based on log10(CFU/ml) are displayed in average ± standard deviation. Dependent variable significance of sample/groups was checked using ANOVA (p-value < 0.05), followed by Tukey Honest Significance Difference (HSD) correction to proof statistical significance between sample/groups (a, b, c). (A) Survivors at 37 °C for 60 s of dwell time at 0-400 MPa, whereby 0 MPa refers to control condition (B) Kinetics of survivors at 350 MPa combined with 37 °C for 0 – 600 s of dwell times, whereby 0 s refers to control condition.

### 4.2.2 Determination of stress application time tolerances

Stress intensity tolerances were exploited and stress responses of *Lb. paracasei* subsp. *paracasei* F19 investigated using MALDI-TOF MS protein profiling. In order to determine stress application time tolerances, respectively, obtained mass spectra of stress responses were statistically analyzed using cluster analysis for the examination of stress response kinetics and discriminant analysis of principle components (DAPC) for grouping of stress responses.

#### 4.2.2.1 Stress response kinetics

Stress responses of 12 stress intensity tolerances with varying application times as well as responses in control condition were investigated on proteome level. Proteomic responses were profiled based on the detection of low molecular weight (lmw) proteins using MALDI-TOF MS protein profiling (3.2.4).

As for the determination of MSPC a recovery phase in Spicher[1] was attached (*), it is yet, for simplification, subsequently discussed as stress response. Besides, the drying process for starter culture preparation was simulated and is listed as drying stress (°).

More than 500 MALDI-TOF mass spectra were recorded within a mass to charge ratio (m/z) of 2,000 to 15,000 and processed to protein expression profiles. In order to determine stress application time tolerances, protein expression profiles of the respective stress intensity tolerance were stacked and stress response kinetics analyzed applying peak-based cluster analysis, respectively. In the following, the analysis of a single stress response kinetic is exemplarily presented for potassium chloride stress, as stress-induced peaks were clearly visible and could be graphically illustrated. The analyses of eleven more stress response kinetics were performed analogously, and the corresponding data and figures can be obtained from Supplementary Part II (II.1.2.2.).

In general, protein expression profiles display peak differences in mass to charge ratio (m/z) and intensity, respectively. Along with the stress application time, peak differences were particularly observed between control and stress protein expression profiles. In the presence of potassium chloride stress, peaks with approx. 6,991 (1), 2,106 (2), 2,122 (3), 2,549 (4) and 2,649 (5) m/z changed in intensity. Noticeably, peak 1 decreased in intensity and visibly reached a minimum of 500 arbitrary units (a.u.) after 60 minutes of stress application. However, with increasing time, peak intensity raised again but did not reach its maximum. Further, numerous peaks were solely detected (2, 3, 4, 5) in the presence of potassium chloride and clearly increased in peak intensity. Especially peak 2, peak 4 and peak 5 showed massive enhancements in peak intensity up to 2,500 a.u. while they were not visible in control conditions (Figure 15).

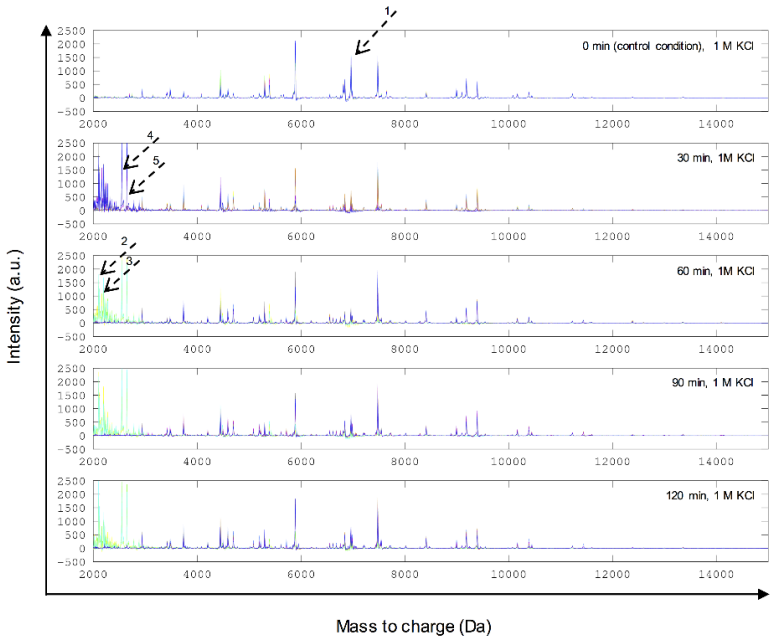


Figure 15: Stacked protein expression profiles of potassium chloride stress (1 M KCl) obtained for *Lb. paracasei* subsp. *paracasei* F19. MALDI-TOF mass spectra in the mass range from 2,000 Da to 15,000 Da were recorded for stress application times of 0 – 120 min, whereby 0 min stress induction refer to control condition. Arrows indicate interesting peaks: arrow 1 marks a single peak at approx. 6,991 m/z (1) with decreasing peak intensity, whereas arrows 2, 3, 4 and 5 mark peaks at 2,106 m/z (2), 2,122 m/z (3), 2,549 m/z (4) and 2,649 m/z (5) with increasing peak intensity.

On the basis of the protein expression profiles, the peak-based hierarchical cluster analyses were successfully performed and stress response kinetics analyzed. In general, stress application time tolerances were identified for all stress intensity tolerances at 60 minutes of stress application, respectively (Table 15). For potassium chloride stress, cluster analysis is presented in Figure 16. The protein expression profile of control condition (0 min) was grouped in a single arm showing a low level of similarity to the analyzed protein expression profiles of stressed cells, which were harbored in a distinct cluster. Note that this pattern was observed for every stress intensity tolerance, respectively (Supplementary Part II, II.1.2.2.). Further, protein expression profiles of 60 and 90 minutes stress application time clustered together displaying highest distance to control. Thus, $T_{max}$ along with the stress application time tolerance were identified at 60 minutes.

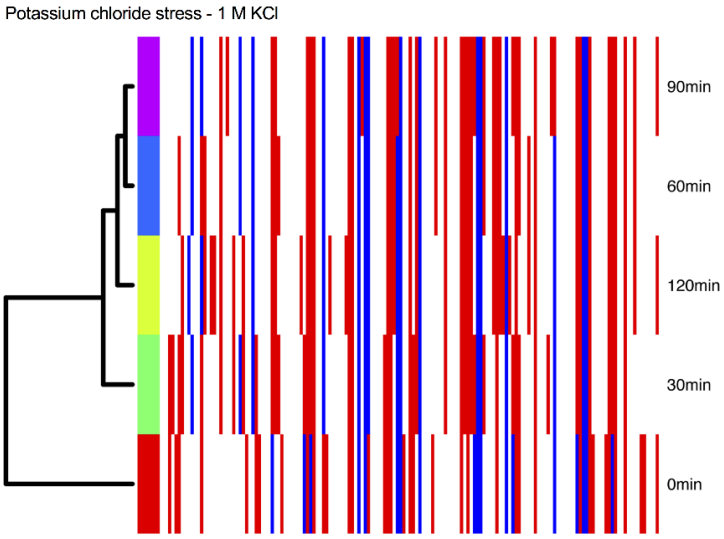


Figure 16: Peak-based cluster analysis of stress response kinetics of sublethal potassium chloride stress (1 M KCl) of *Lb. paracasei* subsp. *paracasei* F19. Cluster analysis is displayed as dendrogram with varying stress application times from 0 min (control) to 90 min in 30 min intervals.

The comparison of the optimal clusters with the stress labelled data revealed that cluster 1 corresponds to the stress response to high hydrostatic pressure stress (HHP), cluster 3 harbors stress responses to alkaline pH stress (pH9) and cluster 2 covers the remaining stress responses (45 °C, 15 °C, D, glu10, H2O2, KCl, lac, NaCl, pH4, suc). One outlier of the grouped stress response to pH9 stress (cluster 3) overlapped with the ellipse of the grouped stress response in cluster 2. Looking at the stress labelled data, stress responses to alkaline pH and HHP stress clearly differed from each other and also to any other stress conditions.

### 4.2.3 Comparable stress conditions for quantitative proteomics

Stress conditions on the basis of identified stress intensity tolerances and stress application time tolerances were identified (sections 4.2.1 and 4.2.2) and are listed in Table 15. These stress conditions are exploited for stress treatments for quantitative proteomics (section 4.3.2).

Table 15: Applied stress treatments employed on *Lb. paracasei* subsp. *paracasei* F19 [320]. Listed are stresses, the corresponding ID and the stress condition, which is specified as the combination of stress intensity tolerance and stress application time tolerance. Regarding the high hydrostatic pressure stress, a recovery phase in Spicher[1] was attached (*) and is yet, for simplification, further discussed as stress. The drying process for starter culture preparation was simulated and is listed as drying stress (#).

| Stress | ID | Stress conditions | |
|---|---|---|---|
| | | Stress intensity tolerance | Stress application time tolerance |
| **pH stress – acid** | pH4 | pH 4 | 60 min |
| **pH stress – alkaline** | pH9 | pH 9 | 60 min |
| **Temperature stress – cold** | 15C | 15 C | 60 min |
| **Temperature stress – heat** | 45C | 45 C | 60 min |
| **Lack of glucose (starvation stress)** | glu10 | 10 % (Spicher[1] v/v) | 60 min |
| **Osmotic stress – potassium chloride** | KCl | 1 M | 60 min |
| **Osmotic stress – sodium chloride** | NaCl | 1 M | 60 min |
| **Osmotic stress – lactose** | Lac | 0.32 M | 60 min |
| **Osmotic stress - sucrose** | Suc | 1.15 M | 60 min |
| **Oxidative stress – hydrogen peroxide** | $H_2O_2$ | 1.40 mM | 60 min |
| **High hydrostatic pressure stress*** | HHP | 350 MPa, 10 min | 60 min* |
| **Drying stress#** | D | RT | 60 min |

## 4.3 Proteome analysis

This chapter corresponds to the publication by Schott *et al.* about the comprehensive analysis of stress responses of *Lactobacillus paracasei* subsp. *paracasei* F19 using genomics and quantitative proteomics [356].

The efficient analysis of bacterial stress responses of *Lb. paracasei* subsp. *paracasei* F19 was accomplished using genomics and quantitative proteomics with chemical labeling. Stress treatments were prepared in biological triplicates based on identified stress conditions (Table 15), cell lysis was carried out and whole-cell protein extracts were subjected to proteolytic digestion with trypsin. Peptide samples were labeled with isobaric tandem mass tags (TMT), and fractionated using off-line hSAX liquid chromatography to reduce sample complexity and alleviate TMT ratio distortion. Full in-depth proteome analysis was performed with LC-MS/MS. For protein identification and quantification, tandem mass spectra were processed with MaxQuant, searched against a protein sequence database based on the whole genome sequence of *Lb. paracasei* subsp. *paracasei* F19, and statistically analyzed in R. Thereby, an overall quality of MaxQuant output of “best” was calculated and differentially expressed proteins (DE) identified. For generating the whole genome sequence, high molecular DNA was isolated and whole genome sequenced via PacBio SMRT sequencing, genome was assembled via SMRT analysis and annotated using RAST and NCBI Prokaryotic Genome Annotation Pipeline. Genome sequence was submitted to GenBank.

In a first section, the general proteomic analysis with respect to identified proteins and properties as well as their functional analysis is presented (section 4.3.1). In a second section, the proteomic analysis of stress responses in reference to control condition is described (section 4.3.2). In a third section, the comparative analysis of stress responses in reference to control condition is documented (section 4.3.3).

Note, that in all three sections the term DE proteins is used. While section two and three solely focus on DE proteins in reference to control condition, section one is about any DE protein. This means: DE protein in reference to any condition (control condition / drying stress / sodium chloride stress etc).

Functional analysis: For the functional analysis, total counts of a given category and the respective proportion in relation to total assignments are calculated. The proportion (coverage) of genes assigned to the respective SEED category will be mentioned in the corresponding subsections and sections. Note that for graphical illustration of biological functions, SEED categories with an overall proportion of less than or equal to 3 % within the genome were summarized and will further refer to the term “Other SEED categories”.

An exception was made for the SEED category “Stress Response” (2.7 %) (section 4.1.2, page 67).

### 4.3.1 General proteomic analysis

#### 4.3.1.1 Identified proteins and properties

Overall, 2159 proteins with at least one unique peptide (False Positive Rate, FPR, 5.4 % on protein level) and 2005 proteins with at least two unique peptides (FPR, 3.1%) were identified. The identified proteins covered 73 % and 68 % of the *in silico* proteome, respectively. Moreover, the protein identifications were based on 21,871 and 21,717 unique peptide identifications (FPR, 0.9 % and 0.9 % on peptide level, respectively) with an average of 10.1 unique peptides per protein identification. 1917 proteins were quantified, of which overall 427 proteins were DE representing the stress proteome (Figure 17A).

Applying the subcellular localization (SCL) prediction of proteins, extracellular, cytoplasmic, cytoplasmic membrane (= cell membrane) and cell wall proteins were found (Figure 17B). Most identified and quantified proteins are cytoplasmic (47 % and 49 %, respectively) and membrane proteins (23 %, respectively) (Table 16). To assess the overall influence of stress, SCL of quantified proteins were compared to SCL of DE proteins using Fisher’s exact test. Thereby, evidence was found that stress significantly (p-value = 0.002) influences the expression of proteins of different SCL. Cells responded to stress with the visual relative enhancement of cell wall and membrane proteins, which was accompanied by the relative reduction of cytoplasmic proteins.

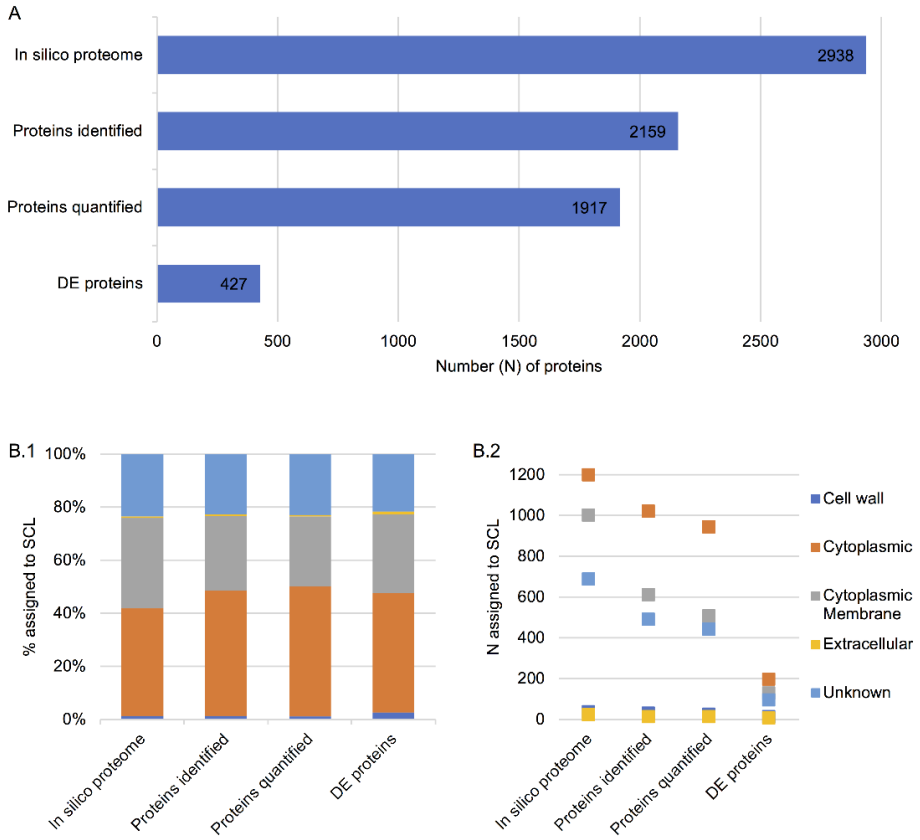


Figure 17: Global proteome characterization. (A) Comparison of *in silico* proteome with identified, quantified and differentially expressed (DE) proteins. (B) Predicted subcellular localization of *in silico* proteome, identified, quantified and DE proteins. Displayed are percentage (%) (B.1) and number (N) (B.2).

Table 16: Predicted subcellular localization (SCL) of *in silico* proteome, identified, quantified and differentially expressed (DE) proteins. Number and percentage are listed.

| SCL | *In silico* proteome | | Proteins identified | | Proteins quantified | | DE proteins | |
|---|---|---|---|---|---|---|---|---|
| **Cell wall** | 36 | 1 % | 27 | 1 % | 23 | 1 % | 11 | 3 % |
| **Cytoplasmic** | 1196 | 41 % | 1019 | 47 % | 940 | 49 % | 193 | 45 % |
| **Membrane** | 999 | 34 % | 609 | 28 % | 505 | 26 % | 127 | 30 % |
| **Extracellular** | 21 | 1 % | 11 | 1 % | 10 | 1 % | 5 | 1 % |
| **Unknown** | 686 | 23 % | 489 | 23 % | 439 | 23 % | 92 | 21 % |

#### 4.3.1.2 Functional analysis

A broad range of biological functions based on the SEED subsystem analysis was detected covering 40 % of the *in silico* proteome of F19. Most abundant proteins were assigned to carbohydrate (23 %) and protein metabolism (12 %), followed by proteins associated with cell wall and capsule biosynthesis, amino acids and derivatives biosynthesis and cofactors/vitamins/prosthetic group biosynthesis (7 %, respectively) (Figure 18). Within these categories, we found proteins related to general metabolic and regulatory functions, e.g. di- and oligosaccharide metabolism, protein biosynthesis, capsular and extracellular polysaccharide biosynthesis, lysine/threonine/methionine/cysteine metabolism, and folate and pterines biosynthesis.

However, for graphical illustration, categories with a constant proportion less than 3 % were summarized as “Other SEED categories” (Respiration; Secondary Metabolism; Phages/Prophages/Transposable elements/Plasmids; Iron Acquisition and Metabolism; Cell Division and Cell Cycle; Nitrogen Metabolism; Potassium Metabolism; Regulation and Cell signaling; Metabolism of Aromatic Compounds; Miscellaneous Metabolism; Sulfur Metabolism; Phosphorus Metabolism; Motility and Chemotaxis; Dormancy and Sporulation).

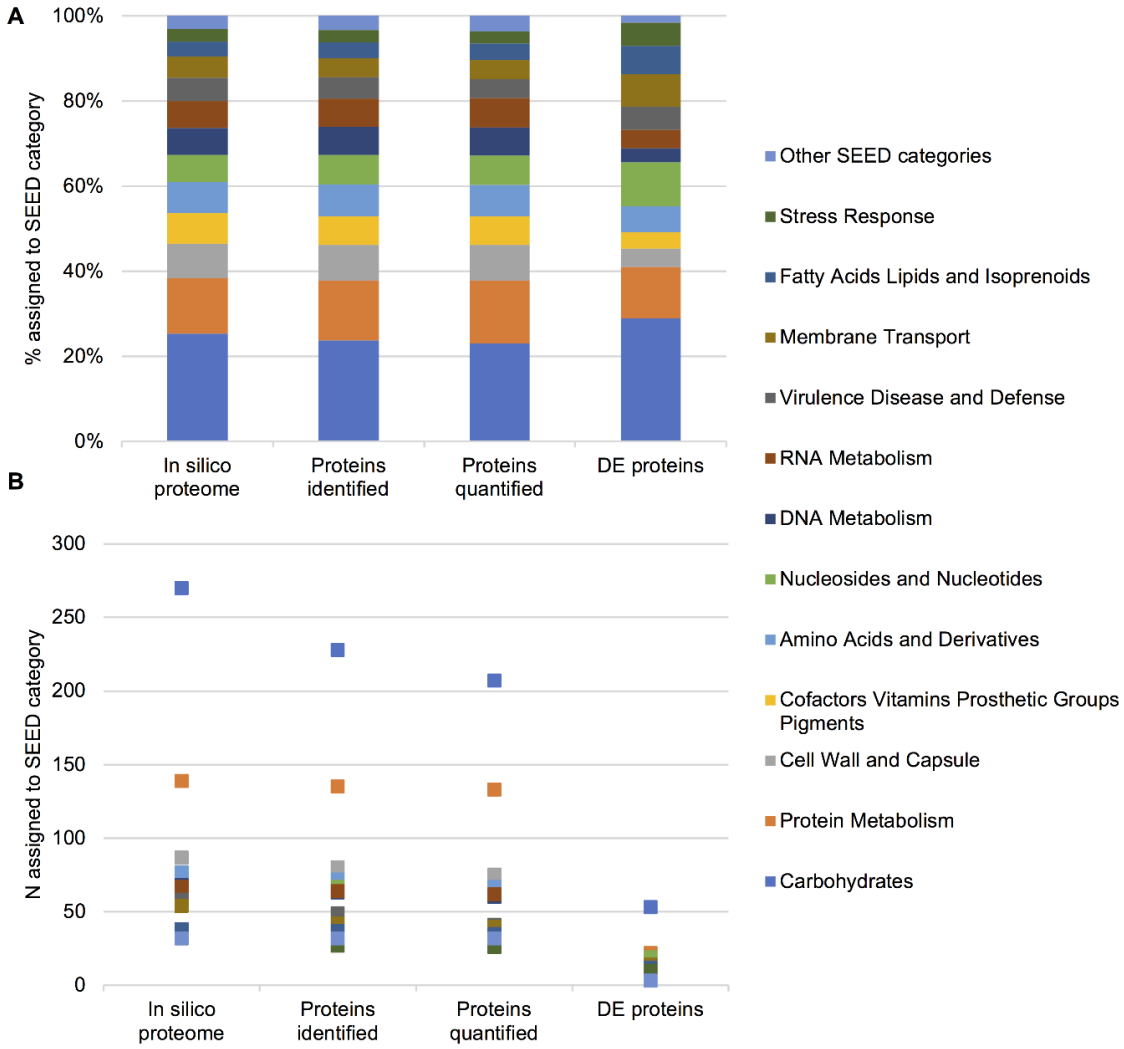


Figure 18: Global analysis of biological functions. Biological functions based on SEED categories. Illustrated are percentage (A) and absolute number (N) (B) of *in silico* proteome, identified, quantified and differentially expressed (DE) proteins. The complete list of predicted SEED category is provided (Table 4, Supplementary Part III).

The respective table listing the assignments of proteins to SEED category can be obtained from Supplementary Part III (Table S5).

To evaluate the influence of stress on biological functions, SEED categories of quantified and DE proteins were compared applying Fisher's exact test. Thereby, evidence was found that stress significantly influences (p-value = 0.001) the expression of proteins of different biological functions. Numerous SEED categories displayed different relative proportions when exposed to stress. Among the top 5 ranked, a relative enhancement based on the associated proteins was revealed for SEED categories carbohydrate metabolism, nucleoside and nucleotide metabolism and membrane transport, whereas a relative reduction was observed for DNA metabolism and cell wall and capsule biosynthesis.

Further, in order to estimate the relative protein investment of the cell in biological functions, the relative protein mass on a proteome-wide scale (% protein mass of the total dry mass) was calculated. During stress, cells invest mostly in proteins of carbohydrate metabolism, followed by nucleosides and nucleotides metabolism and membrane transport (Figure 19), which is in concordance to the relative enhancement of these SEED categories.

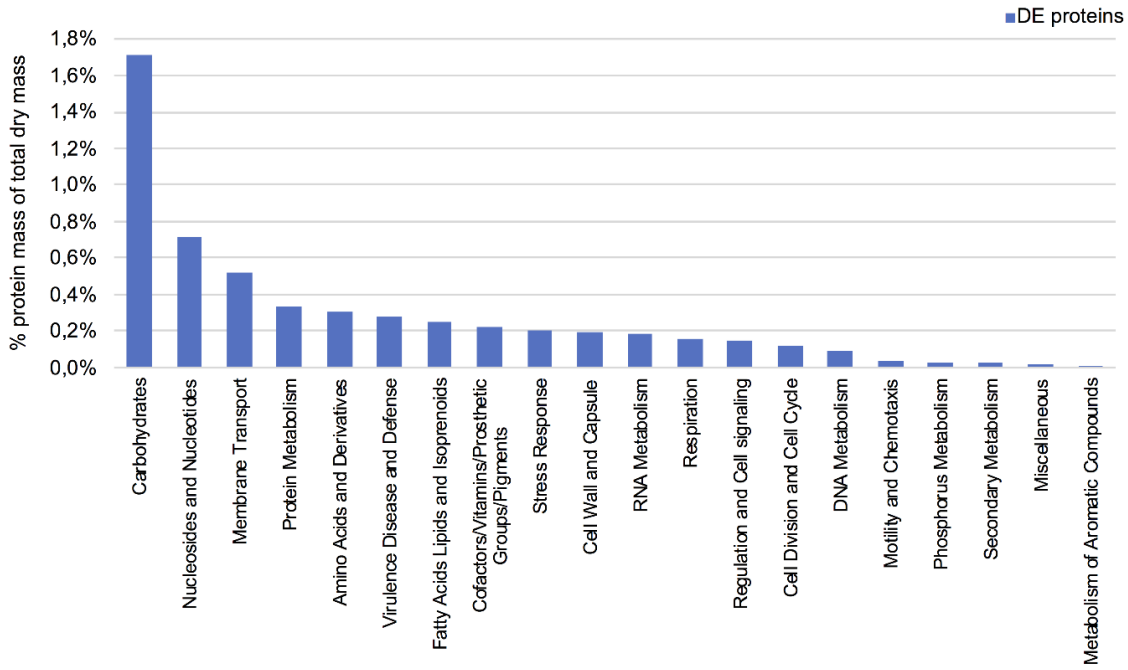


Figure 19: Protein investment of *Lb. paracasei* subsp. *paracasei* F19 during stress. The relative protein investment of the cell in biological functions during stress (DE proteins) is estimated based on the calculation of the relative protein mass on a proteome-wide scale (% protein mass of the total dry mass).

All details regarding functional analysis can be obtained from Table 17.

Table 17: Biological functions based on SEED category of proteins. Displayed are the i*n silico* proteome, identified, quantified and differentially expressed (DE) proteins in the corresponding SEED category. Percentage and absolute number are listed. Top 5 ranked SEED categories influenced by stress are marked: relative enhancement (green), relative reduction (red). Note that categories with a constant proportion less than 3 % are summarized as “Other SEED categories”.

| SEED category | *In silico* proteome | | Proteins identified | | Proteins quantified | | DE proteins | |
|---|---|---|---|---|---|---|---|---|
| **Carbohydrates** | 270 | 23 % | 228 | 22 % | 207 | 21 % | 53 | 27 % |
| **Protein Metabolism** | 139 | 12 % | 135 | 13 % | 133 | 13 % | 22 | 11 % |
| **Cell Wall and Capsule** | 87 | 7 % | 80 | 8 % | 75 | 8 % | 8 | 4 % |
| **Cofactors Vitamins Prosthetic Groups Pigments** | 77 | 7 % | 65 | 6 % | 61 | 6 % | 7 | 4 % |
| **Amino Acids and Derivatives** | 77 | 7 % | 72 | 7 % | 67 | 7 % | 11 | 6 % |
| **Nucleosides and Nucleotides** | 68 | 6 % | 67 | 6 % | 61 | 6 % | 19 | 10 % |
| **DNA Metabolism** | 68 | 6 % | 63 | 6 % | 60 | 6 % | 6 | 3 % |
| **RNA Metabolism** | 67 | 6 % | 64 | 6 % | 62 | 6 % | 8 | 4 % |
| **Virulence, Disease and Defense** | 58 | 5 % | 49 | 5 % | 41 | 4 % | 10 | 5 % |
| **Membrane Transport** | 54 | 5 % | 42 | 4 % | 40 | 4 % | 14 | 7 % |
| **Fatty Acids Lipids and Isoprenoids** | 38 | 3 % | 37 | 4 % | 35 | 4 % | 12 | 6 % |
| **Stress Response** | 32 | 3 % | 27 | 3 % | 26 | 3 % | 10 | 5 % |
| **Other SEED categories** | 139 | 12 % | 127 | 12 % | 122 | 12 % | 19 | 10 % |

### 4.3.2 Proteomic analysis of stress responses

The proteomic analysis of stress responses in reference to control condition is divided in two parts. The first subsection presents a general proteomic analysis in reference to control condition and thus providing an overview of DE proteins. The second section focuses on the proteomic analysis of each individual stress condition in reference to control condition. At this, stress condition-specific analyses are exemplarily depicted based on the comparative analysis of stress responses using cluster analysis (section 4.3.3). As representatives of the formed clusters, stress response analyses of heat, alkaline and drying stress were chosen and are presented in individual subsections, respectively. Consider that the comprehensive stress response analysis of a single stress condition takes about five pages. As the proteomic analysis of stress responses includes twelve stress conditions, the results are offered in Supplementary Part III (III.1.1.1.), where all details are also depicted in individual sections for each stress condition. All relevant data and results, which are necessary to comprehend any thoughts and theories in the discussion, will be recapped explicitly in the discussion.

Note that the following subsection including the associated subsections in Supplementary Part III (III.1.1.1.) are exclusively based on DE proteins during stress in reference to control condition and that this fact will not stressed repeatedly by using terminology such as “in reference to control”, “vs. control”, “in stress”, “DE vs. contr.” or “during stress” etc.

#### 4.3.2.1 General analysis of stress responses

Overall, 188 proteins were DE covering approximately 6 % of the *in silico* proteome (Figure 20A). Further, DE proteins were distributed over the whole genome including chromosome and plasmid (Figure 20B). Out of these proteins, 183 and 5 were chromosomally and plasmid encoded, respectively. With respect to the plasmid encoded proteins, three were annotated as hypothetical proteins, while the remaining ones are a DNA starvation/stationary phase protection protein and a heavy metal-binding protein.

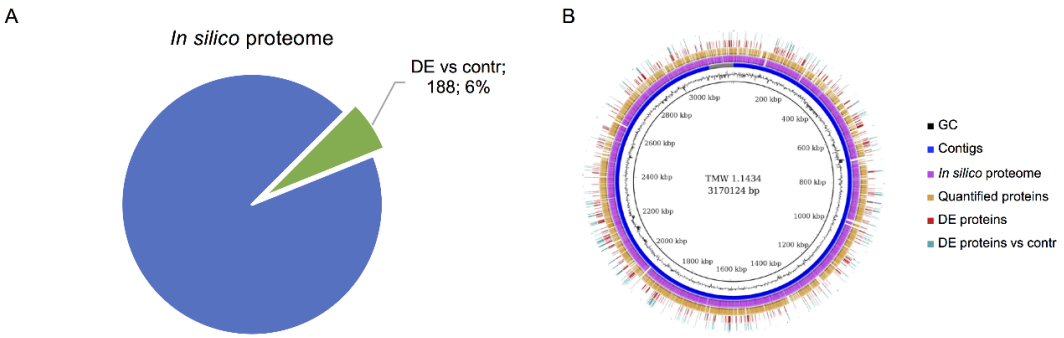


Figure 20: Global analysis of differential protein expression in *Lb. paracasei* subsp. *paracasei* F19 in reference to control condition. (A) Differentially expressed (DE) protein proportion of the *in silico* proteome. (B) BLAST ring image of proteomic properties. All rings are described from the inside to the outside: ring 1 (black) represents the total genome sequence of F19 as reference with bp coordinates; ring 2 (black) shows the GC content; ring 3 (blue) represents the different contigs of F19; ring 4 (purple) shows the coding density, illustrating the *in silico* annotated proteome; ring 5 (orange) represents all quantified proteins; ring 6 (red) shows all differentially expressed (DE) proteins; ring 7(aqua) illustrates differentially expressed (DE) proteins in reference to control condition (vs contr).

#### 4.3.2.2 Analysis of stress responses

##### 4.3.2.2.1 Heat stress

*Identified proteins and properties*

In total, ten proteins were DE during heat stress, of which seven and three proteins were up and downregulated, respectively, as indicated by Log2FC (Figure 21A). Highest upregulation was observed for a hypothetical protein, followed by an uncategorized peptidoglycan-binding protein LysM. LysM was 1-time higher expressed during heat stress. Highest downregulation was identified for acetyl-CoA carboxylase biotin carboxyl carrier protein subunit (accB). accB was 1.3-times lower expressed during heat stress.

The temperature upshift affected proteins of different SCL. Cytoplasmic and cell membrane proteins, as well as proteins of unknown subcellular localization were DE (Figure 21B).

Detailed data of differential protein expression during heat stress can be obtained from Table 18. For the functional analyses and metabolic reconstruction of the proteins, see the following paragraph.

*Functional analysis and metabolic reconstruction*

60 % of DE proteins (3 up and 3 downregulated proteins, respectively) could be assigned to SEED categories and the corresponding classification system. All remaining uncategorized DE proteins were upregulated, of which two were annotated as hypothetical proteins and one as transcriptional regulator.

Figure 21C displays the overall functional analysis of DE proteins during heat stress. As illustrated, this stress condition affects numerous biological functions, which is apparent from SEED classification:

- Protein Metabolism
- Cofactors Vitamins Prosthetic Groups Pigments
- Nucleosides and Nucleotides
- RNA Metabolism
- Fatty Acids Lipids and Isoprenoids
- Secondary Metabolism (see “Other SEED categories”).

DE proteins of the biological function of Protein Metabolism, Nucleosides and Nucleotides and Secondary Metabolism were upregulated, while DE proteins of the biological function of Cofactors Vitamins Prosthetic Groups Pigments, RNA Metabolism and Fatty Acids Lipids and Isoprenoids downregulated (Figure 21A). Details regarding the differential expression, SEED classification and metabolic potential can be obtained from Table 18. Interesting findings are presented hereinafter.

Although upregulated peptidoglycan-binding protein LysM is uncategorized, LysM plays a role in bacterial peptidoglycan signal recognition and in bacterial pathogenesis. LysM harbors a lysin motif (LysM) domain that is responsible for binding to peptidoglycans in the cell wall of gram positive bacteria.

Upregulation was also indicated for a oxidoreductase peptide-methionine (R)-S-oxide reductase that is involved in the biological function of Protein Metabolism. The oxidoreductase peptide-methionine (R)-S-oxide reductase plays a role in protein processing and modification by acting on a sulfur group of donors with a disulfide as acceptor. It is responsible for the reduction of the oxidized form of methionine (R-form of methionine S-oxide) back to methionine and thereby reactivating damaged peptides. Thus, it plays a role in preventing oxidative-stress damage caused by reactive oxygen species.

Downregulated accB is involved in the biological function of Fatty Acids Lipids and Isoprenoids. In particular, it is required for fatty acid metabolism by initiating the fatty acid biosynthesis FASII. accB catalyzes in a two-step reaction first the carboxylation of the carrier protein using biotin carboxylase, followed by the transfer of the carboxyl group using the transcarboxylase in order to form malonyl-CoA for fatty acid biosynthesis.

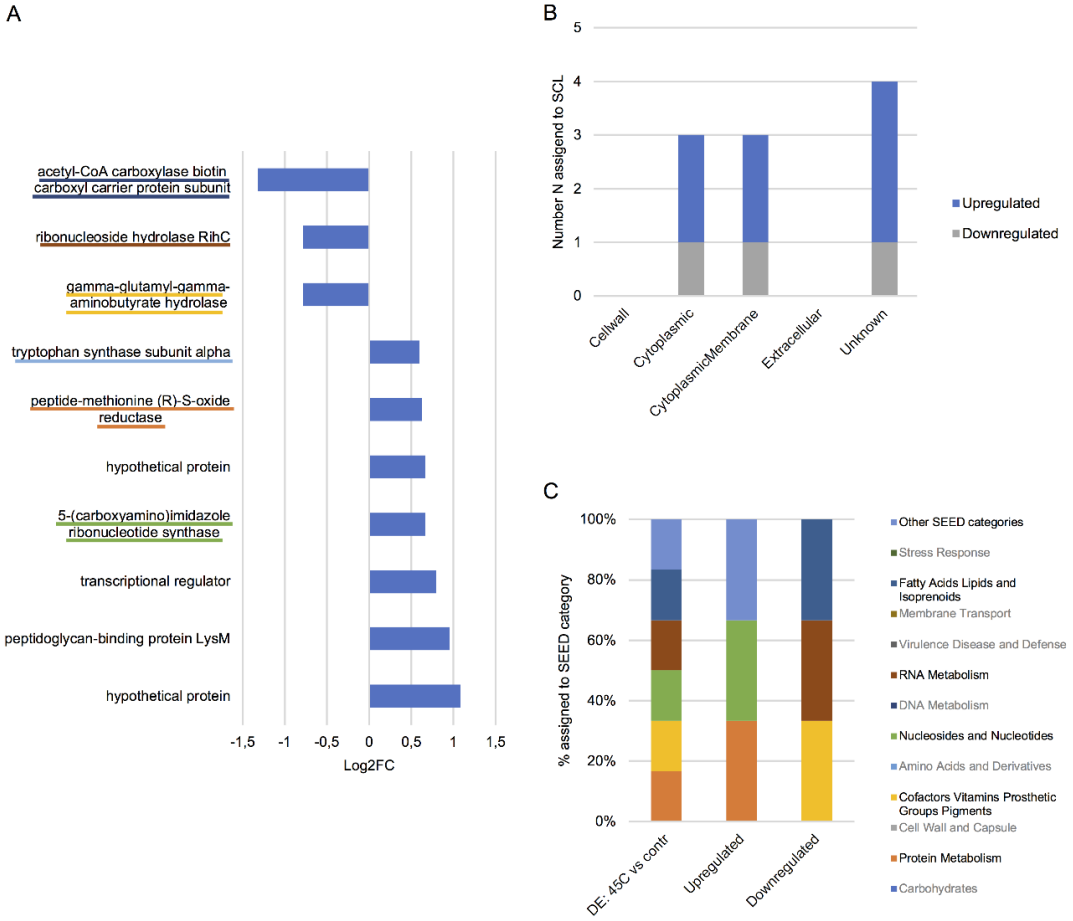


Figure 21: Differential protein expression of *Lb. paracasei* subsp. *paracasei* F19 during heat stress with respect to control condition (DE: 45C vs contr). (A) Differentially expressed (DE) proteins with respective Log2FoldChange (Log2FC) are illustrated. Based on SEED subsystem analysis, assigned SEED category of respective protein is emphasized using a colored underscore (where applicable), whereby color legend of SEED category can be obtained from C. (B) Subcellular localization prediction of DE proteins. (C) Functional analysis of DE proteins based on SEED subsystem analysis. Percentage (%) of assigned proteins are shown with respect to functional SEED category of total DE proteins (DE: 45C vs contr), upregulated and downregulated proteins.

Table 18: Differential protein expression of *Lb. paracasei* subsp. *paracasei* F19 during heat stress with respect to control condition. Listed are DE proteins with respect to NCBI-annotation, Log2FoldChange (Log2FC), log10 p-value (log10.p), SEED category, subcellular localization prediction (SCL) and KO/EC number.

| protein_ID | NCBI-annotation | Log2FC | log10.p | SEED category | SCL | KO number | EC number |
|---|---|---|---|---|---|---|---|
| BBD24_10245 | hypothetical protein | 1.08 | 1.82 | | Unknown | | |
| BBD24_09720 | peptidoglycan-binding protein LysM | 0.95 | 1.73 | | Unknown | | |
| BBD24_00645 | transcriptional regulator | 0.80 | 2.58 | | Cytoplasmic | | |
| BBD24_09025 | 5-(carboxyamino)imidazole ribonucleotide synthase | 0.66 | 2.10 | Nucleosides and Nucleotides | Cytoplasmic Membrane | K01589 | EC 4.1.1.21 |
| BBD24_14215 | hypothetical protein | 0.66 | 1.31 | | Cytoplasmic Membrane | K09167 | |
| BBD24_07900 | peptide-methionine (R)-S-oxide reductase | 0.62 | 1.82 | Protein Metabolism | Unknown | K07305 | EC 1.8.4.12 |
| BBD24_00380 | tryptophan synthase subunit alpha | 0.59 | 2.10 | Secondary Metabolism | Cytoplasmic | K01695 | EC 4.2.1.20 |
| BBD24_02565 | gamma-glutamyl-gamma-aminobutyrate hydrolase | -0.79 | 3.37 | Cofactors Vitamins Prosthetic Groups Pigments | Cytoplasmic | K07010 | EC 2.6.1.85 |
| BBD24_01885 | ribonucleoside hydrolase RihC | -0.79 | 1.66 | RNA Metabolism | Cytoplasmic Membrane | K12700 | EC 3.2.2.1 |
| BBD24_09540 | acetyl-CoA carboxylase biotin carboxyl carrier protein subunit | -1.32 | 1.70 | Fatty Acids Lipids and Isoprenoids | Unknown | | |

#### 4.3.2.2.2 Potassium chloride stress

*Identified proteins and properties*

In total, 22 proteins were DE during potassium chloride stress (approximately 1 % of the *in silico* proteome), of which 12 and 10 proteins were up- and downregulated, respectively, as indicated by Log2FC (Figure 22A). Highest upregulation was observed for a hypothetical protein, followed by two glycine-betaine ABC transporters and one glycine-betaine/L-proline ABC transporter binding protein, which were ≥1.7 times higher expressed during potassium chloride stress. Highest downregulation was identified for uncategorized DUF5011 domain-containing protein, which was 1.1-times lower expressed during potassium chloride stress.

Potassium chloride stress affected proteins of different SCL. Cytoplasmic and cell membrane proteins, as well as cell wall proteins and proteins of unknown subcellular localization were DE (Figure 22B).

Detailed data of differential protein expression during potassium chloride stress can be obtained from Table 19. For the functional analysis and metabolic reconstruction of the proteins, see the following paragraph.

*Functional analysis and metabolic reconstruction*

45 % of DE proteins (7 up and 3 downregulated proteins, respectively) could be assigned to SEED categories and the corresponding classification system. Of the remaining uncategorized DE proteins, 7 and 5 were down and upregulated, respectively, of which overall three were annotated as hypothetical proteins. Further, five uncategorized DE proteins belong to the enzyme class of transferases.

Figure 22C displays the overall functional analysis of DE proteins during potassium chloride stress. As illustrated, this stress condition affects various biological functions, which is apparent from SEED classification:

- Protein Metabolism
- Amino Acids and Derivatives
- RNA Metabolism
- Membrane Transport
- Stress Response
- Respiration (see “Other SEED categories”)

DE proteins of the biological function of Amino Acids and Derivatives, Membrane Transport, Stress Response and Respiration were upregulated, while DE proteins of the biological function of RNA metabolism were downregulated. Within the biological function of Protein Metabolism, we found two DE proteins that were up and

downregulated, respectively (Figure 22A). Details regarding the differential expression, SEED classification and metabolic potential can be obtained from Table 19. Striking findings are presented hereinafter.

Highly upregulated glycine-betaine ABC transporters (proX, proW) and the glycine-betaine/L-proline ABC transporter binding protein (proV) are involved in the biological function of stress response, especially in the osmotic stress response. As members of the ATP-binding cassette (ABC) transporter superfamily, these upregulated transporter proteins form organic ion ABC transporters in the cell membrane that specifically enable the intracellular accumulation of osmoprotectants (osmolytes), such as glycine-betaine and L-proline. Additionally, two more DE proteins were found to be upregulated that are related to ABC transport system, i.e. the uncategorized ABC transporter ATP-binding protein and the peptide ABC transporter substrate-binding protein, which was assigned to the biological function of Membrane Transport. This peptide ABC transporter substrate-binding protein is required for the transport of oligopeptides using an ABC transport system. In total, five proteins were upregulated during potassium chloride stress that are members of the superfamily of ABC transporters.

However, two DE proteins were found to be downregulated during potassium chloride stress that are involved in the biological function of RNA metabolism. Both proteins play a role in RNA processing and modification. Metabolic reconstruction via KEGG color&pathway mapper was performed using the appropriate KO numbers of the proteins. The methylenetetrahydrofolate---tRNA-(uracil54-C5)-methyltransferase (FADH2-oxidizing) (Trm8FO) is metabolically responsible for post-translational modification in mature tRNA. Trm8FO catalyzes the folate-dependent formation of 5-methyl-uridine at position 54 (M-5-U54) in all tRNAs. The pseudouridine synthase catalyzes the formation of uridine to pseudouridine in RNA.

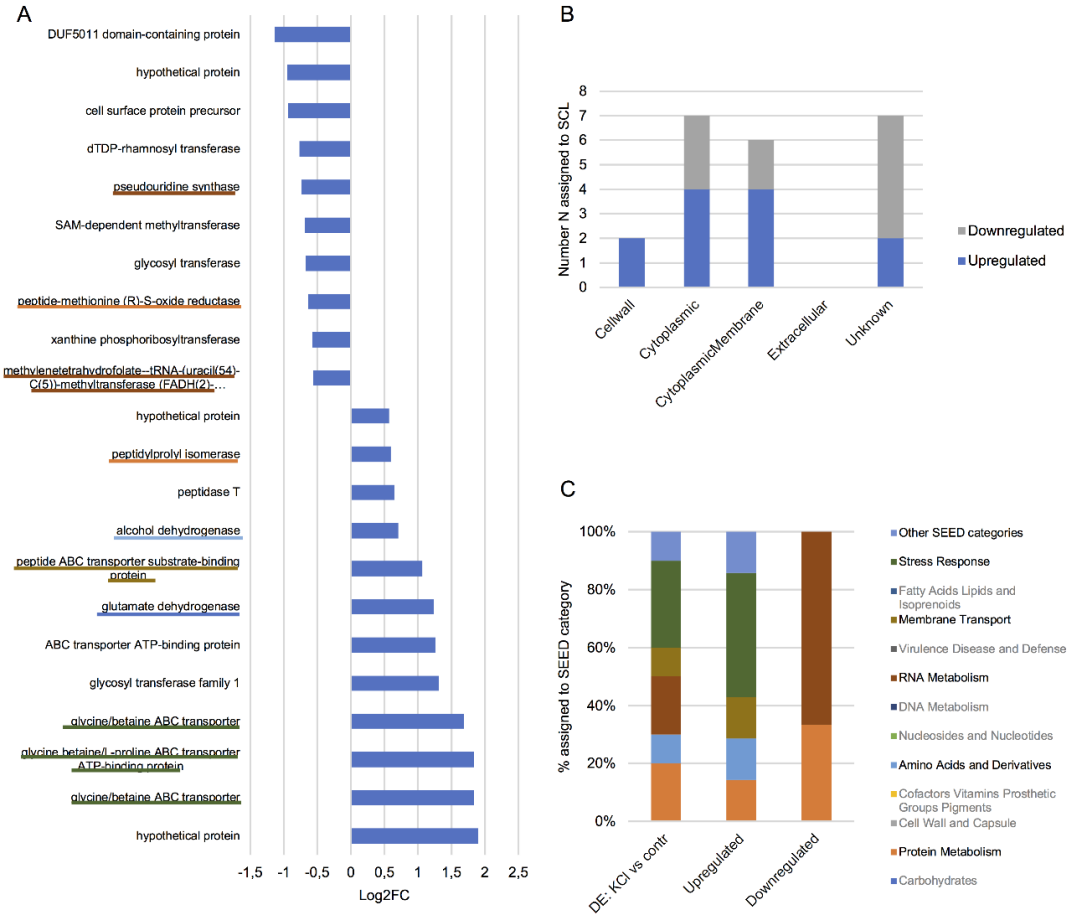


Figure 22: Differential protein expression of *Lb. paracasei* subsp. *paracasei* F19 during potassium chloride stress with respect to control condition (DE: KCl vs contr). (A) Differentially expressed (DE) proteins and respective Log2FoldChanges (Log2FC) are illustrated. Based on SEED subsystem analysis, assigned SEED category of respective protein is emphasized using a colored underscore (where applicable), whereby color legend of SEED category can be obtained from C. (B) Subcellular localization prediction of DE proteins. (C) Functional analysis of DE proteins based on SEED subsystem analysis. Percentage (%) of assigned proteins are shown with respect to functional SEED category of total DE proteins (DE: KCl vs contr), upregulated and downregulated proteins.

Table 19: Differential protein expression of *Lb. paracasei* subsp. *paracasei* F19 during potassium chloride stress with respect to control condition. Listed are DE proteins with respect to NCBI-annotation, Log2FoldChange (Log2FC), log10 p-value (log10.p), SEED category, subcellular localization prediction (SCL) and KO/EC number.

| protein_ID | NCBI-annotation | Log2FC | log10.p | SEED category | SCL | KO number | EC number |
|---|---|---|---|---|---|---|---|
| BBD24_12740 | hypothetical protein | 1.90 | 10.54 | | Unknown | | |
| BBD24_10650 | glycine-betaine ABC transporter | 1.83 | 5.51 | Stress Response | Cytoplasmic Membrane | K02001 | |
| BBD24_10655 | glycine-betaine/L-proline ABC transporter ATP-binding protein | 1.83 | 11.14 | Stress Response | Cytoplasmic Membrane | K02000 | EC 3.6.3.32 |
| BBD24_10645 | glycine-betaine ABC transporter | 1.68 | 10.86 | Stress Response | Cellwall | K02002 | |
| BBD24_14275 | glycosyl transferase family 1 | 1.32 | 4.59 | | Unknown | | |
| BBD24_07940 | ABC transporter ATP-binding protein | 1.27 | 2.84 | | Cytoplasmic Membrane | K01990 | |
| BBD24_03475 | glutamate dehydrogenase | 1.23 | 5.49 | Amino Acids and Derivatives | Cytoplasmic | K00262 | EC 1.4.1.4 |
| BBD24_00895 | peptide ABC transporter substrate-binding protein | 1.07 | 2.88 | Membrane Transport | Cell wall | K15580 | |
| BBD24_14485 | alcohol dehydrogenase | 0.71 | 2.03 | Respiration | Cytoplasmic | K08317 | EC 1.1.1.6 |
| BBD24_01535 | peptidase T | 0.65 | 1.42 | | Cytoplasmic | K01258 | |

| | | | | | | | |
|---|---|---|---|---|---|---|---|
| BBD24_11260 | peptidylprolyl isomerase | 0.60 | 1.30 | Protein Metabolism | Cytoplasmic Membrane | K07533 | |
| BBD24_00915 | hypothetical protein | 0.56 | 1.32 | | Cytoplasmic | | |
| BBD24_07330 | methylenetetrahydrofolate--tRNA-(uracil(54)- C(5))-methyltransferase (FADH(2)-oxidizing) TrmFO | -0.57 | 1.93 | RNA Metabolism | Cytoplasmic | K04094 | |
| BBD24_05875 | xanthine phosphoribosyl transferase | -0.57 | 1.78 | | Cytoplasmic | K03816 | |
| BBD24_07900 | peptide-methionine (R)-S-oxide reductase | -0.64 | 1.96 | Protein Metabolism | Unknown | K07305 | EC 1.8.4.12 |
| BBD24_10180 | glycosyl transferase | -0.68 | 1.73 | | Cytoplasmic Membrane | | |
| BBD24_07790 | SAM-dependent methyltransferase | -0.70 | 1.94 | | Unknown | | |
| BBD24_07145 | pseudouridine synthase | -0.74 | 4.29 | RNA Metabolism | Cytoplasmic | K06178 | EC 4.2.1.70 |
| BBD24_10190 | dTDP-rhamnosyl transferase | -0.77 | 4.09 | | Cytoplasmic Membrane | | |
| BBD24_05795 | cell surface protein precursor | -0.94 | 2.73 | | Unknown | | |
| BBD24_03220 | hypothetical protein | -0.95 | 4.20 | | Unknown | | |
| BBD24_02975 | DUF5011 domain-containing protein | -1.14 | 2.17 | | Unknown | | |

#### 4.3.2.2.3 Drying stress

*Identified proteins and properties*

In total, 58 proteins were DE during drying stress (approximately 2 % of *in silico* proteome), of which 35 and 23 proteins were up and downregulated, respectively, as indicated by Log2FC (Figure 24A). Highest upregulation was observed for two hypothetical proteins, followed by phosphoribosylaminoimidazolesuccinocarboxamide synthase (SAICAR), which was 2.6-times higher expressed during drying stress. Highest downregulation was found for 30S ribosomal protein S16 that was 2.8-times lower expressed during drying. Overall four ribosomal proteins were at least 1.2-times lower expressed.

Desiccation affected proteins of different SCL. Cytoplasmic and cell membrane proteins, as well as proteins of unknown subcellular localization were DE. There were no cell wall or extracellular proteins DE (Figure 24B).

Detailed data of differential protein expression during drying stress can be found in Table 20. For the functional analysis and metabolic reconstruction, see the following paragraph.

*Functional analysis and metabolic reconstruction*

50 % of DE proteins (18 up and 11 downregulated proteins, respectively) could be assigned to SEED categories and the corresponding classification system. Of the remaining uncategorized DE proteins, 12 and 17 were down and upregulated, respectively, of which overall ten were annotated as hypothetical proteins.

Figure 24C displays the overall functional analysis of DE proteins during drying stress. As illustrated, this stress condition affects a wide range of biological functions, which is apparent from SEED classification. Primarily affected SEED categories/biological functions are:

- Carbohydrates
- Protein Metabolism
- Cofactors Vitamins Prosthetic Groups Pigments
- Nucleosides and Nucleotides
- Virulence Disease and Defense (VDD)
- Fatty Acids Lipids and Isoprenoids
- Regulation and Cell signaling (see “Other SEED categories”)

DE proteins of the biological function of Carbohydrates, Nucleosides and Nucleotides, Stress Response and Regulation and Cell signaling were upregulated, while DE proteins of the biological function of Protein Metabolism and VDD were mostly, with the exception

of an amidophosphoribosyltransferase (biological function VDD), downregulated (Figure 24A). Details regarding the differential expression, SEED classification and metabolic potential can be obtained from Table 20. Striking findings are presented hereinafter.

Highly upregulated SAICAR is assigned to the biological function of nucleosides and nucleotides. With nine other DE proteins, this makes a total of ten upregulated proteins that are involved in nucleoside and nucleotide metabolism. Strikingly, this is the largest number of proteins of a biological function that have been DE in the presence of stress. These upregulated proteins are required for either purine or pyrimidine metabolism:

Purine metabolism:

- phosphoribosylaminoimidazolesuccinocarboxamide synthase (SAICAR)
- 5-(carboxyamino)imidazole ribonucleotide synthase (N5-CAIR)
- phosphoribosylamine--glycine-ligase (purD)
- phosphoribosylformylglycinamidine cyclo-ligase (purM)

Pyrimidine metabolism:

- carbamoyl phosphate synthase small subunit (CPSase)
- bifunctional pyr operon transcriptional regulator/uracil phosphoribosyl transferase (pyrR)
- dihydroorotate dehydrogenase B catalytic subunit (pyrDB)
- orotate phosphoribosyltransferase (OPRTase)
- carbamoyl phosphate synthase large subunit (CPSase)

The metabolic reconstruction of these upregulated proteins revealed that they are involved in the first steps of purine and pyrimidine biosynthesis (Figure 23). Particularly, in the synthesis of the intermediate products 5-phosphoribosyl-a-1-pyrophosphate (PRPP), IMP and UMP.

A Purine metabolisms

*in silico* proteome

up regulated protein

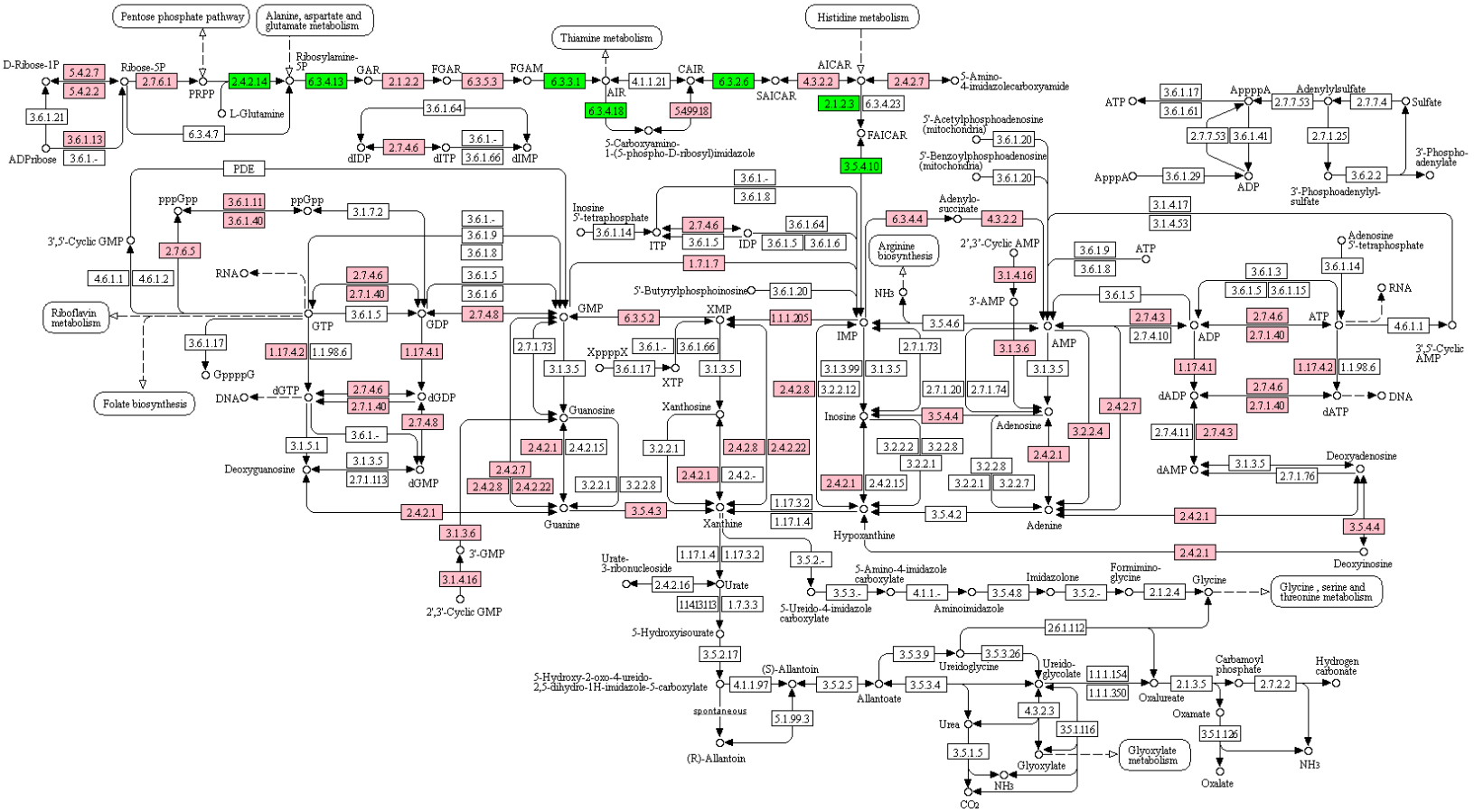

B Pyrimidine metabolisms

*in silico* proteome

up regulated protein

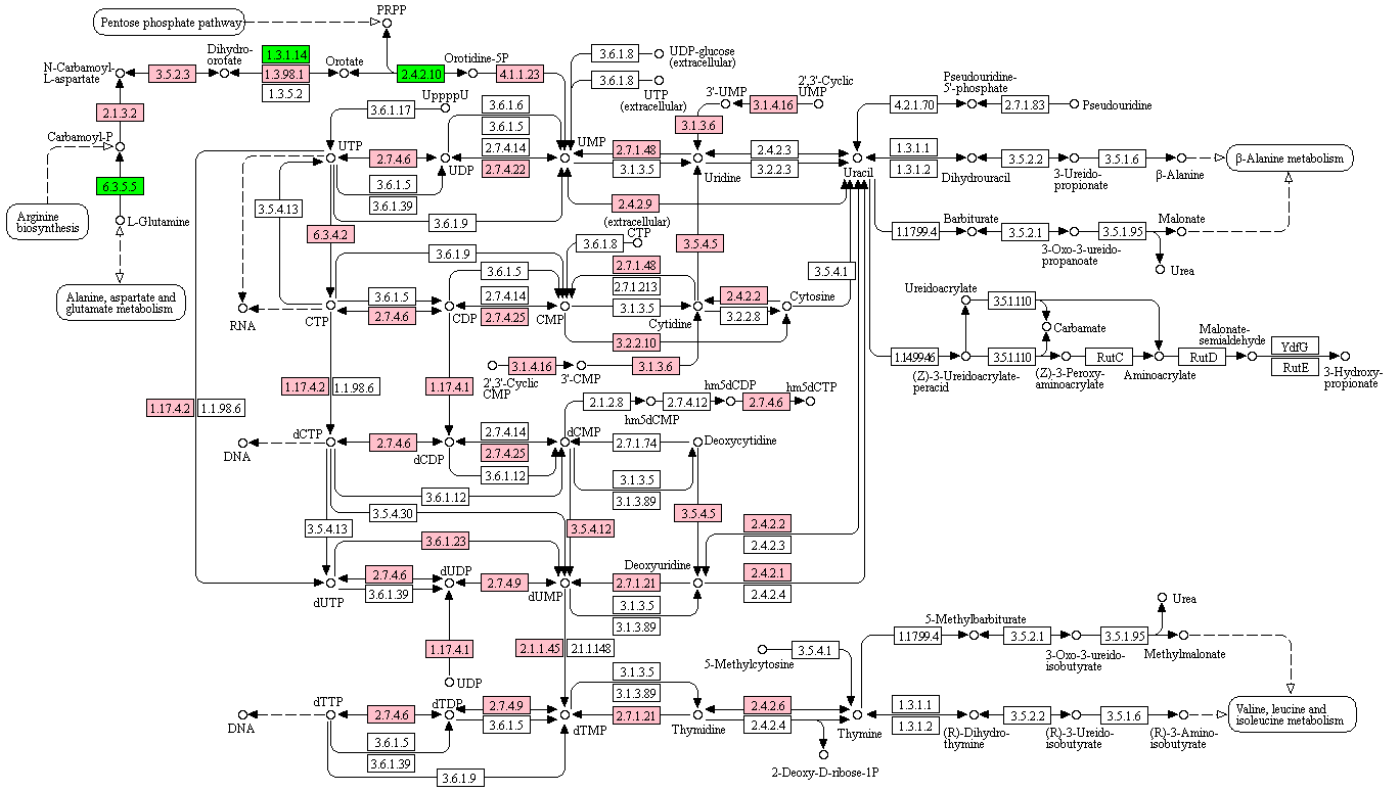


Figure 23: Nucleoside and nucleotide metabolism of *Lb. paracasei* subsp. *paracasei* F19 during drying stress. Metabolic reconstruction of *in silico* proteome (■) and differentially expressed (DE) proteins. Upregulated proteins are emphasized (■).

Highly downregulated 30S ribosomal protein S16 is involved in protein metabolism. Additionally, three other bacterial SSU/LSU ribosomes (50S ribosomal protein L28, 50S ribosomal protein L35, 30S ribosomal protein S14), of which two are involved in protein metabolism, were found to be downregulated. In total, four bacterial SSU/LSU ribosomes that are downregulated during drying stress. As ribosomal proteins, they are involved in protein biosynthesis for translation initiation by interacting with rRNA, for ribosomal assembly and as ribosomal structural constituent.

The 3’ end of the 30S ribosomal protein S16 contains the anti-Shine-Dalgarno sequence and binds upstream to the AUG start codon on the mRNA. S16 is thus responsible for translational initiation. 30S ribosomal protein S14 requires a metal atom zinc as cofactor in order to be catalytically active. It is the major S14 protein in the ribosome and binds 16S rRNA. 30S ribosomal protein S14 is also required for the assembly of 30S particles, particularly for binding of S2 and S3 to the 30S subunit. It further associates the 30S with the 50S subunit and may also be responsible for determining the conformation of the 16S rRNA at the A site. Besides, the 50S ribosomal protein L35, another protein that plays a role in protein biosynthesis (especially translation), is also involved in the biological function of Virulence Disease and Defense (VDD). It is required for invasion and intracellular resistance by acting as mycobacterium virulence operon. The 50S ribosomal protein L28 is required for ribosome assembly. It interacts with 23S rRNA and crosslinks to L9. The interaction of L28 is stimulated by the two 50S ribosomal proteins L15 and L17.

At last, a protein was found to be DE during drying stress that is involved in the biological function of stress response. According to SEED classification, the upregulated DNA starvation/stationary phase protection protein plays a role in the oxidative stress response by binding to DNA in order to protect it against oxidative stress during nutrient starvation.

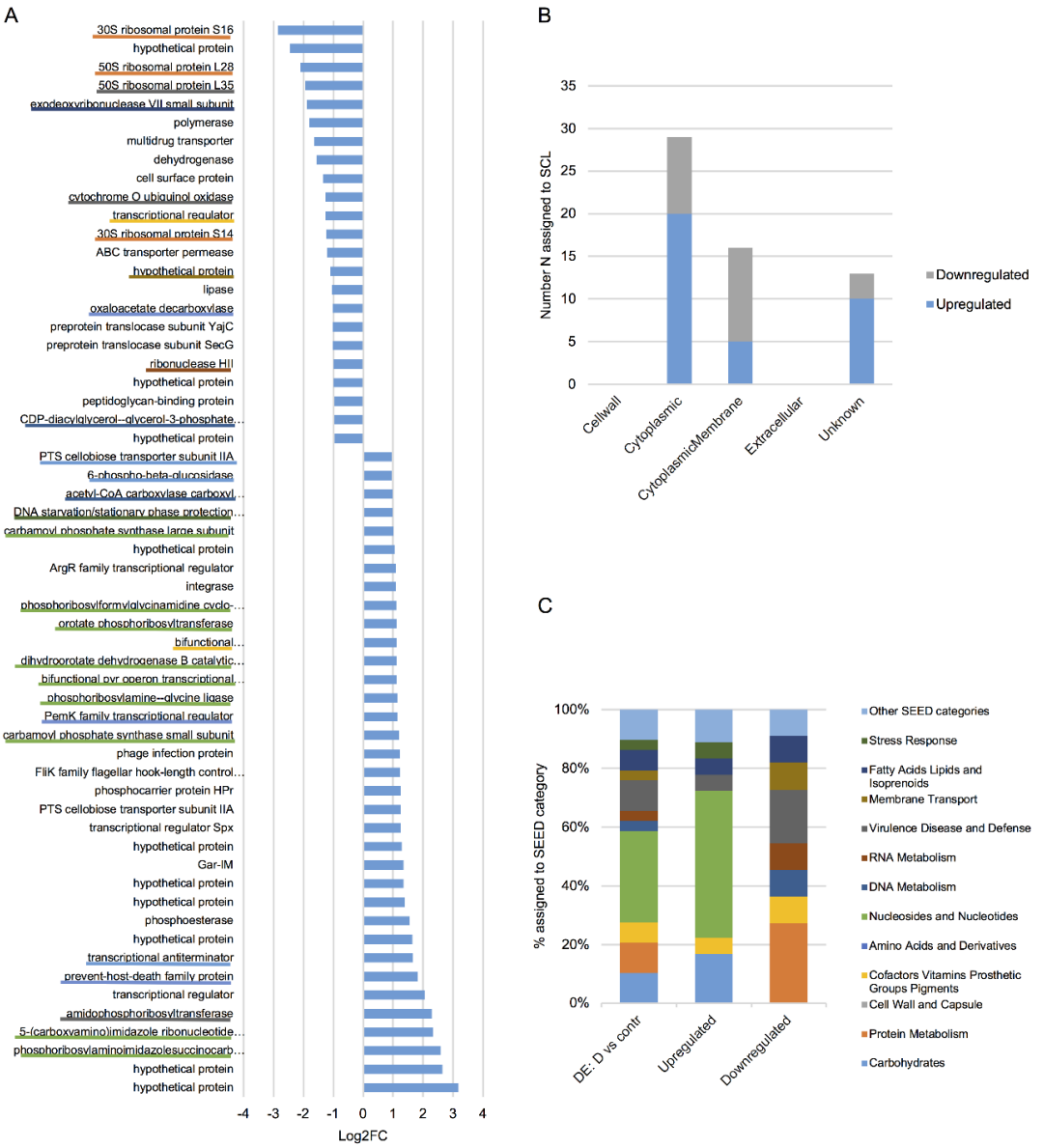


Figure 24: Differential protein expression of *Lb. paracasei* subsp. *paracasei* F19 during drying stress in reference to control condition (DE: D vs contr). (A) Differentially expressed (DE) proteins with respective Log2FoldChange (Log2FC) are illustrated. Based on SEED subsystem analysis, where possible, assigned SEED category of respective protein is emphasized using a colored underscore, whereby color legend of SEED category can be obtained from C. (B) Subcellular localization prediction of DE proteins. (C) Functional analysis of DE proteins based on SEED subsystem analysis. Percentage (%) of assigned proteins are shown with respect to functional SEED category of total DE proteins (DE: D vs contr), upregulated and downregulated proteins.

Table 20: Differential protein expression of *Lb. paracasei* subsp. *paracasei* F19 during drying stress in reference to control condition. Listed are DE proteins with respect to NCBI-annotation, Log2FoldChange (Log2FC), log10 p-value (log10.p), SEED category, subcellular localization prediction (SCL) and KO/EC number.

| protein_ID | NCBI-annotation | Log2FC | log10.p | SEED category | SCL | KO number | EC number |
|---|---|---|---|---|---|---|---|
| BBD24_11955 | hypothetical protein | 3.18 | 9.58 | | Unknown | | |
| BBD24_10375 | hypothetical protein | 2.64 | 4.61 | | Unknown | | |
| BBD24_09020 | Phosphoribosylamino-imidazolesuccinocarboxamide synthase | 2.59 | 6.52 | Nucleosides and Nucleotides | Unknown | K01923 | EC 6.3.2.6 |
| BBD24_09025 | 5-(carboxyamino)imidazole ribonucleotide synthase | 2.33 | 12.08 | Nucleosides and Nucleotides | Cytoplasmic Membrane | K01589 | EC 4.1.1.21 |
| BBD24_09000 | Amidophosphoribosyl-transferase | 2.29 | 3.01 | Virulence Disease and Defense | Cytoplasmic | K00764 | EC 2.4.2.14 |
| BBD24_04390 | transcriptional regulator | 2.06 | 1.68 | | Unknown | | |
| BBD24_03045 | prevent-host-death family protein | 1.83 | 5.43 | Regulation and Cell signaling | Cytoplasmic | K19159 | |
| BBD24_13350 | transcriptional antiterminator | 1.66 | 2 | Carbohydrates | Cytoplasmic | K02538 | |
| BBD24_03750 | hypothetical protein | 1.65 | 5.5 | | Cytoplasmic | | |
| BBD24_01235 | phosphoesterase | 1.55 | 1.32 | | Cytoplasmic | | |

| | | | | | | | |
|---|---|---|---|---|---|---|---|
| BBD24_15015 | hypothetical protein | 1.38 | 1.33 | | Cytoplasmic | | |
| BBD24_15000 | hypothetical protein | 1.35 | 1.79 | | Unknown | | |
| BBD24_00220 | Gar-IM | 1.34 | 2.92 | | Cytoplasmic Membrane | | |
| BBD24_00480 | hypothetical protein | 1.3 | 5.46 | | Unknown | | |
| BBD24_08930 | transcriptional regulator Spx | 1.25 | 1.72 | | Cytoplasmic Membrane | K16509 | |
| BBD24_13110 | PTS cellobiose transporter subunit IIA | 1.25 | 1.52 | | Cytoplasmic | K02759 | |
| BBD24_09050 | phosphocarrier protein HPr | 1.25 | 1.72 | | Cytoplasmic | K11189 | |
| BBD24_13980 | FliK family flagellar hook-length control protein | 1.23 | 6.45 | | Unknown | | |
| BBD24_00870 | phage infection protein | 1.22 | 4.57 | | Cytoplasmic Membrane | K01421 | |
| BBD24_07575 | carbamoyl phosphate synthase small subunit | 1.2 | 4.18 | Nucleosides and Nucleotides | Cytoplasmic | K01956 | EC 6.3.5.5 |
| BBD24_12575 | PemK family transcriptional regulator | 1.14 | 1.31 | Regulation and Cell signaling | Unknown | K07171 | |
| BBD24_08980 | phosphoribosylamine--glycine-ligase | 1.13 | 6.45 | Nucleosides and Nucleotides | Cytoplasmic | K01945 | EC 6.3.4.13 |

| | | | | | | | |
|---|---|---|---|---|---|---|---|
| BBD24_07595 | bifunctional pyr operon transcriptional regulator/ uracil phosphoribosyltransferase | 1.13 | 2.34 | Nucleosides and Nucleotides | Cytoplasmic | K02825 | EC 2.4.2.9 |
| BBD24_07565 | dihydroorotate dehydrogenase B catalytic subunit | 1.13 | 1.39 | Nucleosides and Nucleotides | Cytoplasmic | K17828 | EC 1.3.3.1 |
| BBD24_08985 | bifunctional phosphoribosylaminoimidazole-carboxamide formyltransferase/ IMP cyclohydrolase | 1.13 | 5.57 | Cofactors Vitamins Prosthetic Groups Pigments | Cytoplasmic | K00602 | EC 2.1.2.3 |
| BBD24_07555 | orotate phosphoribosyltransferase | 1.12 | 2.98 | Nucleosides and Nucleotides | Cytoplasmic Membrane | K00762 | EC 2.4.2.10 |
| BBD24_08995 | Phosphoribosylformyl-glycinamidine cyclo-ligase | 1.11 | 2.59 | Nucleosides and Nucleotides | Cytoplasmic | K01933 | EC 6.3.3.1 |
| BBD24_10425 | integrase | 1.09 | 1.63 | | Unknown | | |
| BBD24_08425 | ArgR family transcriptional regulator | 1.08 | 2.74 | | Cytoplasmic | K03402 | |
| BBD24_12980 | hypothetical protein | 1.05 | 1.79 | | Unknown | | |
| BBD24_07570 | carbamoyl phosphate synthase large subunit | 1.01 | 3.35 | Nucleosides and Nucleotides | Cytoplasmic | K01955 | EC 6.3.5.5 |

| | | | | | | | |
|---|---|---|---|---|---|---|---|
| BBD24_14895 | DNA starvation/stationary phase protection protein | 0.98 | 2.28 | Stress Response | Cytoplasmic | | |
| BBD24_10485 | acetyl-CoA carboxylase carboxyl transferase subunit alpha | 0.97 | 1.44 | Fatty Acids Lipids and Isoprenoids | Cytoplasmic | K01962 | EC 6.4.1.2 |
| BBD24_10835 | 6-phospho-beta-glucosidase | 0.96 | 1.42 | Carbohydrates | Cytoplasmic | K01223 | EC 3.2.1.86 |
| BBD24_10320 | PTS cellobiose transporter subunit IIA | 0.96 | 1.32 | Carbohydrates | Cytoplasmic | K02759 | EC 2.7.1.69 |
| BBD24_05400 | hypothetical protein | -0.96 | 1.67 | | Cytoplasmic Membrane | | |
| BBD24_04865 | CDP-diacylglycerol--glycerol-3-phosphate 3-phosphatidyltransferase | -0.98 | 1.53 | Fatty Acids Lipids and Isoprenoids | Cytoplasmic Membrane | K00995 | EC 2.7.8.5 |
| BBD24_10865 | peptidoglycan-binding protein | -0.98 | 2.99 | | Unknown | | |
| BBD24_00820 | hypothetical protein | -0.99 | 2.45 | | Cytoplasmic Membrane | | |
| BBD24_07315 | ribonuclease HII | -0.99 | 3.95 | RNA Metabolism | Cytoplasmic | K03470 | EC 3.1.26.4 |
| BBD24_05140 | preprotein translocase subunit SecG | -1.01 | 2.11 | | Cytoplasmic Membrane | K03075 | |
| BBD24_04165 | preprotein translocase subunit YajC | -1.03 | 2.58 | | Cytoplasmic Membrane | K03210 | |

| | | | | | | | |
|---|---|---|---|---|---|---|---|
| BBD24_09500 | oxaloacetate decarboxylase | -1.03 | 1.88 | Respiration | Cytoplasmic | K01571 | EC 4.1.1.3 |
| BBD24_07240 | lipase | -1.05 | 2.76 | | Unknown | | |
| BBD24_10235 | hypothetical protein | -1.1 | 2.03 | Membrane Transport | Cytoplasmic Membrane | | |
| BBD24_02350 | ABC transporter permease | -1.21 | 1.97 | | Cytoplasmic Membrane | K02004 | |
| BBD24_04810 | 30S ribosomal protein S14 | -1.23 | 2.1 | Protein Metabolism | Cytoplasmic | K02954 | |
| BBD24_05405 | transcriptional regulator | -1.26 | 2.94 | Cofactors Vitamins Prosthetic Groups Pigments | Cytoplasmic | | |
| BBD24_04405 | cytochrome O ubiquinol oxidase | -1.28 | 2.61 | Virulence Disease and Defense | Cytoplasmic Membrane | K03975 | |
| BBD24_00795 | cell surface protein | -1.35 | 5.09 | | Unknown | | |
| BBD24_13580 | dehydrogenase | -1.56 | 1.56 | | Cytoplasmic | K05352 | |
| BBD24_04670 | multidrug transporter | -1.65 | 1.36 | | Cytoplasmic Membrane | | |
| BBD24_10195 | polymerase | -1.81 | 2.02 | | Cytoplasmic Membrane | | |
| BBD24_08440 | exodeoxyribonuclease VII small subunit | -1.88 | 2.73 | DNA Metabolism | Cytoplasmic | K03602 | EC 3.1.11.6 |

| | | | | | | |
|---|---|---|---|---|---|---|
| BBD24_08740 | 50S ribosomal protein L35 | -1.94 | 2.85 | Virulence Disease and Defense | Cytoplasmic | K02916 |
| BBD24_08350 | 50S ribosomal protein L28 | -2.11 | 2.88 | Protein Metabolism | Cytoplasmic | K02902 |
| BBD24_06095 | hypothetical protein | -2.46 | 2.17 | | Cytoplasmic Membrane | K02110 |
| BBD24_08265 | 30S ribosomal protein S16 | -2.84 | 1.38 | Protein Metabolism | Cytoplasmic | K02959 |

### 4.3.3 Comparative analysis of stress responses

Stress responses were compared by detecting uniquely and shared DE proteins and by identifying stress conditions inducing similar stress responses. Interesting and striking findings are exemplarily presented in individual subsections. All details can be obtained from Supplementary Part III (III.1.1.2.).

Note that the following subsection including the associated subsections in Supplementary Part III (III.1.1.2.) are exclusively based on DE proteins during stress in reference to control condition and that this fact will not stressed repeatedly by using terminology such as “in reference to control”, “vs. control”, “in stress”, “DE vs. contr.” or “during stress” etc.

#### 4.3.3.1 Unique and shared differentially expressed proteins

It was investigated whether F19 respond to different stress conditions with shared/unique proteomic stress response mechanisms. Therefore, DE proteins of each stress condition were compared by utilizing Venn diagrams (Figure 25A). Out of 188 DE proteins, 132 proteins were uniquely DE, whereas 56 DE proteins were shared in multiple stress conditions (Figure 25B).

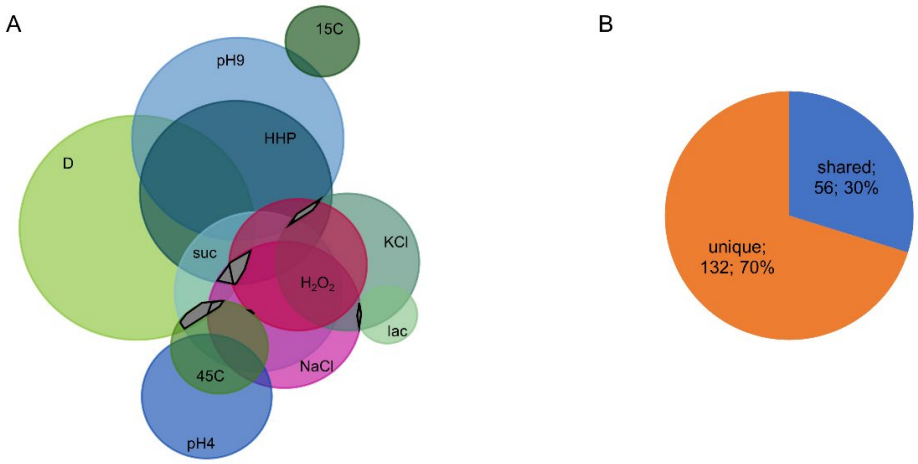


Figure 25: Comparative proteomic analysis of differential protein expression in *Lactobacillus paracasei* subsp. *paracasei* F19 in reference to control condition. Using the Venn diagram, stress condition-specific analyses on basis of DE proteins are compared, and unique and shared DE proteins identified. Stress conditions are color coded: 15C (■), lac (■), 45C (■), D (■), KCl (■), suc (■), pH9 (■), pH4 (■), HHP (■), NaCl (■), $H_2O_2$ (■) (A). The proportion of unique and shared differentially expressed (DE) proteins during stress (B).

Stress conditions that shared most DE proteins are:

1. sodium chloride and sucrose stress (13 DE proteins):

| | | |
|---|---|---|
| Upregulated proteins: | BBD24_09540 | acetyl-CoA carboxylase biotin carboxyl carrier protein subunit |
| Downregulated proteins: | BBD24_00205 | hypothetical protein |
| | BBD24_02975 | DUF5011 domain-containing protein |
| | BBD24_03220 | hypothetical protein |
| | BBD24_04405 | cytochrome O ubiquinol oxidase |
| | BBD24_05525 | hypothetical protein |
| | BBD24_05795 | cell surface protein precursor |
| | BBD24_07145 | pseudouridine synthase |
| | BBD24_07900 | peptide-methionine (R)-S-oxide reductase |
| | BBD24_09375 | hypothetical protein |
| | BBD24_09830 | ABC transporter permease |
| | BBD24_10190 | dTDP-rhamnosyl transferase |
| | BBD24_11030 | hydrolase |

2. high hydrostatic pressure and alkaline stress (13 DE proteins):

| | | |
|---|---|---|
| Upregulated proteins: | BBD24_04740 | phosphohydrolase |
| | BBD24_07565 | dihydroorotate dehydrogenase B catalytic subunit |
| | BBD24_08930 | transcriptional regulator Spx |
| | BBD24_10105 | ATP-dependent Clp protease ATP-binding subunit |
| | BBD24_15055 | hypothetical protein |
| Downregulated proteins: | BBD24_05405 | transcriptional regulator |
| | BBD24_06095 | hypothetical protein |
| | BBD24_08440 | exodeoxyribonuclease VII small subunit |
| | BBD24_10500 | 3-hydroxyacyl-[acyl-carrier-protein] dehydratase FabZ |
| | BBD24_10510 | beta-ketoacyl-[acyl-carrier-protein] synthase II |
| | BBD24_10530 | acyl carrier protein |
| | BBD24_10545 | 3-hydroxyacyl-[acyl-carrier-protein] dehydratase FabZ |
| | BBD24_10865 | peptidoglycan-binding protein |

3. drying and high hydrostatic pressure stress (12 DE proteins):

| | | |
|---|---|---|
| Upregulated proteins: | BBD24_07565 | dihydroorotate dehydrogenase B catalytic subunit |
| | BBD24_08930 | transcriptional regulator Spx |
| Downregulated proteins: | BBD24_00795 | cell surface protein |
| | BBD24_05405 | transcriptional regulator |
| | BBD24_06095 | hypothetical protein |
| | BBD24_07240 | lipase |
| | BBD24_07315 | ribonuclease HII |
| | BBD24_08350 | 50S ribosomal protein L28 |
| | BBD24_08440 | exodeoxyribonuclease VII small subunit |
| | BBD24_08740 | 50S ribosomal protein L35 |
| | BBD24_10195 | polymerase |
| | BBD24_10865 | peptidoglycan-binding protein |

A list of shared/unique DE proteins is presented in Supplementary Part III Table S9 (III.1.1.2.1.). Details regarding the NCBI annotation and the Log2FC can be obtained from the respective stress response section.

Identified unique and shared DE proteins with respect to stress conditions were illustrated applying BRIG (Figure 26).

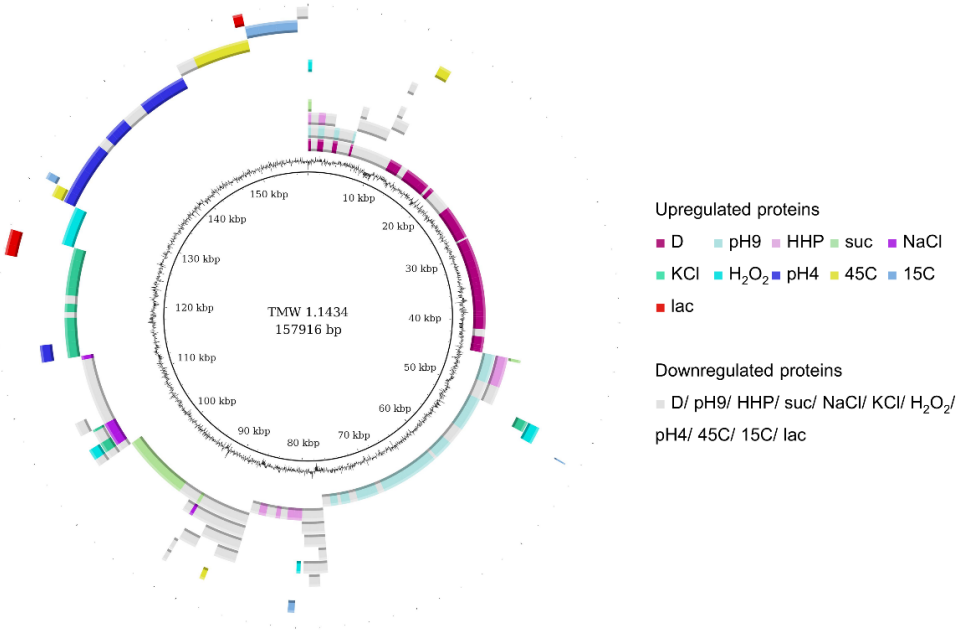


Figure 26: BLAST ring image of DE proteins with respect to stress condition, regulation and comparative alignment of DE proteins. All rings are described from the inside to the outside: ring 1 (black) represents the total sequence of all DE proteins as reference with bp size; ring 2 (black) shows the GC content; ring 3-13 represents all up-/downregulated proteins in the respective stress condition. Upregulation is indicated by different colors depending on the stress condition, while downregulation is color-coded for all stress conditions in grey.

Note that overall 32 shared proteins were downregulated, while only 22 shared proteins were upregulated.

Table 21: Overview of shared and unique proteins with regard to their differentially expression.

| | Shared proteins | Unique proteins | Overall proteins |
|---|---|---|---|
| **Upregulated** | 22 | 88 | 110 |
| **Downregulated** | 32 | 44 | 76 |
| **Mixed regulation** | 2 | 0 | 2 |

### 4.3.3.2 Stress response similarities

Similarities between stress responses induced by different stress conditions were investigated and evaluated using cluster analyses.

Therefore, quantified proteins (1917 proteins) were conducted to hierarchical cluster analysis. Based on their reporter intensities (MS data) in the respective stress condition, similarity coefficients were calculated applying ‘manhattan_bc’, and then using the function ‘hclust’ combined with the cluster method ‘complete linkage’ for plotting. Cluster analysis resulted in a heat map with dendrogram (Figure 27).

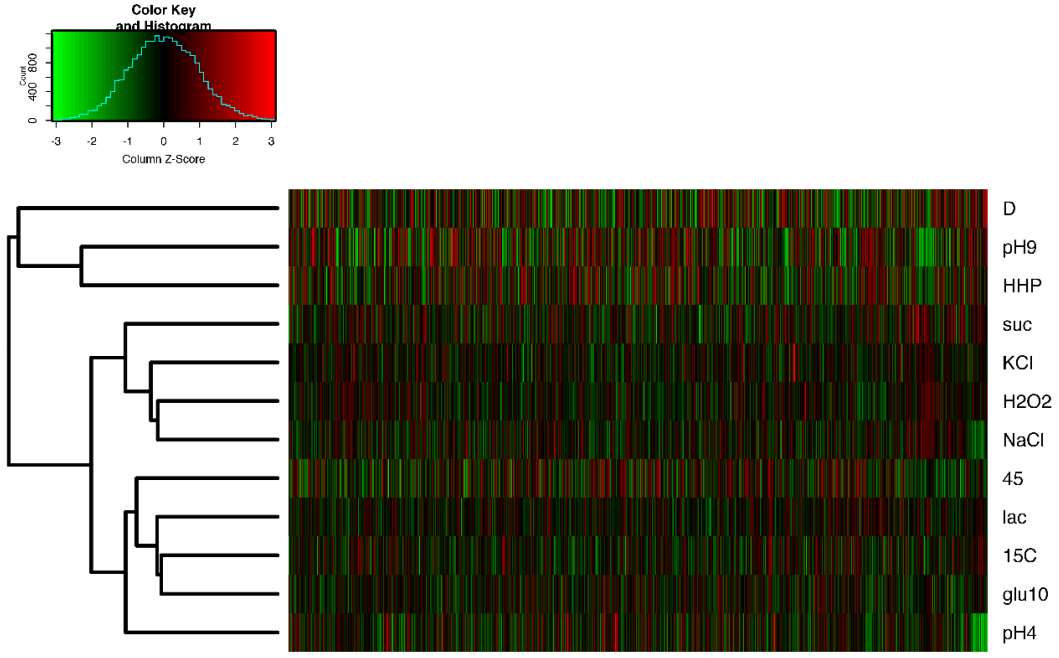


Figure 27: Graphical illustration of stress response similarities of *Lactobacillus paracasei* subsp. *paracasei* F19 using hierarchical cluster analysis. Quantified proteins in reference to control condition are conducted to cluster analysis applying reporter intensities (RI).

A high similarity was identified for drying (D), alkaline (pH9) and high-pressure (HHP) stress response indicating a high similarity between them (cluster 1). With regard to subsection 4.3.3.1, these stresses shared six DE proteins in common, while overall 24 DE proteins were shared in cluster 1 (Figure 28).

Further, potassium chloride (KCl), hydrogen peroxide (H2O2), sodium chloride (NaCl) and sucrose (suc) stress response clustered together indicating a closer relationship (cluster 2). Considering shared and unique proteins (subsection 4.3.3.1), overall 19 DE proteins were shared in cluster 2 (Figure 29). Most shared proteins are a pseudouridine synthase, a hydrolase and cytochrome O ubiquinol oxidase (Table 22).

Last but not least, an additional cluster (cluster 3) was formed by the proteomic responses to acid stress (pH4), heat stress (45C), lactose stress (lac), cold stress (15C) and starvation stress (glu10), indicating a close relation to control condition (contr) and thus a high difference to cluster 1.

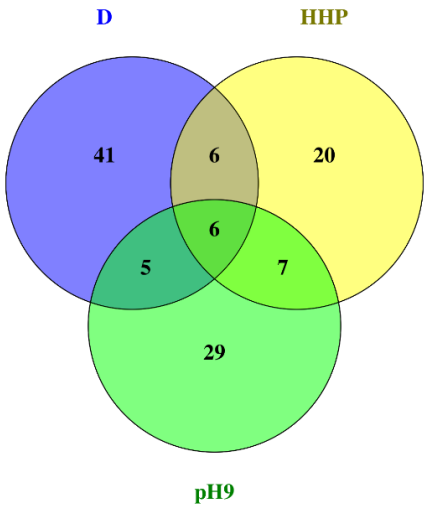


Figure 28: Graphical illustration of shared DE proteins in cluster 1 (D, HHP, pH9) using Venn diagrams. Figure is constructed using Venny 2.0 [357].

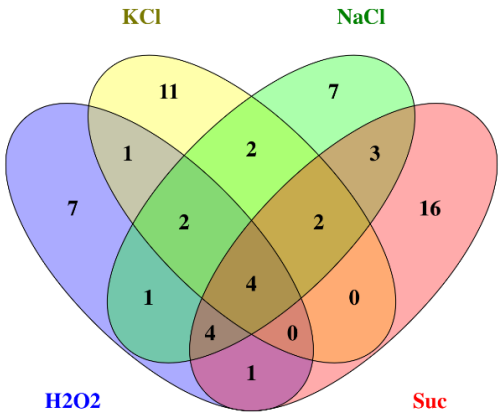


Figure 29: Graphical illustration of shared DE proteins in cluster 2 (KCl, NaCl, suc, H2O2) using Venn diagrams. Figure is constructed using Venny 2.0 [357].

Table 22: Striking proteins shared in sucrose, sodium chloride, potassium chloride and oxidative stress (cluster 2). Listed are NCBI-ID, NCBI-annotation and SEED category with respect to Log2FC in the respective stress condition.

| protein_ID | NCBI-annotation | SEED category | suc | NaCl | KCl | $H_2O_2$ |
|---|---|---|---|---|---|---|
| BBD24_01415 | pyridine nucleotide-disulfide oxidoreductase | | | -0.65 | 0.56 | -0.60 |
| BBD24_02975 | DUF5011 domain-containing protein | | -1.07 | -1.01 | -1.14 | |
| BBD24_04405 | cytochrome O ubiquinol oxidase | Virulence Disease and Defense | -1.58 | -1.52 | | -1.40 |
| BBD24_05795 | cell surface protein precursor | | -1.08 | -1.19 | -0.94 | -0.80 |
| BBD24_07145 | pseudouridine synthase | RNA Metabolism | -0.75 | -0.76 | -0.74 | -0.73 |
| BBD24_07790 | SAM-dependent methyltransferase | | | -0.88 | -0.70 | -0.86 |
| BBD24_07900 | peptide-methionine (R)-S-oxide reductase | Protein Metabolism | -0.75 | -0.92 | -0.64 | |
| BBD24_09830 | ABC transporter permease | | -0.73 | -0.72 | | -0.79 |
| BBD24_10190 | dTDP-rhamnosyl transferase | | -0.84 | -0.85 | -0.77 | -0.80 |
| BBD24_10645 | glycine/betaine ABC transporter | Stress Response | | | 1.68 | |
| BBD24_10650 | glycine/betaine ABC transporter | Stress Response | | | 1.83 | |
| BBD24_10655 | glycine betaine/L-proline ABC transporter ATP-binding protein | Stress Response | | | 1.83 | |
| BBD24_11030 | hydrolase | Membrane Transport | -1.32 | -1.32 | | -1.06 |
| BD24_14275 | glycosyl transferase family 1 | | | 1.00 | 1.32 | 1.19 |

For validation of the evaluated stress response similarities based on quantified proteins, hierarchical cluster analysis was also carried out conducting DE proteins in reference to control (188 DE proteins). At this, based on their reporter intensities (MS data) as well as their Log2FC (protein expression profile) in the respective stress condition, similarity coefficients were calculated.

Regarding cluster analysis of DE proteins based on reporter intensities (RI), a heatmap was again provided (Figure 30). Protein expression similarities of DE proteins based on Log2FC are visualized in Figure 31 and Figure 32, either labeled according to their NCBI-annotation or their biological function based on SEED category.

In both cases, three analogous clusters were formed, which are further congruent to the one of quantified proteins. Further, numerous DE proteins of a biological function cluster together indicating a close relationship according to their differential expression during various stress conditions. Following clusters of biological functions are formed:

- Nucleosides and Nucleotides
- Membrane Transport
- Carbohydrates
- Fatty Acids Lipids and Isoprenoids
- Stress Response

Details regarding DE proteins can be obtained from Supplementary Part III.

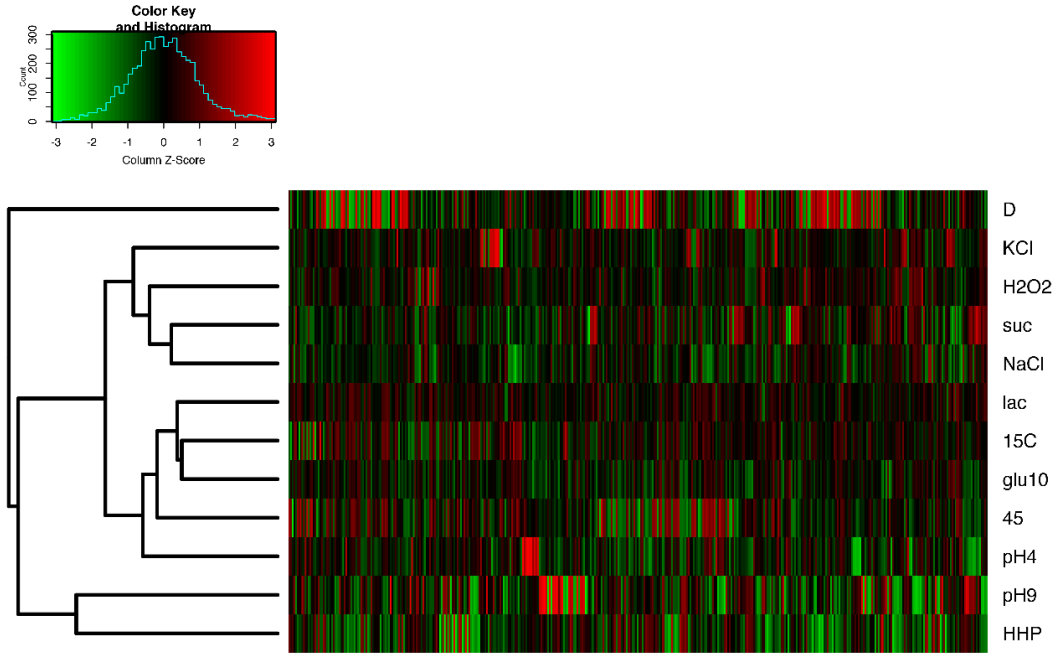


Figure 30: Graphical illustration of stress response similarities of *Lactobacillus paracasei* subsp. *paracasei* F19 using hierarchical cluster analysis. Differentially expressed proteins in reference to control condition are conducted to cluster analysis applying reporter intensities (RI).

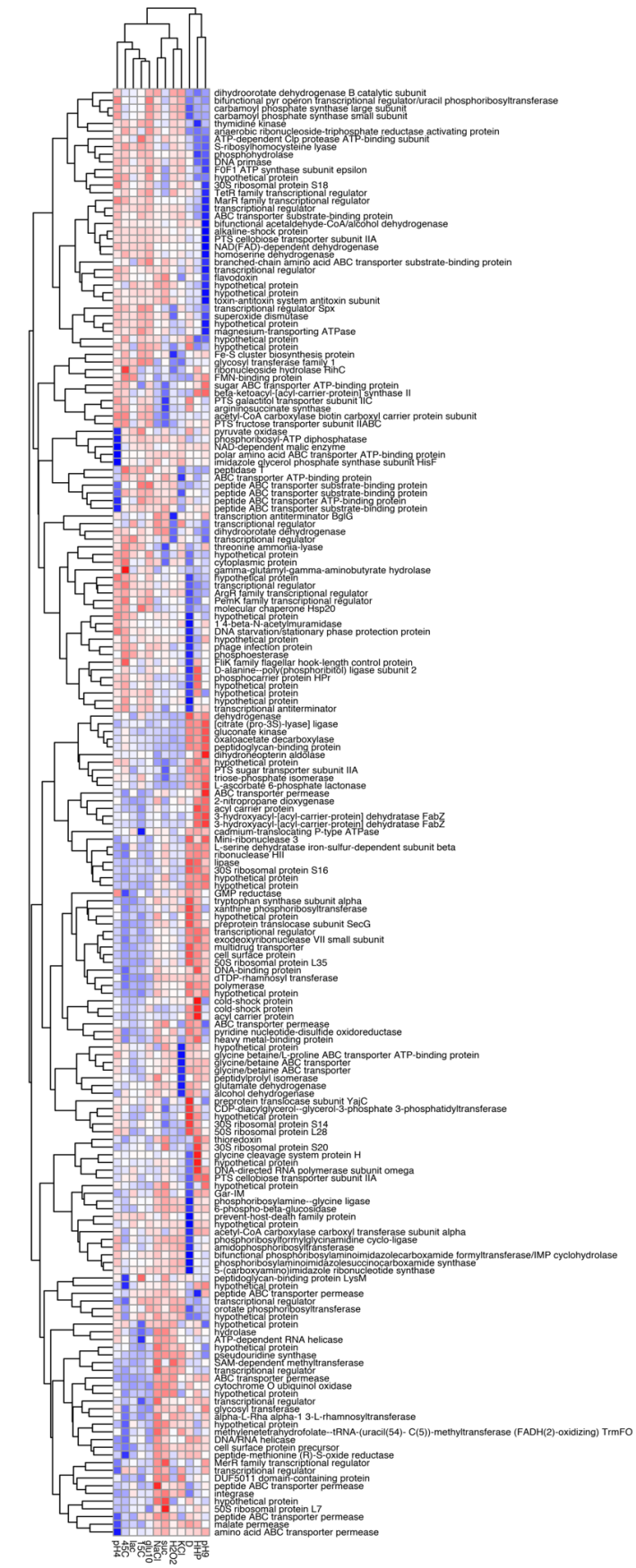


Figure 31: Graphical illustration of protein expression similarities of *Lactobacillus paracasei* subsp. *paracasei* F19 under various stress conditions using cluster analysis. Any differentially expressed protein in reference to control condition is conducted to cluster analysis and similarity coefficient is calculated based on Log2FC. Proteins are labeled according to their NCBI- annotation

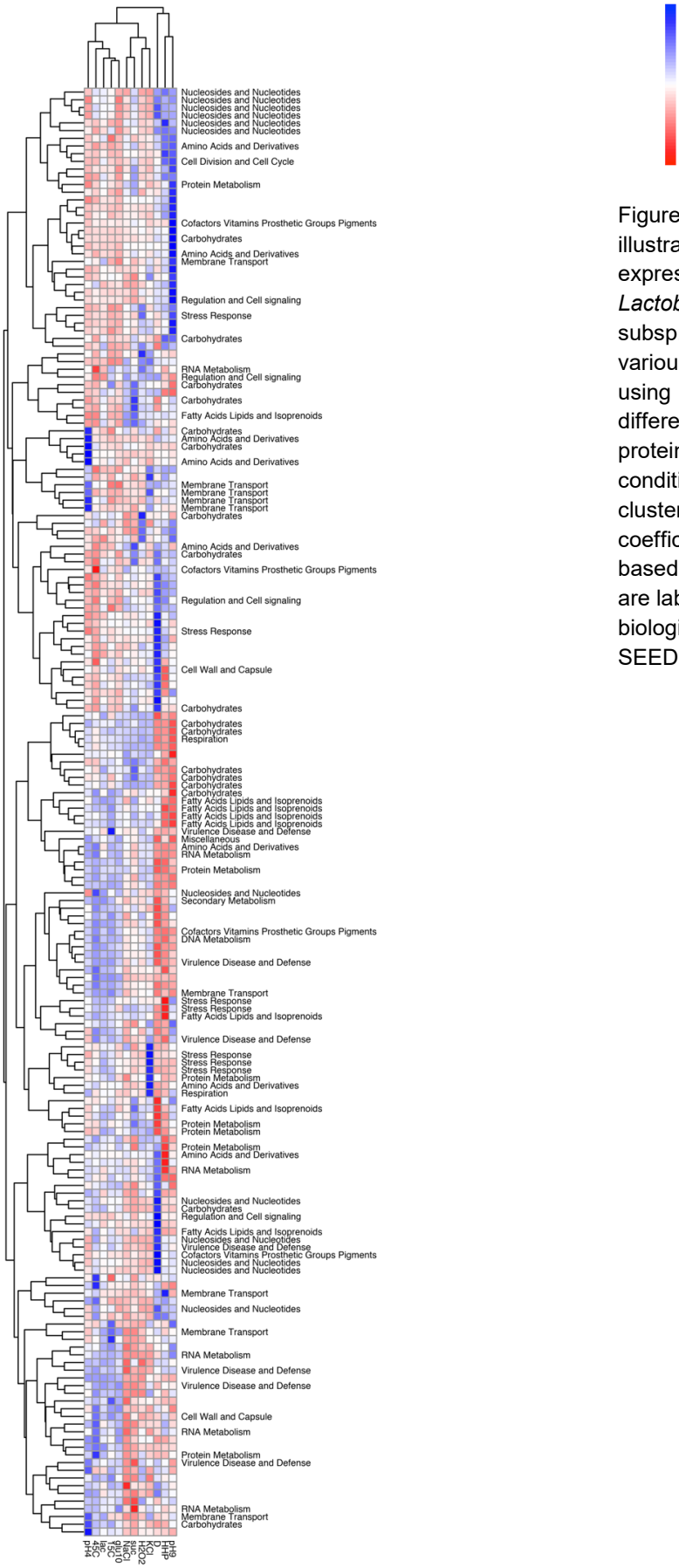


Figure 32: Graphical illustration of protein expression similarities of *Lactobacillus paracasei* subsp. *paracasei* F19 under various stress conditions using cluster analysis. Any differentially expressed protein in reference to control condition is conducted to cluster analysis and similarity coefficient is calculated based on Log2FC. Proteins are labeled according to their biological functions based on SEED category.

# 5 Discussion

This work dissects the stress response of F19 as reflected in the plasticity of its proteome upon sublethal stress application. The following theses can be derived from this investigation:

- A procedure could be established for the selection of stress conditions that have comparable sublethal influence on *Lb. paracasei* subsp. *paracasei* F19's physiology
- MALDI-TOF MS was extended for a fast screening method to profile stress kinetics and identify time points of maximal stages of the stress answer in the proteome.
- Comparable sublethal stress conditions were selected for the analysis of bacterial stress responses utilizing the established procedure.
- An experimental strategy was established for the investigation of bacterial stress responses on basis of genomics and quantitative comparative proteomics.
- A reference genome was set up for database searching.
- Stress response similarities were identified and responses to different stress qualities found to overlap within three groups of stress conditions predicting cross protection against these stresses.
- Optimal pretreatment conditions with sublethal stresses could be found for F19 in order to induce adaptive responses towards drying and to increase survival.
- Optimal preconditioning was predicted applying
- The evaluation of the data assists prediction of changes with respect to fitness and survival and the anticipated probiotic performance of F19.
- The phenotypic plasticity of F19 in response to stresses could be predicted along its proteomic plasticity.

In the subsequent chapters of the discussion these theses will be supported and explained in detail.

## 5.1 Review of the procedure for the selection of stress conditions

This chapter and chapter 5.2 correspond to the publication by Schott et al. [320].

Lactic acid bacteria (LAB) are broadly employed as starter and probiotic cultures in the manufacture of foods. During industrial processes and consumption, LAB encounter numerous stresses resulting in losses of fitness and survival before they even begin to fulfill their biological role in the gut [68, 358]. Hence, a high number of additional fermentation batches with expensive substrates are required in order to yield high quantities of viable, effective cultures. The dairy industry is consequently anxious for a resource-saving production of effective cultures. Optimal survival and preconditioning of LAB would contribute to the culture's industrial performance and health-promoting properties. Consequently, a general understanding of stress response mechanisms is a necessity in order to avoid detrimental damage to the cells and is essential in order to optimize fermentation processes and to improve storage and conservation of the products. Prior work has documented cellular stress response mechanisms of various LAB to different stresses [19, 48]. However, these studies have been limited in comparing detected stress responses since either a single stress was experimentally investigated and comparison was accomplished by reviewing literature only or since several stresses were experimentally investigated, missing the comparability of the induced stresses. Therefore, a procedure was developed that allows the selection of comparable, sublethal stress conditions and serves as primary step in the Comparable, sublethal stress conditions were referred to stresses that have comparable sublethal influence on the F19's physiology. In the following these will be referred to by the term "stress condition" for simplification. Stress conditions were specified as the combination of stress intensity tolerances with stress application time tolerances. Stress intensity tolerances were determined applying growth challenge tests, while stress application time tolerances were determined using MALDI-TOF MS protein profiling. The utilization of growth challenge tests for the determination of sublethal stress intensities is a widely spread method. It was well established in several bacterial physiology studies [347, 359-362] and was recently computer- supported by the statistical program Rproject [363, 364]. The utilization of MADLI-TOF MS for the determination of stress application time tolerances by profiling stress kinetics extents its usual forms of application: MALDI-TOF MS has mostly been used for rapid species identification for the assurance of product quality and safety in food microbiology and biotechnology [365-368], for pathogens identification in clinical diagnostics [369-371] or for biomarker molecules identification in tissues in order to enable the diagnosis of specific illnesses [372-374]. The exploitation of MALDI-TOF MS for profiling stress kinetics is supported by a former study of the chair of Technical Microbiology (TU Munich), in which MALDI-TOF MS protein profiling was

used for the detection and analysis of acid and hop shock induced responses in beer spoiling LAB [342]. Most notably, this is the first study to the author's knowledge to provide a procedure that combines a physiological with a proteomic approach for the comprehensive selection of stress conditions and that enables a primary insight in proteomic stress responses. The developed procedure implements MALDI-TOF MS protein profiling for a substantial analysis of different stress responses in F19 and consequently suggests MALDI-TOF MS protein profiling as a fast and time-saving tool for screening microbial stress responses. However, some limitations are noteworthy. Although the procedure was established for *Lb. paracasei* subsp. *paracasei* F19, the procedure was only reassessed for one other LAB (*Lb. sanfranciscensis*, unpublished data). Future work should therefore include follow-up work designed to evaluate whether the procedure is transferable on other LAB species.

## 5.2 Selection of stress conditions for the analysis of bacterial stress responses

Stresses to which LAB are exposed upon starter culture preparation and transit through the GIT are well known and documented. Nonetheless, there is a battery of them [19, 48, 375, 376]. Principal stresses encountered by LAB upon preparation are drying, temperature, osmotic and oxidative stress, while pH stress dominates during the passage through the GIT [52, 68]. In addition, bacteria are confronted with starvation stress as they spend most of their time in stationary phase with resting growth due to nutrient starvation [19]. In contrast to starvation stress, pressure stress occurs less frequently in natural environments, but is well established in several studies, since pressure induces membrane changes similar to the ones induced by drying stress [156, 171, 377, 378]. Therefore, emphasis was given to these stresses in this work. However, stress responses of microorganisms alter not only depending on the induced stress quality, but also depending on intensity and application time [19, 52]. Thus, a central aim of this study was the selection of stress conditions, which were required to serve as basis for the analysis of bacterial stress responses using quantitative proteomics. In this study, stress conditions were selected by using the developed procedure based on the determination of stress intensity and application time tolerances.

Stress conditions were selected for all induced stresses. These findings extend those of Hörmann *et al.* and Sanders *et al.*, who selected stress conditions solely based on the determination of stress intensity tolerances [347, 359]. In this study, the comparability of the sublethal stress conditions can be facilitated with the determination of stress application time tolerances. In addition to the study of Hörmann *et al*., overall twelve stress conditions were selected in contrast to six. Nonetheless, the identified stress intensity tolerances of *Lb. paracasei* subsp. *paracasei* F19 amount to a similar extent for the ones detected in *L. lactis* and *Lb. sanfranciscensis* [60, 157, 194, 347, 359] and for Shigella and Salmonella [66] indicating that a clear stress response is expected. Most notably, this is the first study to the author’s knowledge to determine a mild sublethal pressure condition that can be analogously used to stress intensity tolerances of other stresses. However, some limitations are worth noting. Although comparable, sublethal stress conditions were selected for *Lb. paracasei* subsp. *paracasei* F19, these stress conditions are specific and thus not transferable to other strains. Moreover, one should consider that the response to the identified mild sublethal pressure condition is more likely a repair response rather than a stress response. Further, stress intensity tolerances for lactose, hydrogen peroxide and temperature stress, as well as stress application time tolerances for oxidative, sucrose, alkaline and heat stress should be reassessed due to

high standard deviations. Future work should therefore reassess the selection of stress conditions in order to confirm its accuracy.

## 5.3 Review of the applied experimental strategy for the investigation of bacterial stress responses

This chapter and chapters 5.4 and 5.5 correspond to the publication by Schott et al. [356].

Mass spectrometry (MS) has emerged as the key technology for the explorative study of complex protein mixtures [379], particularly for the proteome analysis of human tissues [379, 380]. Thereby, MS-based proteomics is the most powerful approach to identify proteins and determine protein expression under different conditions [381-384]. Due to advances in sample preparation, such as multiplex quantitation, and to technological progresses in mass spectrometric instrumentation, a routine identification and quantification of proteins in a single study is enabled. Gradually, quantitative proteomics has been applied to the field of microbiology [380, 385-388], as prior proteomic studies were either of limited scope to understand cellular response mechanisms induced by a sublethal stress (the methodology of 2D gel electrophoresis does not enable the identification of hydrophobic proteins) or were not in the position of multiplex quantification. Nonetheless, several challenges, such as missing model workflow for the analysis of bacterial stress responses and thus missing workflow reproducibility as well as absence of automation capabilities, incomplete sequence coverage or unhandy data processing remain. Hence, one central aim of this study was to develop, implement and benchmark an experimental strategy that addresses these challenges.

In the present work the developed experimental strategy offers an efficient straightforward workflow addressing the challenge of missing workflow reproducibility. This strategy starts with the developed procedure for the selection of comparable, sublethal stress conditions (see chapter 5.1), followed by the stress treatments, the sample preparation, the chemical labeling, the multidimensional tandem mass spectrometry and finally the data analysis using a self-constructed R script, which focuses on the challenge of unhandy data processing and analysis. In parallel, the genome of F19 was sequenced and implemented as reference genome in the database searching to address the challenge of incomplete proteome coverage (chapter 5.4). The developed experimental strategy enabled the quantification of approximately 65 % of the *in silico* proteome, followed by the identification of > 400 differentially expressed proteins stating the stress proteome. This dataset represents one of the largest collections of identified, quantified and DE microbial proteins in a single experiment. To the author's knowledge, there is no other proteomic study of bacterial stress responses that describes an equally large proteome coverage. In addition, the prediction of SCL of proteins and the analysis of biological functions using SEED subsystems enabled the investigation of

stress induced effects. In terms of protein SCL analysis, there was no strong bias between the SCL of the *in silico* proteome and the SCL of the quantified proteins. Further, coverage of all subcellular compartments including proteins of the cell wall and membrane was observed. These findings extend those of Gygi *et al.,* Molloy *et al*. and Hahne *et al.*, indicating that cellular prefractionation of the protein extract during sample preparation is not required [389-391]. The SEED subsystem analysis reflected the large variety of biological functions, enabled the evaluation of the applied stimuli and represented a first insight in the regulation/protein investment of the cell in biological functions upon stress. According to these findings, proteomics is the method of choice for the analysis of physiological responses. Although transcriptomics has emerged as a powerful tool in this field, protein expression levels are still a better proxy for protein activity than mRNA levels [269, 392]. Moreover, proteomics enable the dynamic reflection of both genes and environment at any cell stage as it can be used to identify biological active proteins [269, 392, 393]. And thus, in terms of changing environmental conditions to which organisms respond with changes in its phenotype, proteomics can be the preferable approach for the analysis of phenotypic and proteomic plasticity.

The developed straightforward experimental strategy therefore facilitates the analysis of bacterial stress responses in a comprehensive and multiplexed manner by combining genomics and quantitative proteomics, resulting in resource and time savings. Most notably, in concert with the self-constructed R script for the bioinformatic analysis of proteomic data, data processing can be routinely handled and the whole process can be performed more efficiently. Considering these merits, this strategy has major advantages over other proteomic procedures such as 2D gel electrophoresis, which is on the one hand resource and time consuming and on the other hand limited in the analysis of membrane and dynamic proteins or in the analysis depth itself [394-397]. To conclude, the straightforward experimental strategy based on proteomics and genomics can be the state-of-the-art technique for the analysis of physiological responses. However, some limitations are noteworthy. Although the experimental strategy was efficiently applied to *Lb. paracasei* subsp. *paracasei* F19, it has not been re-examined for other LAB. Further, several challenges, such as missing workflow reproducibility and absence of automation capabilities, remain. Future work should therefore include follow-up work designed to address the remaining challenge of workflow reproducibility by evaluating whether this experimental strategy can be transferred on other strains and also the remaining challenge of automation capabilities.

## 5.4 Establishment of the reference genome for quantitative proteomics

Peptide identification during quantitative proteomics relies on an approach referred to as “database searching” in which measured fragment ion masses are compared to theoretically calculated ones [305]. Therefore, a theoretical search space is generated by a proteolytic *in silico* digest of proteins collected in a database in order to yield theoretical tryptic peptides. However, as already described above, the analysis of proteomic stress responses is only as good as the target database for the consequent mapping of MS data.

In order to address the challenge of incomplete proteome coverage, the genome of *Lb. paracasei* subsp. *paracasei* F19 was sequenced, analyzed and established as reference genome in the database searching. The analysis of the complete genome of F19 resulted in one chromosome and one plasmid consisting of 2,938 ORFs in total. Although LAB include species with completely different genomic preconditions, the genome of *Lb. paracasei* subsp. *paracasei* F19 belongs to the largest LAB genomes [398]. In addition, its functional analysis revealed an enrichment of certain functional categories. While the vast majority of genomically-encoded genes encode either proteins related to basic functions, e.g. carbohydrate or protein metabolism, most abundant plasmid-encoded genes encode for either hypothetical proteins, or products with a non-clearly defined or non-informative biological function. Further, with the establishment of the reference genome for database searching, an extensive proteome coverage of 73 % resulting from identified proteins is enabled. This study therefore indicates that the use of genomics to establish a reference genome can minimize the gap of incomplete sequence coverage.

## 5.5 Stress responses of *Lb. paracasei* subsp. *paracasei* F19

As already described in chapter 5.1, LAB are widely used as starter cultures in the manufacture of foods, such as dairy products, or as probiotics in functional foods. During industrial processes and consumption, LAB are confronted with numerous stresses resulting in an almost complete loss of fitness and living cells [19, 46-50] before they even begin to fulfill their biological role in the gut [68, 358]. Hence, a high number of additional fermentation batches with expensive substrates are required in order to yield high quantities of viable, effective cultures. The dairy industry is consequently anxious for a resource-saving production of effective cultures. Optimal survival of LAB during stress would contribute to the culture's industrial performance and health-promoting properties. Consequently, a general understanding of stress response mechanisms is a necessity in order to avoid detrimental damage to the cells and is essential in order to optimize fermentation processes and to improve storage and conservation of the products. Prior proteomic studies were of limited scope to understand cellular response mechanisms induced by sublethal stress - since the applied methodology 2D gel electrophoresis does not enable the identification of hydrophobic proteins. In this study, stress responses that are induced by stresses which are usually present during industrial processes and consumption are analyzed using the developed straightforward experimental strategy based on genomics and quantitative proteomics.

### 5.5.1 The importance of general stress response mechanisms in starter cultures

Stress can be defined as alterations in the genome, the proteome, or the environment resulting in a decrease in the growth rate or survival of a microorganism [399, 400]. Stress responses are highly important for microorganisms which experience continual changes in factors such as nutrient and water availability, temperature or osmotic pressure in the environments in which they occur. The stresses can be physical, chemical or of biological nature. Some are of environmental origin (i.e. antimicrobials, temperature, available oxygen, osmotic pressure, pH, presence of bile, ethanol concentration), while others can be self-generated (i.e. acidity, starvation/low nutrient availability as a result of metabolism, generation of ROS) [19, 102, 399, 401]. Therefore, both the environmental factors and physiological status of the cells will affect the stress response mechanism. LAB have developed stress-sensing systems that detect these stresses and activate defenses allowing the bacteria to withstand sudden environmental changes or harsh conditions [19, 399, 402]. Activation of defenses against stress conditions depends on regulated gene expression. Although bacteria could theoretically have specific regulators for any stress, this would imply a tremendous genetic burden. Instead, regulators often control several genes and sometimes even other regulators [403] in integrated regulation systems. Bacterial stress responses are therefore based on the coordinated expression of genes that alter cellular processes such as DNA metabolism, cell division, housekeeping, membrane composition, metabolism and transport [19] to increase the bacterial stress tolerance [404]. The integration of these stress responses is achieved through networks of regulators allowing the cell to respond to various complex changes that affect growth and cell survival. The stress-resistance systems can be divided into three classes: (1) specific, induced by a sublethal dose of the stress. This adaptive response usually involves the induction of a specific group of genes or regulators designed to cope with specific stress conditions; (2) general systems where adaptation to a stress condition can render cells resistant to other stress conditions; (3) stationary-phase-associated stress response which involves the induction of numerous regulons designed to overcome several stress conditions. Unlike the adaptive response, the stationary-phase associated response does not require any pre-exposure to stress for resistance development [402] and can be characterized as a genera-type stress response [19]. Cross-resistance, where one stress condition can render cells resistant to other stress conditions, is a general theme among resistance systems in LAB but appears to vary among species [19].

A common regulatory mechanism in the stress response of bacteria involves the modification of sigma factors whose primary role is to bind core RNA polymerase-

conferring promoter specificity [405]. In *Bacillus* and *Listeria*, sigma factor $\sigma^B$ is a major global regulator for stress response in the cells [406, 407]. However, LAB species are lacking an $\sigma^B$ ortholog, while several stress proteins and their regulators are conserved. It is therefore not yet clear how lactobacilli sense and respond to various environmental stimuli and stresses - by global transcriptional regulators or by two-component regulatory systems or both [402]? The unraveling of the occurrence and interaction of different stress responses remains an interesting challenge to which proteomic studies strongly contribute [253, 408, 409].

In this study, stress-induced changes in the proteome of *Lb. paracasei* subsp. *paracasei* F19 were studied in order to characterize underlying stress response mechanisms towards cellular fitness, viability and probiotic activity/performance (see 5.7). F19 responded to stress in general with the relative enhancement of cell membrane and cell wall proteins (cell envelope) accompanied by the relative reduction of cytoplasmic proteins. The differential expression of proteins related to the cell envelope triggered by stress may be consistent with the common notion that changes in its chemical composition, structure and functionality improve cell survival. The cell envelope is the physical barrier separating the cell from its environment and, as such, the first line of defense against detrimental environmental conditions. Maintaining the integrity under changing environmental conditions is a matter of life or death for bacteria [377].

Further, a broad range of F19's biological functions is influenced by stress including carbohydrate metabolism, nucleoside and nucleotide biosynthesis, membrane transport, DNA metabolism and cell wall and capsule biosynthesis. The down-regulation of cell wall and capsule biosynthesis proteins seems to contradict the previous findings of the enhancement of cell wall and membrane proteins (see above). It is important to note that not all proteins which are located in the cell wall or cell membrane are actually involved in its biosynthesis, they can have diverse biological functions instead. Interestingly, an upregulation of cell wall and membrane proteins has been noticed that is involved in fatty acid, lipid and isoprenoid biosynthesis and in stress response confirming that the applied stress condition indeed caused stress responses in F19.

In addition, the analysis of stress responses revealed unique and shared DE proteins (188 proteins in total). Unique DE proteins (70 %) are stress specifically induced, which matches at first sight the widespread conception of stress specific mechanisms [48]. However, almost every third DE protein was shared in several stress conditions, whereby down-regulation overlaps to a much larger extent of almost 60 % of shared proteins than up-regulation. Interestingly, two proteins were respectively shared in several stress

conditions with varying regulation patterns: accB (regulation pattern: pH4↓[10], 45C↓, suc↑[11], NaCl↑), peptide-methionine (R)-S-oxide reductase (regulation pattern: suc↓, NaCl↓, KCl↓, 45C↑). To the author's knowledge, their role in stress has so far only been observed for accB. accB is a component of the acetyl coenzyme A carboxylase complex which is involved in the fatty acid biosynthesis as part of the lipid metabolism. It initiates the fatty acid biosynthesis FASII by catalyzing the reaction to form Malonyl-CoA from Acetyl-CoA. accB has so far been linked to salt stress in *L. lactis* subsp. *lacits* IL1403 [410]. The routing of Acetyl-CoA toward the biosynthesis of fatty acids has previously been observed in *Lb. rhamnosus* GG, *Lb. delbrueckii* subsp. *delbrueckii* CAUH1 and *Lb. bulgaricus* under acid stress [411, 412] and may contribute to the rigidity and impermeability of the cytoplasmic membrane [413, 414]. However, the potential cellular mechanisms of these proteins in sublethal stresses seem diverse since the activity of these proteins is likely to be regulated in response to different types of cellular stress. Most notably, as shared proteins overlap in several different stress conditions, cross-tolerances are indicated.

Based on stress induced changes towards SCL, biological functions and identified unique/shared proteins, this study therefore indicates that stress specific responses are less common than assumed so far. These results provide evidence that in LAB general cellular mechanisms may be more frequently used in counteracting different stress conditions and thus play a key role as general stress responses. These findings were also reported by Hecker et al. [56, 415, 416]. Nonetheless, striking findings including general and specific stress responses are presented for F19 in the following sections.

### 5.5.2 Drying, pressure and alkaline stress induce the stringent response

The comparison of stress responses based on cluster analysis and Venn diagrams revealed a close relationship between drying, pressure and alkaline stress responses. Overall, 24 proteins were shared in drying, pressure and alkaline stress. During these sublethal stresses, F19 upregulated predominantly proteins of the nucleoside and nucleotide biosynthesis. Particularly, upregulated proteins were involved in the first steps of purine[12] and pyrimidine[13] metabolism. These results suggested potentially increased levels of the intermediate products 5-phosphoribosyl-a-1-pyrophosphate (PRPP), IMP and UMP.

[10] ↓ Downregualted protein
[11] ↑ Upregulated protein
[12] SAICAR, N5-CAIR, purD, purM
[13] CPSase, pyrR, pyrDB, OPRTase, CPSase

There are various possible reasons for the potentially increased levels of PRPP, IMP and UMP in *Lb. paracasei* subsp. *paracasei* F19. On the one hand, the potential increase in the PRPP pool can probably be contributed to enhanced levels of $NAD^+$ and $NADP^+$ and thus to oxidative resistance mechanism using NADH oxidase and NADH peroxidase [56, 415, 416]. In particular, PRPP is a common intermediate in both pyrimidine and purine de novo pathways and is used for the biosynthesis of nicotinamide coenzymes ($NAD^+$ and $NADP^+$). $NAD^+$ and $NADP^+$ are linked to the redox potential, as $NAD^+$/$NADP^+$ and NADH/NADPH are used as electron acceptor and donor respectively [102]. Maintaining a low intracellular redox potential is essential for keeping proteins in their reduced active form. However, upon oxidative stress, which can also be caused by drying, the redox potential of the cell is influenced by reactive oxygen species (ROS) which have oxidizing potential, affecting many enzymatic reactions. ROS are highly reactive and toxic. Therefore, LAB posess several mechanisms for their detoxification. One of the most conserved oxidative resistance mechanisms to counteract the effects of oxidative stress results from the coupling of NADH oxidase and NADH peroxidase [417]. At first, oxygen is used for the oxidation of NADH to $NAD^+$ via the NADH oxidase. Thereby $H_2O_2$ is produced, which is subsequently reduced to water by the NADH peroxidase. However, the upregulation of NADH oxidase, NADH peroxidase or any other nicotinamide coenzymes that are linked to the redox potential were not observed during any sublethal stress. Considering this, the potential increase in the PRPP pool in order to enhance levels of $NAD^+$ and $NADP^+$ in *Lb. paracasei* subsp. *paracasei* F19 appears to be unlikely.

On the other hand, the probable enhancement of IMP and UMP in *Lb. paracasei* subsp. *paracasei* F19 is ambiguous and since no other proteins related to nucleotide biosynthesis of purines and pyrimidines are differentially expressed, the role of IMP and UMP enhancement can only be speculated. In the past years, changes in the purine nucleotide pool of guanine have been described in the stringent response (SR), a conserved bacterial stress response [221-226]. The SR induces large-scale transcriptional alterations, such as the decrease in stable RNAs, resulting in a physiological shift to a nongrowth state [417]. In the presence of extreme stress, bacterial cells accumulate the protein alarmone (p)ppGpp that triggers the SR [227, 228, 418-421]. However, the detailed role of (p)ppGpp in the modulation of cell physiology in LAB remains to be established. In *Bacillus (B.) subtilis*, the induction of (p)ppGpp affects the transcription of rRNA genes by reducing the availability of the initiating nucleotide GTP [418], whereby GTP is a growth limiting factor [422]. In this study, *Lb. paracasei* subsp. *paracasei* F19 obtains two genes that code for proteins similar to alarmone (p)ppGpp: the GTP pyrophosphokinases. Interestingly, the adjustment of intracellular growth

processes was confirmed, with the exception of alkaline stress, by a decrease in protein metabolism, particularly by the downregulation of ribosomal proteins belonging to the small and large ribosomal subunit. Besides their roles in the assembly and the structural constituent of the small and large ribosomal subunit, the downregulated 30S ribosomal protein S16 is essential in terms of protein synthesis. Its '3' end, containing the anti-Shine-Dalgarno sequence, binds upstream to the AUG start codon on the mRNA and is thus responsible for translational initiation. Although the detailed role of IMP generation in LAB physiology is unrevealed, the probable increase in the IMP pool in this study, which is caused by upregulated proteins that are involved in purine biosynthesis, appears to be connected to the accumulation of (p)ppGpp. These findings are confirmed by Bittner *et al.* assuming that nucleotide pools may be involved in the modulation of (p)ppGpp production, which may represent a global regulator in sublethal stresses as they induce the SR [423]. Besides transcriptional adaptation based on the SR, it seems likely that bacteria that are subjected to extreme stresses, such as drying, pressure and alkaline stress, may benefit from mechanisms which rapidly adjust the rates of protein and DNA synthesis. All these observations suggest that the probable upregulation of the intracellular IMP and UMP nucleotide pools contribute to translational and replicational adaptations indicating the SR. Thus, drying, pressure and alkaline stress indicate to induce the SR in *Lb. paracasei* subsp. *paracasei* F19.

### 5.5.3 Pseudouridine synthase, hydrolase TolA and cytochrome O ubiquinol play a role in oxidative and osmotic stress

The comparison of stress responses by using cluster analyses revealed similarities between oxidative and osmotic stress – namely hydrogen peroxide, sodium chloride, potassium chloride and sucrose stress. During these stress conditions F19 principally regulated RNA metabolism, Virulence, Disease and Defense (VDD) mechanism and Membrane Transport. Ist das Großschreiben dieser Fachtermini korrekt?Venn diagrams revealed overall 19 shared proteins in hydrogen peroxide, sodium chloride, potassium chloride and sucrose stress, whereby a hypothetical protein, a cell surface protein precursor, a pseudouridine synthase and a dTDP-rhamnosyl transferase were DE in all four stress conditions. However, metabolic potential and biological function was solely revealed for pseudouridine synthase. Two other interesting proteins that were DE in oxidative, sodium chloride and sucrose stress are a hydrolase (TolA) and a cytochrome O ubiquinol oxidase (DedA). In general, all four shared proteins were downregulated.

Pseudouridine synthase, which is involved in RNA metabolism, particularly RNA processing and modification, catalyzes the conversion of uridine to pseudouridine, the most common post-transcriptional modification of RNA including tRNA, rRNA, mRNA and spliceosomal RNAs [424, 425]. Pseudouridine increases the rigidity of the RNA backbone and can enhance base stacking, stabilize base pairs, and alter RNA structure [426]. There are four distinct families of pseudouridine synthases (TruA, TruB, RsuA and RluC/RluD, TruD) that share no global sequence similarity, but which do share the same fold of their catalytic domain(s) and uracil-binding site and are descended from a common molecular ancestor. The deletion of some tRNA pseudouridine synthases results in growth defects in *Escherichia coli* and *Saccharomyces cerevisiae* that can be complemented by catalytically inactive mutants [427-429]. Thus, it was suggested that the pseudouridine synthases may function as RNA chaperones [425, 428-430]. To the author's knowledge, the regulation of pseudouridine synthases has so far not been observed neither in stressed prokaryotic cells nor in any probiotic mechanisms. However, in eukaryotes, Wu *et al.* reported the induction of pseudouridines in yeast under heat shock and in stationary phase [431]. Pseudouridylation is also induced in nutrient deprivation and oxidative stress [432]. In contrast, Rintala-Dempsey and Kothe reported that stress conditions such as pH, osmotic, oxidative and temperature stress led to the downregulation of some pseudouridine synthases in yeast [433], further suggesting some commonalities and overlapping mechanisms in regulating the abundance of these modification enzymes. Thus, the potential mechanisms of pseudouridine synthases in eukaryotic cells in sublethal stresses seem unspecified, as the activity of these enzymes is likely to be regulated in response to different types of

cellular stress and/or depending on the cell cycle [433]. Although the function of pseudouridine synthase has rarely been investigated in prokaryotes, the downregulation of pseudouridine synthase in prokaryotic F19 during oxidative and osmotic stress seems likely according to the findings of Rintala-Dempsey and Kothe. Regarding probiotic mechanisms, one can conclude that pseudouridine synthase is not involved in any probiotic activity since there is no scientific evidence.

The hydrolase TolA, which is involved in membrane transport in F19 is part of the Tol-Pal system. The Tol-Pal system is well conserved in gram-negative bacteria [434], it is also principally required for maintaining outer membrane (OM) integrity, but also involved in transport (uptake) of colicins and filamentous DNA and implicated in pathogenesis. The transport is energized by the proton motive force (PMF). The Tol-Pal system includes three cell membrane proteins TolA, TolQ and TolR, a periplasmic protein TolB, and an outer membrane-anchored peptidoglycan-associated lipoprotein Pal [435-437]. TolA couples the inner membrane complex of itself with TolQ and TolR [438-441] to the outer membrane complex of TolB and Pal [442-446]. TolA plays also a role in the translocation of group A colicins. The downregulation of TolA in this study during oxidative, sodium chloride and sucrose stress is in contradiction to the current scientific notion. Mutation or deletion of any of the *tol* or *pal* genes results in numerous defects, such as periplasmic leakage, increased susceptibility to many toxic compounds and formation of outer membrane vesicles [447, 448]. In addition, several studies reported the upregulation of the TolA protein in stress. Maurer *et al.* and Sistrunk *et al.* observed the induction of TolA in *E. coli* in acid stress [449] and in *Salmonella* in bile stress [450]. To the author's knowledge the downregulation of TolA in stress has so far been connected to any cellular stress response mechanisms. Thus, the potential mechanisms of TolA in sublethal stresses seem unspecified, as activity appears to be modulated in the cell one way or another depending on the stress condition. As the function of TolA has rarely been investigated in prokaryotes, neither on genome nor proteome level, the regulation of TolA in F19 during oxidative and osmotic stress is hard to relate to any current scientific opinion. In addition, its role in probiotic activity could not be demonstrated.

The cytochrome O ubiquinol oxidase was found to be an ortholog to DedA, a protein that is required to produce the antibacterial peptide Colicin V. Consequently, DedA was consequently assigned to the biological function of VDD. Considering that DedA produces a bacteriocin that is active against closely related bacteria, a probiotic property of DedA or cytochrome O ubiquinol oxidase cannot be ruled out at first sight [451, 452]. However, probiotic activity involves upregulation rather than downregulation. Regarding survival and fitness, the cytochrome O ubiquinol oxidase is the main terminal oxidase of

the electron transport chain (ETC) under highly aerobic conditions. In LAB, the activity of ETC is not part of their normal lifestyle. These ETCs need the presence of exogenous cofactors such as heme and menaquinones to operate in LAB. However, a variety of LAB contain rather simple and non-redundant ETCs consisting of NADH dehydrogenase, a menaquinol pool and a *bd/co*-type cytochrome, which enables them to use various intra- and extracellular electron donor and acceptor components for improved bioenergetics [453]. Gaudu *et al.* reported that tolerance to different stresses is improved in the respiratory cell-state [454, 455]. As cytochromes show active oxygen consumption, it leads to low intracellular oxygen levels under aerated conditions and protects against oxidative stress in *Lactococcus lactis* [455]. Accordingly, one would have expected an upregulation of the cytochrome O ubiquinol oxidase in oxidative stress in F19, which was not observed. A possible note for explanation of the downregulation of cytochrome O ubiquinol oxidase in these stresses is provided by Dinamarca. Dinamarca *et al*. reported that the elimination of cytochrome O ubiquinol oxidase led to a decrease in the catabolic repression in *Pseudomonas putida* GPo1 [456]. Thus, this study therefore indicates that, besides its role in the oxidative stress response, cytochrome O ubiquinol oxidase may have an additional role in catabolic repression in *Lb. paracasei* subsp. *paracasei* F19.

From the logical point of view and according to the current scientific notion, the downregulation of pseudouridine synthase, TolA and cytochrome O ubiquinol seems unlikely and questionable. Nonetheless, their significant downregulation in this study and the fact that their differential expression was observed in at least three different sublethal stresses provide compelling evidence that these proteins play a role in oxidative, potassium chloride, sodium chloride and sucrose stress. However, probiotic properties are known for the cytochrome O ubiquinol ortholog DedA but involve its induction rather than its repression. Thus, limitations are clear. Although the results were supported statistically, the potential cellular mechanisms of these proteins in sublethal stresses seem diverse since the activity of these proteins varies between domains and is likely to be regulated in response to different types of cellular stress. Future work should therefore include follow-up work designed to investigate underlying cellular mechanisms in optimal and stress conditions in prokaryotes and eukaryotes and to characterize their specificity and protein interaction partners. Several important questions have to be addressed for each protein to dissect their presumably complex role: How are these genes regulated? Which interaction partners do they have? What are their functions/role under sublethal stresses? Under which conditions are they modified?

### 5.5.4 Osmoregulation in F19 linked to ionic and non-ionic membrane transport systems

The analysis of stress responses induced by osmotic stress - potassium chloride, sucrose and lactose stress - revealed the upregulation of proteins of membrane transport systems.

High osmolality of the extracellular sugar sucrose was associated with the upregulation of the PTS for galactitol and unspecific sugars located next to each other in the genome of F19. PTS is a transmembrane transport system for non-ionic carbohydrates and plays a crucial role in their utilization, as it regulates the activity of metabolic pathways, either through regulation of transcription and/or (in)activation of transporters and key enzymes already present [457]. There is also evidence suggesting that PTS plays a role in stress resistance - high levels of phosphoenolpyruvate phosphotransferase system (PEP-PTS) for glucose appear to improve the acid resistance in *Lb. casei*, *S. mutans* [458-460], *Streptococcus sobrinus* [461] and *Streptococcus macedonicus* [462, 463]. As the induction of PTS in acid stress was not observed in this study, it is more likely that the upregulation of PTS increases the intracellular transport of sucrose. Consequently, it seems that PTS enables the fast equilibration of the extracellular and intracellular concentrations of sucrose in *Lb. paracasei* subsp. *paracasei* F19. These findings are in accordance to Glaasker *et al.*, confirming that *Lb. paracasei* subsp. *paracasei* F19 tends to adapt to changing osmotic sucrose conditions using transmembrane transport systems in order to equilibrate internal and external sugar concentrations [76, 78, 82]. Similar observations have also been reported for *Lb. rhamnosus* and *L. lactis* [71, 153]. In addition, considering the growth challenge tests, growth of *Lb. paracasei* subsp. *paracasei* F19 was much more inhibited under high-osmolality conditions by KCl and NaCl than by equiosmolar concentrations of sucrose or lactose. Glaasker suggested that sucrose and lactose cause only a temporary osmotic stress since the internal and external sugar concentrations equilibrate quickly as a result of sugar uptake. Salt stress (KCl and NaCl), instead, can have a stimulating effect on the accumulation of glycine-betaine [78]. Nonetheless, an upregulation of PTSs was not observed for high osmolality of the extracellular sugar lactose. Reasons for this observation are lacking and can only be speculated on. Possible causes may be the different chemical properties of both sugars (highly soluble sucrose), the use of different transport systems or experimental inaccuracies.

Instead, during lactose as well as potassium chloride stress, proteins of glycine-betaine ABC transport systems were upregulated. These transport systems are involved in osmoregulation since they enable the intracellular accumulation of ionic glycine-betaine.

Glycine-betaine generally augments osmotolerance and acts as osmoprotectant in several LAB, such as *Lb. plantarum*, *Lb. acidophilus* and *L. lactis* [78, 79, 82, 84, 85]. Van der Heide also reported that, beside their role in osmoregulation, the ABC transporter can also function as osmosensor in *L. lactis*. At this, a change in intracellular ionic strength, derived from the intracellular transport of ionic glycine-betaine, serves as a primary signal of osmotic stress which is transmitted via its effect on interactions between membrane lipids and the protein to the transporter [89]. Unfortunately, the intracellular ionic strength as well as the membrane composition was not examined in this study due to experimental limitations.

This study therefore indicates that non-ionic PTS and ionic glycine-betaine ABC transporters appear to improve the osmotic stress resistance in *Lb. paracasei* subsp. *paracasei* F19. Most notably, this is the first study to the authors' knowledge to demonstrate the activity of ionic ABC transporters for osmoprotectants accumulation in sugar (lactose) stress, which until now has only been observed in salt stress. The results provide compelling evidence that F19, like many other LAB, maintains mechanisms of osmoregulation which are linked to transport systems and are activated in both sugar and salt stress. However, some limitations are noteworthy. Although induced mechanisms of osmoregulation linked to transport systems were identified for potassium chloride, sucrose and lactose stress, they were not observed for sodium chloride stress. One would have expected a stress response similar to one evoked by potassium chloride stress. Moreover, despite the upregulation of PTS in sucrose stress, high osmolality of the sugar lactose did not induce the upregulation of PTS. Possible causes can only be speculated on. Future work should therefore include follow-up work designed to reassess the analysis of lactose and sodium chloride stress in order to shed light on the dark.

### 5.5.5 Oxidative, alkaline, pressure and drying stress led to the regulation of stress proteins SOD, ASP, CSP and Dps

Oxidative, alkaline, pressure and drying stress was associated with the regulation of four commonly used stress proteins in F19.

In oxidative stress, F19 induced a superoxide dismutase (SOD) in order to counter the negative effects of oxidation. Note that oxidative stress was stimulated? in this study by the addition of the reactive oxygen species (ROS) $H_2O_2$ which crosses the membrane barrier of the cell and can cause oxidative damage by either reacting with cations ($Fe^{2+}$ and $Cu^{2+}$) or macromolecules (proteins, lipids, nucleic acids) [464, 465] or by inactivating proteins through the oxidation of cysteinyl residues [466]. However, $H_2O_2$ is detoxified by catalases (complete) [467] or NADH peroxide (incomplete) [102] and not by SOD. SOD is responsible for the elimination of ROS $O_2^-$ in a reaction that yields the less toxic ROS $H_2O_2$ [104]. Nonetheless, the induction of SOD in the presence of $H_2O_2$ has previously been observed in four Lactobacillus strains (*Lb. casei* Zhang, *Lb. rhamnosus*, *Lb. gasseri*, *Lb. acidophilus* NCFM) [468]. In addition, SOD was also induced in alkaline stress in F19. These findings extend those of Giard *et al*.. confirming that SOD is one of the main key players in the antioxidant mechanisms helping to counteract any deleterious effects of oxidation caused by different stresses [211]. Consequently, SOD may obtain a role in cross-protection against alkaline and acid stress as well as glucose starvation [211]. Besides its importance in the antioxidant mechanisms, its role in $H_2O_2$ detoxification is unclear.

Speaking of alkaline stress, F19 remarkably enhanced the transcription of an alkaline-shock protein (ASP) in an environment of high pH. The upregulation of an ASP has only been observed in another study by Kuroda *et al*. who reported a positive regulation of the alkaline-shock protein ASP23 in *Staphylococcus aureus* [469]. Most notably, this is the first study to the author's knowledge that confirms the regulation of ASP in an alkaline environment in LAB. The results in this study provide compelling evidence that the ASP plays a key role in alkaline pH tolerance in bacteria. Although the results were supported statistically, this study and the study by Kuroda are lacking any information regarding the regulation of ASP, its functionality, mechanism and interaction partners.

Another commonly used stress protein in LAB is the cold-shock protein (CSP), which is induced at low temperatures. Surprisingly, in this study, F19 regulated two CSPs in the presence of pressure stress. CSPs are generally induced in cold stress in LAB and can normally be considered to support transcription and translation, as they bind to single-stranded nucleic acids in order to resolve secondary structures formed at low temperatures. The differential expressions of CSPs in pressure treated cells are in

accordance to the results of Wemekamp-Kamphuis *et al*. who observed the regulation of CSPs in *Listeria monocytogenes* LO28 for supporting transcription and translation in pressure stress [203]. While they reported an increased level of CSPs in *Listeria monocytogenes* LO28, the downregulation of CSPs was observed in F19. In addition, CSPs were neither up- nor downregulated at temperature downshifts in F19. Most notably, this is the first study to the author's knowledge to report that pressure-treated cells led to the downregulation of CSPs. Thus, the interpretation of the results is speculative. Besides their role in supporting transcription and translation under stress, CSPs appear to have additional functionalities or, in contrast, they seem to underlie some intracellular commonalities and overlapping mechanisms that regulate the abundance of CSPs. Thus, the potential mechanisms of CSPs in sublethal stresses seem unspecified as the activity of these enzymes is likely to be regulated in response to different quantities and qualities of cellular stress.

Besides the regulation of SOD, ASP and CSP a DNA starvation/stationary phase protection protein (Dps) was induced during drying stress in F19. Dps is conserved to a remarkable high degree in more than 300 bacterial species [470]. It is known to play a multifaceted role in bacterial stress mediation [470] based on four intrinsic properties of the protein: DNA binding (i), metal binding and sequestration (ii), ferroxidase activity (iii) as well as the ability to affect gene regulation (iv). Most important properties are presented in the following. Dps monomers assemble into a dodecameric functional unit with an outer diameter of ~90 Å and an interior core diameter of ~45 Å [471, 472]. These dodecamers pack with DNA into a three-dimensional hexagonal structure [473-475], also called biocrystal, whereby the positively charged DNA backbone most probably interact with Dps through basic residues on the dodecamer surfaces [476]. During stationary phase, Dps condenses the chromosome such that most other macromolecules are excluded. By directly binding the chromosome, Dps can shield DNA from damage caused by peroxides and other agents. It is also likely that Dps increases the efficiency and accuracy of the repair process by recruiting repair enzymes or other proteins to the chromosome [477]. Further, Dps is a structural homolog of ferritin, the primary iron storage protein of virtually all organisms [476, 478], and was found in *Listeria innocua* [479] and *Halobacterium salinarium* [480]. Ferritins are functionally defined by the ability to bind iron and the presence of a ferroxidase activity. Although Dps and ferritin monomers have the same four-helix-bundle tertiary structure and form multiprotein spheres with hollow cores, respectively,the fundamental difference between Dps and the ferritins is that Dps binds DNA. Monomers of Dps and ferritin form pores respectively which can accommodate positively charged ions, such as iron [476]. It was observed recently that Dps acts as an iron storage protein, participating in its binding, oxidation,

and mineralization [481]. While oxidizing and mineralizing iron, Dps serves two purposes: both processes lead to quenching of $H_2O_2$ and prevent it from reacting with ferrous iron in the Fenton reaction (i) and mineralization (ii). For better understanding, the underlying mechanism is described in the following. In DPS, Fe(II) is generally oxidized at the ferroxidase active site, precipitating as insoluble ferric oxyhydroxide, Fe(III), and is stored in the protein's hollow core. While ferritins use primarily dioxygen as the oxidant [478], the Dps ferroxidase consumes $H_2O_2$ as the oxidant in two ways, both for oxidation and for mineralization [482]. According to Zhao *et al*., this reaction is summarized in: $2Fe^2 + H_2O_2 + 2H_2O_2 \rightarrow 2\mathrm{FeOOH} + 4H^+$. Fe(II) is oxidized to Fe(III) by $H_2O_2$ and oxidized Fe(III) is mineralized to insoluble ferric(III) oxohydroxide at the core of the dodecamer. Fe(III) is stored in the DPS core. The trapped iron is sequestered from the cytosol, a reducing environment that can convert it back into reactive $Fe^{2+}$. This prevents it from interacting with $H_2O_2$ formed during various metabolic activities. Zhao also demonstrated that Dps appears to have a weak catalase activity neutralizing hydrogen peroxide and resulting in two potentially deleterious reactants which are converted to harmless products [482]. In *E. coli*, Dps is among the most abundant proteins in stationary-phase [471], but is also regulated in various stress responses including protection from oxidative damage, particularly against peroxides during exponential phase [471, 483]. In addition, Dps was also induced in *L. plantarum* WCFS1 during growth in ethanol [484]. Considering the properties, prior studies and findings in this study, the induction of Dps during drying stress in F19 is plausible. Dps seems to act as general stress protein in different stresses since its importance in DNA binding, metal binding and sequestration and ferroxidase activity is ubiquitous.

The results in this study provide compelling evidence of the regulation of the stress proteins SOD, ASP, CSP and Dps in oxidative, alkaline, pressure and drying stress in F19, respectively. However, limitations are worth noting. Although the results were supported statistically, several questions should be addressed. Although the importance of SOD in the antioxidant mechanisms is clear, what role does it play in the detoxification of $H_2O_2$ or in an alkaline environment? Does it directly influence the detoxification of $H_2O_2$? Are there interaction partners? Future-work should therefore include follow-up work designed to evaluate cellular functions and mechanisms of SOD in the presence of the ROS $H_2O_2$ and alkaline environment. Regarding ASP, any information regarding the regulation of ASP, its functionality, mechanism and interaction partners is lacking. Consequently, future work should address those limitations. In terms of CSP, future work should focus on functionalities, intracellular commonalities and overlapping mechanisms that regulate the abundance of CSPs in different sublethal stresses.

## 5.6 The exploitation of pressure and alkaline stress for optimal preconditioning of starter cultures

Drying stress represents a central stress in the life of a starter culture. It amalgamates numerous stresses, like oxidative, starvation and osmotic stress. In addition, during industrial preparation starter cultures, such as F19, are confronted with temperature stress depending on the applied drying procedure (freeze-drying, low-temperature-vacuum-drying). As starter cultures lose cellular fitness and viability during industrial preparation [19, 46-50], the dairy industry is anxious for a resource-saving production of effective starter cultures. Optimal survival of LAB during stress would contribute to the starter culture's industrial performance and health-promoting properties. While numerous approaches focused on the technological improvement of the starter culture preparation, other approaches laid focus on enhancing the starter culture's effectiveness and viability by increasing LAB's cellular fitness towards encountered stresses. Thereby, the most promising approach appears to be the concept of preconditioning (pretreatment of LAB with sublethal stresses), as adaptive responses are developed leading to increased stress protection [485, 486].

In this study, optimal preconditioning of F19 towards drying stress was predicted. Therefore, induced stress responses were analyzed and compared applying cluster analysis. Stress responses with the biggest overlap of shared DE proteins towards drying stress were identified using Venn diagrams. A high similarity of drying and alkaline (pH9) stress or drying and pressure (HHP) stress was identified. These stresses shared in total 24 DE proteins. Their role and function are described in section 5.5.2. F19 responds to these stresses with the regulation of predominantly cell wall and cell membrane proteins. These findings extend those of Santivarangkna *et al*., confirming that the cell membrane and even cell wall are the principle sites of bacteria inactivation caused by drying [487]. Based on similarities and identified proteins, the cell membrane and cell wall in F19 appear to be the principle site of its inactivation caused by pressure and alkaline stress. In order to survive changing conditions, it is essential for bacteria to maintain an intact cell membrane [377]. Several studies reported about the inactivation of the cell envelope. Jordan *et al.* observed that the fluidity of the bacterial cell membrane decreases in pressure stress, leading to the loss of membrane integrity and thus functionality. By increasing the ratio of saturated to unsaturated fatty acids in the cell membrane, bacteria maintain their membrane integrity in pressurized stress conditions [377]. Analogously, these effects have also been described for bacterial cells exposed to drying, where the decreasing water content results in a reduced cell membrane fluidity and thus to membrane phase transitions from the liquid crystalline to gel phase [156, 171, 378]. In

case of pH stress, Quivey *et al*. reported the production of unsaturated membrane fatty acids in an acidic environment [133, 488] concluding the opposite for alkaline stress in this study and thus being in accordance to what is known for drying and pressure stress.

This study therefore indicates that F19 responds to drying, pressure and alkaline stress in similar ways. These stress conditions induce the stringent response and may reduce membrane fluidity resulting in membrane phase transitions. Most notably, this is the first study to the author's knowledge to investigate the influence of alkaline stress on F19's physiology, whereby the cell envelope appears to be the first line of defense and is probably among the major site of cellular damage. Further, based on similarities and identified proteins between these stress conditions, compelling evidence is provided demonstrating that pressure and alkaline stress can be exploited for optimal preconditioning of LAB, specifically F19, towards drying and thus for the preparation of effective starter cultures. Therefore, an optimal preconditioning in the form of an alkaline stress (pH 9, 60 min) or a mild sublethal high hydrostatic pressure stress (350 MPa, 10 min) followed by a repair phase (60 min) means a fitness and efficiency increase of *Lb. paracasei* subsp. *paracasei* F19. However, some limitations are worth noting. Although the hypothesis was supported statistically, identified optimal preconditioning was not verified in industrial starter culture preparation. Future work should therefore include follow-up work designed to evaluate whether preconditioning of F19 using pressure and alkaline stress increases its viability as starter culture and whether the identified optimal preconditioning can be transferred on other LAB that are used as starter cultures.

## 5.7 Probiotic activity and performance of *Lactobacillus paracasei* subsp. *paracasei* F19

Probiotic bacteria have become progressively popular over the last three decades as a result of growing scientific evidence based on *in vitro* and *in vivo* data pointing to their beneficial health effects on humans. These findings have coincided with the increasing consumer awareness of the relationship between health and nutrition providing a supporting environment for the development of the functional food concept. This functional food concept describes foods or food ingredients as exhibiting positive effects on the consumers' health beyond their nutritive value [489]. Similar to starter LAB, probiotic LAB need to be able to resist technological stresses during preparation to maintain high viable counts and must survive the harsh conditions in the GI tract after consumption [48]. Consequently, the stress physiology of probiotic LAB is of great interest as it provides insight in its probiotic activity and performance during stress. Although several health effects are associated with the application of probiotics, the majority of probiotic mechanisms of action are not exactly known but rather suggested [27, 33, 34]. Further, probiotic performance varies with the utilized LAB [83, 489]. In this study, underlying stress responses based on DE proteins of *Lb. paracasei* subsp. *paracasei* F19 were also evaluated towards its probiotic activity and performance.

Based on the fact that pseudouridine synthase, hydrolase TolA and cytochrome O ubiquinol were shared in most stress conditions, these proteins were initially examined for their probiotic activity and performance. Therefore, see section 5.5.3. Although their involvement in stress resistance towards oxidative and osmotic stress could be demonstrated, their evaluation with respect to probiotic activity and performance, which was discussed in the same section, could not be discovered. Another promising protein of DE proteins with probiotic activity appears to be the peptidoglycan-binding protein LysM, which F19 induced during a temperature upshift. LysM protein binds noncovalently to peptidoglycan (PG) and chitin by interacting with N-acetylglucosamine moieties [490]. Therefore, it uses the specific LysM domain, which is a widespread protein module. LysM was originally identified in bacterial cell walls degrading enzymes. Several proteins that contain the domain, such as TspA, FsaP and Intimin, respectively, *Neisseria meningitidis* [491], *Francisella tularensis* [492] and *E. coli* [493] are involved in adherence to human cells and in bacterial pathogenesis [490]. As a result of horizontal gene transfer from bacteria, LysM is yet present in many other bacterial proteins including proteins of eukaryotes, making it to a general peptidoglycan-binding protein [490]. An example of biotechnological application of LysM is the use of the LysM domain of AcmA to bind antigens to non-genetically modified gram-positive bacteria for oral

immunization purposes [494, 495]. Based on the specific adhesion properties of LysM to PG, LysM is also applied for modulating host–microbe interactions, cell immobilization for entrapping microbes or enzymes, proteins antibiotics and various other chemical compounds, separating/purifying matrices, detecting bacteria and fungi and displaying surface enzymes [496]. Considering these scientific evidences, it is suggested that the identified peptidoglycan-binding protein LysM is related to probiotic activity in F19 as it could impact intercellular actions by binding to other cells, i.e. for trans cell lysis between species in mixed cultures, for aggregation, for immune modulation by competitive exclusion of pathogens as well as for prevention of pathogen adhesion to mucosal and epithelial surfaces and their colonization. These findings correspond to the common notion that probiotics decrease colonization of pathogenic organisms in the GI tract by competitively blocking their adhesion to the epithelium [29]. In addition, the induction of LysM during heat stress noted in this study indicated that a pretreatment of F19 with a sublethal heat stress may increase levels of LysM and thus raise binding to PG resulting in an enhanced probiotic performance.

The findings in this study provide compelling evidence of probiotic activity of F19 utilizing the peptidoglycan-binding protein LysM and suggest that a pretreatment with a temperature upshift may contribute to its probiotic performance. However, there are limitations that are noteworthy. Although the data were statistically supported, the potential cellular mechanism of LysM in F19 are unknown and yet to be determined. Furthermore, its predicted probiotic activity and performance evoked by LysM should be examined. Future work should therefore include follow-up work designed to investigate underlying probiotic mechanisms using *in vitro* and *in vivo* tests.

## 5.8 Phenotypic and proteomic plasticity of F19

Prior evolutionary studies have documented that the ability of individual genotype to produce different phenotypes in response to distinct environmental conditions, also known as phenotypic plasticity [266], is of crucial importance for the fate of organisms in a changing environment [265]. A typical example for phenotypic plasticity is the polymorphism in insects [497]. Although plasticity has usually been thought to be an evolutionary adaptation to environmental variation (Darwinian selection) allowing individuals to fit their phenotype to different environments by expressing different traits, it nowadays also refers to the ability of an individual organism to change its phenotypic state or activity (e.g. its metabolism) in response to environmental stress [267, 273]. However, these studies have either been evolutionary studies focusing on phenotypic plasticity with respect to evolutionary adaptation or have been proteomic studies with focus on proteomic plasticity as response to a single environmental stress in eukaryotic cells. In this study proteomic plasticity in response to several different environmental stresses was investigated using quantitative proteomics in prokaryotic LAB F19.

*Lb. paracasei* subsp. *paracasei* F19 adapts to environmental stress with the plastic regulation of proteins depending on the encountered stresses. Stresses in general primarily affected cell membrane and cell wall proteins (cell envelope). While in drying, pressure and alkaline stress, F19 induced transcriptional and replicational adaptations using the stringent response, it utilized osmoregulation linked to ionic and non-ionic membrane transport systems in osmotic stress. Further, stress specific (ASP) and general stress (Dps) proteins are regulated in oxidative, alkaline, pressure and drying stress. Proteins, whose functionality and role in environmental stress has so far not been observed, were found to play a role in oxidative and osmotic stress. These findings extend those of Bedon *et al*., confirming that under environmental stresses one can observe a shift of the protein expression pattern, defining a new cellular phenotype that possibly can improve the organism's fitness [277]. This study therefore provides compelling evidence for demonstrating stress-induced phenotypic and proteomic plasticity in *Lb. paracasei* subsp. *paracasei* F19. This plasticity probably favors F19's fitness and survival in changing environments. However, a major gap remains as this has not been tested, leaving these findings descriptive. In addition, for quite a bunch of identified proteins which are regulated in environmental stress, the regulation, mechanism and functionality are unknown. And most probably differs depending on strain and species. Future work should address these limitations and fill the gaps.

# 6 Summary

Lactic acid bacteria (LAB) have a significant impact on human culture, traditions and well-being. Their economic importance is tremendously increasing due to the industrialization of and consumer appreciation for food. Consequently, the reliability of starter cultures is important in terms of quality and functional properties (aroma and texture), growth performance (fast growth, rapid acidification of the substrate, phage and bacteriocin resistance) and robustness of strains (during starter handling, storage and preservation by lyophilization, freezing, or spray-drying). Moreover, the need for robust LAB is even more important in the development of new applications such as probiotic food (functional food). Probiotics should survive the production and handling procedures as well as the environmental conditions which they encounter in the product to which they are added. Such products are dairy-related products (i.e. fermented milks, frozen fermented dairy desserts, ice cream, cheese). Furthermore, once they are consumed and encounter stressful conditions in the GI tract, they need to survive and be metabolically active.

The aim of this study was to understand stress response mechanisms of LAB in order to avoid detrimental damage to the cells, to optimize preparation and fermentation processes and to improve storage and conservation of the products. Therefore, stresses that frequently occur during industrial processes and consumption are characterized and evaluated for their cellular fitness, viability and probiotic activity / performance using the example of *Lb. paracasei* subsp. *paracasei* F19, a LAB that has been utilized as starter and probiotic culture.

In order to compare stress responses, stress conditions needed to be selected that have comparable sublethal influence on *Lb. paracasei* subsp. *paracasei* F19's physiology. The selection of these comparable stress conditions is performed by applying an established procedure that is based on the determination of stress intensity tolerances with stress application time tolerances. Stress intensity tolerances were determined using growth challenge tests. Stress application time tolerances were determined applying MALDI-TOF MS as a fast screening method to profile stress kinetics and to identify time points of maximal stages of the stress answer in the proteome. In this study, twelve stress conditions were selected including pH, temperature, starvation, osmotic, oxidative, high hydrostatic pressure and drying stress that comparably affect the physiology of F19.

For the investigation of stress responses another experimental strategy was established on the basis of genomics and quantitative proteomics. Applying genomics, a reference genome was set up for quantitative proteomics. Therefore, the complete genome of F19

was obtained in this study and assembled in one chromosome and one plasmid. Its functional analysis revealed an enrichment of certain functional categories. While the vast majority of genomically-encoded genes encodes either proteins related to basic functions, e.g. carbohydrate or protein metabolism, most abundant plasmid-encoded genes encode for either hypothetical proteins or products with a non-clearly defined or non-informative biological function. The developed experimental strategy enabled the identification of 2159 proteins, which corresponds to an extensive proteome coverage of 73 %. Further, approximately 65 % of the *in silico* proteome were quantified, of which > 400 proteins were differentially expressed (DE). This dataset represents one of the largest collections of identified, quantified and DE microbial proteins in a single experiment. This straightforward experimental strategy based on genomics and proteomics can be the state-of-the-art technique for the analysis of physiological responses.

Stress-induced changes in the proteome of F19 were detected, based on identified DE proteins. F19 responded to stress in general with a relative enhancement of cell membrane and cell wall proteins (cell envelope) accompanied by a relative reduction of cytoplasmic proteins. Further, a broad range of F19's biological functions is influenced by stress, among others carbohydrate metabolism, nucleoside and nucleotide biosynthesis, membrane transport, DNA metabolism and cell wall and capsule biosynthesis. The analysis of stress responses in reference to control condition revealed unique and shared DE proteins (188 proteins in total), whereby almost every third DE protein was shared in several stress conditions. General cellular mechanisms may be more frequently used in F19 in counteracting different stress conditions and thus play key roles as general stress responses. This indicates that stress specific responses are less in common than it has been assumed so far.

Similarities of stress responses were identified by using cluster analysis and Venn diagrams. At this, stress responses overlap and form three groups predicting cross-protection against the respective stresses within a group. Similarities were found for response to alkaline, high hydrostatic pressure and drying stress, for responses to sucrose, sodium chloride, potassium chloride and oxidative (hydrogen peroxide) stress, as well as for responses to temperature, lactose, starvation and acid stress.

During drying, pressure and alkaline stress, F19 upregulated proteins of the nucleoside and nucleotide biosynthesis. Particularly, upregulated proteins were involved in the first steps of purine (SAICAR, N5-CAIR, purD, purM) and pyrimidine (CPSase, pyrR, pyrDB, OPRTase, CPSase) metabolism suggesting potential increased levels of the intermediate products PRPP, IMP or UMP. Moreover, ribosomal proteins belonging to the small (30S ribosomal protein S1, 30S ribosomal protein S14) and large (50S

ribosomal protein L28, 50S ribosomal protein L35) ribosomal subunit were downregulated during the sublethal stress treatment. These ribosomal proteins are essential in terms of translation initiation and ribosome assembly. Changes in the nucleotide pools and transcriptional and replicational adaptations have been described in the stringent response (SR), a conserved bacterial stress response that induces large-scale transcriptional alterations such as the decrease in stable RNAs. Hence, it was concluded that *Lb. paracasei* subsp. *paracasei* F19 induces the stringent response during drying, pressure and alkaline stress by which translational and replicational adaptations take place. These adaptations lead to a physiological shift of F19 to a nongrowth state.

During hydrogen peroxide, sodium chloride, potassium chloride and sucrose stress F19 principally regulated RNA metabolism, Virulence, Disease and Defense (VDD) mechanism and Membrane Transport. At this, pseudouridine synthase, hydrolase TolA and cytochrome O ubiquinol were significantly downregulated. A probiotic activity of these proteins could be excluded. According to the current scientific notion, the potential mechanisms of these proteins in sublethal stresses seems further unspecified as the activity of this enzyme is likely to be regulated in response to different types of cellular stress and/or depending on the cell cycle. Commonalities and overlapping mechanisms in regulating the abundance of these modification enzymes are possible. Nonetheless, their significant downregulation in this study and the fact that their differential expression was observed in at least three different sublethal stress treatments provide compelling evidence that these proteins play a role in oxidative, potassium chloride, sodium chloride and sucrose stress.

During potassium chloride, sucrose and lactose stress, F19 induced proteins of membrane transport systems. High extracellular osmolality of the sugar sucrose was associated with the upregulation of the PTS for galactitol and unspecific sugars which are located next to each other in the genome of F19. PTS is a transmembrane transport system for non-ionic carbohydrates and plays a crucial role in their utilization as it regulates the activity of metabolic pathways, either through regulation of transcription and/or (in)activation of transporters and key enzymes already present. During lactose as well as during potassium chloride stress, F19 uses glycine-betaine ABC transport systems that enable the intracellular accumulation of the ionic osmoprotectant glycine-betaine. Consequently, it was suggested that non-ionic PTS and ionic glycine-betaine ABC transporters appear to improve the osmotic stress resistance in *Lb. paracasei* subsp. *paracasei* F19.

In the presence of oxidative, alkaline, pressure and drying stress, F19 regulated specific (ASP) and general (Dps) proteins as well as proteins with predicted cross-protection

against other stress conditions (SOD, CSP). Sublethal oxidative and alkaline stress were associated with the induction of SOD, which is one of the main key proteins in the antioxidant stress mechanism helping to counteract any deleterious effects of oxidation [211]. Although SOD is primarily induced during oxidative stress, it has also been observed to induce cross-protection against acid stress and glucose starvation. Consequently, SOD seems to have an additional role in cross-protection against alkaline stress in F19. Another commonly used stress protein in LAB is the cold-shock protein (CSP). CSPs are generally induced in cold stress in LAB and support transcription and translation as they bind to single-stranded nucleic acids in order to resolve secondary structures formed at low temperatures. Surprisingly, in this study, F19 regulated two CSPs in the presence of pressure stress. Thus, it is suggested that CSPs appear to have additional functionalities or seem to underlie some intracellular commonalities and overlapping mechanisms that regulate the abundance of CSPs in different stresses including pressure stress. While, in an alkaline environment, F19 induced the specific stress protein ASP, of which cellular mechanisms are lacking and yet to be determined, F19 induced Dps when exposed to drying. Although Dps was found to be primarily regulated under starvation, it is known to be a general stress protein since its importance in DNA binding, metal binding and sequestration and ferroxidase activity is ubiquitous.

Besides the comparison of stress responses in order to identify similarities and possible cross-protections among them, the data were evaluated on survival and fitness during industrial preparation processes of F19. Drying stress represents a central stress in the life of a starter culture or probiotic. It amalgamates numerous stresses, including oxidative, starvation and osmotic stress. In addition, upon industrial preparation and transit through GI tract, starter and probiotic LAB, such as F19, are as well confronted with temperature and pH stress. Optimal survival and fitness during these stresses would contribute on the one hand to their industrial performance and on the other hand to their health-promoting properties. The enhancement of the culture's effectiveness and viability by increasing LAB's cellular fitness towards encountered stresses is promising. At this, the pretreatment of LAB with sublethal stresses, whereby adaptive responses are developed leading to increased stress protection, is essential. This concept is also known under the term preconditioning. In this study, optimal preconditioning towards drying was predicted for F19 applying high hydrostatic pressure (350 MPa for 10 min, attached recovery phase 10 min) or alkaline pH (pH9, 60 min) pretreatments.

Furthermore, the data were also evaluated on anticipated probiotic activity / performance of F19. Probiotic activity was projected for *Lb. paracasei* subsp. *paracasei* F19 based on specific adhesion properties of LysM to peptidoglycans. LysM can impact intercellular actions by binding to other cells, e.g. for trans cell lysis between species in mixed

cultures, for aggregation, for immune modulation by competitive exclusion of pathogens as well as for prevention of pathogen adhesion to mucosal and epithelial surfaces and their colonization. These findings correspond to the common notion that probiotics decrease colonization of pathogenic organisms in the GI tract by competitively blocking their adhesion to the epithelium. Further, a pretreatment of F19 with heat stress was predicted to contribute to increased levels of LysM and consequently to F19's probiotic performance.

Stress-induced phenotypic and proteomic plasticity was demonstrated for *Lb. paracasei* subsp. *paracasei* F19 as it adapts to environmental stress by the plastic regulation of proteins depending on the encountered stresses. While proteins of the cell envelope are primarily affected by stress and represent the major target of stress damage, F19 plastically regulates cellular mechanisms depending on the encountered stress (see above). This plasticity probably favors F19's fitness and survival in changing environments. In general, one can observe a shift of the protein expression pattern under environmental stresses, defining a new cellular phenotype that possibly can improve F19's fitness. However, a major gap remains as the plasticity has not been tested for survival and fitness leaving these findings descriptive.

# 7 Zusammenfassung

Milchsäurebakterien (LAB) haben einen bedeutenden Einfluss auf die menschliche Kultur, Traditionen und das Wohlbefinden. Ihre wirtschaftliche Bedeutung nimmt aufgrund der Industrialisierung und der Wertschätzung des Verbrauchers für Nahrungsmittel enorm zu. Folglich ist die Zuverlässigkeit von Starterkulturen wichtig in Bezug auf Qualität und funktionelle Eigenschaften (Aroma und Textur), Wachstumsperformance (schnelles Wachstum, schnelle Ansäuerung des Substrats, Phagen- und Bakteriozinresistenz) und Robustheit der Stämme (während der Handhabung, Lagerung und Konservierung durch Lyophilisierung, Einfrieren oder Sprühtrocknung). Zudem ist die Notwendigkeit eines robusten LAB bei der Entwicklung neuer Anwendungen wie beispielsweise probiotischer Nahrungsmittel (Functional Food) noch wichtiger. Probiotika sollten die Herstellungs- und Handhabungsverfahren sowie die Umweltbedingungen in dem Produkt, dem sie zugesetzt werden, , überleben. Solche Produkte sind milchbezogene Produkte wie fermentierte Milch, gefrorene fermentierte Milchdesserts, Eiscreme, Käse. Darüber hinaus müssen sie überleben und metabolisch aktiv sein sobald sie konsumiert sind und stressigen Bedingungen im Magen-Darm-Trakt begegnen.

Das Ziel dieser Studie war es, die Stressreaktionsmechanismen von LAB zu verstehen um schädliche Zellschädigungen zu vermeiden, die Präparations- und Fermentationsprozesse zu optimieren sowie die Lagerung und Konservierung der Produkte zu verbessern. Daher werden Stressarten, die bei industriellen Prozessen und beim Konsum häufig auftreten, charakterisiert und hinsichtlich der zellulären Fitness, Lebensfähigkeit und probiotischen Aktivität / Performance am Beispiel von *Lb. paracasei* subsp. *paracasei* F19, einem LAB, welches als Starter- und probiotische Kultur verwendet wird, bewertet.

Um die hervorgerufenen Stressantworten zu vergleichen, mussten Stressbedingungen ausgewählt werden, die einen vergleichbaren subletalen Einfluss auf die Physiologie von *Lb paracasei* subsp. *paracasei* F19 haben. Die Auswahl dieser vergleichbaren Stressbedingungen erfolgt nach einem festgelegten Verfahren, das auf der Ermittlung von Stressintensitätstoleranzen kombiniert mit Stressdauertoleranzen basiert. Die Stressintensitätstoleranzen wurden mittels Wachstumsexperimenten unter Stresseinfluss bestimmt. Stressdauertoleranzen wurden unter Verwendung von MALDI-TOF MS als einem schnellen Screening-Verfahren zum Profilieren von Stresskinetiken und zum Identifizieren von Zeitpunkten maximaler Stressantwort im Proteom bestimmt. In dieser Studie wurden zwölf Stressbedingungen ausgewählt, welche die Physiologie

von F19 vergleichbar beeinflussen. Dies sind unter anderem pH, Temperatur-, Hunger-, osmotischer, oxidativer, Hochdruck- und Trocknungsstress.

Zur Untersuchung von Stressantworten wurde eine weitere experimentelle Strategie, basierend auf Genomik und quantitativer Proteomik, etabliert. Mittels Genomik wurde ein Referenzgenom für die quantitative Proteomik erstellt. In dieser Studie konnte das vollständige Genom von F19 zu einem Chromosom und einem Plasmid assembliert werden.. Die Funktionsanalyse des gesamten Genoms, welche mittels SEED Subsystem Analyse durchgeführt wurde, ergab eine Anreicherung bestimmter Funktionskategorien. Während die überwiegende Mehrheit der chromosomalen Gene Proteine kodieren, die mit Grundfunktionen wie Kohlenhydrat- oder Proteinmetabolismus verwandt sind, kodieren die am häufigsten vorkommenden Plasmidgene entweder hypothetische Proteine oder Produkte mit einer nicht klar definierten oder nicht informativen biologischen Funktion. Die entwickelte experimentelle Strategie ermöglichte die Identifizierung von 2158 Proteinen, was einer Proteomabdeckung von 73 % entspricht. Ferner wurden ca. 65 % des *in silico* Proteoms quantifiziert, von denen > 400 Proteine differentiell exprimiert wurden (DE). Dieser Datensatz repräsentiert eine der größten Sammlungen von identifizierten, quantifizierten und DE mikrobiellen Proteinen in einem einzigen Experiment. Diese einfache experimentelle Strategie, die auf Genomik und Proteomik basiert, kann die State-of-the-Art Technik für die Analyse von physiologischen Reaktionen sein.

Stressinduzierte Veränderungen im Proteom von F19 wurden anhand von identifizierten DE Proteinen nachgewiesen. F19 reagierte auf Stress im Allgemeinen mit einer relativen Verstärkung von Zellmembran- und Zellwandproteinen (Zellhülle), begleitet von einer relativen Reduktion cytoplasmatischer Proteine. Darüber hinaus ist eine Vielzahl der biologischen Funktionen von F19 durch Stress beeinflusst, unter anderem Kohlenhydratstoffwechsel, Nukleosid- und Nukleotidbiosynthese, Membrantransport, DNA-Metabolismus und Zellwand- und Kapselbiosynthese. Die Analyse von Stressantworten in Bezug auf Kontrollbedingungen ergab eindeutige und gemeinsame DE Proteine (insgesamt 188 Proteine), wobei fast jedes dritte DE Protein in verschiedenen Stressbedingungen geteilt wurde. Allgemeine zelluläre Mechanismen werden in F19 häufiger verwendet um unterschiedlichen Stressbedingungen entgegenzuwirken und spielen somit eine Schlüsselrolle als allgemeine Stressreaktionen. Dies deutet darauf hin, dass stressspezifische Reaktionen weniger häufig als bisher angenommen sind.

Ähnlichkeiten von Stressantworten wurden mithilfe von Clusteranalysen und Venn-Diagrammen identifiziert. Dabei überlagern sich die Stressreaktionen und bilden drei Gruppen, die einen Kreuzschutz gegen die jeweiligen Stressbedingungen innerhalb

einer Gruppe vorhersagen. Ähnlichkeiten wurden für Reaktionen auf alkalischen, hohen hydrostatischen Druck- und Trocknungsstress, für Reaktionen auf Saccharose-, Natriumchlorid-, Kaliumchlorid- und oxidativen Stress (Wasserstoffperoxide) sowie für Reaktionen auf Temperatur-, Laktose-, Hunger- und Säurestress gefunden.

In Trocknungs-, Druck- und alkalischem Stress regulierte F19 die Proteine der Nukleosid- und Nukleotidbiosynthese. Insbesondere waren die hochregulierten Proteine an den ersten Schritten des Purin- (SAICAR-, N5-CAIR-, purD-, purM-) und Pyrimidin- (CPSase-, pyrR-, pyrDB-, OPRTase-, CPSase-) Metabolismus beteiligt, was auf potentiell erhöhte Spiegel der Zwischenprodukte PRPP, IMP oder UMP hindeutet. Darüber hinaus wurden ribosomale Proteine der kleinen (30S ribosomales Protein S1, 30S ribosomales Protein S14) und der großen ribosomalen Untereinheit (50S ribosomales Protein L28, 50S ribosomales Protein L35) während dieser subletalen Stressbehandlung herunterreguliert. Diese ribosomalen Proteine sind essentiell in Bezug auf die Translationsinitiation und die Ribosomengruppierung. Veränderungen in den Nukleotidpools und Transkriptions- und Replikationsadaptionen wurden in der stringenten Antwort (SR) beschrieben, einer konservierten bakteriellen Stressantwort, die Transkriptionsveränderungen im großen Maßstab wie die Abnahme stabiler RNAs induziert. Hieraus wurde gefolgert, dass *Lb. paracasei* subsp. *paracasei* F19 die stringente Reaktion unter Trocknungs-, Druck- und alkalischem Stress induziert, wodurch eine Translations- und Replikationsanpassung erfolgen. Diese Anpassungen führen zu einer physiologischen Verschiebung von F19 zu einem nicht wachsenden Zellzustand.

In Wasserstoffperoxid-, Natriumchlorid-, Kaliumchlorid- und Saccharose-Stress reguliert F19 hauptsächlich RNA-Metabolismus, Virulenz-, Krankheits- und Abwehrmechanismus (VDD) und Membrantransport. Dabei werden eine Pseudouridinsynthase, eine Hydrolase TolA und ein Cytochrom O Ubichinol signifikant herunterreguliert. Eine probiotische Aktivität dieser Proteine konnte ausgeschlossen werden. Nach heutigem wissenschaftlichen Verständnis scheinen zudem die potentiellen Mechanismen dieser Proteine bei subletalen Stressfaktoren weiter nicht spezifiziert zu sein, da die Aktivität dieser Enzyme voraussichtlich als Reaktion auf verschiedene Arten von Zellstress und/oder Zellzyklus reguliert wird. Gemeinsamkeiten und Überlappungsmechanismen, die die Häufigkeit dieser Modifikationsenzyme regulieren, sind möglich. Trotzdem liefern ihre signifikante Herunterregulierung in dieser Studie und die Tatsache, dass ihre differentielle Expression bei mindestens drei verschiedenen subletalen Stressbehandlungen beobachtet wurde, einen überzeugenden Beweis, dass diese Proteine bei oxidativem, Kaliumchlorid-, Natriumchlorid- und Saccharosestress eine Rolle spielen.

Unter Belastung mit Kaliumchlorid-, Saccharose- und Laktosestress induzierte F19 zudem Membrantransportproteine. Eine hohe extrazelluläre Osmolalität des Zuckers Saccharose war mit der Induktion des Phosphotransferasesystems (PTS) für Galactit und unspezifische Zucker assoziiert, welche im Genom von F19 nebeneinander liegen. PTS ist ein Transmembrantransportsystem für nicht-ionische Kohlenhydrate und spielt eine entscheidende Rolle bei deren Verwendung, da es die Aktivität von Stoffwechselwegen reguliert, entweder durch Regulierung der Transkription und/oder (In)Aktivierung von bereits vorhandenen Transportern und Schlüsselenzymen. Sowohl in Laktose- als auch in Kaliumchloridstress verwendet F19 Glycin-Betain-ABC-Transportsysteme, die die intrazelluläre Anreicherung des ionischen Osmoprotectants Glycin-Betain ermöglichen. Folglich scheinen nicht-ionische PTS und ionische Glycin-Betain-ABC-Transporter die osmotische Stressresistenz in *Lb. paracasei* subsp. *paracasei* F19 zu verbessern.

In Gegenwart von oxidativem alkalischem Druck- und Trocknungsstress regulierte F19 spezifische (ASP) und allgemeine (Dps) Proteine sowie Proteine mit vorhergesagtem Kreuzschutz gegen andere Stressbedingungen (SOD, CSP). Sublethaler oxidativer und alkalischer Stress wurden mit der Induktion von SOD in Verbindung gebracht, welches eines der wichtigsten Schlüsselproteine im antioxidativen Stressmechanismus ist. SOD hilft den schädlichen Auswirkungen der Oxidation entgegenzuwirken [211]. Obwohl SOD hauptsächlich in oxidativem Stress induziert wird, wurde auch ein Kreuzschutz gegen Säurestress und Glucose-Hunger beobachtet. In F19 scheint SOD zudem eine zusätzliche Rolle beim Kreuzschutz gegen alkalischen Stress zu haben. Ein weiteres, häufig verwendetes Stressprotein in LAB ist das Cold-Shock-Protein (CSP). CSPs werden im Allgemeinen bei niedrigen Temperaturen in LAB induziert und unterstützen Transkription und Translation, da sie an einzelsträngige Nucleinsäuren binden, um bei Kältestress gebildete Sekundärstrukturen aufzulösen. Überraschenderweise regulierte F19 in dieser Studie zwei CSPs in Gegenwart von Hochdruckstress. Demnach scheinen CSPs zusätzliche Funktionalitäten zu haben oder es liegen intrazelluläre Gemeinsamkeiten und Überlappungsmechanismen zugrunde, die die Häufigkeit von CSPs bei verschiedenen Stressfaktoren, einschließlich Druckbelastung, regulieren. Während in einer alkalischen Umgebung F19 das spezifische Stressprotein ASP induzierte, dessen zelluläre Mechanismen nicht bekannt und noch zu bestimmen sind, induzierte F19 das Protein Dps unter Trocknungsstress. Obwohl festgestellt wurde, dass Dps hauptsächlich unter Hunger reguliert wird, ist bekannt, dass es ein allgemeines Stressprotein ist, da seine Bedeutung in der DNA-Bindung, Metallbindung und Sequestrierung und Ferroxidaseaktivität allgegenwärtig ist.

Neben dem Vergleich von Stressantworten zur Identifizierung von Ähnlichkeiten und möglichem Kreuzschutz wurden die Daten im Hinblick auf Überleben und Fitness während industrieller Präparationsprozesse ausgewertet. Trocknungsstress stellt eine zentrale Belastung im Leben einer Starterkultur oder eines Probiotikums dar. Er vereint zahlreiche Stressfaktoren wie oxidativen Stress, Hunger und osmotischen Stress. Bei der industriellen Präparation und dem Transport durch den GI-Trakt werden außerdem Starter und probiotisches LAB, wie F19, zusätzlich mit Temperatur- und pH-Stress konfrontiert. Optimales Überleben und Fitness bei diesen Belastungen würde einerseits zu ihrer industriellen Leistungsfähigkeit und andererseits zu gesundheitsfördernden Eigenschaften der Milchsäurebakterien beitragen. Die Verbesserung der Wirksamkeit und Lebensfähigkeit der Kulturen durch Erhöhung der zellulären Fitness von LAB gegenüber auftretenden Stressarten ist vielversprechend. Hierbei ist die Vorbehandlung von LAB mit subletalen Stressbedingungen, bei der adaptive Antworten entwickelt werden, die zu erhöhtem Stressschutz führen, essentiell. Dieses Konzept ist auch unter dem Begriff Vorkonditionierung bekannt. In dieser Studie wurde eine optimale Vorkonditionierung von F19 gegenüber Trocknung unter Anwendung von hohem hydrostatischem Druck (350 MPa für 10 min, anhaftende Erholungsphase 10 min) oder alkalischem pH (pH 9, 60 min) vorhergesagt.

Darüber hinaus wurden die Daten auch hinsichtlich der erwarteten probiotischen Aktivität/Leistung von F19 ausgewertet. Probiotische Aktivität wurde für *Lb. paracasei* subsp. *paracasei* F19 basierend auf spezifischen Adhäsionseigenschaften von LysM an Peptidoglykane nachgewiesen. LysM zeigt interzelluläre Wirkungen durch Bindung an andere Zellen. Dadurch kann eine Trans-Zelllyse zwischen Spezies in Mischkulturen, eine Aggregation, eine Immunmodulation durch kompetitiven Ausschluss von Pathogenen sowie eine Verhinderung der Adhäsion von Pathogenen an Schleimhaut- und Epitheloberflächen und deren Besiedelung erfolgen. Diese Ergebnisse entsprechen der allgemeinen Vorstellung, dass Probiotika die Kolonisierung von pathogenen Organismen im Gastrointestinaltrakt durch kompetitive Blockierung ihrer Adhäsion an das Epithel verringern. Ferner wurde vorhergesagt, dass eine Vorbehandlung von F19 mit Hitzestress zu einem erhöhten LysM-Spiegel führt und folglich zur probiotischen Leistung von F19 beiträgt.

Stressinduzierte phänotypische und proteomische Plastizität konnte für *Lb. paracasei* subsp. *paracasei* F19 nachgewiesen werden. F19 passt sich an die Umweltbelastung an, indem es die Expression von Proteinen plastisch in Abhängigkeit von den auftretenden Stressarten reguliert. Hier zeigt sich, dass in erster Linie Proteine der Zellhülle von Stress betroffen sind und so das Hauptangriffsziel der Stressschädigung darstellen. Des Weiteren reguliert F19 zelluläre Mechanismen in Abhängigkeit der

Stressbedingungen (siehe oben). Diese Plastizität begünstigt wahrscheinlich die Fitness und das Überleben von F19 in sich verändernden Umgebungen. Im Allgemeinen kann man eine Verschiebung des Proteinexpressionsmusters unter Umweltstress beobachten, was einen neuen zellulären Phänotyp definiert, der möglicherweise die Fitness von F19 verbessern kann.

# 8 References


1. Nations, F.a.A.O.o.t.U., *FAOSTAT*, in *Commodity Balances, Livestock and Fish, Primary Equivalent*. 2017, FAO: Rome, Italy.
2. Nations, F.a.A.O.o.t.U., *The Global Dairy Sector: Facts*. 2013.
3. Heseker, B. and H. Heseker, *Nährstoffe in Lebensmitteln: die große Energie- und Nährwerttabelle ; mit Zusatztabellen zu sekundären Pflanzenstoffen*. 2007: Umschau-Zeitschr.-Verlag Breidenstein.
4. Hill, C., et al., *Expert consensus document: The International Scientific Association for Probiotics and Prebiotics consensus statement on the scope and appropriate use of the term probiotic.* Nature Reviews Gastroenterology and Hepatology, 2014. **11**(8): p. 506.
5. Organization, F.a.A.O.o.t.U.N.a.W.H., *Joint FAO/WHO working group report on drafting guidelines for the evaluation of probiotics in food*, F.a.A.O.o.t.U. Nations, Editor. 2002.
6. Organization, F.a.A.O.o.t.U.N.a.W.H., *Health and nutritional properties of probiotics in food including powder milk with live lactic acid bacteria*, W.H. Organization, Editor. 2001.
7. council, T.e.p.a.o.t., *on the provision of food information to consumers, amending Regulations (EC) No 1924/2006 and (EC) No 1925/2006 of the European Parliament and of the Council, and repealing Commission Directive 87/250/EEC, Council Directive 90/496/EEC, Commission Directive 1999/10/EC, Directive 2000/13/EC of the European Parliament and of the Council, Commission Directives 2002/67/EC and 2008/5/EC and Commission Regulation (EC) No 608/2004*, EU, Editor. 2011.
8. Krämer, J., *Lebensmittel-Mikrobiologie*. Vol. 1421. 2007, Stuttgart: UTB. 416.
9. Altieri, C., et al., *Lactic acid bacteria as starter cultures.* Starter Cultures in Food Production: p. 1-15.
10. Caplice, E. and G.F. Fitzgerald, *Food fermentations: role of microorganisms in food production and preservation.* Int J Food Microbiol, 1999. **50**(1-2): p. 131-49.
11. Ray, B. and M. Daeschel, *Food biopreservatives of microbial origin.* Food biopreservatives of microbial origin., 1992.
12. Wood, B.J., *Microbiology of fermented foods*. 2012: Springer Science & Business Media.
13. Holzapfel, W. and B.J. Wood, *The genera of lactic acid bacteria*. Vol. 2. 2012: Springer Science & Business Media.
14. Hansen, E.B., *Commercial bacterial starter cultures for fermented foods of the future.* Int J Food Microbiol, 2002. **78**(1-2): p. 119-31.
15. Leroy, F. and L. De Vuyst, *Lactic acid bacteria as functional starter cultures for the food fermentation industry.* Trends in Food Science & Technology, 2004. **15**(2): p. 67-78.
16. Kongo, J.M., *Lactic Acid Bacteria as Starter-Cultures for Cheese Processing: Past, Present and Future Developments*. 2013.
17. Lacroix, C. and S. Yildirim, *Fermentation technologies for the production of probiotics with high viability and functionality.* Curr Opin Biotechnol, 2007. **18**(2): p. 176-83.

18. Heller, K.J., *Probiotic bacteria in fermented foods: product characteristics and starter organisms.* Am J Clin Nutr, 2001. **73**(2 Suppl): p. 374S-379S.
19. van de Guchte, M., et al., *Stress responses in lactic acid bacteria.* Antonie Van Leeuwenhoek, 2002. **82**(1-4): p. 187-216.
20. FAO/WHO, *Report of a Joint FAO WHO Expert Consultation on Evaluation of Health and Nutritional Properties of Probiotics in Food Including Powder Milk with Live Lactic Acid Bacteria*. 2001.
21. Holzapfel, W.H., et al., *Taxonomy and important features of probiotic microorganisms in food and nutrition.* Am J Clin Nutr, 2001. **73**(2 Suppl): p. 365S-373S.
22. Santosa, S., E. Farnworth, and P.J. Jones, *Probiotics and their potential health claims.* Nutrition reviews, 2006. **64**(6): p. 265-274.
23. Alvarez-Olmos, M.I. and R.A. Oberhelman, *Probiotic agents and infectious diseases: a modern perspective on a traditional therapy.* Clinical infectious diseases, 2001. **32**(11): p. 1567-1576.
24. Doron, S. and S.L. Gorbach, *Probiotics: their role in the treatment and prevention of disease.* Expert review of anti-infective therapy, 2006. **4**(2): p. 261-275.
25. Pham, M., D.A. Lemberg, and A.S. Day, *Probiotics: sorting the evidence from the myths.* Med J Aust, 2008. **188**(5): p. 304-8.
26. Senok, A.C., A.Y. Ismaeel, and G.A. Botta, *Probiotics: facts and myths.* Clin Microbiol Infect, 2005. **11**(12): p. 958-66.
27. Vanderhoof, J.A. and R. Young, *Probiotics in the United States.* Clin Infect Dis, 2008. **46 Suppl 2**(Supplement_2): p. S67-72; discussion S144-51.
28. Goldin, B.R., *Health benefits of probiotics.* Br J Nutr, 1998. **80**(4): p. S203-7.
29. Macintyre, A. and T.C. Cymet, *Probiotics: the benefits of bacterial cultures.* Compr Ther, 2005. **31**(3): p. 181-5.
30. Scarpellini, E., et al., *Probiotics: which and when?* Dig Dis, 2008. **26**(2): p. 175-82.
31. Farnworth, E.R., *The evidence to support health claims for probiotics.* J Nutr, 2008. **138**(6): p. 1250S-4S.
32. Goldin, B.R. and S.L. Gorbach, *Clinical indications for probiotics: an overview.* Clin Infect Dis, 2008. **46 Suppl 2**(Supplement_2): p. S96-100; discussion S144-51.
33. Schrezenmeir, J. and M. de Vrese, *Probiotics, prebiotics, and synbiotics—approaching a definition–.* The American journal of clinical nutrition, 2001. **73**(2): p. 361s-364s.
34. Williams, N.T., *Probiotics.* American Journal of Health-System Pharmacy, 2010. **67**(6): p. 449-458.
35. Vanderhoof, J.A. and R.J. Young, *Current and potential uses of probiotics.* Ann Allergy Asthma Immunol, 2004. **93**(5 Suppl 3): p. S33-7.
36. Silva, M., et al., *Antimicrobial substance from a human Lactobacillus strain.* Antimicrob Agents Chemother, 1987. **31**(8): p. 1231-3.
37. Chan, R.C., et al., *Competitive exclusion of uropathogens from human uroepithelial cells by Lactobacillus whole cells and cell wall fragments.* Infect Immun, 1985. **47**(1): p. 84-9.

38. Mack, D.R., et al., *Probiotics inhibit enteropathogenic E. coli adherence in vitro by inducing intestinal mucin gene expression.* Am J Physiol, 1999. **276**(4 Pt 1): p. G941-50.

39. Reid, G., et al., *Potential uses of probiotics in clinical practice.* Clin Microbiol Rev, 2003. **16**(4): p. 658-72.

40. Ljungh, Å., J. Lan, and N. Yanagisawa, *Isolation, Selection and Characteristics of Lactobacillus paracasei subsp. paracasei F19.* Microbial Ecology in Health and Disease, 2009. **14**(1): p. 4-6.

41. Lee, Y.K. and S. Salminen, *Handbook of probiotics and prebiotics*. 2009: John Wiley & Sons.

42. Bauer, S.A.W., U. Kulozik, and P. Foerst, *Drying Kinetics and Survival of Bacteria Suspensions ofL. paracaseiF19 in Low-Temperature Vacuum Drying.* Drying Technology, 2013. **31**(13-14): p. 1497-1503.

43. Ohlson, K., et al., *Lactobacillus F19-a probiotic strain suitable for consumer products.* Microbial ecology in health and disease, 2002. **14**(1): p. 27-32.

44. Di Cerbo, A. and B. Palmieri, *Lactobacillus Paracasei subsp. Paracasei F19; a farmacogenomic and clinical update.* Nutr Hosp, 2013. **28**(6): p. 1842-50.

45. Crittenden, R., et al., *Lactobacillus paracasei subsp. paracasei F19: Survival, Ecology and Safety in the Human Intestinal Tract - A Survey of Feeding Studies within the PROBDEMO Project.* Microbial Ecology in Health and Disease, 2009. **14**(1): p. 22-26.

46. Santivarangkna, C., U. Kulozik, and P. Foerst, *Inactivation mechanisms of lactic acid starter cultures preserved by drying processes.* J Appl Microbiol, 2008. **105**(1): p. 1-13.

47. Meryman, H.T., R.J. Williams, and M.S. Douglas, *Freezing injury from "solution effects" and its prevention by natural or artificial cryoprotection.* Cryobiology, 1977. **14**(3): p. 287-302.

48. Papadimitriou, K., et al., *Stress Physiology of Lactic Acid Bacteria.* Microbiol Mol Biol Rev, 2016. **80**(3): p. 837-90.

49. Duwat, P., et al., *Lactococcus lactis, a bacterial model for stress responses and survival.* Int J Food Microbiol, 2000. **55**(1-3): p. 83-6.

50. Johnson, E., *Microbial adaptation and survival in foods*, in *Microbial stress adaptation and food safety*. 2002. p. 84-85.

51. Beales, N., *Adaptation of Microorganisms to Cold Temperatures, Weak Acid Preservatives, Low pH, and Osmotic Stress: A Review.* Comprehensive Reviews in Food Science and Food Safety, 2004. **3**(1): p. 1-20.

52. Vinusha, K.S., et al., *Proteomic studies on lactic acid bacteria: A review.* Biochem Biophys Rep, 2018. **14**: p. 140-148.

53. Hecker, M., W. Schumann, and U. Volker, *Heat-shock and general stress response in Bacillus subtilis.* Mol Microbiol, 1996. **19**(3): p. 417-28.

54. Kohlstedt, M., et al., *Adaptation of Bacillus subtilis carbon core metabolism to simultaneous nutrient limitation and osmotic challenge: a multi-omics perspective.* Environ Microbiol, 2014. **16**(6): p. 1898-917.

55. Rosen, R., et al., *Stress-induced proteins of Agrobacterium tumefaciens.* FEMS Microbiol Ecol, 2001. **35**(3): p. 277-285.

56. Hecker, M. and U. Völker, *General stress proteins in Bacillus subtilis.* FEMS Microbiology Ecology, 1990. **7**(2-3): p. 197-213.

57. Hartke, A., et al., *Starvation-Induced Stress Resistance in Lactococcus lactis subsp. lactis IL1403.* Appl Environ Microbiol, 1994. **60**(9): p. 3474-8.

58. Hormann, S., et al., *Comparative proteome approach to characterize the high-pressure stress response of Lactobacillus sanfranciscensis DSM 20451(T).* Proteomics, 2006. **6**(6): p. 1878-85.

59. Kilstrup, M., et al., *Induction of heat shock proteins DnaK, GroEL, and GroES by salt stress in Lactococcus lactis.* Appl Environ Microbiol, 1997. **63**(5): p. 1826-37.

60. Scheyhing, C.H., et al., *Barotolerance is inducible by preincubation under hydrostatic pressure, cold-, osmotic- and acid-stress conditions in Lactobacillus sanfranciscensis DSM 20451T.* Lett Appl Microbiol, 2004. **39**(3): p. 284-9.

61. Hansen, L.J.J., et al., *Freeze-drying of live virus vaccines: A review.* Vaccine, 2015. **33**(42): p. 5507-5519.

62. Rey, L., *Freeze-drying/lyophilization of pharmaceutical and biological products*. 2016: CRC Press.

63. Leslie, S.B., et al., *Trehalose and sucrose protect both membranes and proteins in intact bacteria during drying.* Applied and environmental microbiology, 1995. **61**(10): p. 3592-3597.

64. Kets, E., P. Teunissen, and J. De Bont, *Effect of compatible solutes on survival of lactic Acid bacteria subjected to drying.* Applied and Environmental Microbiology, 1996. **62**(1): p. 259-261.

65. Elbein, A.D., et al., *New insights on trehalose: a multifunctional molecule.* Glycobiology, 2003. **13**(4): p. 17R-27R.

66. Flessa, S., *Drying Stress and Survival of Shigella and Salmonella in Food Derived Model Systems*, in *Technische Mikrobiologie*. 2005, Technische Universität München.

67. Garay-Arroyo, A., et al., *Highly hydrophilic proteins in prokaryotes and eukaryotes are common during conditions of water deficit.* J Biol Chem, 2000. **275**(8): p. 5668-74.

68. Mills, S., et al., *Enhancing the stress responses of probiotics for a lifestyle from gut to product and back again.* Microb Cell Fact, 2011. **10 Suppl 1**: p. S19.

69. Crowe, J.H., J.F. Carpenter, and L.M. Crowe, *The role of vitrification in anhydrobiosis.* Annu Rev Physiol, 1998. **60**(1): p. 73-103.

70. De Angelis, M. and M. Gobbetti, *Environmental stress responses in Lactobacillus: a review.* Proteomics, 2004. **4**(1): p. 106-22.

71. Prasad, J., P. McJarrow, and P. Gopal, *Heat and osmotic stress responses of probiotic Lactobacillus rhamnosus HN001 (DR20) in relation to viability after drying.* Appl Environ Microbiol, 2003. **69**(2): p. 917-25.

72. Waśko, A., M. Polak-Berecka, and W. Gustaw, *Increased viability of probiotic Lactobacillus rhamnosus after osmotic stress.* Acta alimentaria, 2013. **42**(4): p. 520-528.

73. Yi, X., E. Kot, and A. Bezkorovainy, *Properties of NADH oxidase from Lactobacillus delbrueckii ssp bulgaricus.* Journal of the Science of Food and Agriculture, 1998. **78**(4): p. 527-534.

74. Csonka, L.N. and A.D. Hanson, *Prokaryotic osmoregulation: genetics and physiology.* Annu Rev Microbiol, 1991. **45**(1): p. 569-606.

75. Kets, E., P. Teunissen, and J. de Bont, *Effect of compatible solutes on survival of lactic Acid bacteria subjected to drying.* Appl Environ Microbiol, 1996. **62**(1): p. 259-61.

76. Poolman, B. and E. Glaasker, *Regulation of compatible solute accumulation in bacteria.* Mol Microbiol, 1998. **29**(2): p. 397-407.

77. Panoff, J.M., B. Thammavongs, and M. Gueguen, *Cryoprotectants lead to phenotypic adaptation to freeze-thaw stress in Lactobacillus delbrueckii ssp. bulgaricus CIP 101027T.* Cryobiology, 2000. **40**(3): p. 264-9.

78. Glaasker, E., et al., *Physiological response of Lactobacillus plantarum to salt and nonelectrolyte stress.* J Bacteriol, 1998. **180**(17): p. 4718-23.

79. Hutkins, R.W., W.L. Ellefson, and E.R. Kashket, *Betaine Transport Imparts Osmotolerance on a Strain of Lactobacillus acidophilus.* Appl Environ Microbiol, 1987. **53**(10): p. 2275-81.

80. Kets, E.P.W. and J.A.M. Bont, *Protective effect of betaine on survival ofLactobacillus plantarumsubjected to drying.* FEMS Microbiology Letters, 1994. **116**(3): p. 251-255.

81. Pichereau, V., et al., *The osmoprotectant glycine betaine inhibits salt-induced cross-tolerance towards lethal treatment in Enterococcus faecalis.* Microbiology, 1999. **145 ( Pt 2)**: p. 427-35.

82. Glaasker, E., W.N. Konings, and B. Poolman, *Osmotic regulation of intracellular solute pools in Lactobacillus plantarum.* J Bacteriol, 1996. **178**(3): p. 575-82.

83. Tsakalidou, E. and K. Papadimitriou, *Stress responses of lactic acid bacteria*. 2011: Springer Science & Business Media.

84. Obis, D., et al., *Genetic and biochemical characterization of a high-affinity betaine uptake system (BusA) in Lactococcus lactis reveals a new functional organization within bacterial ABC transporters.* J Bacteriol, 1999. **181**(20): p. 6238-46.

85. Van Der Heide, T. and B. Poolman, *Glycine betaine transport in Lactococcus lactis is osmotically regulated at the level of expression and translocation activity.* Journal of bacteriology, 2000. **182**(1): p. 203-206.

86. Bouvier, J., et al., *Characterization of OpuA, a glycine-betaine uptake system of Lactococcus lactis.* J Mol Microbiol Biotechnol, 2000. **2**(2): p. 199-205.

87. Obis, D., A. Guillot, and M.Y. Mistou, *Tolerance to high osmolality of Lactococcus lactis subsp. lactis and cremoris is related to the activity of a betaine transport system.* FEMS Microbiol Lett, 2001. **202**(1): p. 39-44.

88. Patzlaff, J.S., T. van der Heide, and B. Poolman, *The ATP/substrate stoichiometry of the ATP-binding cassette (ABC) transporter OpuA.* J Biol Chem, 2003. **278**(32): p. 29546-51.

89. van der Heide, T., M.C. Stuart, and B. Poolman, *On the osmotic signal and osmosensing mechanism of an ABC transport system for glycine betaine.* EMBO J, 2001. **20**(24): p. 7022-32.

90. Guillot, A., D. Obis, and M.Y. Mistou, *Fatty acid membrane composition and activation of glycine-betaine transport in Lactococcus lactis subjected to osmotic stress.* Int J Food Microbiol, 2000. **55**(1-3): p. 47-51.

91. Nilsson, D., et al., *A Lactococcus lactis gene encodes a membrane protein with putative ATPase activity that is homologous to the essential Escherichia coli ftsH gene product.* Microbiology, 1994. **140**(10): p. 2601-2610.

92. Poquet, I., et al., *HtrA is the unique surface housekeeping protease in Lactococcus lactis and is required for natural protein processing.* Molecular microbiology, 2000. **35**(5): p. 1042-1051.

93. Liu, S.-Q., et al., *Influence of Reduced Water Activity on Lactose Metabolism by Lactococcus lactis subsp. cremorisat Different pH Values.* Applied and environmental microbiology, 1998. **64**(6): p. 2111-2116.

94. Uguen, P., et al., *Influence of osmolarity and the presence of an osmoprotectant on lactococcus lactis growth and bacteriocin production.* Appl Environ Microbiol, 1999. **65**(1): p. 291-3.

95. De Felipe, F.L., et al., *Cofactor engineering: a novel approach to metabolic engineering in Lactococcus lactis by controlled expression of NADH oxidase.* Journal of Bacteriology, 1998. **180**(15): p. 3804-3808.

96. Condon, S., *Responses of lactic acid bacteria to oxygen.* FEMS Microbiology Reviews, 1987. **3**(3): p. 269-280.

97. Stewart, E.J., F. Aslund, and J. Beckwith, *Disulfide bond formation in the Escherichia coli cytoplasm: an in vivo role reversal for the thioredoxins.* EMBO J, 1998. **17**(19): p. 5543-50.

98. Pebay, M., et al., *Characterization of the gor gene of the lactic acid bacterium Streptococcus thermophilus CNRZ368.* Res Microbiol, 1995. **146**(5): p. 371-83.

99. Bolotin, A., et al., *Low-redundancy sequencing of the entire Lactococcus lactis IL1403 genome.* Antonie Van Leeuwenhoek, 1999. **76**(1-4): p. 27-76.

100. Turner, M.S., et al., *The bspA locus of Lactobacillus fermentum BR11 encodes an L-cystine uptake system.* J Bacteriol, 1999. **181**(7): p. 2192-8.

101. Guerzoni, M.E., R. Lanciotti, and P.S. Cocconcelli, *Alteration in cellular fatty acid composition as a response to salt, acid, oxidative and thermal stresses in Lactobacillus helveticus.* Microbiology, 2001. **147**(8): p. 2255-2264.

102. Miyoshi, A., et al., *Oxidative stress in Lactococcus lactis.* Genet Mol Res, 2003. **2**(4): p. 348-59.

103. van Niel, E.W., K. Hofvendahl, and B. Hahn-Hagerdal, *Formation and conversion of oxygen metabolites by Lactococcus lactis subsp. lactis ATCC 19435 under different growth conditions.* Appl Environ Microbiol, 2002. **68**(9): p. 4350-6.

104. Sanders, J.W., et al., *Stress response in Lactococcus lactis: cloning, expression analysis, and mutation of the lactococcal superoxide dismutase gene.* J Bacteriol, 1995. **177**(18): p. 5254-60.

105. Archibald, F.S. and I. Fridovich, *Manganese, superoxide dismutase, and oxygen tolerance in some lactic acid bacteria.* Journal of Bacteriology, 1981. **146**(3): p. 928-936.

106. Duwat, P., et al., *Respiration capacity of the fermenting bacterium Lactococcus lactis and its positive effects on growth and survival.* J Bacteriol, 2001. **183**(15): p. 4509-16.

107. Yamamoto, Y., et al., *Respiration metabolism of Group B Streptococcus is activated by environmental haem and quinone and contributes to virulence.* Molecular microbiology, 2005. **56**(2): p. 525-534.

108. Fahey, R.C., et al., *Occurrence of glutathione in bacteria.* J Bacteriol, 1978. **133**(3): p. 1126-9.

109. Engesser, D.M. and W.P. Hammes, *Non-heme catalase activity of lactic acid bacteria.* Systematic and applied microbiology, 1994. **17**(1): p. 11-19.

110. van de Guchte, M., S.D. Ehrlich, and E. Maguin, *Production of growth-inhibiting factors by Lactobacillus delbrueckii.* J Appl Microbiol, 2001. **91**(1): p. 147-53.

111. Marty-Teysset, C., F. De La Torre, and J.-R. Garel, *Increased Production of Hydrogen Peroxide byLactobacillus delbrueckii subsp. bulgaricus upon Aeration: Involvement of an NADH Oxidase in Oxidative Stress.* Applied and environmental microbiology, 2000. **66**(1): p. 262-267.

112. Knauf, H.J., R.F. Vogel, and W.P. Hammes, *Cloning, sequence, and phenotypic expression of katA, which encodes the catalase of Lactobacillus sake LTH677.* Applied and environmental microbiology, 1992. **58**(3): p. 832-839.

113. Hertel, C., et al., *Oxygen-dependent regulation of the expression of the catalase gene katA of Lactobacillus sakei LTH677.* Appl Environ Microbiol, 1998. **64**(4): p. 1359-65.

114. Kono, Y. and I. Fridovich, *Isolation and characterization of the pseudocatalase of Lactobacillus plantarum.* J Biol Chem, 1983. **258**(10): p. 6015-9.

115. Igarashi, T., Y. Kono, and K. Tanaka, *Molecular cloning of manganese catalase from Lactobacillus plantarum.* J Biol Chem, 1996. **271**(47): p. 29521-4.

116. Duwat, P., S.D. Ehrlich, and A. Gruss, *The recA gene of Lactococcus lactis: characterization and involvement in oxidative and thermal stress.* Mol Microbiol, 1995. **17**(6): p. 1121-31.

117. Rallu, F., et al., *Acid- and multistress-resistant mutants of Lactococcus lactis : identification of intracellular stress signals.* Mol Microbiol, 2000. **35**(3): p. 517-28.

118. Presser, K.A., D.A. Ratkowsky, and T. Ross, *Modelling the growth rate of Escherichia coli as a function of pH and lactic acid concentration.* Appl Environ Microbiol, 1997. **63**(6): p. 2355-60.

119. Hartke, A., et al., *The Lactic Acid Stress Response of Lactococcus lactis subsp. lactis.* Curr Microbiol, 1996. **33**(3): p. 194-9.

120. Belli, W.A. and R.E. Marquis, *Adaptation of Streptococcus mutans and Enterococcus hirae to acid stress in continuous culture.* Appl Environ Microbiol, 1991. **57**(4): p. 1134-8.

121. Flahaut, S., et al., *Relationship between stress response towards bile salts, acid and heat treatment inEnterococcus faecalis.* FEMS Microbiology Letters, 1996. **138**(1): p. 49-54.

122. O'Sullivan, E. and S. Condon, *Relationship between acid tolerance, cytoplasmic pH, and ATP and H+-ATPase levels in chemostat cultures of Lactococcus lactis.* Applied and environmental microbiology, 1999. **65**(6): p. 2287-2293.

123. Kim, W.S., et al., *Assessment of stress response of the probiotic Lactobacillus acidophilus.* Curr Microbiol, 2001. **43**(5): p. 346-50.

124. Takahashi, N. and T. Yamada, *Acid-induced acid tolerance and acidogenicity of non-mutans streptococci.* Oral Microbiol Immunol, 1999. **14**(1): p. 43-8.

125. Champomier-Verges, M.C., et al., *Lactic acid bacteria and proteomics: current knowledge and perspectives.* J Chromatogr B Analyt Technol Biomed Life Sci, 2002. **771**(1-2): p. 329-42.

126. Hutkins, R.W. and N.L. Nannen, *pH Homeostasis in Lactic Acid Bacteria1.* Journal of Dairy Science, 1993. **76**(8): p. 2354-2365.

127. Guzzo, J., et al., *Regulation of stress response in Oenococcus oeni as a function of environmental changes and growth phase.* International journal of food microbiology, 2000. **55**(1-3): p. 27-31.

128. Arikado, E., et al., *Enzyme level of enterococcal F1Fo-ATPase is regulated by pH at the step of assembly.* The FEBS Journal, 1999. **259**(1-2): p. 262-268.

129. Kullen, M.J. and T.R. Klaenhammer, *Identification of the pH-inducible, proton-translocating F1F0-ATPase (atpBEFHAGDC) operon of Lactobacillus acidophilus by differential display: gene structure, cloning and characterization.* Mol Microbiol, 1999. **33**(6): p. 1152-61.

130. Kashket, E.R., *Bioenergetics of lactic acid bacteria: cytoplasmic pH and osmotolerance.* FEMS Microbiology Letters, 1987. **46**(3): p. 233-244.

131. Kashket, E.R. and S.L. Barker, *Effects of potassium ions on the electrical and pH gradients across the membrane of Streptococcus lactis cells.* J Bacteriol, 1977. **130**(3): p. 1017-23.

132. Cunin, R., et al., *Biosynthesis and metabolism of arginine in bacteria.* Microbiol Rev, 1986. **50**(3): p. 314-52.

133. Quivey Jr, R.G., W.L. Kuhnert, and K. Hahn, *Adaptation of oral streptococci to low pH.* 2000.

134. Hanna, M.N., et al., *uvrA Is an Acid-Inducible Gene Involved in the Adaptive Response to Low pH inStreptococcus mutans.* Journal of bacteriology, 2001. **183**(20): p. 5964-5973.

135. Hahn, K., R. Faustoferri, and R. Quivey, *Induction of an AP endonuclease activity in Streptococcus mutans during growth at low pH.* Molecular microbiology, 1999. **31**(5): p. 1489-1498.

136. Quivey Jr, R.G., et al., *Acid adaptation in Streptococcus mutans UA159 alleviates sensitization to environmental stress due to RecA deficiency.* FEMS microbiology letters, 1995. **126**(3): p. 257-261.

137. Farrow, J.A. and M.D. Collins, *Enterococcus hirae, a new species that includes amino acid assay strain NCDO 1258 and strains causing growth depression in young chickens.* International Journal of Systematic and Evolutionary Microbiology, 1985. **35**(1): p. 73-75.

138. NAKAGAWA, A. and K. KITAHARA, *Taxonomic studies on the genus Pediococcus.* The Journal of General and Applied Microbiology, 1959. **5**(3): p. 95-126.

139. Nyanga-Koumou, A.P., et al., *Response mechanisms of lactic acid bacteria to alkaline environments: a review.* Crit Rev Microbiol, 2012. **38**(3): p. 185-90.

140. Kakinuma, Y., *Lowering of cytoplasmic pH is essential for growth of Streptococcus faecalis at high pH.* J Bacteriol, 1987. **169**(9): p. 4403-5.

141. Kakinuma, Y. and K. Igarashi, *Active potassium extrusion regulated by intracellular pH in Streptococcus faecalis.* J Biol Chem, 1988. **263**(28): p. 14166-70.

142. Kakinuma, Y. and K. Igarashi, *Potassium/proton antiport system of growing Enterococcus hirae at high pH.* J Bacteriol, 1995. **177**(8): p. 2227-9.

143. Kakinuma, Y. and K. Igarashi, *Isolation and properties of Enterococcus hirae mutants defective in the potassium/proton antiport system.* J Bacteriol, 1999. **181**(13): p. 4103-5.

144. Kobayashi, H., *A proton-translocating ATPase regulates pH of the bacterial cytoplasm.* J Biol Chem, 1985. **260**(1): p. 72-6.

145. Kobayashi, H., N. Murakami, and T. Unemoto, *Regulation of the cytoplasmic pH in Streptococcus faecalis.* J Biol Chem, 1982. **257**(22): p. 13246-52.

146. Flahaut, S., et al., *Alkaline stress response in Enterococcus faecalis: adaptation, cross-protection, and changes in protein synthesis.* Appl Environ Microbiol, 1997. **63**(2): p. 812-4.

147. Knorr, D., *Novel approaches in food-processing technology: new technologies for preserving foods and modifying function.* Curr Opin Biotechnol, 1999. **10**(5): p. 485-91.

148. Senorans, J., E. Ibanez, and A. Cifuentes, *New trends in food processing.* Crit Rev Food Sci Nutr, 2003. **43**(5): p. 507-26.

149. Ross, A.I., et al., *Combining nonthermal technologies to control foodborne microorganisms.* Int J Food Microbiol, 2003. **89**(2-3): p. 125-38.

150. Sancho, F., et al., *Effect of ultra-high hydrostatic pressure on hydrosoluble vitamins.* Journal of Food Engineering, 1999. **39**(3): p. 247-253.

151. Buzrul, S., *Evaluation of Different Dose-Response Models for High Hydrostatic Pressure Inactivation of Microorganisms.* Foods, 2017. **6**(9): p. 79.

152. Guan, D., H. Chen, and D.G. Hoover, *Inactivation of Salmonella typhimurium DT 104 in UHT whole milk by high hydrostatic pressure.* Int J Food Microbiol, 2005. **104**(2): p. 145-53.

153. Molina-Hoppner, A., et al., *Protective effect of sucrose and sodium chloride for Lactococcus lactis during sublethal and lethal high-pressure treatments.* Appl Environ Microbiol, 2004. **70**(4): p. 2013-20.

154. Van Opstal, I., et al., *Inactivation of Bacillus cereus spores in milk by mild pressure and heat treatments.* Int J Food Microbiol, 2004. **92**(2): p. 227-34.

155. Clery-Barraud, C., et al., *Combined effects of high hydrostatic pressure and temperature for inactivation of Bacillus anthracis spores.* Appl Environ Microbiol, 2004. **70**(1): p. 635-7.

156. Bartlett, D.H., *Pressure effects on in vivo microbial processes.* Biochim Biophys Acta, 2002. **1595**(1-2): p. 367-81.

157. Drews, O., et al., *High pressure effects step-wise altered protein expression in Lactobacillus sanfranciscensis.* Proteomics, 2002. **2**(6): p. 765-74.

158. Molina-Hoppner, A., et al., *Effects of pressure on cell morphology and cell division of lactic acid bacteria.* Extremophiles, 2003. **7**(6): p. 511-6.

159. Abe, F. and K. Horikoshi, *The biotechnological potential of piezophiles.* Trends Biotechnol, 2001. **19**(3): p. 102-8.

160. Kato, C. and D.H. Bartlett, *The molecular biology of barophilic bacteria.* Extremophiles, 1997. **1**(3): p. 111-6.

161. Mozhaev, V.V., et al., *Exploiting the effects of high hydrostatic pressure in biotechnological applications.* Trends in Biotechnology, 1994. **12**(12): p. 493-501.

162. Balny, C. and P. Masson, *Effects of high pressure on proteins.* Food Reviews International, 1993. **9**(4): p. 611-628.

163. Landau, J.V., *Induction, transcription and translation in Escherichia coli: a hydrostatic pressure study.* Biochim Biophys Acta, 1967. **149**(2): p. 506-12.

164. Yayanos, A.A. and E.C. Pollard, *A study of the effects of hydrostatic pressure on macromolecular synthesis in Escherichia coli.* Biophys J, 1969. **9**(12): p. 1464-82.

165. Gross, M., et al., *Pressure-induced dissociation of ribosomes and elongation cycle intermediates. Stabilizing conditions and identification of the most sensitive functional state.* Eur J Biochem, 1993. **218**(2): p. 463-8.

166. DeLong, E.F. and A.A. Yayanos, *Adaptation of the membrane lipids of a deep-sea bacterium to changes in hydrostatic pressure.* Science, 1985. **228**(4703): p. 1101-3.

167. Kamimura, K., et al., *Effects of growth pressure and temperature on Fatty Acid composition of a barotolerant deep-sea bacterium.* Appl Environ Microbiol, 1993. **59**(3): p. 924-6.

168. Wirsen, C.O., et al., *Membrane lipids of a psychrophilic and barophilic deep-sea bacterium.* Current Microbiology, 1986. **14**(6): p. 319-322.

169. Allen, E.E., D. Facciotti, and D.H. Bartlett, *Monounsaturated but not polyunsaturated fatty acids are required for growth of the deep-sea bacteriumPhotobacterium profundum SS9 at high pressure and low temperature.* Applied and Environmental Microbiology, 1999. **65**(4): p. 1710-1720.

170. Kato, M. and R. Hayashi, *Effects of high pressure on lipids and biomembranes for understanding high-pressure-induced biological phenomena.* Biosci Biotechnol Biochem, 1999. **63**(8): p. 1321-8.

171. Balny, C., P. Masson, and K. Heremans, *High pressure effects on biological macromolecules: from structural changes to alteration of cellular processes.* Biochim Biophys Acta, 2002. **1595**(1-2): p. 3-10.

172. Casadei, M.A., et al., *Role of membrane fluidity in pressure resistance of Escherichia coli NCTC 8164.* Appl Environ Microbiol, 2002. **68**(12): p. 5965-72.

173. Malone, A.S., T.H. Shellhammer, and P.D. Courtney, *Effects of high pressure on the viability, morphology, lysis, and cell wall hydrolase activity of Lactococcus lactis subsp. cremoris.* Appl Environ Microbiol, 2002. **68**(9): p. 4357-63.

174. Mañas, P. and B.M. Mackey, *Morphological and physiological changes induced by high hydrostatic pressure in exponential-and stationary-phase cells of Escherichia coli: relationship with cell death.* Applied and environmental microbiology, 2004. **70**(3): p. 1545-1554.

175. Garcia-Graells, C., K.J. Hauben, and C.W. Michiels, *High-pressure inactivation and sublethal injury of pressure-resistant Escherichia coli mutants in fruit juices.* Appl Environ Microbiol, 1998. **64**(4): p. 1566-8.

176. Alpas, H., et al., *Interactions of high hydrostatic pressure, pressurization temperature and pH on death and injury of pressure-resistant and pressure-sensitive strains of foodborne pathogens.* International Journal of Food Microbiology, 2000. **60**(1): p. 33-42.

177. Pagan, R., et al., *Enhanced acid sensitivity of pressure-damaged Escherichia coli O157 cells.* Appl Environ Microbiol, 2001. **67**(4): p. 1983-5.

178. Molina-Gutierrez, A., et al., *In situ determination of the intracellular pH of Lactococcus lactis and Lactobacillus plantarum during pressure treatment.* Appl Environ Microbiol, 2002. **68**(9): p. 4399-406.

179. Perrier-Cornet, J.-M., et al., *High-pressure inactivation of Saccharomyces cerevisiae and Lactobacillus plantarum at subzero temperatures.* Journal of biotechnology, 2005. **115**(4): p. 405-412.

180. Ulmer, H.M., M.G. Ganzle, and R.F. Vogel, *Effects of high pressure on survival and metabolic activity of Lactobacillus plantarum TMW1.460.* Appl Environ Microbiol, 2000. **66**(9): p. 3966-73.

181. Korakli, M., et al., *Metabolism of Lactobacillus sanfranciscensis under high pressure: investigations using stable carbon isotopes*, in *Progress in Biotechnology*. 2002, Elsevier. p. 287-294.

182. Marquis, R.E. and G.R. Bender, *Barophysiology of prokaryotes and proton-translocating ATPases.* Current perspectives in high pressure biology, 1987: p. 65-73.

183. Abe, F. and K. Horikoshi, *Analysis of intracellular pH in the yeast Saccharomyces cerevisiae under elevated hydrostatic pressure: a study in baro- (piezo-) physiology.* Extremophiles, 1998. **2**(3): p. 223-8.

184. Zobell, C.E. and A.B. Cobet, *Growth, reproduction, and death rates of Escherichia coli at increased hydrostatic pressures.* Journal of bacteriology, 1962. **84**(6): p. 1228-1236.

185. Zobell, C.E. and A.B. Cobet, *Filament formation by Escherichia coli at increased hydrostatic pressures.* Journal of bacteriology, 1964. **87**(3): p. 710-719.

186. Aertsen, A. and C.W. Michiels, *SulA-dependent hypersensitivity to high pressure and hyperfilamentation after high-pressure treatment of Escherichia coli lon mutants.* Res Microbiol, 2005. **156**(2): p. 233-7.

187. Welch, T.J., et al., *Stress response of Escherichia coli to elevated hydrostatic pressure.* J Bacteriol, 1993. **175**(22): p. 7170-7.

188. Sato, T., et al., *The dynamism of Escherichia coli under high hydrostatic pressure—repression of the FtsZ-ring formation and chromosomal DNA condensation*, in *Progress in Biotechnology*. 2002, Elsevier. p. 233-238.

189. Ishii, A., et al., *Effects of high hydrostatic pressure on bacterial cytoskeleton FtsZ polymers in vivo and in vitro.* Microbiology, 2004. **150**(Pt 6): p. 1965-72.

190. Kawarai, T., et al., *SulA-independent filamentation of Escherichia coli during growth after release from high hydrostatic pressure treatment.* Appl Microbiol Biotechnol, 2004. **64**(2): p. 255-62.

191. Certes, A.-A., *De l'Action des hautes pressions sur les phénomènes de la putréfaction et sur la vitalité des micro-organismes d'eau douce et d'eau de mer, par A. Certes*. 1884: Gauthier-Villars.

192. Groß, M., et al., *Response of bacteria and fungi to high-pressure stress as investigated by two-dimensional polyacrylamide gel electrophoresis.* Electrophoresis, 1994. **15**(1): p. 1559-1565.

193. Aertsen, A., et al., *Heat shock protein-mediated resistance to high hydrostatic pressure in Escherichia coli.* Appl Environ Microbiol, 2004. **70**(5): p. 2660-6.

194. Scheyhing, C.H., *Hochdruckinduzierte Genexpression bei Bakterien*. 2003, Technische Universität München.

195. Drews, O., *Differential proteome analysis of selected lactic acid bacteria, stress response and database construction*. 2005, Technische Universität München.

196. Hörmann, S., *Hochdruckinduzierte Stressantwort bei Lactobacillus sanfranciscensis DSM 20451T*. 2007, Technische Universität München.

197. Ishii, A., et al., *Analysis of hydrostatic pressure effects on transcription in Escherichia coli by DNA microarray procedure.* Extremophiles, 2005. **9**(1): p. 65-73.

198. Ananta, E. and D. Knorr, *Evidence on the role of protein biosynthesis in the induction of heat tolerance of Lactobacillus rhamnosus GG by pressure pre-treatment.* Int J Food Microbiol, 2004. **96**(3): p. 307-13.

199. Ananta, E. and D. Knorr, *Pressure-induced thermotolerance of Lactobacillus rhamnosus GG.* Food research international, 2003. **36**(9-10): p. 991-997.

200. Bartlett, D.H., C. Kato, and K. Horikoshi, *High pressure influences on gene and protein expression.* Res Microbiol, 1995. **146**(8): p. 697-706.

201. Abee, T. and J.A. Wouters, *Microbial stress response in minimal processing.* Int J Food Microbiol, 1999. **50**(1-2): p. 65-91.

202. Desmond, C., et al., *Improved stress tolerance of GroESL-overproducing Lactococcus lactis and probiotic Lactobacillus paracasei NFBC 338.* Appl Environ Microbiol, 2004. **70**(10): p. 5929-36.

203. Wemekamp-Kamphuis, H.H., et al., *Enhanced levels of cold shock proteins in Listeria monocytogenes LO28 upon exposure to low temperature and high hydrostatic pressure.* Applied and Environmental Microbiology, 2002. **68**(2): p. 456-463.

204. Poolman, B., et al., *Bioenergetic consequences of lactose starvation for continuously cultured Streptococcus cremoris.* J Bacteriol, 1987. **169**(4): p. 1460-8.

205. Konings, W.N., et al., *The role of transport processes in survival of lactic acid bacteria. Energy transduction and multidrug resistance.* Antonie Van Leeuwenhoek, 1997. **71**(1-2): p. 117-28.

206. Tonon, T. and A. Lonvaud-Funel, *Metabolism of arginine and its positive effect on growth and revival of Oenococcus oeni.* J Appl Microbiol, 2000. **89**(3): p. 526-31.

207. Kunji, E., et al., *Physiological responses of Lactococcus lactis ML3 to alternating conditions of growth and starvation.* Archives of microbiology, 1993. **159**(4): p. 372-379.

208. Lange, R. and R. Hengge-Aronis, *Growth phase-regulated expression of bolA and morphology of stationary-phase Escherichia coli cells are controlled by the novel sigma factor sigma S.* J Bacteriol, 1991. **173**(14): p. 4474-81.

209. Giard, J.C., et al., *Starvation-induced multiresistance in Enterococcus faecalis JH2-2.* Curr Microbiol, 1996. **32**(5): p. 264-71.

210. Hartke, A., et al., *Survival of Enterococcus faecalis in an oligotrophic microcosm: changes in morphology, development of general stress resistance, and analysis of protein synthesis.* Appl Environ Microbiol, 1998. **64**(11): p. 4238-45.

211. Giard, J.C., et al., *The stress proteome of Enterococcus faecalis.* Electrophoresis, 2001. **22**(14): p. 2947-54.

212. Stuart, M.R., L.S. Chou, and B.C. Weimer, *Influence of carbohydrate starvation and arginine on culturability and amino acid utilization of lactococcus lactis subsp. lactis.* Appl Environ Microbiol, 1999. **65**(2): p. 665-73.

213. Champomier Vergès, M.-C., et al., *Relationships between arginine degradation, pH and survival in Lactobacillus sakei.* FEMS Microbiology Letters, 1999. **180**(2): p. 297-304.

214. Kornberg, A., N.N. Rao, and D. Ault-Riche, *Inorganic polyphosphate: a molecule of many functions.* Annual review of biochemistry, 1999. **68**(1): p. 89-125.

215. Rao, N. and A. Kornberg, *Inorganic polyphosphate regulates responses of Escherichia coli to nutritional stringencies, environmental stresses and survival in the stationary phase*, in *Inorganic Polyphosphates*. 1999, Springer. p. 183-195.

216. Kuroda, A., et al., *Role of inorganic polyphosphate in promoting ribosomal protein degradation by the Lon protease in E. coli.* Science, 2001. **293**(5530): p. 705-8.

217. Hengge-Aronis, R., *Survival of hunger and stress: the role of rpoS in early stationary phase gene regulation in E. coli.* Cell, 1993. **72**(2): p. 165-8.

218. Hengge-Aronis, R., *Interplay of global regulators and cell physiology in the general stress response of Escherichia coli.* Curr Opin Microbiol, 1999. **2**(2): p. 148-52.

219. Bernhardt, J., et al., *Specific and general stress proteins in Bacillus subtilis–a two-dimensional protein electrophoresis study.* Microbiology, 1997. **143**(3): p. 999-1017.

220. Voelker, U., et al., *Separate mechanisms activate sigma B of Bacillus subtilis in response to environmental and metabolic stresses.* J Bacteriol, 1995. **177**(13): p. 3771-80.

221. Mechold, U., et al., *Functional analysis of a relA/spoT gene homolog from Streptococcus equisimilis.* J Bacteriol, 1996. **178**(5): p. 1401-11.

222. Whitehead, K.E., G.M. Webber, and R.R. England, *Accumulation of ppGpp in Streptococcus pyogenes and Streptococcus rattus following amino acid starvation.* FEMS Microbiol Lett, 1998. **159**(1): p. 21-6.

223. Crosse, A.M., D.L. Greenway, and R.R. England, *Accumulation of ppGpp and ppGp in Staphylococcus aureus 8325-4 following nutrient starvation.* Lett Appl Microbiol, 2000. **31**(4): p. 332-7.

224. Wendrich, T.M. and M.A. Marahiel, *Cloning and characterization of a relA/spoT homologue from Bacillus subtilis.* Mol Microbiol, 1997. **26**(1): p. 65-79.

225. Kvint, K., A. Farewell, and T. Nyström, *RpoS-dependent promoters require guanosine tetraphosphate for induction even in the presence of high levels of ςS.* Journal of Biological Chemistry, 2000. **275**(20): p. 14795-14798.

226. Wehmeier, L., et al., *The role of the Corynebacterium glutamicum rel gene in (p)ppGpp metabolism.* Microbiology, 1998. **144 ( Pt 7)**(7): p. 1853-62.

227. Chatterji, D. and A.K. Ojha, *Revisiting the stringent response, ppGpp and starvation signaling.* Curr Opin Microbiol, 2001. **4**(2): p. 160-5.

228. Steiner, K. and H. Malke, *Life in protein-rich environments: the relA-independent response of Streptococcus pyogenes to amino acid starvation.* Mol Microbiol, 2000. **38**(5): p. 1004-16.

229. Phadtare, S. and M. Inouye, *The Cold Shock Response.* EcoSal Plus, 2008. **3**(1).

230. Wouters, J.A., et al., *The role of cold-shock proteins in low-temperature adaptation of food-related bacteria.* Syst Appl Microbiol, 2000. **23**(2): p. 165-73.

231. Jiang, W., L. Fang, and M. Inouye, *The role of the 5'-end untranslated region of the mRNA for CspA, the major cold-shock protein of Escherichia coli, in cold-shock adaptation.* J Bacteriol, 1996. **178**(16): p. 4919-25.

232. Fang, L., et al., *Promoter-independent cold-shock induction of cspA and its derepression at 37 C by mRNA stabilization.* Molecular microbiology, 1997. **23**(2): p. 355-364.

233. Yamanaka, K., M. Mitta, and M. Inouye, *Mutation analysis of the 5' untranslated region of the cold shock cspA mRNA of Escherichia coli.* J Bacteriol, 1999. **181**(20): p. 6284-91.

234. Brandi, A., et al., *Post-transcriptional regulation of CspA expression in Escherichia coli.* Mol Microbiol, 1996. **19**(2): p. 231-40.

235. Goldenberg, D., I. Azar, and A.B. Oppenheim, *Differential mRNA stability of the cspA gene in the cold-shock response of Escherichia coli.* Mol Microbiol, 1996. **19**(2): p. 241-8.

236. Kaan, T., B. Jurgen, and T. Schweder, *Regulation of the expression of the cold shock proteins CspB and CspC in Bacillus subtilis.* Mol Gen Genet, 1999. **262**(2): p. 351-4.

237. Graumann, P., et al., *Cold shock stress-induced proteins in Bacillus subtilis.* J Bacteriol, 1996. **178**(15): p. 4611-9.

238. Bae, W., P.G. Jones, and M. Inouye, *CspA, the major cold shock protein of Escherichia coli, negatively regulates its own gene expression.* J Bacteriol, 1997. **179**(22): p. 7081-8.

239. Xia, B., H. Ke, and M. Inouye, *Acquirement of cold sensitivity by quadruple deletion of the cspA family and its suppression by PNPase S1 domain in Escherichia coli.* Mol Microbiol, 2001. **40**(1): p. 179-88.

240. Graumann, P., et al., *A family of cold shock proteins in Bacillus subtilis is essential for cellular growth and for efficient protein synthesis at optimal and low temperatures.* Molecular microbiology, 1997. **25**(4): p. 741-756.

241. Jiang, W., Y. Hou, and M. Inouye, *CspA, the major cold-shock protein of Escherichia coli, is an RNA chaperone.* Journal of Biological Chemistry, 1997. **272**(1): p. 196-202.

242. Hanna, M.M. and K. Liu, *Nascent RNA in transcription complexes interacts with CspE, a small protein in E. coli implicated in chromatin condensation1.* Journal of molecular biology, 1998. **282**(2): p. 227-239.

243. Phadtare, S. and M. Inouye, *Sequence-selective interactions with RNA by CspB, CspC and CspE, members of the CspA family of Escherichia coli.* Mol Microbiol, 1999. **33**(5): p. 1004-14.

244. Somero, G.N., *Proteins and temperature.* Annu Rev Physiol, 1995. **57**(1): p. 43-68.

245. Earnshaw, R., J. Appleyard, and R. Hurst, *Understanding physical inactivation processes: combined preservation opportunities using heat, ultrasound and pressure.* International Journal of Food Microbiology, 1995. **28**(2): p. 197-219.

246. Teixeira, P., et al., *Identification of sites of injury in Lactobacillus bulgaricus during heat stress.* J Appl Microbiol, 1997. **83**(2): p. 219-26.

247. Hansen, M.C., et al., *Changes in rRNA levels during stress invalidates results from mRNA blotting: fluorescence in situ rRNA hybridization permits renormalization for estimation of cellular mRNA levels.* J Bacteriol, 2001. **183**(16): p. 4747-51.

248. Whitaker, R.D. and C.A. Batt, *Characterization of the Heat Shock Response in Lactococcus lactis subsp. lactis.* Appl Environ Microbiol, 1991. **57**(5): p. 1408-12.

249. Auffray, Y., et al., *Heat shock-induced protein synthesis inLactococcus lactis subsp. lactis.* Current microbiology, 1992. **24**(5): p. 281-284.

250. Salotra, P., et al., *Expression of DnaK and GroEL homologs in Leuconostoc esenteroides in response to heat shock, cold shock or chemical stress.* FEMS Microbiol Lett, 1995. **131**(1): p. 57-62.

251. Flahaut, S., et al., *Relationship between stress response towards bile salts, acid and heat treatment in Enterococcus faecalis.* FEMS microbiology letters, 1996. **138**(1): p. 49-54.

252. Guzzo, J., et al., *A small heat shock protein from Leuconostoc oenos induced by multiple stresses and during stationary growth phase.* Lett Appl Microbiol, 1997. **24**(5): p. 393-6.

253. Gouesbet, G., G. Jan, and P. Boyaval, *Two-dimensional electrophoresis study of Lactobacillus delbrueckii subsp. bulgaricus thermotolerance.* Appl Environ Microbiol, 2002. **68**(3): p. 1055-63.

254. Zuber, U. and W. Schumann, *CIRCE, a novel heat shock element involved in regulation of heat shock operon dnaK of Bacillus subtilis.* J Bacteriol, 1994. **176**(5): p. 1359-63.

255. Petersohn, A., et al., *Global analysis of the general stress response ofBacillus subtilis.* Journal of bacteriology, 2001. **183**(19): p. 5617-5631.

256. Price, C.W., et al., *Genome-wide analysis of the general stress response in Bacillus subtilis.* Mol Microbiol, 2001. **41**(4): p. 757-74.

257. Derre, I., G. Rapoport, and T. Msadek, *CtsR, a novel regulator of stress and heat shock response, controls clp and molecular chaperone gene expression in gram-positive bacteria.* Mol Microbiol, 1999. **31**(1): p. 117-31.

258. Svensater, G., B. Sjogreen, and I.R. Hamilton, *Multiple stress responses in Streptococcus mutans and the induction of general and stress-specific proteins.* Microbiology, 2000. **146 ( Pt 1)**(1): p. 107-17.

259. Nussey, D.H., A.J. Wilson, and J.E. Brommer, *The evolutionary ecology of individual phenotypic plasticity in wild populations.* J Evol Biol, 2007. **20**(3): p. 831-44.

260. Gabriel, W., *How stress selects for reversible phenotypic plasticity.* J Evol Biol, 2005. **18**(4): p. 873-83.

261. Garland, T., Jr. and S.A. Kelly, *Phenotypic plasticity and experimental evolution.* J Exp Biol, 2006. **209**(Pt 12): p. 2344-61.

262. Fuller, A., et al., *Physiological mechanisms in coping with climate change.* Physiol Biochem Zool, 2010. **83**(5): p. 713-20.

263. Scheiner, S.M. and R.F. Lyman, *The genetics of phenotypic plasticity I. Heritability.* Journal of Evolutionary Biology, 1989. **2**(2): p. 95-107.

264. Bradshaw, W. and C. Holzapfel, *Genetic response to rapid climate change: it's seasonal timing that matters.* Molecular ecology, 2008. **17**(1): p. 157-166.

265. Somero, G., *The physiology of climate change: how potentials for acclimatization and genetic adaptation will determine 'winners' and 'losers'.* Journal of Experimental Biology, 2010. **213**(6): p. 912-920.

266. Pigliucci, M., C.J. Murren, and C.D. Schlichting, *Phenotypic plasticity and evolution by genetic assimilation.* J Exp Biol, 2006. **209**(Pt 12): p. 2362-7.

267. Fusco, G. and A. Minelli, *Phenotypic plasticity in development and evolution: facts and concepts. Introduction.* Philos Trans R Soc Lond B Biol Sci, 2010. **365**(1540): p. 547-56.

268. Singh, O.V. and N.S. Nagaraj, *Transcriptomics, proteomics and interactomics: unique approaches to track the insights of bioremediation.* Brief Funct Genomic Proteomic, 2006. **4**(4): p. 355-62.

269. Feder, M.E. and J.C. Walser, *The biological limitations of transcriptomics in elucidating stress and stress responses.* J Evol Biol, 2005. **18**(4): p. 901-10.

270. Karr, T.L., *Application of proteomics to ecology and population biology.* Heredity (Edinb), 2008. **100**(2): p. 200-6.

271. Lemos, M.F., et al., *Proteins in ecotoxicology - how, why and why not?* Proteomics, 2010. **10**(4): p. 873-87.

272. Mallick, P. and B. Kuster, *Proteomics: a pragmatic perspective.* Nat Biotechnol, 2010. **28**(7): p. 695-709.

273. Silvestre, F., V. Gillardin, and J. Dorts, *Proteomics to assess the role of phenotypic plasticity in aquatic organisms exposed to pollution and global warming*. 2012, Oxford University Press.

274. Pan, C., et al., *Comparative proteomic phenotyping of cell lines and primary cells to assess preservation of cell type-specific functions.* Mol Cell Proteomics, 2009. **8**(3): p. 443-50.

275. Doolittle, W.F. and C. Sapienza, *Selfish genes, the phenotype paradigm and genome evolution.* Nature, 1980. **284**(5757): p. 601-3.

276. Khaitovich, P., et al., *A neutral model of transcriptome evolution.* PLoS Biol, 2004. **2**(5): p. E132.

277. Bedon, F., et al., *Proteomic plasticity of two Eucalyptus genotypes under contrasted water regimes in the field.* Plant Cell Environ, 2012. **35**(4): p. 790-805.

278. Morgan, C., et al., *Plasticity demonstrated in the proteome of a parasitic nematode within the intestine of different host strains.* Proteomics, 2006. **6**(16): p. 4633-4645.

279. Martínez-Fernández, M.n., et al., *Proteomic comparison between two marine snail ecotypes reveals details about the biochemistry of adaptation.* Journal of proteome research, 2008. **7**(11): p. 4926-4934.

280. Martínez-Fernández, M., M.P. de la Cadena, and E. Rolán-Alvarez, *The role of phenotypic plasticity on the proteome differences between two sympatric marine snail ecotypes adapted to distinct micro-habitats.* BMC evolutionary biology, 2010. **10**(1): p. 65.

281. Aebersold, R. and M. Mann, *Mass-spectrometric exploration of proteome structure and function.* Nature, 2016. **537**(7620): p. 347-55.

282. Steen, H. and M. Mann, *The ABC's (and XYZ's) of peptide sequencing.* Nat Rev Mol Cell Biol, 2004. **5**(9): p. 699-711.

283. Giansanti, P., et al., *Six alternative proteases for mass spectrometry-based proteomics beyond trypsin.* Nat Protoc, 2016. **11**(5): p. 993-1006.

284. Tsiatsiani, L. and A.J. Heck, *Proteomics beyond trypsin.* FEBS J, 2015. **282**(14): p. 2612-26.

285. Swaney, D.L., C.D. Wenger, and J.J. Coon, *Value of Using Multiple Proteases for Large-Scale Mass Spectrometry-Based Proteomics.* Journal of Proteome Research, 2010. **9**(3): p. 1323-1329.

286. Zhou, F., et al., *Online nanoflow reversed phase-strong anion exchange-reversed phase liquid chromatography-tandem mass spectrometry platform for efficient and in-depth proteome sequence analysis of complex organisms.* Anal Chem, 2011. **83**(18): p. 6996-7005.

287. Manadas, B., et al., *Peptide fractionation in proteomics approaches.* Expert Review of Proteomics, 2010. **7**(5): p. 655-663.

288. Ritorto, M.S., et al., *Hydrophilic strong anion exchange (hSAX) chromatography for highly orthogonal peptide separation of complex proteomes.* J Proteome Res, 2013. **12**(6): p. 2449-57.

289. Wolters, D.A., M.P. Washburn, and J.R. Yates, 3rd, *An automated multidimensional protein identification technology for shotgun proteomics.* Anal Chem, 2001. **73**(23): p. 5683-90.

290. Savaryn, J.P., T.K. Toby, and N.L. Kelleher, *A researcher's guide to mass spectrometry-based proteomics.* Proteomics, 2016. **16**(18): p. 2435-43.

291. Scheltema, R.A., et al., *The Q Exactive HF, a Benchtop mass spectrometer with a pre-filter, high-performance quadrupole and an ultra-high-field Orbitrap analyzer.* Mol Cell Proteomics, 2014. **13**(12): p. 3698-708.

292. Michalski, A., et al., *Mass spectrometry-based proteomics using Q Exactive, a high-performance benchtop quadrupole Orbitrap mass spectrometer.* Mol Cell Proteomics, 2011. **10**(9): p. M111 011015.

293. Nilsson, T., et al., *Mass spectrometry in high-throughput proteomics: ready for the big time.* Nat Methods, 2010. **7**(9): p. 681-5.

294. Fenn, J.B., et al., *Electrospray ionization for mass spectrometry of large biomolecules.* Science, 1989. **246**(4926): p. 64-71.

295. Wilm, M. and M. Mann, *Analytical properties of the nanoelectrospray ion source.* Anal Chem, 1996. **68**(1): p. 1-8.

296. Karas, M., U. Bahr, and T. Dulcks, *Nano-electrospray ionization mass spectrometry: addressing analytical problems beyond routine.* Fresenius J Anal Chem, 2000. **366**(6-7): p. 669-76.

297. Makarov, A., *Electrostatic Axially Harmonic Orbital Trapping: A High-Performance Technique of Mass Analysis.* Analytical Chemistry, 2000. **72**(6): p. 1156-1162.

298. Perry, R.H., R.G. Cooks, and R.J. Noll, *Orbitrap mass spectrometry: instrumentation, ion motion and applications.* Mass Spectrom Rev, 2008. **27**(6): p. 661-99.

299. Hu, Q., et al., *The Orbitrap: a new mass spectrometer.* J Mass Spectrom, 2005. **40**(4): p. 430-43.

300. Zubarev, R.A. and A. Makarov, *Orbitrap mass spectrometry*. 2013, ACS Publications.

301. Scigelova, M., et al., *Fourier transform mass spectrometry.* Mol Cell Proteomics, 2011. **10**(7): p. M111 009431.

302. McLafferty, F.W., *Tandem mass spectrometry.* Science, 1981. **214**(4518): p. 280-7.

303. Roepstorff, P. and J. Fohlman, *Proposal for a common nomenclature for sequence ions in mass spectra of peptides.* Biomed Mass Spectrom, 1984. **11**(11): p. 601.

304. Michalski, A., J. Cox, and M. Mann, *More than 100,000 detectable peptide species elute in single shotgun proteomics runs but the majority is inaccessible to data-dependent LC-MS/MS.* J Proteome Res, 2011. **10**(4): p. 1785-93.

305. Nesvizhskii, A.I., O. Vitek, and R. Aebersold, *Analysis and validation of proteomic data generated by tandem mass spectrometry.* Nat Methods, 2007. **4**(10): p. 787-97.

306. Tyanova, S., T. Temu, and J. Cox, *The MaxQuant computational platform for mass spectrometry-based shotgun proteomics.* Nat Protoc, 2016. **11**(12): p. 2301-2319.

307. Jeong, K., S. Kim, and N. Bandeira, *False discovery rates in spectral identification.* BMC Bioinformatics, 2012. **13 Suppl 16**: p. S2.

308. Nesvizhskii, A.I., *A survey of computational methods and error rate estimation procedures for peptide and protein identification in shotgun proteomics.* J Proteomics, 2010. **73**(11): p. 2092-123.

309. Nesvizhskii, A.I. and R. Aebersold, *Analysis, statistical validation and dissemination of large-scale proteomics datasets generated by tandem MS.* Drug Discov Today, 2004. **9**(4): p. 173-81.

310. Nesvizhskii, A.I., et al., *A statistical model for identifying proteins by tandem mass spectrometry.* Anal Chem, 2003. **75**(17): p. 4646-58.

311. Keller, A., et al., *Empirical statistical model to estimate the accuracy of peptide identifications made by MS/MS and database search.* Anal Chem, 2002. **74**(20): p. 5383-92.

312. Elias, J.E. and S.P. Gygi, *Target-decoy search strategy for increased confidence in large-scale protein identifications by mass spectrometry.* Nat Methods, 2007. **4**(3): p. 207-14.

313. Cox, J., et al., *Accurate proteome-wide label-free quantification by delayed normalization and maximal peptide ratio extraction, termed MaxLFQ.* Mol Cell Proteomics, 2014. **13**(9): p. 2513-26.

314. Cox, J. and M. Mann, *MaxQuant enables high peptide identification rates, individualized p.p.b.-range mass accuracies and proteome-wide protein quantification.* Nat Biotechnol, 2008. **26**(12): p. 1367-72.

315. Cox, J., et al., *Andromeda: a peptide search engine integrated into the MaxQuant environment.* J Proteome Res, 2011. **10**(4): p. 1794-805.

316. Bantscheff, M., et al., *Quantitative mass spectrometry in proteomics: critical review update from 2007 to the present.* Anal Bioanal Chem, 2012. **404**(4): p. 939-65.

317. Bantscheff, M., et al., *Quantitative mass spectrometry in proteomics: a critical review.* Analytical and Bioanalytical Chemistry, 2007. **389**(4): p. 1017-1031.

318. Thompson, A., et al., *Tandem Mass Tags: A Novel Quantification Strategy for Comparative Analysis of Complex Protein Mixtures by MS/MS.* Analytical Chemistry, 2003. **75**(8): p. 1895-1904.

319. De Man, J.C., d.M. Rogosa, and M.E. Sharpe, *A medium for the cultivation of lactobacilli.* Journal of applied Bacteriology, 1960. **23**(1): p. 130-135.

320. Schott, A.S., et al., *MALDI-TOF Mass Spectrometry Enables a Comprehensive and Fast Analysis of Dynamics and Qualities of Stress Responses of Lactobacillus paracasei subsp. paracasei F19.* PLoS One, 2016. **11**(10): p. e0165504.

321. Eid, J., et al., *Real-time DNA sequencing from single polymerase molecules.* Science, 2009. **323**(5910): p. 133-8.

322. McCarthy, A., *Third generation DNA sequencing: pacific biosciences' single molecule real time technology.* Chem Biol, 2010. **17**(7): p. 675-6.

323. Chin, C.S., et al., *Nonhybrid, finished microbial genome assemblies from long-read SMRT sequencing data.* Nat Methods, 2013. **10**(6): p. 563-9.

324. Altschul, S.F., et al., *Basic local alignment search tool.* J Mol Biol, 1990. **215**(3): p. 403-10.

325. Camacho, C., et al., *BLAST+: architecture and applications.* BMC Bioinformatics, 2009. **10**: p. 421.

326. Krumsiek, J., R. Arnold, and T. Rattei, *Gepard: a rapid and sensitive tool for creating dotplots on genome scale.* Bioinformatics, 2007. **23**(8): p. 1026-8.

327. Aziz, R.K., et al., *The RAST Server: rapid annotations using subsystems technology.* BMC Genomics, 2008. **9**: p. 75.

328. Seaver, S.M., et al., *High-throughput comparison, functional annotation, and metabolic modeling of plant genomes using the PlantSEED resource.* Proc Natl Acad Sci U S A, 2014. **111**(26): p. 9645-50.

329. Overbeek, R., et al., *The SEED and the Rapid Annotation of microbial genomes using Subsystems Technology (RAST).* Nucleic Acids Res, 2014. **42**(Database issue): p. D206-14.

330. Behr, J., et al., *The Identification of Novel Diagnostic Marker Genes for the Detection of Beer Spoiling Pediococcus damnosus Strains Using the BlAst Diagnostic Gene findEr.* PLoS One, 2016. **11**(3): p. e0152747.

331. Angiuoli, S.V., et al., *Toward an online repository of Standard Operating Procedures (SOPs) for (meta)genomic annotation.* OMICS, 2008. **12**(2): p. 137-41.

332. Burks, C., et al., *The GenBank nucleic acid sequence database.* Comput Appl Biosci, 1985. **1**(4): p. 225-33.

333. Clark, K., et al., *GenBank.* Nucleic Acids Res, 2016. **44**(D1): p. D67-72.

334. Vesth, T., et al., *CMG-biotools, a free workbench for basic comparative microbial genomics.* PLoS One, 2013. **8**(4): p. e60120.

335. Gardy, J.L., et al., *PSORTb v.2.0: expanded prediction of bacterial protein subcellular localization and insights gained from comparative proteome analysis.* Bioinformatics, 2005. **21**(5): p. 617-23.

336. Yu, N.Y., et al., *PSORTb 3.0: improved protein subcellular localization prediction with refined localization subcategories and predictive capabilities for all prokaryotes.* Bioinformatics, 2010. **26**(13): p. 1608-15.

337. Gardy, J.L., et al., *PSORT-B: Improving protein subcellular localization prediction for Gram-negative bacteria.* Nucleic Acids Res, 2003. **31**(13): p. 3613-7.

338. Kanehisa, M. and S. Goto, *KEGG: kyoto encyclopedia of genes and genomes.* Nucleic Acids Res, 2000. **28**(1): p. 27-30.

339. Kanehisa, M., et al., *Data, information, knowledge and principle: back to metabolism in KEGG.* Nucleic Acids Res, 2014. **42**(Database issue): p. D199-205.

340. Okuda, S., et al., *KEGG Atlas mapping for global analysis of metabolic pathways.* Nucleic Acids Res, 2008. **36**(Web Server issue): p. W423-6.

341. Kanehisa, M., et al., *KEGG as a reference resource for gene and protein annotation.* Nucleic Acids Res, 2016. **44**(D1): p. D457-62.

342. Schurr, B.C., J. Behr, and R.F. Vogel, *Detection of acid and hop shock induced responses in beer spoiling Lactobacillus brevis by MALDI-TOF MS.* Food Microbiol, 2015. **46**(0): p. 501-506.

343. Bast, E., *Mikrobiologische methoden*. 1998: Fischer.

344. Lenz, C.A. and R.F. Vogel, *Effect of sporulation medium and its divalent cation content on the heat and high pressure resistance of Clostridium botulinum type E spores.* Food Microbiol, 2014. **44**: p. 156-67.

345. Lenz, C.A. and R.F. Vogel, *Differential effects of sporulation temperature on the high pressure resistance of Clostridium botulinum type E spores and the*

*interconnection with sporulation medium cation contents.* Food Microbiol, 2015. **46**: p. 434-442.

346. Kahm, M., et al., *grofit: Fitting Biological Growth Curves with R.* Journal of Statistical Software, 2010. **33**(7): p. 1-21.
347. Sanders, J.W., G. Venema, and J. Kok, *Environmental stress responses inLactococcus lactis.* FEMS Microbiology Reviews, 1999. **23**(4): p. 483-501.
348. Kern, C.C., et al., *Optimization of Matrix-Assisted-Laser-Desorption-Ionization-Time-Of-Flight Mass Spectrometry for the identification of bacterial contaminants in beverages.* J Microbiol Methods, 2013. **93**(3): p. 185-91.
349. Kern, C.C., R.F. Vogel, and J. Behr, *Identification and differentiation of brewery isolates of Pectinatus sp. by Matrix-Assisted-Laser Desorption–Ionization Time-Of-Flight Mass Spectrometry (MALDI-TOF MS).* European Food Research and Technology, 2014. **238**(5): p. 875-880.
350. Mantini, D., et al., *A computational platform for MALDI-TOF mass spectrometry data: application to serum and plasma samples.* J Proteomics, 2010. **73**(3): p. 562-70.
351. Eaton, J.W., D. Bateman, and S. Hauberg, *{GNU Octave} version 3.0.1 manual: a high-level interactive language for numerical computations*. 2009: Create Space Independent Publishing Platform.
352. Octave, C., *GNU Octave 3.8.1*. 2014.
353. Rappsilber, J., Y. Ishihama, and M. Mann, *Stop and go extraction tips for matrix-assisted laser desorption/ionization, nanoelectrospray, and LC/MS sample pretreatment in proteomics.* Anal Chem, 2003. **75**(3): p. 663-70.
354. Bielow, C., G. Mastrobuoni, and S. Kempa, *Proteomics Quality Control: Quality Control Software for MaxQuant Results.* J Proteome Res, 2016. **15**(3): p. 777-87.
355. Alikhan, N.F., et al., *BLAST Ring Image Generator (BRIG): simple prokaryote genome comparisons.* BMC Genomics, 2011. **12**(1): p. 402.
356. Schott, A.S., et al., *Quantitative Proteomics for the Comprehensive Analysis of Stress Responses of Lactobacillus paracasei subsp. paracasei F19.* J Proteome Res, 2017. **16**(10): p. 3816-3829.
357. Oliveros, J.C., *Venny. An interactive tool for comparing lists with Venn's diagrams.* 2007-2015.
358. Corcoran, B.M., et al., *Life under stress: the probiotic stress response and how it may be manipulated.* Curr Pharm Des, 2008. **14**(14): p. 1382-99.
359. Hörmann, S., *Hochdruckinduzierte Stressantwort bei Lactobacillus sanfranciscensis DSM 20451T*, in *Fakultät Wissenschaftszentrum Weihenstephan*. 2007, Technische Universität München: München. p. 225.
360. Zwietering, M.H., et al., *Modeling of the bacterial growth curve.* Appl Environ Microbiol, 1990. **56**(6): p. 1875-81.
361. Dalgaard, P., et al., *Estimation of bacterial growth rates from turbidimetric and viable count data.* Int J Food Microbiol, 1994. **23**(3-4): p. 391-404.
362. Pruitt, K.M., R.E. DeMuth, and M.E. Turner, Jr., *Practical application of generic growth theory and the significance of the growth curve parameters.* Growth, 1979. **43**(1): p. 19-35.
363. Kahm, M., et al., *Fitting Biological Growth Curves with {R}*. Journal of Statistical Software, 2010. **33**(7): p. 1-21.

364. Team, R.C., *R: A Language and Environment for Statistical Computing*. 2013, R Foundation for Statistical Computing: Vienna, Austria.

365. Claydon, M.A., et al., *The rapid identification of intact microorganisms using mass spectrometry.* Nat Biotechnol, 1996. **14**(11): p. 1584-6.

366. Demirev, P.A., et al., *Microorganism identification by mass spectrometry and protein database searches.* Anal Chem, 1999. **71**(14): p. 2732-8.

367. Demirev, P.A., et al., *Top-down proteomics for rapid identification of intact microorganisms.* Anal Chem, 2005. **77**(22): p. 7455-61.

368. Wieme, A.D., et al., *Identification of beer-spoilage bacteria using matrix-assisted laser desorption/ionization time-of-flight mass spectrometry.* Int J Food Microbiol, 2014. **185**: p. 41-50.

369. Alispahic, M., et al., *Species-specific identification and differentiation of Arcobacter, Helicobacter and Campylobacter by full-spectral matrix-associated laser desorption/ionization time of flight mass spectrometry analysis.* J Med Microbiol, 2010. **59**(Pt 3): p. 295-301.

370. Hsieh, S.Y., et al., *Highly efficient classification and identification of human pathogenic bacteria by MALDI-TOF MS.* Mol Cell Proteomics, 2008. **7**(2): p. 448-56.

371. Peel, T.N., et al., *Matrix-assisted laser desorption ionization time of flight mass spectrometry and diagnostic testing for prosthetic joint infection in the clinical microbiology laboratory.* Diagn Microbiol Infect Dis, 2015. **81**(3): p. 163-8.

372. Chen, C.Y., C.C. Chang, and C.W. Lin, *Clinical application of immunomagnetic reduction for quantitative measurement of insulin-like growth factor binding protein-1 in the prediction of pregnant women with preterm premature rupture of membranes.* Clin Chim Acta, 2015. **438**: p. 337-41.

373. Rodrigo, M.A., et al., *MALDI-TOF MS as evolving cancer diagnostic tool: a review.* J Pharm Biomed Anal, 2014. **95**: p. 245-55.

374. Teunissen, C.E., et al., *Identification of biomarkers for diagnosis and progression of MS by MALDI-TOF mass spectrometry.* Mult Scler, 2011. **17**(7): p. 838-50.

375. Taskila, S., *Industrial production of starter cultures*, in *Starter Cultures in Food Production*. 2017, John Wiley & Sons, Ltd. p. 79-100.

376. Altieri, C., et al., *Lactic acid bacteria as starter cultures*, in *Starter Cultures in Food Production*. 2017, John Wiley & Sons, Ltd. p. 1-15.

377. Jordan, S., M.I. Hutchings, and T. Mascher, *Cell envelope stress response in Gram-positive bacteria.* FEMS Microbiol Rev, 2008. **32**(1): p. 107-46.

378. Allen, E.E., D. Facciotti, and D.H. Bartlett, *Monounsaturated but not polyunsaturated fatty acids are required for growth of the deep-sea bacterium Photobacterium profundum SS9 at high pressure and low temperature.* Appl Environ Microbiol, 1999. **65**(4): p. 1710-20.

379. Aebersold, R. and M. Mann, *Mass spectrometry-based proteomics.* Nature, 2003. **422**(6928): p. 198-207.

380. Lill, J., *Proteomic tools for quantitation by mass spectrometry.* Mass Spectrom Rev, 2003. **22**(3): p. 182-94.

381. Geiger, T., et al., *Super-SILAC mix for quantitative proteomics of human tumor tissue.* Nat Methods, 2010. **7**(5): p. 383-5.

382. Schmidt, C., et al., *Mass spectrometry-based relative quantification of proteins in precatalytic and catalytically active spliceosomes by metabolic labeling (SILAC),*

*chemical labeling (iTRAQ), and label-free spectral count.* RNA, 2014. **20**(3): p. 406-20.

383. Blagoev, B., et al., *Temporal analysis of phosphotyrosine-dependent signaling networks by quantitative proteomics.* Nat Biotechnol, 2004. **22**(9): p. 1139-45.

384. Mann, M., *Functional and quantitative proteomics using SILAC.* Nat Rev Mol Cell Biol, 2006. **7**(12): p. 952-8.

385. Gygi, S.P., et al., *Quantitative analysis of complex protein mixtures using isotope-coded affinity tags.* Nat Biotechnol, 1999. **17**(10): p. 994-9.

386. Ong, S.E. and M. Mann, *Mass spectrometry-based proteomics turns quantitative.* Nat Chem Biol, 2005. **1**(5): p. 252-62.

387. Coombs, K.M., *Quantitative proteomics of complex mixtures.* Expert Rev Proteomics, 2011. **8**(5): p. 659-77.

388. Bantscheff, M. and B. Kuster, *Quantitative mass spectrometry in proteomics.* Anal Bioanal Chem, 2012. **404**(4): p. 937-8.

389. Molloy, M.P., et al., *Extraction of membrane proteins by differential solubilization for separation using two-dimensional gel electrophoresis.* Electrophoresis, 1998. **19**(5): p. 837-44.

390. Gygi, S.P., et al., *Evaluation of two-dimensional gel electrophoresis-based proteome analysis technology.* Proc Natl Acad Sci U S A, 2000. **97**(17): p. 9390-5.

391. Hahne, H., et al., *A comprehensive proteomics and transcriptomics analysis of Bacillus subtilis salt stress adaptation.* J Bacteriol, 2010. **192**(3): p. 870-82.

392. Suarez, R.K. and C.D. Moyes, *Metabolism in the age of 'omes'.* J Exp Biol, 2012. **215**(Pt 14): p. 2351-7.

393. Rifai, N., M.A. Gillette, and S.A. Carr, *Protein biomarker discovery and validation: the long and uncertain path to clinical utility.* Nat Biotechnol, 2006. **24**(8): p. 971-83.

394. Rabilloud, T. and C. Lelong, *Two-dimensional gel electrophoresis in proteomics: a tutorial.* J Proteomics, 2011. **74**(10): p. 1829-41.

395. Han, X., A. Aslanian, and J.R. Yates, 3rd, *Mass spectrometry for proteomics.* Curr Opin Chem Biol, 2008. **12**(5): p. 483-90.

396. Baggerman, G., et al., *Gel-based versus gel-free proteomics: a review.* Comb Chem High Throughput Screen, 2005. **8**(8): p. 669-77.

397. Renzone, G., et al., *Differential proteomic analysis in the study of prokaryotes stress resistance.* Ann Ist Super Sanita, 2005. **41**(4): p. 459-68.

398. Geissler, A., *Lifestyle of beer spoiling lactic acid bacteria*. 2016, Technische Universität München.

399. Spano, G. and S. Massa, *Environmental stress response in wine lactic acid bacteria: beyond Bacillus subtilis.* Crit Rev Microbiol, 2006. **32**(2): p. 77-86.

400. Sugimoto, S., M. Abdullah Al, and K. Sonomoto, *Molecular chaperones in lactic acid bacteria: physiological consequences and biochemical properties.* J Biosci Bioeng, 2008. **106**(4): p. 324-36.

401. Bruno-Barcena, J.M., M.A. Azcarate-Peril, and H.M. Hassan, *Role of antioxidant enzymes in bacterial resistance to organic acids.* Appl Environ Microbiol, 2010. **76**(9): p. 2747-53.

402. Lorca, G.L. and G.F. de Valdez, *Lactobacillus stress responses.* Lactobacillus molecular biology: from genomics to probiotics. Calister Academic Press, Norfolk, United Kingdom, 2009: p. 115-137.

403. VanBogelen, R.A., et al., *Mapping regulatory networks in microbial cells.* Trends Microbiol, 1999. **7**(8): p. 320-8.

404. Koonin, E., et al., *Bacterial Stress Responses*, in *In A Comparative Genomic View of the Microbial Stress Response*. 2000, ASM Press.

405. Haldenwang, W.G., *The sigma factors of Bacillus subtilis.* Microbiol Rev, 1995. **59**(1): p. 1-30.

406. Volker, U., et al., *Analysis of the induction of general stress proteins of Bacillus subtilis.* Microbiology, 1994. **140 ( Pt 4)**(4): p. 741-52.

407. Becker, L.A., et al., *Identification of the Gene Encoding the Alternative Sigma Factor çB from Listeria monocytogenesand Its Role in Osmotolerance.* Journal of bacteriology, 1998. **180**(17): p. 4547-4554.

408. Marceau, A., et al., *Evidence for involvement of at least six proteins in adaptation of Lactobacillus sakei to cold temperatures and addition of NaCl.* Applied and environmental microbiology, 2004. **70**(12): p. 7260-7268.

409. Pieterse, B., et al., *Unravelling the multiple effects of lactic acid stress on Lactobacillus plantarum by transcription profiling.* Microbiology, 2005. **151**(Pt 12): p. 3881-94.

410. Xie, Y., et al., *DNA Macroarray profiling of Lactococcus lactis subsp. lactis IL1403 gene expression during environmental stresses.* Appl Environ Microbiol, 2004. **70**(11): p. 6738-47.

411. Koponen, J., et al., *Effect of acid stress on protein expression and phosphorylation in Lactobacillus rhamnosus GG.* J Proteomics, 2012. **75**(4): p. 1357-74.

412. Zhai, Z., et al., *Proteomic characterization of the acid tolerance response in L actobacillus delbrueckii subsp. bulgaricus CAUH1 and functional identification of a novel acid stress-related transcriptional regulator L db0677.* Environmental microbiology, 2014. **16**(6): p. 1524-1537.

413. Cotter, P.D. and C. Hill, *Surviving the acid test: responses of gram-positive bacteria to low pH.* Microbiol Mol Biol Rev, 2003. **67**(3): p. 429-53, table of contents.

414. Fernandez, A., et al., *Rerouting of pyruvate metabolism during acid adaptation in Lactobacillus bulgaricus.* Proteomics, 2008. **8**(15): p. 3154-63.

415. Hecker, M. and U. Volker, *General stress response of Bacillus subtilis and other bacteria.* Adv Microb Physiol, 2001. **44**: p. 35-91.

416. Hecker, M. and U. Volker, *Non-specific, general and multiple stress resistance of growth-restricted Bacillus subtilis cells by the expression of the sigmaB regulon.* Mol Microbiol, 1998. **29**(5): p. 1129-36.

417. Kilstrup, M., et al., *Nucleotide metabolism and its control in lactic acid bacteria.* FEMS Microbiol Rev, 2005. **29**(3): p. 555-90.

418. Potrykus, K. and M. Cashel, *(p)ppGpp: still magical?* Annu Rev Microbiol, 2008. **62**: p. 35-51.

419. Barker, M.M., T. Gaal, and R.L. Gourse, *Mechanism of regulation of transcription initiation by ppGpp. II. Models for positive control based on properties of RNAP mutants and competition for RNAP.* J Mol Biol, 2001. **305**(4): p. 689-702.

420. Barker, M.M., et al., *Mechanism of regulation of transcription initiation by ppGpp. I. Effects of ppGpp on transcription initiation in vivo and in vitro.* J Mol Biol, 2001. **305**(4): p. 673-88.

421. O'Farrell, P.H., *The suppression of defective translation by ppGpp and its role in the stringent response.* Cell, 1978. **14**(3): p. 545-57.

422. Krasny, L. and R.L. Gourse, *An alternative strategy for bacterial ribosome synthesis: Bacillus subtilis rRNA transcription regulation.* EMBO J, 2004. **23**(22): p. 4473-83.

423. Bittner, A.N., A. Kriel, and J.D. Wang, *Lowering GTP level increases survival of amino acid starvation but slows growth rate for Bacillus subtilis cells lacking (p)ppGpp.* J Bacteriol, 2014. **196**(11): p. 2067-76.

424. Grosjean, H. and R. Benne, *Modification and Editing of RNA*. 1998: ASM press Washington, DC.

425. Machnicka, M.A., et al., *MODOMICS: a database of RNA modification pathways--2013 update.* Nucleic Acids Res, 2013. **41**(Database issue): p. D262-7.

426. Ge, J. and Y.T. Yu, *RNA pseudouridylation: new insights into an old modification.* Trends Biochem Sci, 2013. **38**(4): p. 210-8.

427. Persson, B.C., et al., *The gene for a tRNA modifying enzyme, m5U54-methyltransferase, is essential for viability in Escherichia coli.* Proc Natl Acad Sci U S A, 1992. **89**(9): p. 3995-8.

428. Johansson, M.J. and A.S. Bystrom, *Dual function of the tRNA(m(5)U54)methyltransferase in tRNA maturation.* RNA, 2002. **8**(3): p. 324-35.

429. Gutgsell, N., et al., *Deletion of the Escherichia coli pseudouridine synthase gene truB blocks formation of pseudouridine 55 in tRNA in vivo, does not affect exponential growth, but confers a strong selective disadvantage in competition with wild-type cells.* RNA, 2000. **6**(12): p. 1870-81.

430. Wolin, S.L., *Two for the price of one: RNA modification enzymes as chaperones.* Proc Natl Acad Sci U S A, 2016. **113**(50): p. 14176-14178.

431. Wu, G., et al., *U2 snRNA is inducibly pseudouridylated at novel sites by Pus7p and snR81 RNP.* EMBO J, 2011. **30**(1): p. 79-89.

432. Vandivier, L.E. and B.D. Gregory, *Chapter Eight - Reading the Epitranscriptome: New Techniques and Perspectives*, in *The Enzymes*, G.F. Chanfreau, Editor. 2017, Academic Press. p. 269-298.

433. Rintala-Dempsey, A.C. and U. Kothe, *Eukaryotic stand-alone pseudouridine synthases - RNA modifying enzymes and emerging regulators of gene expression?* RNA Biol, 2017. **14**(9): p. 1185-1196.

434. Sturgis, J.N., *Organisation and evolution of the tol-pal gene cluster.* J Mol Microbiol Biotechnol, 2001. **3**(1): p. 113-22.

435. Lazzaroni, J.C., J.F. Dubuisson, and A. Vianney, *The Tol proteins of Escherichia coli and their involvement in the translocation of group A colicins.* Biochimie, 2002. **84**(5-6): p. 391-7.

436. Lloubes, R., et al., *The Tol-Pal proteins of the Escherichia coli cell envelope: an energized system required for outer membrane integrity?* Res Microbiol, 2001. **152**(6): p. 523-9.

437. Cascales, E., et al., *Pal lipoprotein of Escherichia coli plays a major role in outer membrane integrity.* J Bacteriol, 2002. **184**(3): p. 754-9.

438. Lazzaroni, J.C., et al., *Transmembrane alpha-helix interactions are required for the functional assembly of the Escherichia coli Tol complex.* J Mol Biol, 1995. **246**(1): p. 1-7.

439. Derouiche, R., et al., *Protein complex within Escherichia coli inner membrane. TolA N-terminal domain interacts with TolQ and TolR proteins.* J Biol Chem, 1995. **270**(19): p. 11078-84.

440. Germon, P., et al., *Mutational analysis of the Escherichia coli K-12 TolA N-terminal region and characterization of its TolQ-interacting domain by genetic suppression.* J Bacteriol, 1998. **180**(24): p. 6433-9.

441. Journet, L., et al., *Role of TolR N-terminal, central, and C-terminal domains in dimerization and interaction with TolA and tolQ.* J Bacteriol, 1999. **181**(15): p. 4476-84.

442. Clavel, T., et al., *TolB protein of Escherichia coli K-12 interacts with the outer membrane peptidoglycan-associated proteins Pal, Lpp and OmpA.* Mol Microbiol, 1998. **29**(1): p. 359-67.

443. Bouveret, E., et al., *Peptidoglycan-associated lipoprotein-TolB interaction. A possible key to explaining the formation of contact sites between the inner and outer membranes of Escherichia coli.* J Biol Chem, 1995. **270**(19): p. 11071-7.

444. Bouveret, E., et al., *In vitro characterization of peptidoglycan-associated lipoprotein (PAL)-peptidoglycan and PAL-TolB interactions.* J Bacteriol, 1999. **181**(20): p. 6306-11.

445. Ray, M.C., et al., *Identification by genetic suppression of Escherichia coli TolB residues important for TolB-Pal interaction.* J Bacteriol, 2000. **182**(3): p. 821-4.

446. Cascales, E. and R. Lloubes, *Deletion analyses of the peptidoglycan-associated lipoprotein Pal reveals three independent binding sequences including a TolA box.* Mol Microbiol, 2004. **51**(3): p. 873-85.

447. Webster, R.E., *The tol gene products and the import of macromolecules into Escherichia coli.* Mol Microbiol, 1991. **5**(5): p. 1005-11.

448. Bernadac, A., et al., *Escherichia coli tol-pal mutants form outer membrane vesicles.* J Bacteriol, 1998. **180**(18): p. 4872-8.

449. Maurer, L.M., et al., *pH regulates genes for flagellar motility, catabolism, and oxidative stress in Escherichia coli K-12.* J Bacteriol, 2005. **187**(1): p. 304-19.

450. Sistrunk, J.R., et al., *Survival of the Fittest: How Bacterial Pathogens Utilize Bile To Enhance Infection.* Clin Microbiol Rev, 2016. **29**(4): p. 819-36.

451. Lebeer, S., J. Vanderleyden, and S.C.J. De Keersmaecker, *Genes and Molecules of Lactobacilli Supporting Probiotic Action.* Microbiology and Molecular Biology Reviews, 2008. **72**(4): p. 728-764.

452. Moslehi-Jenabian, S., D.S. Nielsen, and L. Jespersen, *Application of Molecular Biology and Genomics of Probiotics for Enteric Cytoprotection*, in *Probiotic Bacteria and Enteric Infections: Cytoprotection by Probiotic Bacteria*, J.J. Malago, J.F.J.G. Koninkx, and R. Marinsek-Logar, Editors. 2011, Springer Netherlands: Dordrecht. p. 133-153.

453. Brooijmans, R., W.M. de Vos, and J. Hugenholtz, *Electron transport chains of lactic acid bacteria - walking on crutches is part of their lifestyle.* F1000 Biol Rep, 2009. **1**: p. 34.

454. Gaudu, P., et al., *Respiration capacity and consequences in Lactococcus lactis.* Antonie Van Leeuwenhoek, 2002. **82**(1-4): p. 263-9.

455. Rezaiki, L., et al., *Respiration metabolism reduces oxidative and acid stress to improve long-term survival of Lactococcus lactis.* Mol Microbiol, 2004. **53**(5): p. 1331-42.

456. Dinamarca, M.A., A. Ruiz-Manzano, and F. Rojo, *Inactivation of cytochrome o ubiquinol oxidase relieves catabolic repression of the Pseudomonas putida GPo1 alkane degradation pathway.* J Bacteriol, 2002. **184**(14): p. 3785-93.

457. Poolman, B., *Transporters and their roles in LAB cell physiology.* Antonie Van Leeuwenhoek, 2002. **82**(1-4): p. 147-64.

458. Wu, R., et al., *Proteomic analysis of responses of a new probiotic bacterium Lactobacillus casei Zhang to low acid stress.* Int J Food Microbiol, 2011. **147**(3): p. 181-7.

459. Len, A.C., D.W. Harty, and N.A. Jacques, *Proteome analysis of Streptococcus mutans metabolic phenotype during acid tolerance.* Microbiology, 2004. **150**(Pt 5): p. 1353-66.

460. Gong, Y., et al., *Global transcriptional analysis of acid-inducible genes in Streptococcus mutans: multiple two-component systems involved in acid adaptation.* Microbiology, 2009. **155**(Pt 10): p. 3322-32.

461. Nascimento, M.M., et al., *Adaptive acid tolerance response of Streptococcus sobrinus.* J Bacteriol, 2004. **186**(19): p. 6383-90.

462. Papadimitriou, K., et al., *Acid tolerance of Streptococcus macedonicus as assessed by flow cytometry and single-cell sorting.* Appl Environ Microbiol, 2007. **73**(2): p. 465-76.

463. Papadimitriou, K., et al., *RNA arbitrarily primed PCR and fourier transform infrared spectroscopy reveal plasticity in the acid tolerance response of Streptococcus macedonicus.* Appl Environ Microbiol, 2008. **74**(19): p. 6068-76.

464. Fridovich, I., *Oxygen toxicity: a radical explanation.* J Exp Biol, 1998. **201**(Pt 8): p. 1203-9.

465. Farr, S.B. and T. Kogoma, *Oxidative stress responses in Escherichia coli and Salmonella typhimurium.* Microbiol Rev, 1991. **55**(4): p. 561-85.

466. Storz, G. and J.A. Imlay, *Oxidative stress.* Curr Opin Microbiol, 1999. **2**(2): p. 188-94.

467. Zamocky, M. and F. Koller, *Understanding the structure and function of catalases: clues from molecular evolution and in vitro mutagenesis.* Prog Biophys Mol Biol, 1999. **72**(1): p. 19-66.

468. Zhao, B.B., et al., *Protective effect of surface layer proteins isolated from four Lactobacillus strains on hydrogen-peroxide-induced HT-29 cells oxidative stress.* Int J Biol Macromol, 2017. **102**: p. 76-83.

469. Kuroda, M., T. Ohta, and H. Hayashi, *Isolation and the gene cloning of an alkaline shock protein in methicillin resistant Staphylococcus aureus.* Biochem Biophys Res Commun, 1995. **207**(3): p. 978-84.

470. Chiancone, E. and P. Ceci, *The multifaceted capacity of Dps proteins to combat bacterial stress conditions: Detoxification of iron and hydrogen peroxide and DNA binding.* Biochim Biophys Acta, 2010. **1800**(8): p. 798-805.

471. Almiron, M., et al., *A novel DNA-binding protein with regulatory and protective roles in starved Escherichia coli.* Genes Dev, 1992. **6**(12B): p. 2646-54.

472. Wolf, S.G., et al., *DNA protection by stress-induced biocrystallization.* Nature, 1999. **400**(6739): p. 83-5.

473. Jenkins, D.E., J.E. Schultz, and A. Matin, *Starvation-induced cross protection against heat or H2O2 challenge in Escherichia coli.* J Bacteriol, 1988. **170**(9): p. 3910-4.

474. Byun, M.W., et al., *Gamma irradiation and ozone treatment for inactivation of Escherichia coli O157:H7 in culture media.* J Food Prot, 1998. **61**(6): p. 728-30.

475. Fehniger, T.E., J.D. Radolf, and M.A. Lovett, *Properties of an ordered ring structure formed by recombinant Treponema pallidum surface antigen 4D.* J Bacteriol, 1986. **165**(3): p. 732-9.

476. Grant, R.A., et al., *The crystal structure of Dps, a ferritin homolog that binds and protects DNA.* Nat Struct Biol, 1998. **5**(4): p. 294-303.

477. Adamcik, J., et al., *Effect of bacteria growth temperature on the distribution of supercoiled DNA and its thermal stability.* Electrophoresis, 2002. **23**(19): p. 3300-9.

478. Harrison, P.M. and P. Arosio, *The ferritins: molecular properties, iron storage function and cellular regulation.* Biochim Biophys Acta, 1996. **1275**(3): p. 161-203.

479. Bozzi, M., et al., *A novel non-heme iron-binding ferritin related to the DNA-binding proteins of the Dps family in Listeria innocua.* J Biol Chem, 1997. **272**(6): p. 3259-65.

480. Reindel, S., et al., *The DpsA-homologue of the archaeon Halobacterium salinarum is a ferritin.* Biochim Biophys Acta, 2002. **1598**(1-2): p. 140-6.

481. Ilari, A., et al., *Iron incorporation into Escherichia coli Dps gives rise to a ferritin-like microcrystalline core.* J Biol Chem, 2002. **277**(40): p. 37619-23.

482. Zhao, G., et al., *Iron and hydrogen peroxide detoxification properties of DNA-binding protein from starved cells. A ferritin-like DNA-binding protein of Escherichia coli.* J Biol Chem, 2002. **277**(31): p. 27689-96.

483. Martinez, A. and R. Kolter, *Protection of DNA during oxidative stress by the nonspecific DNA-binding protein Dps.* J Bacteriol, 1997. **179**(16): p. 5188-94.

484. van Bokhorst-van de Veen, H., et al., *Short- and long-term adaptation to ethanol stress and its cross-protective consequences in Lactobacillus plantarum.* Appl Environ Microbiol, 2011. **77**(15): p. 5247-56.

485. Alonso, S., *Novel Preservation Techniques for Microbial Cultures*, in *Novel Food Fermentation Technologies*. 2016, Springer. p. 7-33.

486. Bergenholtz, A.S., et al., *A case study on stress preconditioning of a Lactobacillus strain prior to freeze-drying.* Cryobiology, 2012. **64**(3): p. 152-9.

487. Santivarangkna, C., et al., *Damage of cell envelope of Lactobacillus helveticus during vacuum drying.* J Appl Microbiol, 2007. **102**(3): p. 748-56.

488. Fozo, E.M. and R.G. Quivey, Jr., *Shifts in the membrane fatty acid profile of Streptococcus mutans enhance survival in acidic environments.* Appl Environ Microbiol, 2004. **70**(2): p. 929-36.

489. Kechagia, M., et al., *Health Benefits of Probiotics: A Review.* ISRN Nutrition, 2013. **2013**: p. 481651.

490. Girbe, B., et al., *LysM, a widely distributed protein motif for binding to (peptido)glycans.* Molecular Microbiology, 2008. **68**(4): p. 838-847.

491. Oldfield, N.J., et al., *T-cell stimulating protein A (TspA) of Neisseria meningitidis is required for optimal adhesion to human cells.* Cellular microbiology, 2007. **9**(2): p. 463-478.

492. Melillo, A., et al., *Identification of a Francisella tularensis LVS outer membrane protein that confers adherence to A549 human lung cells.* FEMS microbiology letters, 2006. **263**(1): p. 102-108.

493. Bateman, A. and M. Bycroft, *The structure of a LysM domain from E. coli membrane-bound lytic murein transglycosylase D (MltD) 1.* Journal of molecular biology, 2000. **299**(4): p. 1113-1119.

494. van Roosmalen, M.L., et al., *Mucosal vaccine delivery of antigens tightly bound to an adjuvant particle made from food-grade bacteria.* Methods, 2006. **38**(2): p. 144-9.

495. Bosma, T., et al., *Novel Surface Display System for Proteins on Non-Genetically Modified Gram-Positive Bacteria.* Applied and Environmental Microbiology, 2006. **72**(1): p. 880-889.

496. Visweswaran, G.R.R., et al., *Exploiting the peptidoglycan-binding motif, LysM, for medical and industrial applications.* Applied Microbiology and Biotechnology, 2014. **98**(10): p. 4331-4345.

497. Whitman, D., *Phenotypic plasticity of insects: mechanisms and consequences*. 2009: CRC Press.

# 9 Supplementary Part I – Material and Methods

## 9.1 Devices, chemicals and consumables

Table S 1: Devices used in this work

| Device | Model | Manufacturer |
|---|---|---|
| Balance | SI-234 | Denver Instrument, Bohemia, NY, USA |
| Balance | SBA 52 | Scaltec Instruments, Heiligenstadt, Germany |
| Balance | SPO 61 | Scaltec Instruments, Heiligenstadt, Germany |
| Balance | BP 210 S | Sartorius AG, Göttingen, Germany |
| Balance | 572-37 | KERN & SOHN GmbH, Balingen-Frommern, Germany |
| Centrifuge | Z 216 MK | Hermle Labortechnik GmbH, Wehingen, Germany |
| Centrifuge | Z382 K | Hermle Labortechnik GmbH, Wehingen, Germany |
| Centrifuge | Z383 K | Hermle Labortechnik GmbH, Wehingen, Germany |
| Centrifuge | 1-14 | Sigma Laborzentrifugen GmbH, Osterode am Harz, Germany |
| Centrifuge | 6-16 K | Sigma Laborzentrifugen GmbH, Osterode am Harz, Germany |
| Centrifuge | MCF-1350 | LMS Consult GmbH & Co. KG, Brigachtal, Germany |
| Centrifuge | Rotina 380 | Andreas Hettich GmbH & Co.KG, Tuttlingen, Germany |
| Colony counter | BZG 30 | WTW Wissenschaftlich-Technische Werkstätten GmbH, Weilheim, Germany |
| Electronically controlled manual dispenser | Multipette® stream | Eppendorf AG, Hamburg, Germany |
| First-dimension focusing unit | IEF100 | Hoefer, Inc., Holliston, MA, USA |
| Freeze-dryer | FreeZone Plus 2.5 freeze dry system | Labconco, Kansas City, MO, USA |
| French Press | HTU DIGI-F-Press | Andreas Hettich GmbH & Co.KG, Schwäbisch Gmünd, Germany |

| | | |
|---|---|---|
| Heating block | Dri-Block DB-3 | Bibby Scientific Limited, Staffordshire, UK |
| Heating magnetic stirrer | AREC | VELP Scientifica Srl, Usmate, Italy |
| Heating magnetic stirrer | Wise Stir MSH-20A | ©WITEG Labortechnik GmbH, Wertheim, Germany |
| Heating magnetic stirrer | RCT basic | IKA®-Werke GmbH & CO. KG, Staufen, Germany |
| Homogenisator | SONOPLUS GM 2070 | Bandelin electronic GmbH & Co. KG, Berlin, Germany |
| Incubator | TC 135 S | Tintometer GmbH, Lovibond® Water Testing, Dortmund, Germany |
| Incubator | Brutschrank B5042 | Heraeus Instruments, Hanau, Germany |
| Laminar airflow clean bench | HERA safe | Heraeus Instruments, Hanau, Germany |
| Laminar airflow clean bench | Kojair®, Biowizard Golden Line | KOJAIR TECH OY, Vilppula, Finland |
| Large Format Vertical Gel Electrophoresis Unit | SE900 | Hoefer, Inc., Holliston, MA, USA |
| Magnetic stirrer | AREC heating magnetic stirrer | VELP® Scientifica, Usmate, Italy |
| MALDI-TOF mass spectrometer (MS) | Microflex LT | Bruker Daltronics, Bremen, Germany |
| Microplate reader | Sunrise | Tecan Deutschland GmbH, Crailsheim, Germany |
| Microplate reader | SPECTROstar Nano | BMG LABTECH GmbH, Ortenberg, Germany |
| Microwave oven | intellowave | LG Electronics Deutschland GmbH, Ratingen, Germany |
| pH electrode | InLab® Semi-Micro pH, pH 0-12 | Mettler-Toledo GmbH, Gießen, Germany |
| pH electrode | InLab® 412, pH 0-14 | Mettler-Toledo GmbH, Gießen, Germany |
| Pipettes | Pipetman (2 µL, 20 µL, 100 µL, 200 µL, 1000 µL) | Gilson International B.V, Deutschland, Limburg-Offheim, Germany |
| Pipetting robot | RoboSeq® 4204 S | MWG Biotech AG, Ebersberg, Germany |
| Power Supply | EPS 3501 XL | GE Healthcare Europe GmbH, Freiburg, Germany |

| | | |
|---|---|---|
| Scanner | Bio-5000 | Microtek, Hsinchu, Taiwan |
| Shaker | UNITWIST300 | UniEquip Laborgerätebau- und Vertriebs GmbH, Planegg, Germany |
| Spectrophotometer | Novaspec II | Pharmacia Biotech, Uppsala, Sweden |
| Spectrophotometer | NovaspecPlus | Pharmacia Biotech, Uppsala, Sweden |
| Thermostatic circulator | MultiTempIII | Pharmacia Biotech, Uppsala, Sweden |
| Ultra sonic water bath | Sonorex Super RK103H | Bandelin electronic GmbH & Co. KG, Berlin, Germany |
| Vacuum concentration centrifuge | UNIVAPO | UniEquip Laborgerätebau- und Vertriebs GmbH, Planegg, Germany |
| Vacuum pump | ILMVAC Rotary Vane Pump PK 8DP | Gardner Denver Thomas GmbH, Ilmenau, Germany |
| Vacuum pump | PC 3003 VARIO | VACUUBRAND GMBH + CO KG, Wertheim, Germany |
| Vacuum regulator | CVC 3000 | VACUUBRAND GMBH + CO KG, Wertheim, Germany |
| Vortex mixer | Vortex Genie 2 | Scientific Industries Inc., Bohemia, NY, USA |
| Vortex mixer | Vortex | STARLAB GmbH, Hamburg, Germany |
| Water bath | E100 LAUDA | Lauda DR. R. Wobser GmbH & Co. KG, Lauda-Königshofen, Germany |
| Water bath | W19 HAAKE | Thermo Haake GmbH, Karlsruhe, Germany |

Table S 2: Chemicals used in this work.

| Chemical | Specification | Manufacturer |
|---|---|---|
| Acetic acid | 100 %, glacial | Carl Roth GmbH & Co. KG, Karlsruhe, Germany |
| Acetonitrile | ≥ 99.9 % | Carl Roth GmbH & Co. KG, Karlsruhe, Germany |
| Acetonitrile | Fluka, LC-MS Ultra CHROMASOLV®, tested for UHPLC-MS | SIGMA-ALDRICH, Steinheim, Germany |
| Acetonitrile | anhydrous, 99.8 % | SIGMA-ALDRICH, Steinheim, Germany |
| Acrylamide/Bis solution | 29:1; 30 % (w/v) | SERVA, Heidelberg, Germany |
| Agar | european agar | Difco, BD sciences, Heidelberg, Germany |
| Albumin Fraction V | ≥ 98 %, powdered, for molecular biology | Carl Roth GmbH & Co. KG, Karlsruhe, Germany |
| Antifoam B emulsion | | SIGMA-ALDRICH, Steinheim, Germany |
| Bio-Rad Protein Assay Dye Reagent Concentrate | 5 ˣ conc. solution for Colloidal Coomassie staining of protein gels | Bio-Rad Laboratories GmbH, München, Germany |
| Bromophenol Blue | for electrophoresis | SIGMA-ALDRICH, Steinheim, Germany |
| Bruker Matrix HCCA (α-cyano-4-hydroxycinnamic acid solution) | - | Bruker Daltronics GmbH, Bremen, Germany |
| Cholamidopropyldimethylammonio-1-propanesulfonic acid; CHAPS | > 98 % | GERBU Biotechnik GmbH, Heidelberg, Germany |
| D(-)-Fructose | - | OMNI Life Science GmbH & Co. KG, Bremen, Germany |
| D(+)-Glucose monohydrate | for microbiology | Merck, Darmstadt, Germany |
| di-Ammonium hydrogen citrate | ≥ 98 %, extra pure | Carl Roth GmbH & Co. KG, Karlsruhe, Germany |
| di-Sodium hydrogen phosphate dihydrate; $Na_2HPO_4 * 2H_2O$ | for analysis | Merck, Darmstadt, Germany |
| DTT | - | SIGMA-ALDRICH, Steinheim, Germany |

| | | |
|---|---|---|
| DTT | ≥ 99 %, analytical grade | GERBU Biotechnik GmbH, Heidelberg, Germany |
| EDTA (ethylenediaminetetraacetic acid) | for molecular biology | SIGMA-ALDRICH, Steinheim, Germany |
| Ethanol, absolute | ≥ 99.8 % | VWR, International, Foutenay-sous-Bois, France |
| Ethanol, denatured | 99 %; with 1 % methylethylketone | Chemikalien und Laborbedarf Nierle, Freising, Germany |
| Formaldehyde solution; $CH_2O$, 37 % | p.a. | Carl Roth GmbH & Co. KG, Karlsruhe, Germany |
| Formic acid | 98 - 100 %, p.a. | Merck, Darmstadt, Germany |
| Formic acid | Fluka, eluent additive for LC-MS | SIGMA-ALDRICH, Steinheim, Germany |
| Gluconic acid sodium salt | ≥ 99 %, for synthesis | Carl Roth GmbH & Co. KG, Karlsruhe, Germany |
| Glycerol | anhydrous, ultra pure | J. T. Baker, Deventer, Netherlands |
| Glycine | for molecular biology and electrophoresis | GERBU Biotechnik GmbH, Heidelberg, Germany |
| Hydrochloric acid solution; HCl, 37 % | p.a. | Carl Roth GmbH & Co. KG, Karlsruhe, Germany |
| Hydrogen peroxide; $H_2O_2$, 30 % | for analysis | Merck, Darmstadt, Germany |
| Hydroxylamine solution | 50 wt. % in H2O, 99.999 % | SIGMA-ALDRICH, Steinheim, Germany |
| Imidazole | puriss. p.a., ≥ 99.5 % (GC) | SIGMA-ALDRICH, Steinheim, Germany |
| Immobiline DryStrip Cover Fluid | for electrophoresis | VWR, International, Foutenay-sous-Bois, France |
| Iodoacetamide; $ICH_2CONH_2$ | vial of 56 mg, for analysis | SIGMA-ALDRICH, Steinheim, Germany |
| Iodoacetamide; $ICH_2CONH_2$ | ≥ 99 % | AppliChem GmbH, Darmstadt, Germany |
| IPG Chamber Cleaner | For electrophoresis | SERVA, Heidelberg, Germany |

| | | |
|---|---|---|
| Iron(II) sulphate heptahydrate; $FeSO_4 * 7H_2O$ | Fluka, puriss. p.a., ACS reagent | SIGMA-ALDRICH, Steinheim, Germany |
| Lactose monohydrate | for microbiology | GERBU Biotechnik GmbH, Heidelberg, Germany |
| L-Cysteine-HCl monohydrate | ≥ 98.5 % | Carl Roth GmbH & Co. KG, Karlsruhe, Germany |
| Lysozyme | cryst., from chicken egg white min. 100 000 units/mg | SERVA, Heidelberg, Germany |
| Magnesium sulphate heptahydrate; $MgSO_4 * 7H_2O$ | ACS, Reag. Ph Eur | Merck, Darmstadt, Germany |
| MALDI-TOF MS bacterial test standard | - | Bruker Daltronics, Bremen, Germany |
| Maltose monohydrate | for microbiology | Merck, Darmstadt, Germany |
| Manganese(II) sulphate monohydrate; $MnSO_4 * H_2O$ | ≥99 %, p.a., ACS | Carl Roth GmbH & Co. KG, Karlsruhe, Germany |
| Meat extract | for microbiology | Merck, Darmstadt, Germany |
| Methanol | ≥ 99.9 % | Carl Roth GmbH & Co. KG, Karlsruhe, Germany |
| Molecular weight marker for peptides | for SDS-PAGE; Mw range 2.5 - 17 kDa | SIGMA-ALDRICH, Steinheim, Germany |
| Paraffin oil | puriss., meets analytical specification of Ph. Eur., BP, viscous liquid | SIGMA-ALDRICH, Steinheim, Germany |
| Pefabloc® SC | - | SIGMA-ALDRICH, Steinheim, Germany |
| Peptone from casein | for microbiology | Merck, Darmstadt, Germany |
| Potassium chloride; KCl | ≥ 99.5 %, p.a. | Carl Roth GmbH & Co. KG, Karlsruhe, Germany |
| Potassium dihydrogen phosphate, $KH_2PO_4$ | ≥ 99 %, p.a. | Carl Roth GmbH & Co. KG, Karlsruhe, Germany |
| Potassium hydroxide; KOH | p.a. | Merck, Darmstadt, Germany |
| Protease inhibitor, cOmplete™ | Roche, Protease Inhibitor Cocktail Tablets provided in glass vials | SIGMA-ALDRICH, Steinheim, Germany |
| SERDOLIT® MB-1 | analytical grade | SERVA, Heidelberg, Germany |

| | | |
|---|---|---|
| SERVA HPE™ IPG Overlay | for electrophoresis | SERVA, Heidelberg, Germany |
| SERVALYT™ 3-10 | Iso-Dalt, for 2D Electrophoresis | SERVA, Heidelberg, Germany |
| SIGMA*FAST*™ Protease Inhibitor Tablets | for general use | SIGMA-ALDRICH, Steinheim, Germany |
| Silver nitrate; $AgNO_3$ | ≥ 99.9 %, p.a. | Carl Roth GmbH & Co. KG, Karlsruhe, Germany |
| Sodium carbonate; $NaCO_3$ | ≥ 99.8 %, p.a. | Carl Roth GmbH & Co. KG, Karlsruhe, Germany |
| Sodium chloride; NaCl | ≥ 99.5 %, p.a., ACS, ISO | Carl Roth GmbH & Co. KG, Karlsruhe, Germany |
| Sodium hydroxide solution; NaOH, 50 % | - | J. T. Baker, Deventer, Netherlands |
| Sodium hydroxide; NaOH | ≥ 99 %, p.a. | Carl Roth GmbH & Co. KG, Karlsruhe, Germany |
| Sodium n-dodecyl sulphate (SDS) | research grade | SERVA, Heidelberg, Germany |
| Sodium thiosulfate pentahydrate; $Na_2O_3S_2 * 5 H_2O$ | EMSURE® ACS, ISO, Reag. Ph Eur, for electrophoresis | Merck, Darmstadt, Germany |
| Sucrose | for density gradients, biochemical use, electrophoresis | GERBU Biotechnik GmbH, Heidelberg, Germany |
| TEMED (N,N,N',N'-tetramethylethylen-diamine) | for electrophoresis | SIGMA-ALDRICH, Steinheim, Germany |
| Thiourea | Fluka, puriss. p.a., ACS reagent, ≥ 99.0 % | SIGMA-ALDRICH, Steinheim, Germany |
| Thiourea | for analysis, ACS, Reag. Ph Eur | Merck, Darmstadt, Germany |
| Triethylammonium bicarbonate buffer; TEAB | 1.0 M, pH 8.5±0.1, for analysis | SIGMA-ALDRICH, Steinheim, Germany |
| Trifluoroacetic acid | ≥ 99.9 % | Carl Roth GmbH & Co. KG, Karlsruhe, Germany |
| Tris; Tris(hydroxymethyl)-aminomethane | ultra pure | MP Biomedicals, Solon, Ohio, USA |
| Tris; Tris(hydroxymethyl)-aminomethane | analytical grade | GERBU Biotechnik GmbH, Heidelberg, Germany |
| Tris-HCl | 99.89 % | GERBU Biotechnik GmbH, Heidelberg, Germany |

| | | |
|---|---|---|
| Trypsin | sequencing grade modified | Promega GmbH, Mannheim, Germany |
| Tryptone/Peptone ex casein | granulated | Carl Roth GmbH & Co. KG, Karlsruhe, Germany |
| Tween® 80 (Polyoxyethylenesorbitan monooleate) | for cell culture and bacteriology | GERBU Biotechnik GmbH, Heidelberg, Germany |
| Urea | ≥ 99.5 %, pharmaceutical grade | GERBU Biotechnik GmbH, Heidelberg, Germany |
| Water | Chromasolv®, for HPLC | SIGMA-ALDRICH, Steinheim, Germany |
| Water | J.T.Baker®, for HPLC, electrophoresis | VWR International GmbH, Heidelberg, Germany |
| Yeast extract | for bacteriology | Carl Roth GmbH & Co. KG, Karlsruhe, Germany |

Table S 3: Consumables used in this work.

| Item | Specification | Manufacturer |
|---|---|---|
| Acrylic cuvettes | 10 x 10 x 45 mm, 10 x 4 x 45 mm | Sarstedt AG & Co., Nümbrecht, Germany |
| Combitips | Combitips advanced®, sterile, 1 ml | Eppendorf AG, Hamburg, Germany |
| Cryo pure tubes | 1.8 ml white, non-pyrogenic, non-mutagenic, non-cytotoxic | Sarstedt AG & Co., Nümbrecht, Germany |
| Electrode Wicks IEF106 | Two Sealed Bags of 252 Wicks per Bag | Hoefer, Inc., Holliston, MA, USA |
| Empore™ SPE Disks | Supelco, C18, diam. 47 mm, pk of 20 | SIGMA-ALDRICH, Steinheim, Germany |
| Folded filters | cellulose, 65 g/m2 | Munktell & Filtrak GmbH, Bärenstein, Germany |
| Hinged Glas Cassette for SE 900 | for electrophoresis | Hoefer, Inc., Holliston, MA, USA |
| HPLC column | Aeris-PEPTIDE 3.6 µm XB-C18 column, 150 x 4.6 mm | Phenomenex, Torrance, CA, USA |
| HPLC column | Gemini 5 µm C18 110 Å column, 150 x 3 mm | Phenomenex, Torrance, CA, USA |
| HPLC column | YMC Triart C18 RP, ID: 100 x 2.0 mm, 3 µm particles, 12 nm pores | YMC, Dinslaken, Germany |
| HPLC column | LiChrospher® 10 µm 100 RP-18 endcapped, 250 x 10 mm | Merck, Darmstadt, Germany |
| HPLC vial crimp caps | Verex seal, 11 mm Dia. Crimp, PTFE/rubber red | Phenomenex, Torrance, CA, USA |
| HPLC vials | Verex vial, crimp, 2 ml, clear 33, no patch | Phenomenex, Torrance, CA, USA |
| MALDI-TOF MS stainless steel target plate | MSP 96 | Bruker Daltronics, Bremen, Germany |
| Membrane filter units | Phenex™, RC-membrane, 0.2 µm, 4 mm non-sterile PP housing, lure/slip | Phenomenex, Torrance, CA, USA |
| Membrane filters | 47 mm, cellulose, 0.2 µm | Sartorius AG, Göttingen, Germany |
| Microtitre plates | 96 well, flat bottom with lid | Sarstedt AG & Co., Nümbrecht, Germany |

| | | |
|---|---|---|
| PageRuler™ Plus Prestained Protein Ladder | 10 to 250 kDa | Thermo Fisher Scientific, Waltham, MA, USA |
| Petri dishes | 92 x 16 mm, without ventilation cams | Sarstedt AG & Co., Nümbrecht, Germany |
| Pipette tips | PIPETMAN TIPS Diamond; 0.1-20 µL | Gilson International B.V, Deutschland, Limburg-Offheim, Germany |
| Pipette tips | 1-200 µL, 100-1000 µL | Peske GmbH, Karlsruhe, Germany |
| Reaction tubes | 200 µL, 1.5 ml, 2ml | Eppendorf AG, Hamburg, Germany |
| Running Cups IEF108 | Ten Sets of Running Cups (Each Set Containing Six Sample Cups) | Hoefer, Inc., Holliston, MA, USA |
| Serva IPG *Blue*strip | pH 3-6/18cm, pH4-7/24cm | SERVA, Heidelberg, Germany |
| Sterile filters | Filtropur S 0.2 and S 0.45, sterile non-pyrogenic, | Sarstedt AG & Co., Nümbrecht, Germany |
| Sterile reagent and centrifuge tubes | 5 ml, 15 ml, 50 ml | Sarstedt AG & Co., Nümbrecht, Germany |
| Syringes | single use, pyrogenfree, sterile; 2 ml, 10 ml, 20 ml | Dispomed Witt oHG, Gelnhausen, Germany |
| TMT10plex™ Isobaric Label Reagent Set | for mass spectrometry, 1x 5 mg | Thermo Fisher Scientific, Waltham, MA, USA |

## 9.2 R script for bioinformatical analysis of proteomic data

```
#setwd("~/Documents")
library("DESeq")
library("RColorBrewer")
library("gplots")
library("adegenet")
library("Heatplus")
library("pracma")
library("car")
library("coin")
library("plyr")
library("randomForest")
library("scales")
library("DescTools")
library("multcompView")
library("colorspace")
library("dataframes2xls")
library("vegan")
library("cluster")
library("e1071")
library("rpart")
```

```
#functions#################################################################
#histogram
histnorm3=function(COUNT, condition, ...)
{
 if (length(COUNT)>0)
 {
  hist(COUNT, breaks = 100, freq=FALSE, main = paste("Histogram of" , condition), ...)
  rug(COUNT)

  COUNT.NA <- COUNT
  COUNT.NA[COUNT.NA == -Inf] <- NA
  mn <- mean(COUNT.NA, na.rm = TRUE)
  stdev <- sd(COUNT.NA, na.rm = TRUE)
  x <- COUNT
  curve(dnorm(x, mean = mn, sd= stdev), add=TRUE, col="red", lty="dotted", xaxt="n")
  quant <- quantile(COUNT.NA, na.rm = TRUE)
  abline(v=quant[2], col="blue")
  abline(v=quant[3], col="red")
  abline(v=quant[4], col="blue")

  mtext(paste("mean ", round(mn, 1), "; sd ", round(stdev, 1), "; N ", length(COUNT),sep=""), side=1,
 cex=.75)
  return(quant)
 } # fi
} # histnorm
#functions#################################################################

#settings
quantil_normalization <- TRUE
shift1 <- FALSE
p.sig <- 0.05
p.high.sig <- 0.01

#68???95???99.7 rule


#step 1 read data remove contaminants#############################
#read experimental data
raw.data <- read.table("proteinGroups.txt", header=TRUE, sep="\t", comment.char = "", quote="")

#read experimental design
exp.design <- read.table("SampleID_MSMS_AS.csv", header=TRUE, sep=";", comment.char = "",
 quote="", stringsAsFactors = FALSE)

#new meta data table
meta.data <- read.table("Metadfile.csv", header=TRUE, sep=";", comment.char = "", quote="",
 stringsAsFactors = FALSE)

#experimental design (replicates are labeled identically)
message("Number of samples: ", length(exp.design$condition))

#output dir
dir.create("output", showWarnings = TRUE, recursive = FALSE, mode = "0777")

#remove contaminants
step1.raw.data.nocont<- raw.data[!(raw.data$Only.identified.by.site=="+" | raw.data$Reverse=="+" |
 raw.data$Potential.contaminant=="+"), ]
```

```
protein.IDs <- step1.raw.data.nocont$Protein.IDs

#get fasta description if needed
headers <- as.data.frame(step1.raw.data.nocont$Fasta.headers)
rownames(headers) <- protein.IDs

#extract intensity columns
step1.data<- step1.raw.data.nocont[ , grepl( 'Reporter.intensity.[0-9].P' , names( step1.raw.data.nocont
 ) ) ]
#use protein accessions (IDs) as label
rownames(step1.data) <- protein.IDs

# Rename columns
for (i in 1:length(exp.design$ID.raw)) {
colnames(step1.data)[colnames(step1.data)==exp.design$ID.raw[i]] <- exp.design$ID.sample[i]
}

#step 2 remove zero rows and separate zeroblocks#################
step2.data<-step1.data

# remove rows with 0s only
step2.data<- step2.data[!rowSums(!step2.data)==ncol(step2.data), ]
histnorm3(rowSums(step2.data==0), "data zero blocks distribution")

#move 0 blocks to new dataframe
step2.data.nozeroblocks<- step2.data[!(rowSums(!step2.data[, 1:10])==10 | rowSums(!step2.data[,
 11:20])==10 | rowSums(!step2.data[, 21:30])==10 | rowSums(!step2.data[, 31:40])==10 |
 rowSums(!step2.data[, 41:50])==10), ]
step2.data.zeroblocks<- step2.data[(rowSums(!step2.data[, 1:10])==10 | rowSums(!step2.data[,
 11:20])==10 | rowSums(!step2.data[, 21:30])==10 | rowSums(!step2.data[, 31:40])==10 |
 rowSums(!step2.data[, 41:50])==10), ]
histnorm3(rowSums(step2.data.nozeroblocks==0), "data no zeroblocks")


#step 3 between run normalisation################################
#continue with data with no zeroblocks
step3.data <- step2.data.nozeroblocks

#Hannes normalization start#######################################
#normalize runs (replicates are labeled differently)
#get position of PS for run normalization
PS1.pos <- grep("PS1", colnames(step3.data))
PS2.pos <- grep("PS2", colnames(step3.data))
PS.pos <- c(PS1.pos, PS2.pos)
runs <- length(PS1.pos)

#calculate row means
all_row_means<- rowMeans(step3.data[, PS.pos], na.rm = FALSE, dims = 1)
all_row_means[is.na(all_row_means)]

#test for na in data
if (!isempty(step3.data[is.na(step3.data)])) {
 warning("step3.data contains non numeric elements")
}

step3.data.norm <- step3.data

for(i in 1:runs) {
```

```
 j <- i-1
 row_means <- (step3.data.norm[ ,PS1.pos[i]] + step3.data[ , PS2.pos[i]])/2
 #shift data 1 up (remove zeros)
 if (shift1) {
  row_means <- row_means + 1
 }
 norm_factor <- all_row_means/row_means
 histnorm3(norm_factor, paste("normfactor before outlier elimination: run ",  i))
 #test for na's in dataset
 if (!isempty(norm_factor[is.na(norm_factor)])) {
  warning("norm_factor contains non numeric elements")
 }
 if (!isempty(norm_factor[is.infinite(norm_factor)])) {
  warning("norm_factor contains infinite elements")
 }
 #quantile normalization
 if (quantil_normalization) {
  quant <- quantile(norm_factor, c(0.00, 0.01, 0.50, 0.99), na.rm = TRUE)
  norm_factor[is.na(norm_factor)] <- quant[2]
  norm_factor[is.infinite(norm_factor)] <- quant[4]
  norm_factor[norm_factor < quant[2]] <- quant[2]
  norm_factor[norm_factor > quant[4]] <- quant[4]
 }
 # simple normfactor gap filling by 1
 else {
  norm_factor[is.na(norm_factor)] <- 1
  norm_factor[is.infinite(norm_factor)] <- 1
 }
 if (!isempty(norm_factor[is.na(norm_factor)])) {
  warning("norm_factor contains non numeric elements")
 }
 step3.data.norm[, (1+j*10):(10+j*10)] <- apply(step3.data.norm[, (1+j*10):(10+j*10)], 2, "*",
 norm_factor)
 histnorm3(norm_factor, paste("normfactor after outlier elimination: run ",  i))
}

#in rows with only 0 counts/intensities a division by 0 leads to NaN (replace by 0 again)
if (!isempty(step3.data.norm[is.na(step3.data.norm)])) {
 warning("step3.data.norm contains non numeric elements")
}

#only true samples are procecced further (10plex, first two are always calibration standards)
step3.data.filter <- step3.data.norm[, c(3:10, 13:20, 23:30, 33:40, 43:49)]
#Hannes normalization end#########################################

#sort columns (we don't need experiment blocks any more)
step3.data.filter <- step3.data.filter[ , order(names(step3.data.filter))]

step4.data <- step3.data.filter
histnorm3(as.matrix(step4.data), "step4.data runs normalised")

#step 4 between sample normalisation#############################

#DESeq normalization start#######################################
#normalize samples (replicates are labeled equal)
#for analysis float values are converted to int (count data)
step4.data.int <- round(step4.data, digits=0)
#remove PS and blanks from exp.design
```

```
exp.design.noPS <- exp.design[!(exp.design$condition == "PS" | exp.design$condition == "blank"), ]
exp.design.noPS.sort <- exp.design.noPS[order(exp.design.noPS$ID.sample), ]
#create cds object
cds = newCountDataSet(step4.data.int, exp.design.noPS.sort$condition)
cds = estimateSizeFactors(cds)
#print plot size factors
sizeFactors(cds)
plot(sizeFactors(cds))

#normalized count data
step4.data.norm <- counts(cds, normalized=TRUE)
#DESeq normalization end##########################################
histnorm3(step4.data.norm, "step4.data DESeq normalised")

#step 5 log2 transform ##########################################
step5.data <- step4.data.norm

#log2 transform
if (TRUE) {
  step5.data <- log2(step5.data)
  step5.data[step5.data == -Inf] <- 0
}

#step 6 transpose data ##########################################
step6.data <- step5.data
histnorm3(step6.data, "step6.data log2 transformed")

#transpose data
step6.data.t  <- as.data.frame(t(step6.data))
step6.data.t.cond <- as.data.frame(cbind(exp.design.noPS.sort$condition, step6.data.t))
colnames(step6.data.t.cond)[colnames(step6.data.t.cond)=="exp.design.noPS.sort$condition"] <-
  "condition"

#step 7 MANOVA ##################################################
step7.data <- step6.data.t.cond

#withingroupvariance
withingroupvariance <- apply(step7.data[,2:4],2,function(x) tapply(x, step7.data$condition ,var))
#betweengroupvariance
betweengroupvariance <- apply(apply(step7.data[,2:4],2,function(x)
  tapply(x,step7.data$condition,var)),2,mean)
#TODO:do anything

#replace 0 by NA
step7.data[step7.data == 0] <- NA
protein.IDs.contain.zero<- colnames(step7.data[apply(step7.data, 2, function(x) any(x %in% NA))])

#anova analysis
fit.pvalues <- apply(step7.data[,2:ncol(step7.data)],2, function(x) summary(aov (x ~ condition, data =
  step7.data))[[1]][[1,"Pr(>F)"]])

fit.tukey.hsd <- as.data.frame(t(apply(step7.data[,2:ncol(step7.data)],2, function(x)
  t(as.data.frame(extract_p(TukeyHSD(aov (x ~ condition, data = step7.data))))))))

anova.step7.data  <- cbind(fit.pvalues, fit.tukey.hsd)

#naming of anova test
combos <- combn(levels(as.factor(exp.design.noPS.sort$condition)),2)
```

```
condition.combinations <- paste(combos[1, ], combos[2, ], sep="-")

cond.string <- c("ANOVA-P-VALUE")

anova.colnames <- c(cond.string, condition.combinations)

colnames(anova.step7.data) <- anova.colnames

write.table(anova.step7.data, file =
 "output/data_no_zeroblocks_anova_pvalue_all_proteins_vs_all.csv", sep="\t", dec=".", row.names =
 TRUE, col.names = NA)

#log2 fold changes
step7.data.mean <- t(step7.data[, -1])
step7.data.mean[step7.data.mean == 0] <- NA
for (i in 1:13) {
 j <- i-1
 tmp.mean <- apply(step7.data.mean[, (1+j*3):(3+j*3)], 1, mean, na.rm=TRUE)
 tmp.sd <- apply(step7.data.mean[, (1+j*3):(3+j*3)], 1, sd, na.rm=TRUE)
 if (i == 1) {
  condition.protein.sd <- tmp.sd
  condition.protein.mean <- tmp.mean
 } else {
  condition.protein.sd <- cbind(condition.protein.sd, tmp.sd)
  condition.protein.mean <- cbind(condition.protein.mean, tmp.mean)
 }

}

step7.condition.protein.sd <- as.data.frame(condition.protein.sd)
colnames(step7.condition.protein.sd) <- levels(as.factor(exp.design.noPS.sort$condition))
step7.condition.protein.mean <- as.data.frame(condition.protein.mean)
colnames(step7.condition.protein.mean) <- levels(as.factor(exp.design.noPS.sort$condition))


#volcanoPlot all conditions vs all conditions filter
par(mfrow=c(1,1))
condition.names <- levels(as.factor(exp.design.noPS.sort$condition))
all.sig.proteins.IDs <-NULL
for (single.conditions in condition.names) {
anova.contr.vs.all <- anova.step7.data[ , grepl( single.conditions , names(anova.step7.data) ) ]
volc.max.x.axis <- 1.1*max(step7.condition.protein.mean[,1:ncol(step7.condition.protein.mean)]-
 step7.condition.protein.mean$contr)
volc.min.x.axis <- 0.9*min(step7.condition.protein.mean[,1:ncol(step7.condition.protein.mean)]-
 step7.condition.protein.mean$contr)
volc.max.y.axis <- max(-log10(anova.step7.data[ , grepl( single.conditions , names(anova.step7.data) ) ]))

comparison.names.split <- strsplit(colnames(anova.contr.vs.all), "-")
dat.all.cond <- NULL
sig.proteins <- NULL
for (i in 1:length(comparison.names.split)) {
 sig.level=-log10(p.sig)

 if (comparison.names.split[[i]][1] == single.conditions) {
  cond<- comparison.names.split[[i]][2]
 } else {
  cond <- comparison.names.split[[i]][1]
```

```
 }

 cmd <- paste("step7.condition.protein.mean$`", cond, "`-step7.condition.protein.mean$`",
 single.conditions, "`", sep = "")
 y<- eval(parse(text = cmd))
 sd <- sd(y)
 #y <- step7.condition.protein.mean$pH9-step7.condition.protein.mean$contr
 log10.p<- -log10(anova.contr.vs.all[, i])
 dat <- cbind(y, log10.p)
 rownames(dat) <- rownames(step7.condition.protein.mean)
 colnames(dat) <- c("log2FoldChange", "log10p")
 #bind all conditions
 dat.cond <- dat
 colnames(dat.cond) <-paste(paste(cond, single.conditions, sep="-"), colnames(dat.cond), sep = "-")
 dat.all.cond <- cbind(dat.all.cond, dat.cond)

 dat <- as.data.frame(dat)


 dat.sig <- dat[dat[, 2] > sig.level & (dat$log2FoldChange > 2*sd | dat$log2FoldChange < -2*sd), ]
 color.sig <- rgb(red=1.0, green=0.1, blue=0.1, alpha=0.5)
 color.notsig <- rgb(red=0.1, green=0.1, blue=1.0, alpha=0.1)
 plot(dat$log2FoldChange, dat$log10p, pch=16, col = ifelse(dat$log10p > sig.level &
 (dat$log2FoldChange > 2*sd | dat$log2FoldChange < -2*sd) , color.sig, color.notsig), main=paste(cond,
 single.conditions, sep="-"), xlim=c(volc.min.x.axis, volc.max.x.axis), ylim=c(0, volc.max.y.axis))

 if (nrow(dat.sig) > 0) {
   text(dat.sig$log2FoldChange, dat.sig$log10p, labels=rownames(dat.sig), cex= 0.7 )
 }

 lines(c(2*sd,2*sd), c(0, volc.max.y.axis) , col="Blue")
 lines(c(-2*sd,-2*sd), c(0, volc.max.y.axis) , col="Blue")
 lines(c(volc.min.x.axis, volc.max.x.axis), c(sig.level,sig.level) , col="Red")

 #export volcano-plots
 tiff(file = paste("output/Volcano_", cond, "_vs_", single.conditions, ".tiff"), width=11.681,
 height=7.431, units="in",type="cairo", res=600, compression="lzw")
 plot(dat$log2FoldChange, dat$log10p, pch=16, col = ifelse(dat$log10p > sig.level &
 (dat$log2FoldChange > 2*sd | dat$log2FoldChange < -2*sd) , color.sig, color.notsig), main=paste(cond,
 single.conditions, sep="-"), xlim=c(volc.min.x.axis, volc.max.x.axis), ylim=c(0, volc.max.y.axis))

 if (nrow(dat.sig) > 0) {
   text(dat.sig$log2FoldChange, dat.sig$log10p, labels=rownames(dat.sig), cex= 0.7 )
 }

 lines(c(2*sd,2*sd), c(0, volc.max.y.axis) , col="Blue")
 lines(c(-2*sd,-2*sd), c(0, volc.max.y.axis) , col="Blue")
 lines(c(volc.min.x.axis, volc.max.x.axis), c(sig.level,sig.level) , col="Red")
 dev.off()

 #headers[rownames(dat.sig), ]
 sig.proteins.tmp <- cbind(rownames(dat.sig), rep(cond, length(rownames(dat.sig))), dat.sig,
 as.character(headers[rownames(dat.sig), ]))
 sig.proteins<- rbind(sig.proteins, sig.proteins.tmp)

}

#significant DE proteins table###################################
```

```
colnames(sig.proteins) <- c("protein_ID", "condition", "log2foldchange", "log10.p", "annotation")
write.table(sig.proteins, file = paste("output/sign_DE_proteins_vs_", single.conditions, ".csv", sep = ""),
 sep="\t", dec=".", row.names = FALSE)

#all vs condition all proteins table############################
write.table(dat.all.cond, file = paste("output/all_proteins_vs_", single.conditions, ".csv", sep = ""),
 sep="\t", dec=".", row.names = TRUE, col.names = NA)
#all vs condition significant proteins table####################
sig.proteins.IDs <- sig.proteins$protein_ID
sig.proteins.IDs.uniq<- as.character(unique(unlist(sig.proteins.IDs)))
write.table(dat.all.cond[sig.proteins.IDs.uniq, ], file = paste("output/sign_DE_proteins_all_cond_vs_",
 single.conditions, ".csv", sep = ""), sep="\t", dec=".", row.names = TRUE, col.names = NA)
all.sig.proteins.IDs <- c(all.sig.proteins.IDs, sig.proteins.IDs.uniq)
}
all.sig.proteins.IDs.uniq<- as.character(unique(unlist(all.sig.proteins.IDs)))


#####################################################################
#Step 8 - prepare zeroblock-data for further usage # # # # if possible include normalization (between
 run)
step2.data.zeroblocks -> step2.data.zeroblocks.raw.intensities

step2.data.zeroblocks <- step2.data.zeroblocks.raw.intensities

# only true samples are procecced further (10plex, first two are always calibration standards)
step2.data.zeroblocks.filter <- step2.data.zeroblocks[, c(3:10, 13:20, 23:30, 33:40, 43:49)]

#sort columns (we don't need experiment blocks any more)
step2.data.zeroblocks.filter <- step2.data.zeroblocks.filter[ , order(names(step2.data.zeroblocks.filter))]

step8.data <- step2.data.zeroblocks.filter
histnorm3(as.matrix(step8.data), "step8.data runs normalised")


# log2 transform
if (TRUE) {
 step8.data.log2 <- log2(step8.data)
 step8.data.log2[step8.data.log2 == -Inf] <- 0
}

step9.data <- step8.data.log2
histnorm3(as.matrix(step9.data), "step8.data log2 transformed")

#step 9 transpose data ########################################

#transpose data
step9.data.t  <- as.data.frame(t(step9.data))
step9.data.t.cond <- as.data.frame(cbind(exp.design.noPS.sort$condition, step9.data.t))
colnames(step9.data.t.cond)[colnames(step9.data.t.cond)=="exp.design.noPS.sort$condition"] <-
 "condition"
step10.data <- step9.data.t.cond

#step 10 log2 fold changes#####################################
step10.data.mean <- t(step10.data[, -1])
step10.data.mean[step10.data.mean == 0] <- NA
for (i in 1:13) {
 j <- i-1
 tmp.mean <- apply(step10.data.mean[, (1+j*3):(3+j*3)], 1, mean, na.rm=TRUE)
```

```
 tmp.sd <- apply(step10.data.mean[, (1+j*3):(3+j*3)], 1, sd, na.rm=TRUE)
 if (i == 1) {
  condition.protein.sd <- tmp.sd
  condition.protein.mean <- tmp.mean
 } else {
  condition.protein.sd <- cbind(condition.protein.sd, tmp.sd)
  condition.protein.mean <- cbind(condition.protein.mean, tmp.mean)
 }

}

step10.condition.protein.sd <- as.data.frame(condition.protein.sd)
colnames(step10.condition.protein.sd) <- levels(as.factor(exp.design.noPS.sort$condition))
step10.condition.protein.mean <- as.data.frame(condition.protein.mean)
colnames(step10.condition.protein.mean) <- levels(as.factor(exp.design.noPS.sort$condition))

step11.data <- step10.condition.protein.mean

dat.all.store <- NULL
for (single.conditions in condition.names) {

 comparison.names.split <- strsplit(colnames(anova.contr.vs.all), "-")
 dat.all.cond <- NULL

 for (i in 1:length(comparison.names.split)) {

  if (comparison.names.split[[i]][1] == single.conditions) {
   cond<- comparison.names.split[[i]][2]
  } else {
   cond <- comparison.names.split[[i]][1]
  }

  cmd2 <- paste("step10.condition.protein.mean$`", cond, "`-step10.condition.protein.mean$`",
single.conditions, "`", sep = "")
  y2<- eval(parse(text = cmd2))
  sd <- sd(y2)
  dat <- cbind(y2)
  rownames(dat) <- rownames(step10.condition.protein.mean)
  colnames(dat) <- c("log2FoldChange")
  #bind all conditions
  dat.cond <- dat
  colnames(dat.cond) <-paste(paste(cond, single.conditions, sep="-"), colnames(dat.cond), sep = "-")
  dat.all.cond <- cbind(dat.all.cond, dat.cond)

  dat <- as.data.frame(dat)

 }

 dat.all.store <- cbind(dat.all.store, dat.all.cond)

 }

######write some tables zeroblock-data#########################
write.table(dat.all.store , file = paste("output/data_zeroblocks_all_proteins_vs_all_log2fold.csv", sep =
 ""), sep="\t", dec=".", row.names = TRUE, col.names = NA)
write.table(step11.data, file = "output/data_zeroblocks_logtransformed_means.csv", sep="\t", dec=".",
 row.names = TRUE, col.names = NA)
```

```
write.table(step9.data, file = "output/data_zeroblocks_logtransformed_reps.csv", sep="\t", dec=".",
 row.names = TRUE, col.names = NA)

###########End Step 8 - prepare zeroblock-data##################

###########write some tables data###############
log.transformed.data.means.and.sd.wo.zeroblocks <- cbind(step7.condition.protein.mean,
 step7.condition.protein.sd)
log.transformed.data.means.and.sd.wo.zeroblocks.ordered <-
 log.transformed.data.means.and.sd.wo.zeroblocks[ ,
 order(names(log.transformed.data.means.and.sd.wo.zeroblocks))]
write.table(log.transformed.data.means.and.sd.wo.zeroblocks.ordered, file =
 "output/data_no_zeroblocks_logtransformed.csv", sep="\t", dec=".", row.names = TRUE, col.names =
 NA)
write.table(step7.data[,all.sig.proteins.IDs.uniq], file = "output/all_sign_proteins_log_data.csv",
 sep="\t", dec=".", row.names = TRUE, col.names = TRUE)

#create figures#####################################################
#prepare colors
hmcol = colorRampPalette(c("green", "black", "red"))(n = 50)

#prepare data for heatmap#########################################
#prepare data for heatmap-creation - raw intensities all proteins with zeroblocks
step2.data.hm <- step2.data[, c(3:10, 13:20, 23:30, 33:40, 43:49)]
step2.data.hm.ordered<- step2.data.hm[ , order(names(step2.data.hm))]
step2.data.hm.t  <- as.data.frame(t(step2.data.hm.ordered))
step2.data.hm.t.cond <- as.data.frame(cbind(exp.design.noPS.sort$condition, step2.data.hm.t))
colnames(step2.data.hm.t.cond)[colnames(step2.data.hm.t.cond)=="exp.design.noPS.sort$condition"]
 <- "condition"
step2.data.hm.final <- step2.data.hm.t.cond

#prepare data for heatmap-creation - raw intensities all proteins without zeroblocks
step3.data.hm <- step3.data[, c(3:10, 13:20, 23:30, 33:40, 43:49)]
step3.data.hm.ordered<- step3.data.hm[ , order(names(step3.data.hm))]
step3.data.hm.t  <- as.data.frame(t(step3.data.hm.ordered))
step3.data.hm.t.cond <- as.data.frame(cbind(exp.design.noPS.sort$condition, step3.data.hm.t))
colnames(step3.data.hm.t.cond)[colnames(step3.data.hm.t.cond)=="exp.design.noPS.sort$condition"]
 <- "condition"
step3.data.hm.final <- step3.data.hm.t.cond

#prepare data for heatmap-creation - after Hannes (between run normalisation) !!!
step4.data.hm.t  <- as.data.frame(t(step4.data))
step4.data.hm.t.cond <- as.data.frame(cbind(exp.design.noPS.sort$condition, step4.data.hm.t))
colnames(step4.data.hm.t.cond)[colnames(step4.data.hm.t.cond)=="exp.design.noPS.sort$condition"]
 <- "condition"
step4.data.hm.final <- step4.data.hm.t.cond

#prepare data for heatmap-creation - after DESeq normalisation
step5.data.hm.t  <- as.data.frame(t(step5.data))
step5.data.hm.t.cond <- as.data.frame(cbind(exp.design.noPS.sort$condition, step5.data.hm.t))
colnames(step5.data.hm.t.cond)[colnames(step5.data.hm.t.cond)=="exp.design.noPS.sort$condition"]
 <- "condition"
step5.data.hm.final <- step5.data.hm.t.cond

#create heatmaps#################################################
#raw intensities all proteins with zeroblocks
tiff(file="output/heatmap_1_raw_all_proteins_w_zeroblocks.tiff", width=11.681, height=7.431,
 units="in",type="cairo", res=600, compression="lzw")
```

```
par(lwd=3)
heatmap.2(as.matrix(step2.data.hm.final[, 2:ncol(step2.data.hm.final)] ), col = hmcol, labCol=FALSE,
 scale=c("none"), labRow=rownames(step2.data.hm.final) ,trace="none", Rowv = TRUE, Colv = FALSE,
 dendrogram = c("row"), hclust=function(x) hclust(x,method="average"), distfun = function(x)
 dist(x,method = 'minkowski'), margin=c(2, 5))
dev.off()

#raw intensities all proteins without zeroblocks
tiff(file="output/heatmap_2_raw_all_proteins_wo_zeroblocks.tiff", width=11.681, height=7.431,
 units="in",type="cairo", res=600, compression="lzw")
par(lwd=3)
heatmap.2(as.matrix(step3.data.hm.final[, 2:ncol(step3.data.hm.final)] ), col = hmcol, labCol=FALSE,
 scale=c("none"), labRow=rownames(step3.data.hm.final) ,trace="none", Rowv = TRUE, Colv = FALSE,
 dendrogram = c("row"), hclust=function(x) hclust(x,method="average"), distfun = function(x)
 dist(x,method = 'minkowski'), margin=c(2, 5))
dev.off()

#normalized (between run, Hannes) intensities all proteins without zeroblocks
tiff(file="output/heatmap_3_NormHannes_all_proteins_wo_zeroblocks.tiff", width=11.681,
 height=7.431, units="in",type="cairo", res=600, compression="lzw")
par(lwd=3)
heatmap.2(as.matrix(step4.data.hm.final[, 2:ncol(step4.data.hm.final)] ), col = hmcol, labCol=FALSE,
 scale=c("none"), labRow=rownames(step4.data.hm.final) ,trace="none", Rowv = TRUE, Colv = FALSE,
 dendrogram = c("row"), hclust=function(x) hclust(x,method="average"), distfun = function(x)
 dist(x,method = 'minkowski'), margin=c(2, 5))
dev.off()

#normalized (between run) intensities and between samples (DESeq) all proteins without zeroblocks
tiff(file="output/heatmap_4_NormDESeq_all_proteins_wo_zeroblocks.tiff", width=11.681,
 height=7.431, units="in",type="cairo", res=600, compression="lzw")
par(lwd=3)
heatmap.2(as.matrix(step5.data.hm.final[, 2:ncol(step5.data.hm.final)] ), col = hmcol, labCol=FALSE,
 scale=c("none"), labRow=rownames(step5.data.hm.final) ,trace="none", Rowv = TRUE, Colv = FALSE,
 dendrogram = c("row"), hclust=function(x) hclust(x,method="average"), distfun = function(x)
 dist(x,method = 'minkowski'), margin=c(2, 5))
dev.off()

#only signgicantly DE proteins - log2-transformed
tiff(file="output/heatmap_5_Log2_trans_all_signDE.tiff", width=11.681, height=7.431,
 units="in",type="cairo", res=600, compression="lzw")
par(lwd=3)
heatmap.2(as.matrix(step7.data[, all.sig.proteins.IDs.uniq]), col = hmcol, labCol=FALSE, scale=c("none"),
 labRow=rownames(step7.data) ,trace="none", Rowv = TRUE, Colv = FALSE, dendrogram = c("row"),
 hclust=function(x) hclust(x,method="average"), distfun = function(x) dist(x,method = 'minkowski'),
 margin=c(2, 5))
dev.off()

#normalized and log2-transformed - all proteins
tiff(file="output/heatmap_6_Log2_trans_all_proteins.tiff", width=11.681, height=7.431,
 units="in",type="cairo", res=600, compression="lzw")
par(lwd=3)
heatmap.2(as.matrix(step7.data[, 2:ncol(step7.data)]), col = hmcol, labCol=FALSE, scale=c("none"),
 labRow=rownames(step7.data) ,trace="none", Rowv = TRUE, Colv = FALSE, dendrogram = c("row"),
 hclust=function(x) hclust(x,method="average"), distfun = function(x) dist(x,method = 'minkowski'),
 margin=c(2, 5))
dev.off()

#################################################################
```

```
#do discriminant analysis of principal components (DAPC)

#prepare data
DAPC.df <- step7.data
for(i in 2:ncol(DAPC.df)){
 DAPC.df[is.na(DAPC.df[,i]), i] <- mean(DAPC.df[,i], na.rm = TRUE)
}

data_start <- min(grep("BBD24_", colnames(DAPC.df)))

#OPTIONAL - manually change labels
rep_labels <- FALSE
if(rep_labels) {
 change_label <- "LABEL7"
 change_label_pos <- grep(change_label, colnames(DAPC.df))
 find_list <-   c("MRS")
 replace_list <- c("mMRS")
 size_lists <- length(replace_list)

 for(i in 1:size_lists) {
  DAPC.df[, change_label] <- sub(find_list[i], replace_list[i], DAPC.df[, change_label])
 }
 DAPC.df[, change_label] <- factor(DAPC.df[, change_label])
}

#DO: set!!!! max grps
max_grps <- 13

#first approach "natural grouping" ##############################
grp <- find.clusters(DAPC.df[ , data_start:ncol(DAPC.df)], max.n.clust=max_grps, pca.select="percVar",
 perc.pca=75, scale=FALSE, center=FALSE, n.iter=1e5, n.start=1000)
dapc1 <- dapc(DAPC.df[ , data_start:ncol(DAPC.df)], grp$grp, pca.select="percVar", perc.pca=75)

#plotting
scatter(dapc1)
scatter(dapc1, grp=DAPC.df$condition)
scatter(dapc1, grp=as.factor(rownames(DAPC.df)))

#see contributions
contrib <- loadingplot(dapc1$var.contr, axis=1, thres=.02, lab.jitter=1)

#second approach "natural grouping" - interactive ##############
grp <- find.clusters(DAPC.df[ , data_start:ncol(DAPC.df)], max.n.clust=max_grps, pca.select="percVar",
 perc.pca=75, scale=FALSE, center=FALSE, n.iter=1e5, n.start=1000)
dapc2 <- dapc(DAPC.df[ , data_start:ncol(DAPC.df)], grp$grp)

#plotting
scatter(dapc2)
scatter(dapc2, grp=as.factor(rownames(DAPC.df)))
scatter(dapc2, grp=DAPC.df$condition)

tiff(file="output/DAPC_nat.tiff", width=11.681, height=7.431, units="in",type="cairo", res=600,
 compression="lzw")
scatter(dapc2, grp=DAPC.df$condition)
dev.off()

#see contributions
contrib <- loadingplot(dapc2$var.contr, axis=1, thres=.02, lab.jitter=1)
```

```
#third approach - "forced grouping" ############################
dapc3 <- dapc(DAPC.df[ , data_start:ncol(DAPC.df)], grp=DAPC.df$condition, pca.select="percVar",
 perc.pca=75, n.da=length(levels(DAPC.df$condition))-1)

#plotting
scatter(dapc3)

tiff(file="output/DAPC_forced_step7.data.tiff", width=11.681, height=7.431, units="in",type="cairo",
 res=600, compression="lzw")
scatter(dapc3)
dev.off()

#see contributions
contrib <- loadingplot(dapc3$var.contr, axis=1, thres=.02, lab.jitter=1)
```

# 10 Supplementary Part II - Results

## 10.1 Genomics

### 10.1.1 Genome analysis

Table S 4: Functional analysis of *Lb. paracasei* subsp. *paracasei* F19 using SEED subsystem analysis. The total number of assigned proteins to SEED categories with respect to whole genome, chromosome (chr) and plasmid (pl) is listed.

| SEED category | genome | chr | pl |
|---|---|---|---|
| **Carbohydrates** | 270 | 265 | 5 |
| **Protein Metabolism** | 139 | 139 | 0 |
| **Cell Wall and Capsule** | 87 | 86 | 1 |
| **Cofactors Vitamins Prosthetic Groups Pigments** | 77 | 77 | 0 |
| **Amino Acids and Derivatives** | 77 | 75 | 2 |
| **Nucleosides and Nucleotides** | 68 | 68 | 0 |
| **DNA Metabolism** | 68 | 66 | 2 |
| **RNA Metabolism** | 67 | 67 | 0 |
| **Virulence Disease and Defense** | 58 | 53 | 5 |
| **Membrane Transport** | 54 | 54 | 0 |
| **Fatty Acids Lipids and Isoprenoids** | 38 | 38 | 0 |
| **Stress Response** | 32 | 31 | 1 |
| **Cell Division and Cell Cycle** | 32 | 30 | 2 |
| **Regulation and Cell signaling** | 30 | 30 | 0 |
| **Miscellaneous** | 20 | 19 | 1 |
| **Respiration** | 14 | 14 | 0 |
| **Phosphorus Metabolism** | 13 | 13 | 0 |
| **Iron acquisition and metabolism** | 6 | 6 | 0 |
| **Sulfur Metabolism** | 5 | 5 | 0 |
| **Secondary Metabolism** | 4 | 4 | 0 |
| **Nitrogen Metabolism** | 4 | 4 | 0 |
| **Potassium metabolism** | 4 | 4 | 0 |

| | | | |
|---|---|---|---|
| **Dormancy and Sporulation** | 3 | 3 | 0 |
| **Metabolism of Aromatic Compounds** | 2 | 2 | 0 |
| **Phages Prophages Transposable elements Plasmids** | 1 | 1 | 0 |
| **Motility and Chemotaxis** | 1 | 1 | 0 |

## 10.2 Selection of comparable stress conditions

### 10.2.1 Determination of stress intensity tolerances

#### 10.2.1.1 Sublethal stress conditions

##### 10.2.1.1.1 Starvation stress

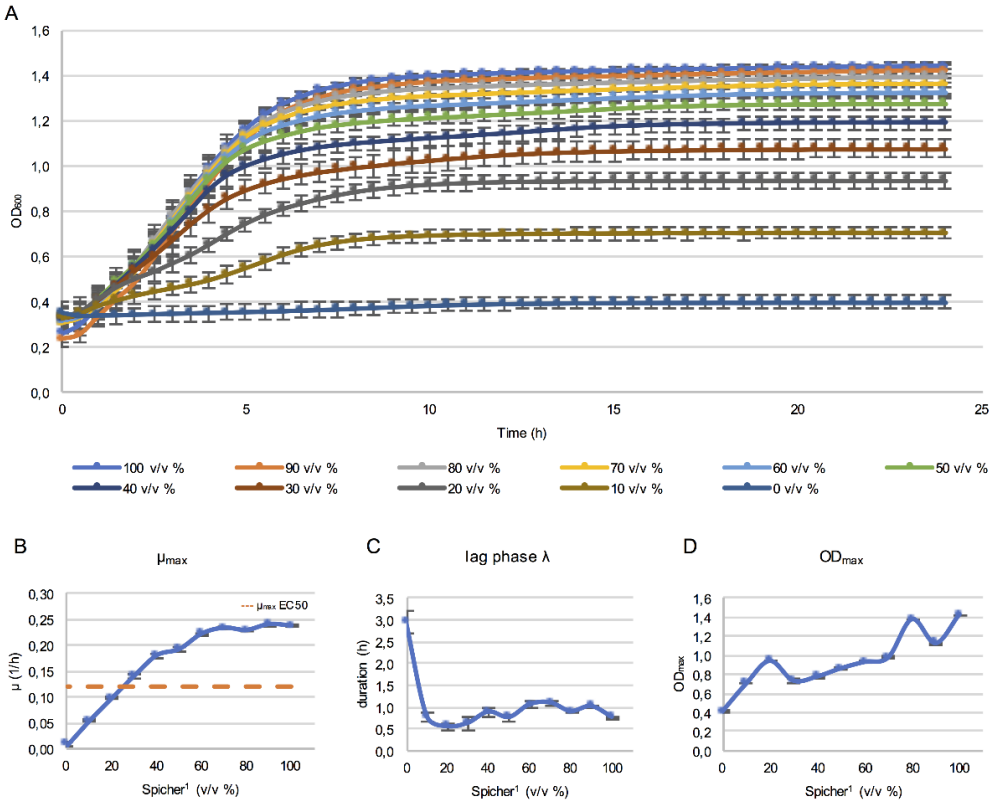


Figure S 1: Growth curve analysis of *Lb. paracasei* subsp. *paracasei* F19 in the presence of starvation stress. Growth curves are illustrated for all applied concentrations (A). Growth parameters maximum specific growth rate ($\mu_{max}$), duration of lag phase λ and maximum turbidity ($OD_{max}$) were extracted for all growth data obtained and plotted against the Spicher[1] concentration (B) $\mu_{max}$ and λ were affected by the induced stress quality and $OD_{max}$ remained more or less constant. EC50 was estimated based on the calculation of $\mu_{max}$ EC50 (---). Note that normalization was conducted for the calculation of $\mu_{max}$ and λ.

### 10.2.1.1.2 Oxidative stress

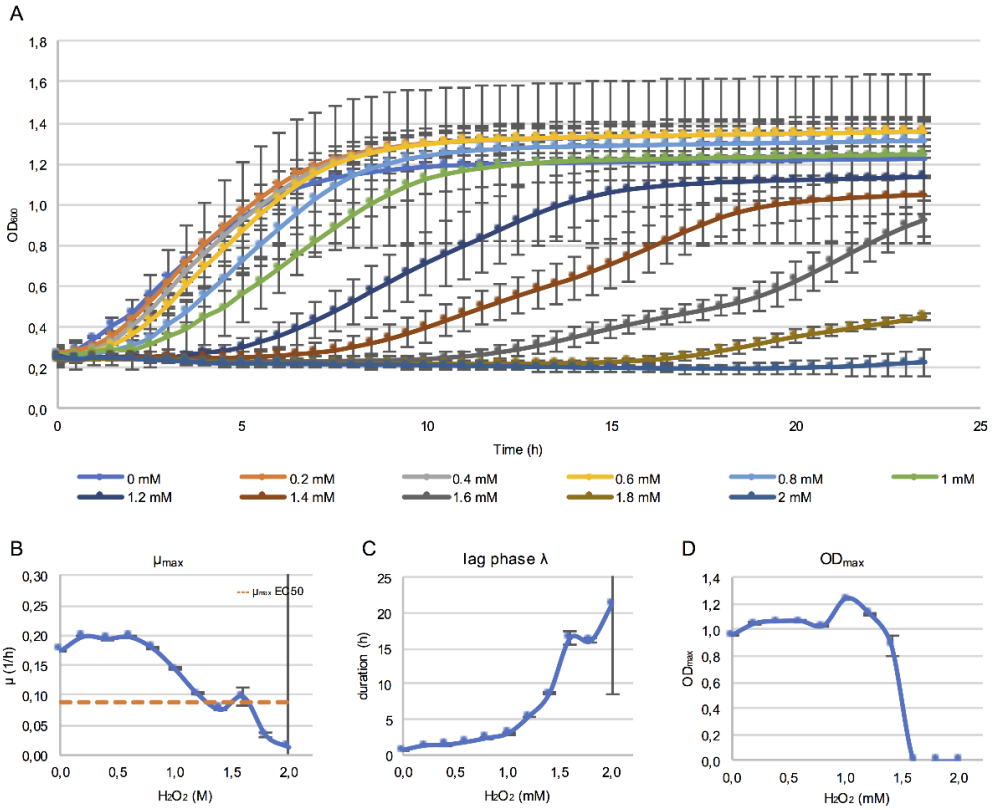


Figure S 2: Growth curve analysis of *Lb. paracasei* subsp. *paracasei* F19 in the presence of oxidative stress. Growth curves are illustrated for all applied concentrations (A). Growth parameters maximum specific growth rate ($\mu_{max}$), duration of lag phase λ and maximum turbidity ($OD_{max}$) were extracted for all growth data obtained and plotted against the $H_2O_2$ concentration (B) $\mu_{max}$, λ and $OD_{max}$ were affected by the induced stress quality. EC50 was estimated based on the calculation of $\mu_{max}$ EC50 (---). Note that normalization was conducted for the calculation of $\mu_{max}$ and λ.

### 10.2.1.1.3 Lactose stress

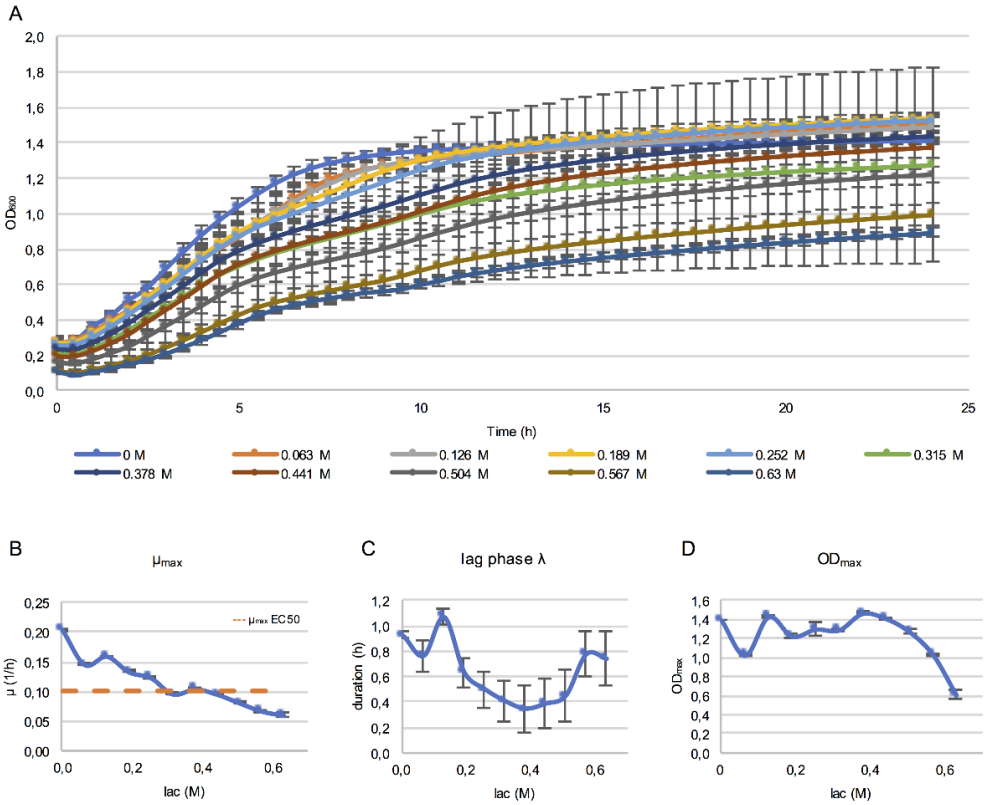


Figure S 3: Growth curve analysis of *Lb. paracasei* subsp. *paracasei* F19 in the presence of lactose stress. Growth curves are illustrated for all applied concentrations (A). Growth parameters maximum specific growth rate ($\mu_{max}$), duration of lag phase λ and maximum turbidity ($OD_{max}$) were extracted for all growth data obtained and plotted against the lactose concentration (B) $\mu_{max}$ and $OD_{max}$ were affected by the induced stress quality and λ remained more or less constant. EC50 was estimated based on the calculation of $\mu_{max}$ EC50 (---). Note that normalization was conducted for the calculation of $\mu_{max}$ and λ.

### 10.2.1.1.4 Sucrose stress

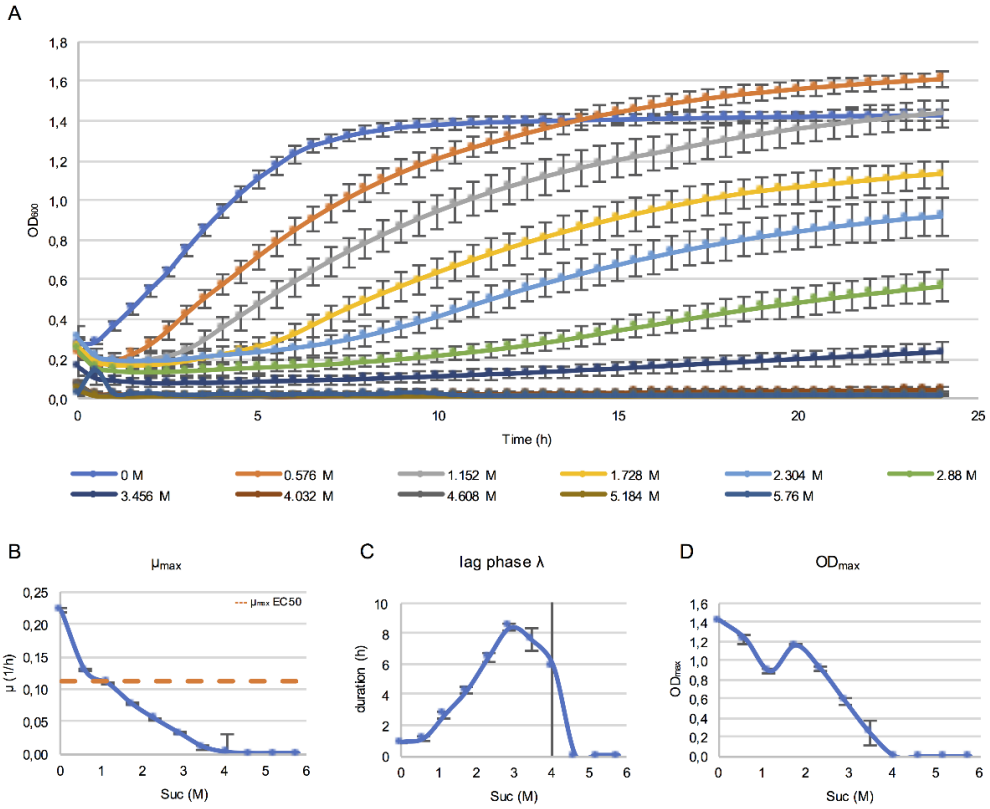


Figure S 4: Growth curve analysis of *Lb. paracasei* subsp. *paracasei* F19 in the presence of sucrose stress. Growth curves are illustrated for all applied concentrations (A). Growth parameters maximum specific growth rate ($\mu_{max}$), duration of lag phase λ and maximum turbidity ($OD_{max}$) were extracted for all growth data obtained and plotted against the sucrose concentration (B) $\mu_{max}$, λ and $OD_{max}$ were affected by the induced stress quality. EC50 was estimated based on the calculation of $\mu_{max}$ EC50 (---). Note that normalization was conducted for the calculation of $\mu_{max}$ and λ.

### 10.2.1.1.5 Sodium chloride stress

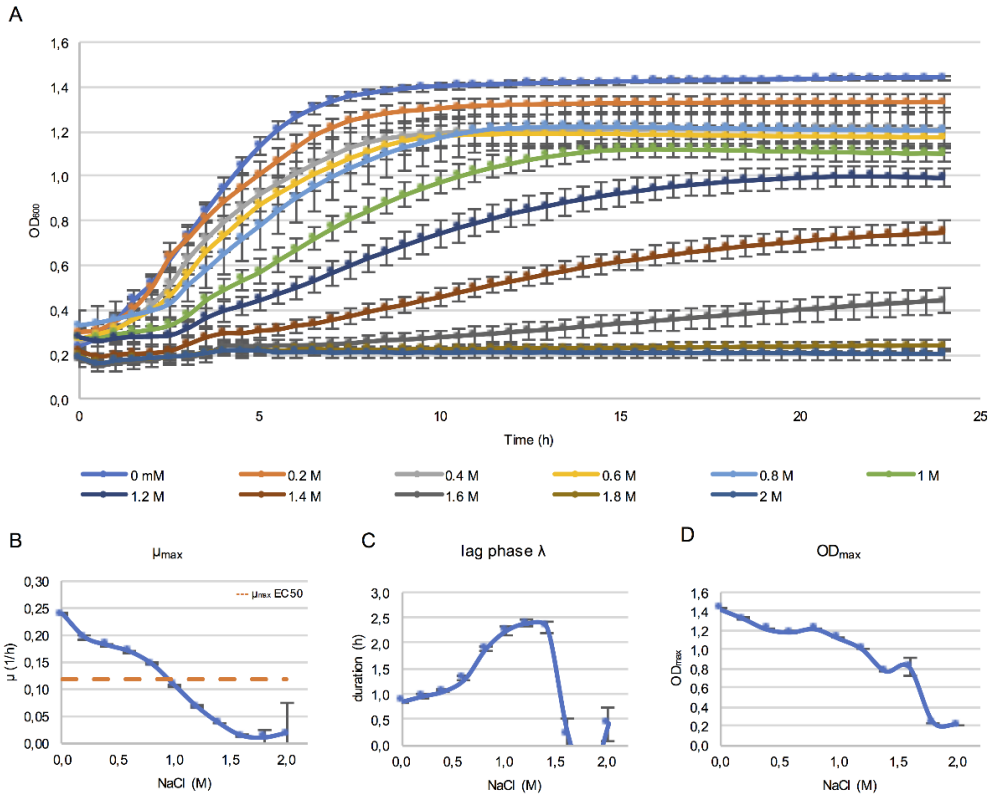


Figure S 5: Growth curve analysis of *Lb. paracasei* subsp. *paracasei* F19 in the presence of sodium chloride stress. Growth curves are illustrated for all applied concentrations (A). Growth parameters maximum specific growth rate ($\mu_{max}$), duration of lag phase λ and maximum turbidity ($OD_{max}$) were extracted for all growth data obtained and plotted against the NaCl concentration (B) $\mu_{max}$, λ and $OD_{max}$ were affected by the induced stress quality. EC50 was estimated based on the calculation of $\mu_{max}$ EC50 (---). Note that normalization was conducted for the calculation of $\mu_{max}$ and λ.

### 10.2.1.1.6 pH stress

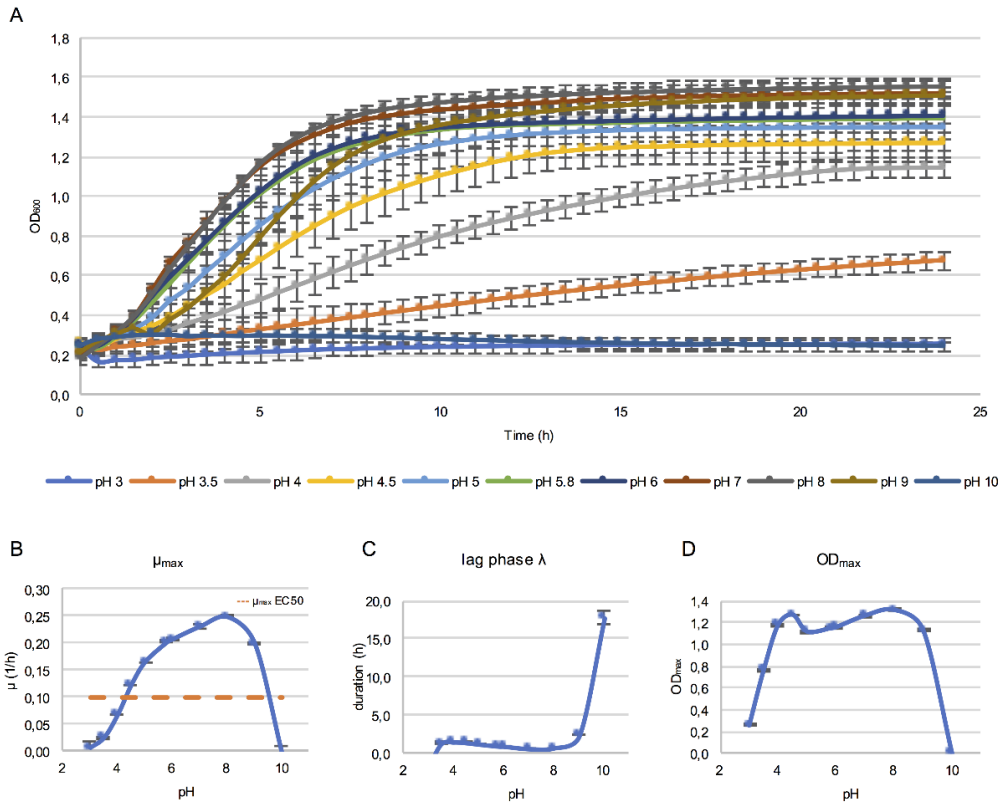


Figure S 6: Growth curve analysis of *Lb. paracasei* subsp. *paracasei* F19 in the presence of pH stress. Growth curves are illustrated for all applied pH conditions (A). Growth parameters maximum specific growth rate ($\mu_{max}$), duration of lag phase λ and maximum turbidity ($OD_{max}$) were extracted for all growth data obtained and plotted against the pH (B) $\mu_{max}$, λ and $OD_{max}$ were affected by the induced stress quality. EC50 was estimated based on the calculation of $\mu_{max}$ EC50 (---). Note that normalization was conducted for the calculation of $\mu_{max}$ and λ.

#### 10.2.1.1.7 Temperature stress

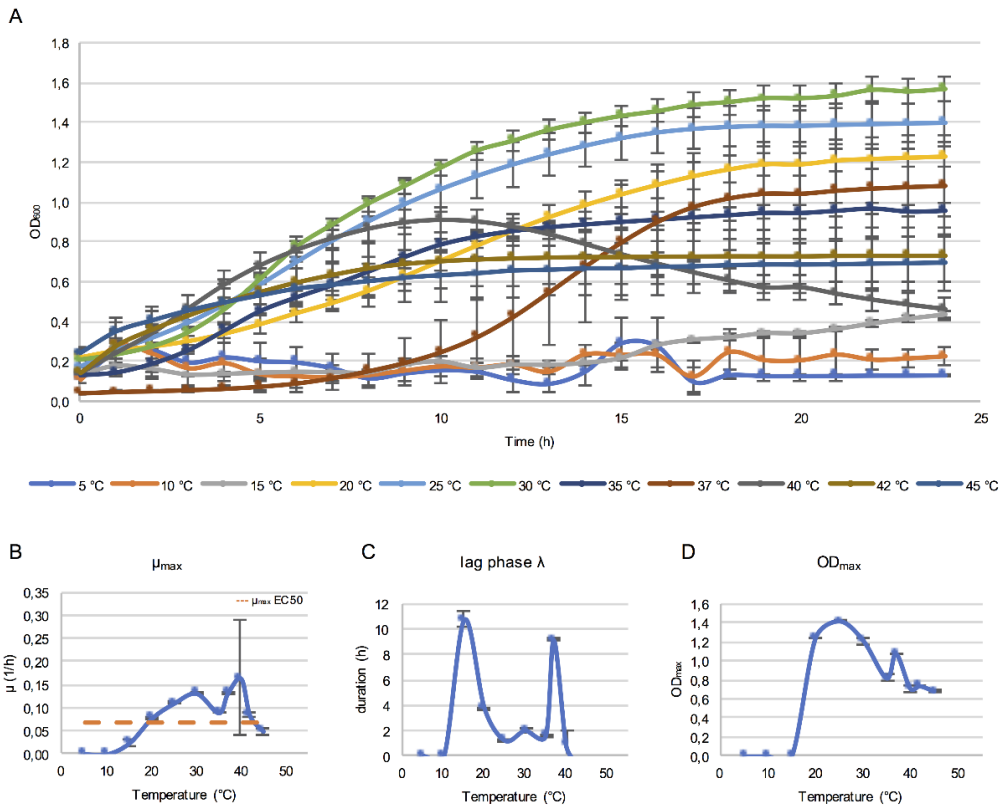


Figure S 7: Growth curve analysis of *Lb. paracasei* subsp. *paracasei* F19 in the presence of temperature stress. Growth curves are illustrated for all applied concentrations (A). Growth parameters maximum specific growth rate ($\mu_{max}$), duration of lag phase λ and maximum turbidity ($OD_{max}$) were extracted for all growth data obtained and plotted against the temperature (B) $\mu_{max}$, λ and $OD_{max}$ were affected by the induced stress quality. EC50 was estimated based on the calculation of $\mu_{max}$ EC50 (---). Note that normalization was conducted for the calculation of $\mu_{max}$ and λ.

## 10.2.2 Determination of stress application time tolerances

### 10.2.2.1 Stress response kinetics

The cluster analyses of sublethal sodium chloride (NaCl), alkaline pH (pH9) and lactose (lac) stress are shown in S2 Fig, demonstrating analogies among the cluster formation. The analyzed mass spectra of the stress samples were separated, based on the sampling points, in two sub-clusters. Concerning the stress treatments with sodium chloride or alkaline pH, one sub-cluster harbored spectra of 90 and 120 minutes duration of stress induction (late phase of stress response), demonstrating higher variability to each other and any other sampling point of the stress response. Thus, the other sub-cluster consisted of 30 and 60 minutes stress application. Regarding the stress treatment with lactose, the stress responses of 60 and 120 minutes duration of stress induction

grouped in a sub-cluster revealing higher similarity and low distance to each other than to the other sub-cluster, which harbored stress responses of 30 and 90 minutes of stress induction.

The hierarchical clustering of glucose-starvation (glu10), potassium chloride (KCl), acidic pH (pH4), sucrose (suc), hydrogen peroxide ($H_2O_2$) or temperature (15 °C, 45 °C) stress treatment grouped the analyzed mass spectra of the stress samples in solely one cluster (S2 Fig). In case of glucose-starvation, potassium chloride or acidic pH stress, the analyzed mass spectra of 60 and 90 minutes duration of stress induction showed lowest distance to each other than to the rest of the sampling points - 30 minutes and 120 minutes duration of stress application. For sucrose or heat stress (45 °C), the stress responses of 90 and 120 minutes duration of stress induction displayed a lower distance to each other and thus indicated a higher similarity to each other than to stress responses after 30 and 60 minutes of stress induction. Regarding the stress treatment with hydrogen peroxide, the lowest distance of the cluster was detected for stress responses of 30 and 90 minutes duration of stress induction, whereas the cluster analysis of cold stress (15 °C) detected the highest similarity between stress responses of 60 and 120 minutes of stress induction.

#### 10.2.2.1.1 Starvation stress

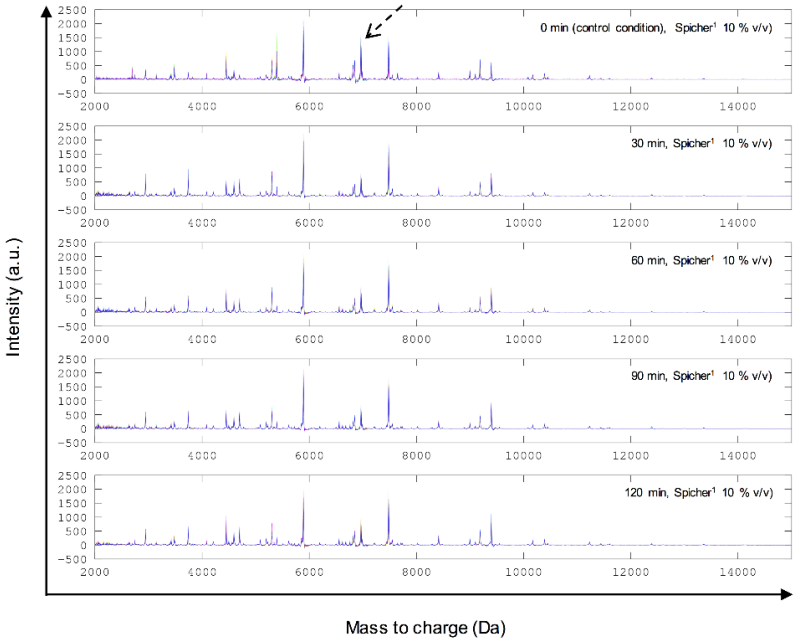


Figure S 8: Stacked protein expression profiles of starvation stress (Spicher[1] 10% v/v) obtained for *Lb. paracasei* subsp. *paracasei* F19. MALDI-TOF mass spectra in the mass range from 2,000 Da to 15,000 Da were recorded for stress application times of 0 – 120 min, whereby 0 min stress induction refer to control condition. Arrows indicate interesting peaks.

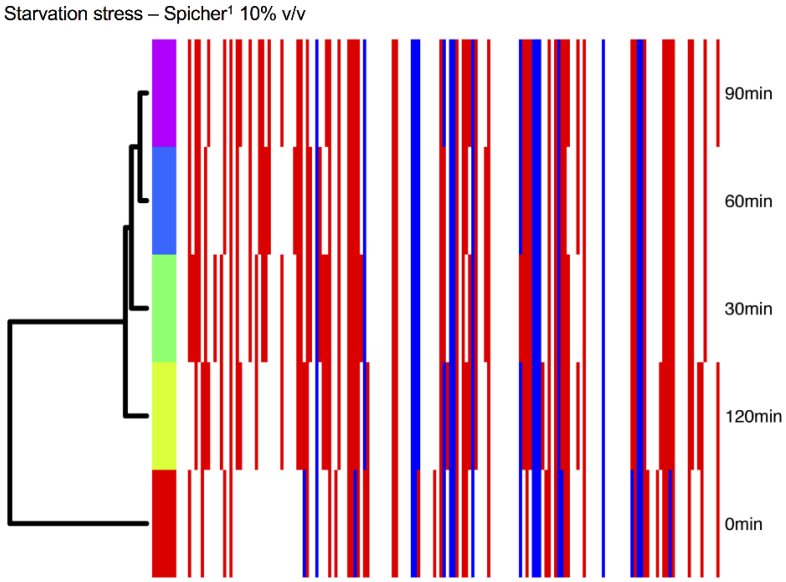


Figure S 9: Peak-based cluster analysis of stress response kinetics of starvation stress (Spicher[1] 10 % v/v) of *Lb. paracasei* subsp. *paracasei* F19. Cluster analysis is displayed as dendrogram with varying stress application times from 0 min (control) to 90 min in 30 min intervals

### 10.2.2.1.2 Oxidative stress

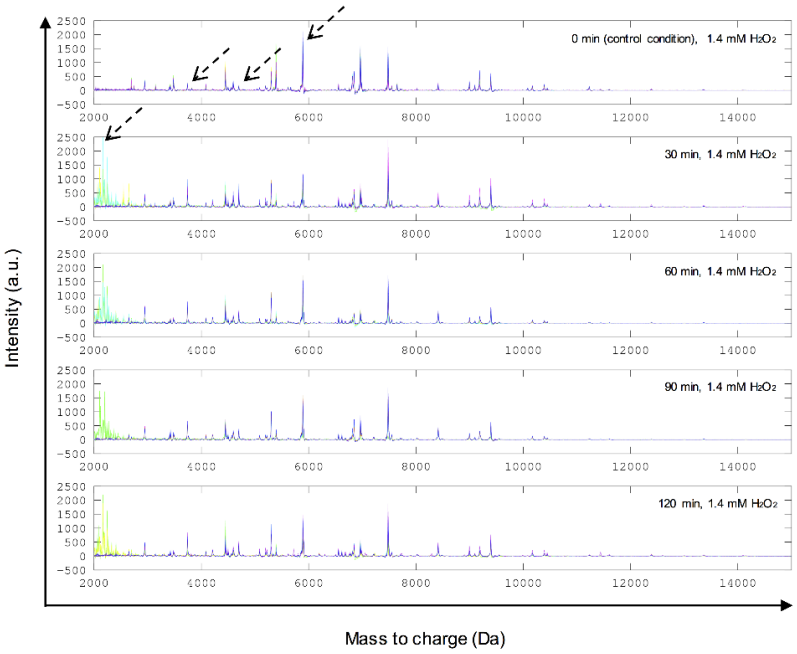


Figure S 10: Stacked protein expression profiles of oxidative stress (H2O2) obtained for Lb. paracasei subsp. paracasei F19. MALDI-TOF mass spectra in the mass range from 2,000 Da to 15,000 Da were recorded for stress application times of 0 – 120 min, whereby 0 min stress induction refer to control condition. Arrows indicate interesting peaks.

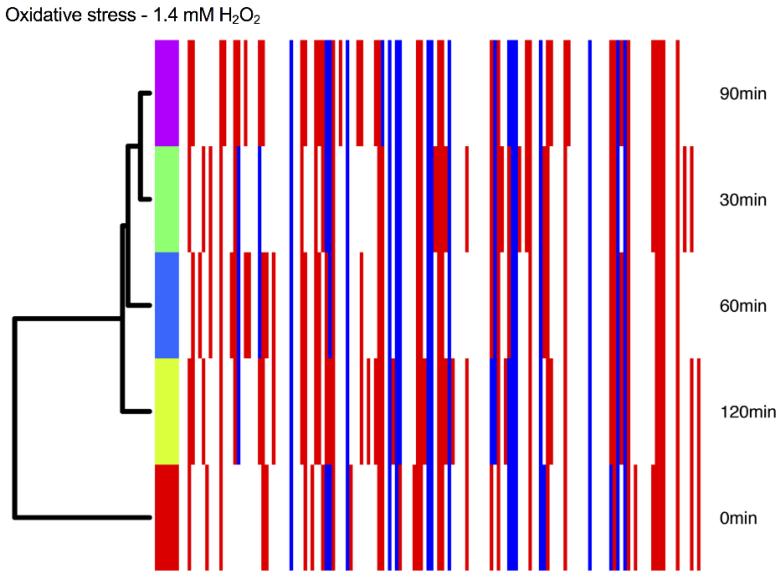


Figure S 11: Peak-based cluster analysis of stress response kinetics of oxidative stress (1.4mM H2O2) of Lb. paracasei subsp. paracasei F19. Cluster analysis is displayed as dendrogram with varying stress application times from 0 min (control) to 90 min in 30 min intervals.

#### 10.2.2.1.3 Lactose stress

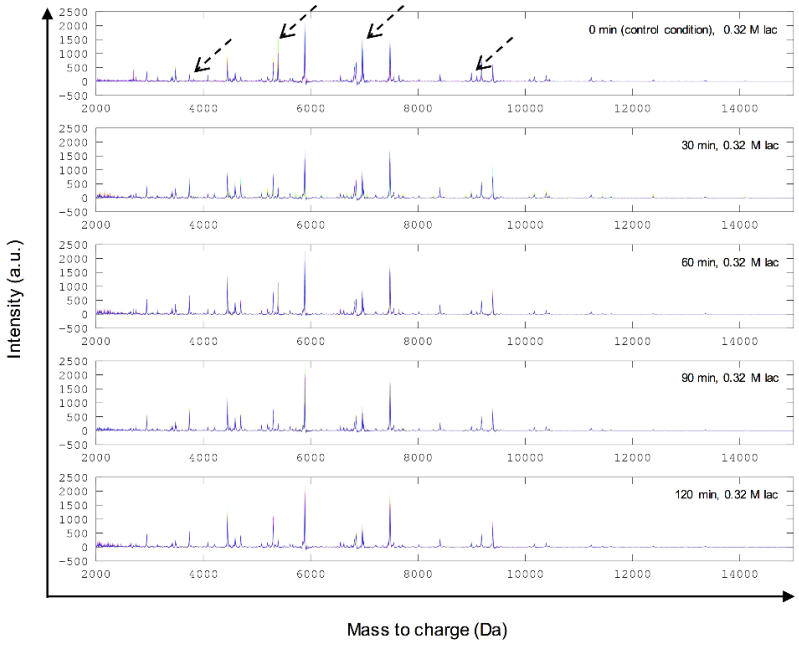


Figure S 12: Stacked protein expression profiles of lactose stress (lac) obtained for Lb. paracasei subsp. paracasei F19. MALDI-TOF mass spectra in the mass range from 2,000 Da to 15,000 Da were recorded for stress application times of 0 – 120 min, whereby 0 min stress induction refer to control condition. Arrows indicate interesting peaks.

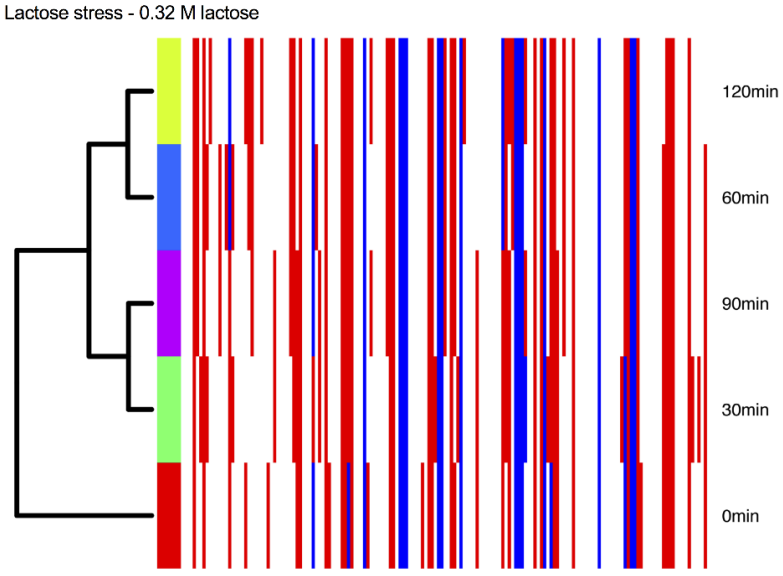


Figure S 13: Peak-based cluster analysis of stress response kinetics of lactose stress (0.32 M lactose) of Lb. paracasei subsp. paracasei F19. Cluster analysis is displayed as dendrogram with varying stress application times from 0 min (control) to 90 min in 30 min intervals.

### 10.2.2.1.4 Sucrose Stress

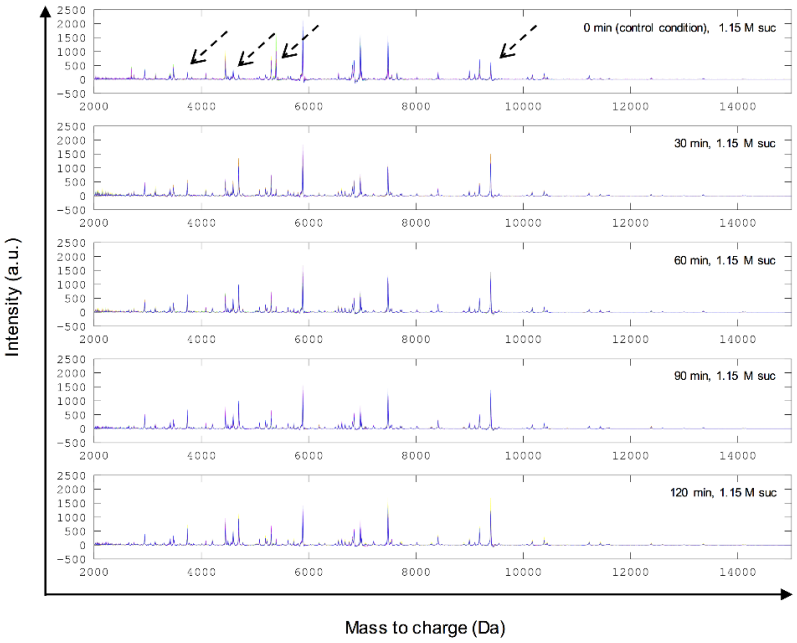


Figure S 14: Stacked protein expression profiles of sucrose stress (suc) obtained for Lb. paracasei subsp. paracasei F19. MALDI-TOF mass spectra in the mass range from 2,000 Da to 15,000 Da were recorded for stress application times of 0 – 120 min, whereby 0 min stress induction refer to control condition. Arrows indicate interesting peaks.

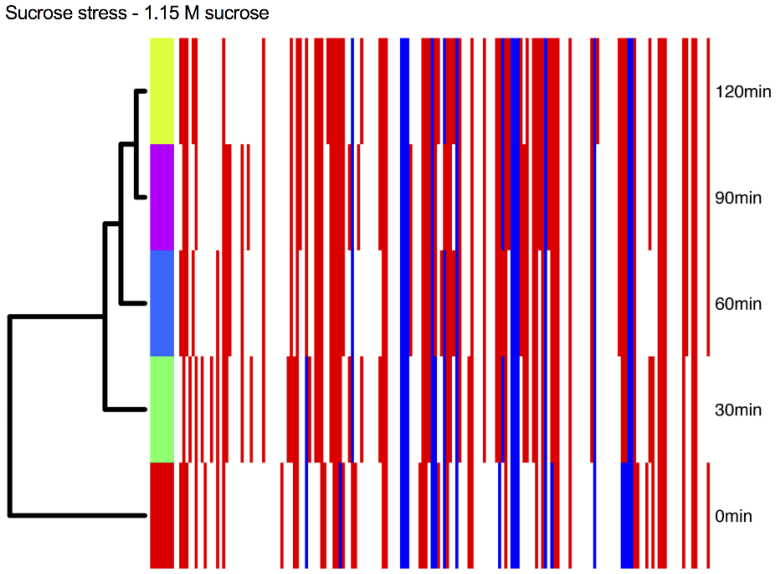


Figure S 15: Peak-based cluster analysis of stress response kinetics of sucrose stress (1.15 M suc) of Lb. paracasei subsp. paracasei F19. Cluster analysis is displayed as dendrogram with varying stress application times from 0 min (control) to 90 min in 30 min intervals.

### 10.2.2.1.5 Sodium chloride stress

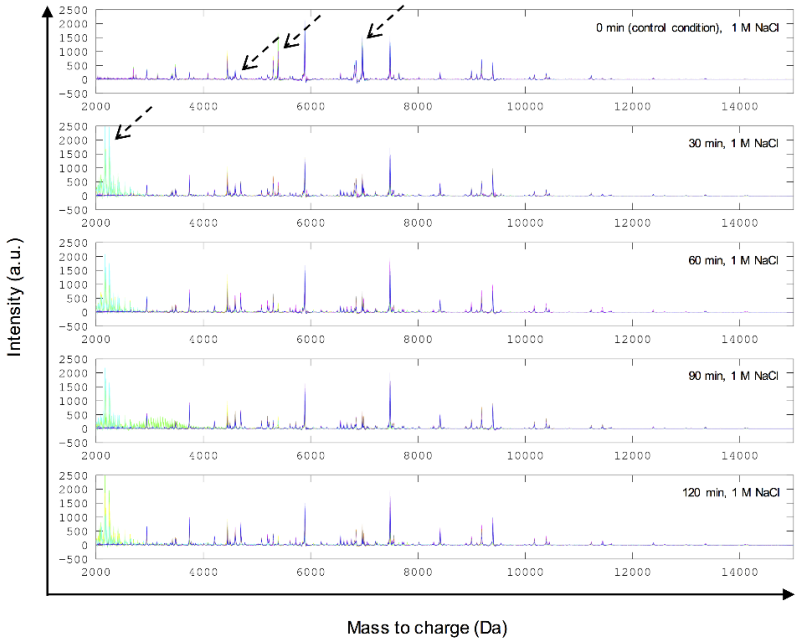


Figure S 16: Stacked protein expression profiles of sodium chloride stress (NaCl) obtained for Lb. paracasei subsp. paracasei F19. MALDI-TOF mass spectra in the mass range from 2,000 Da to 15,000 Da were recorded for stress application times of 0 – 120 min, whereby 0 min stress induction refer to control condition. Arrows indicate interesting peaks.

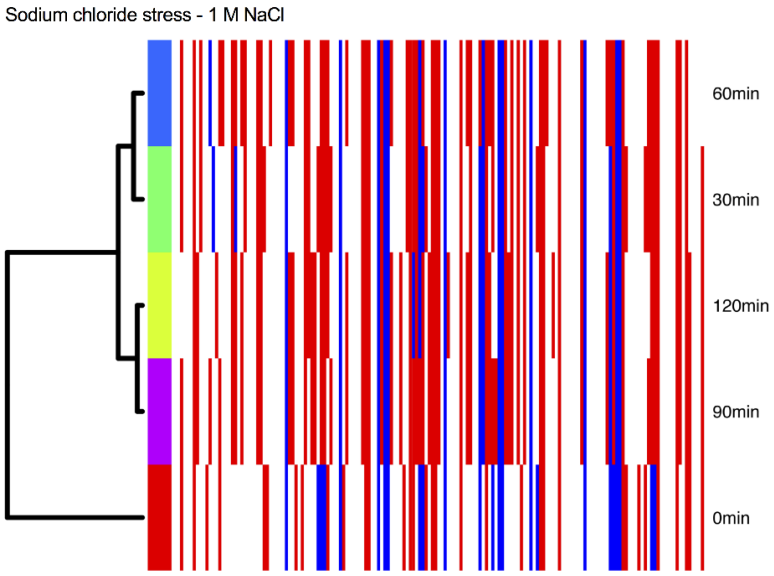


Figure S 17: Peak-based cluster analysis of stress response kinetics of sodium chloride stress (1 M NaCl) of Lb. paracasei subsp. paracasei F19. Cluster analysis is displayed as dendrogram with varying stress application times from 0 min (control) to 90 min in 30 min intervals.

### 10.2.2.1.6 pH4 stress

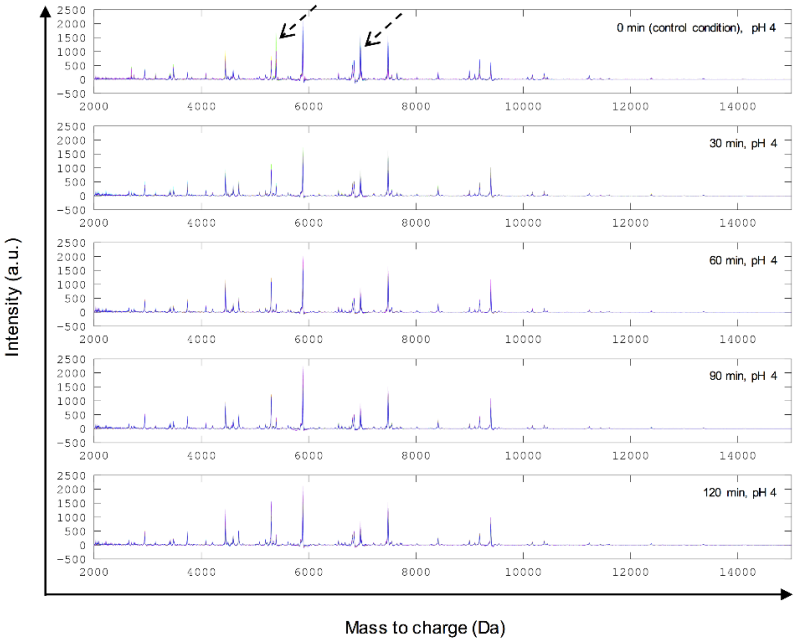


Figure S 18: Stacked protein expression profiles of acid stress (pH4) obtained for Lb. paracasei subsp. paracasei F19. MALDI-TOF mass spectra in the mass range from 2,000 Da to 15,000 Da were recorded for stress application times of 0 – 120 min, whereby 0 min stress induction refer to control condition. Arrows indicate interesting peaks.

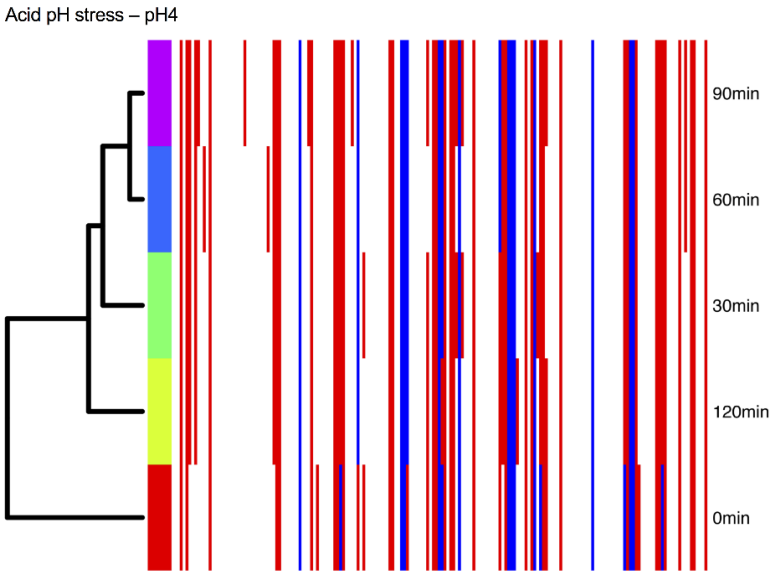


Figure S 19: Peak-based cluster analysis of stress response kinetics of acid pH stress (pH4) of Lb. paracasei subsp. paracasei F19. Cluster analysis is displayed as dendrogram with varying stress application times from 0 min (control) to 90 min in 30 min intervals.

### 10.2.2.1.7 pH9 stress

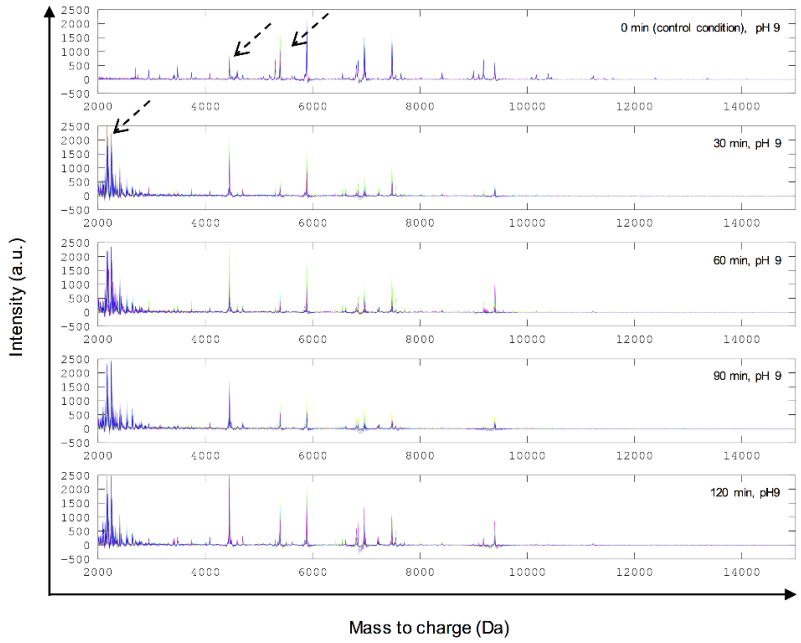


Figure S 20: Stacked protein expression profiles of alkaline stress (pH9) obtained for Lb. paracasei subsp. paracasei F19. MALDI-TOF mass spectra in the mass range from 2,000 Da to 15,000 Da were recorded for stress application times of 0 – 120 min, whereby 0 min stress induction refer to control condition. Arrows indicate interesting peaks.

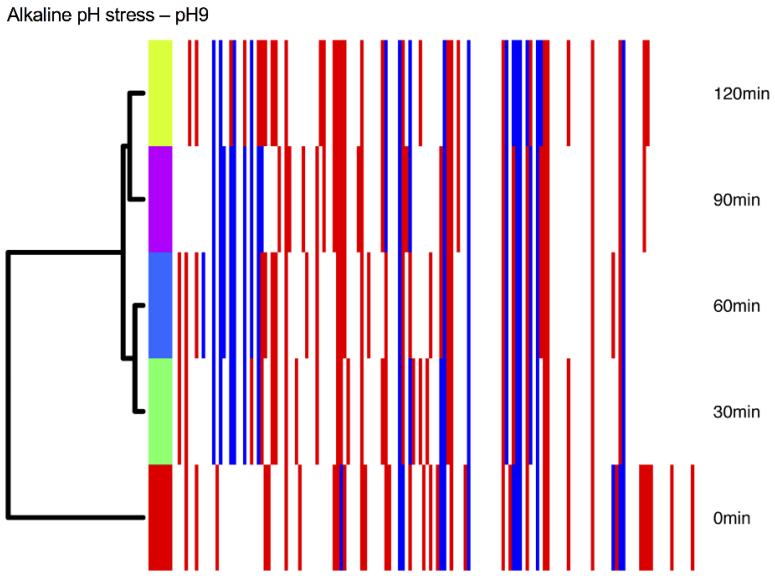


Figure S 21: Peak-based cluster analysis of stress response kinetics of alkaline pH stress (pH9) of Lb. paracasei subsp. paracasei F19. Cluster analysis is displayed as dendrogram with varying stress application times from 0 min (control) to 90 min in 30 min intervals.

### 10.2.2.1.8 Cold stress

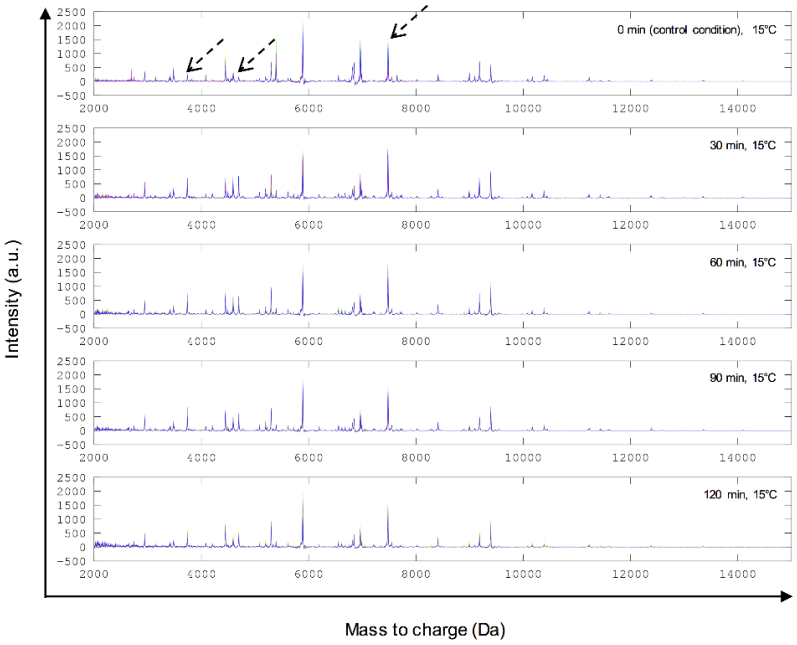


Figure S 22: Stacked protein expression profiles of cold stress (15°C) obtained for Lb. paracasei subsp. paracasei F19. MALDI-TOF mass spectra in the mass range from 2,000 Da to 15,000 Da were recorded for stress application times of 0 – 120 min, whereby 0 min stress induction refer to control condition. Arrows indicate interesting peaks.

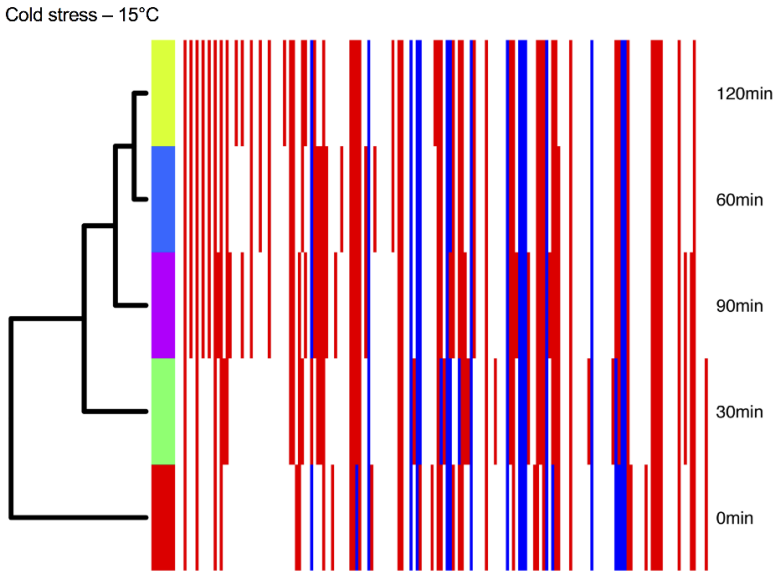


Figure S 23: Peak-based cluster analysis of stress response kinetics of cold stress (15°C) of Lb. paracasei subsp. paracasei F19. Cluster analysis is displayed as dendrogram with varying stress application times from 0 min (control) to 90 min in 30 min intervals.

### 10.2.2.1.9 Heat stress

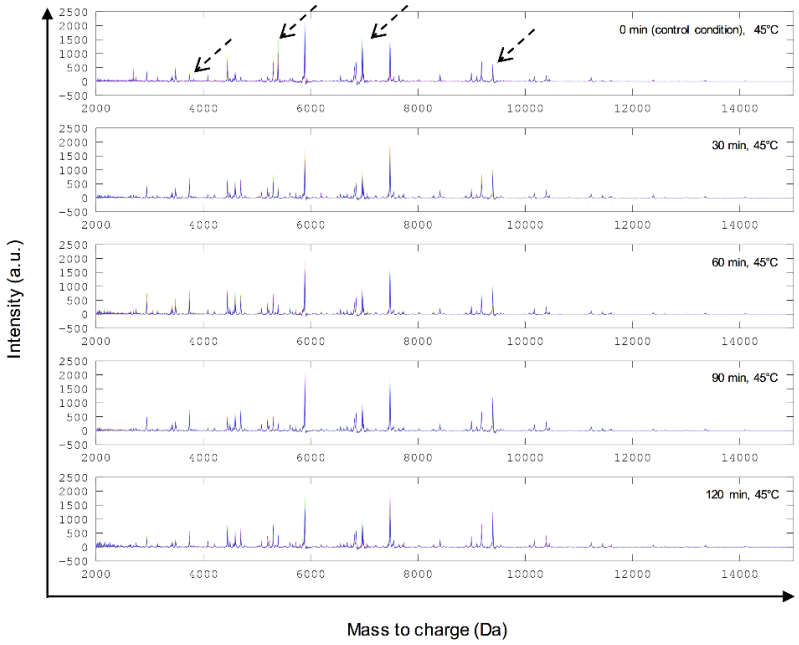


Figure S 24: Stacked protein expression profiles of heat stress (45°C) obtained for Lb. paracasei subsp. paracasei F19. MALDI-TOF mass spectra in the mass range from 2,000 Da to 15,000 Da were recorded for stress application times of 0 – 120 min, whereby 0 min stress induction refer to control condition. Arrows indicate interesting peaks.

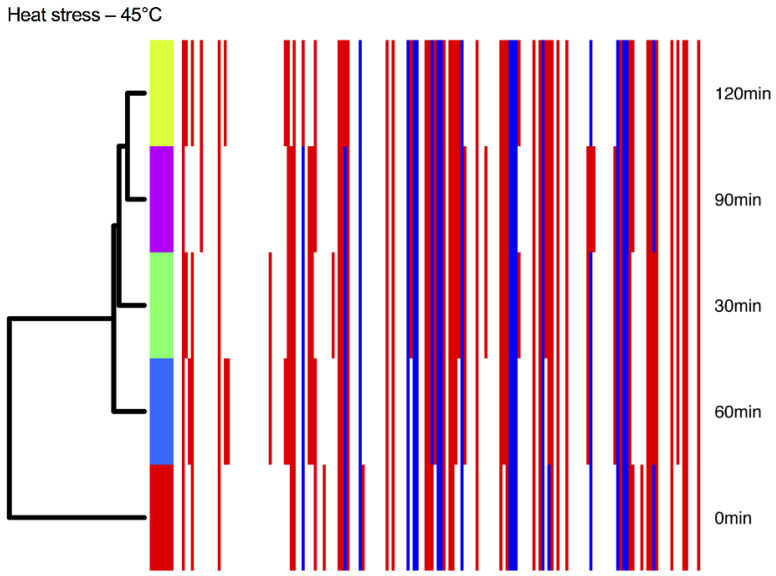


Figure S 25: Peak-based cluster analysis of stress response kinetics of heat stress (45°C) of Lb. paracasei subsp. paracasei F19. Cluster analysis is displayed as dendrogram with varying stress application times from 0 min (control) to 90 min in 30 min intervals.

### 10.2.2.1.10 High hydrostatic pressure stress

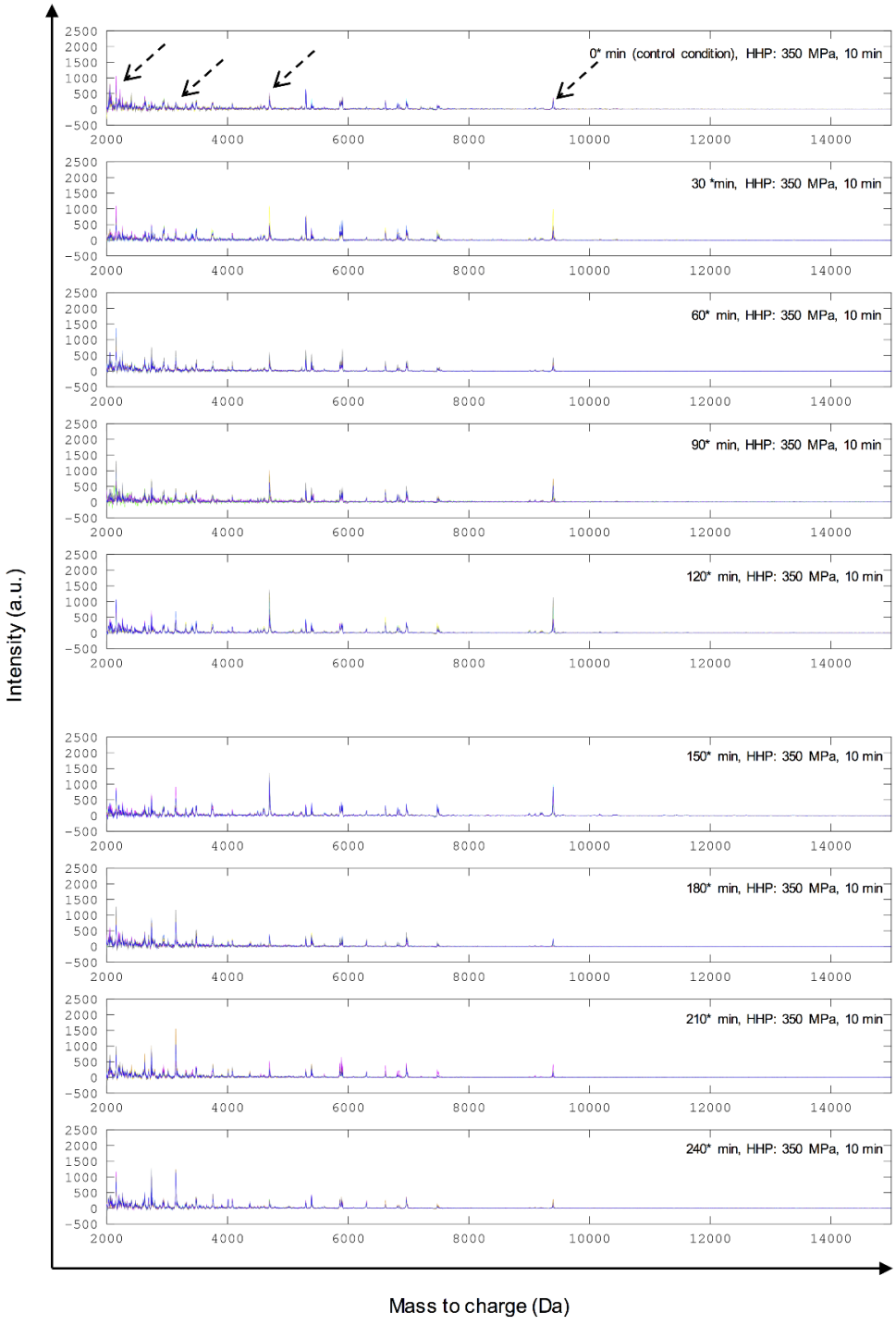


Figure S 26: Stacked protein expression profiles of high hydrostatic pressure stress (HHP) obtained for Lb. paracasei subsp. paracasei F19. MALDI-TOF mass spectra in the mass range from 2,000 Da to 15,000 Da were recorded for stress application times of 0 – 120 min, whereby 0 min stress induction refer to control condition. Arrows indicate interesting peaks.

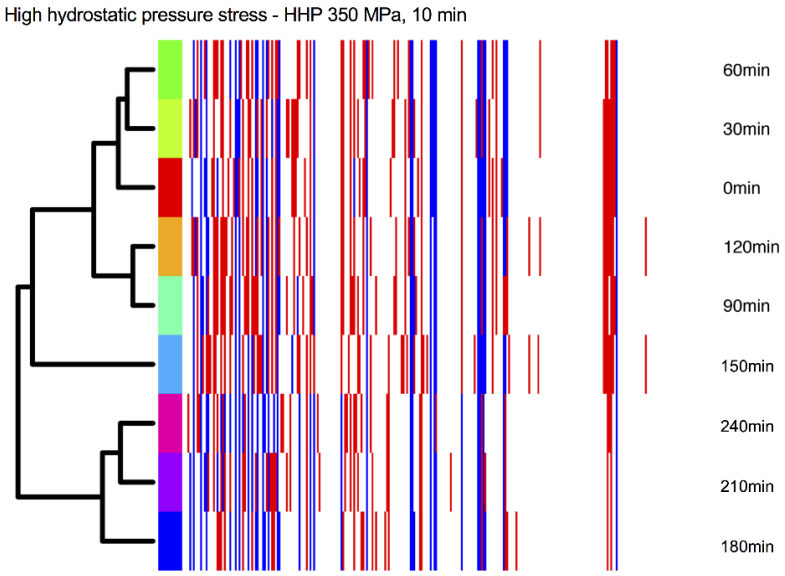


Figure S 27: Peak-based cluster analysis of stress response kinetics of high hydrostatic pressure stress (HHP 350 MPa, 10 min) of Lb. paracasei subsp. paracasei F19. Cluster analysis is displayed as dendrogram with varying stress application times from 0 min (control) to 240 min in 30 min.

### 10.2.2.1.11 Drying stress

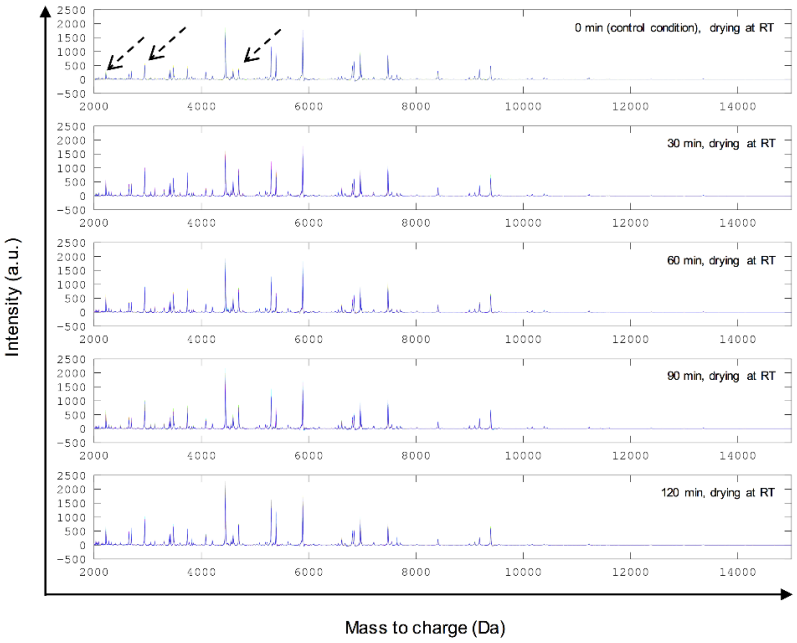


Figure S 28: Stacked protein expression profiles of drying stress obtained for Lb. paracasei subsp. paracasei F19. MALDI-TOF mass spectra in the mass range from 2,000 Da to 15,000 Da were recorded for stress application times of 0 – 120 min, whereby 0 min stress induction refer to control condition. Arrows indicate interesting peaks.

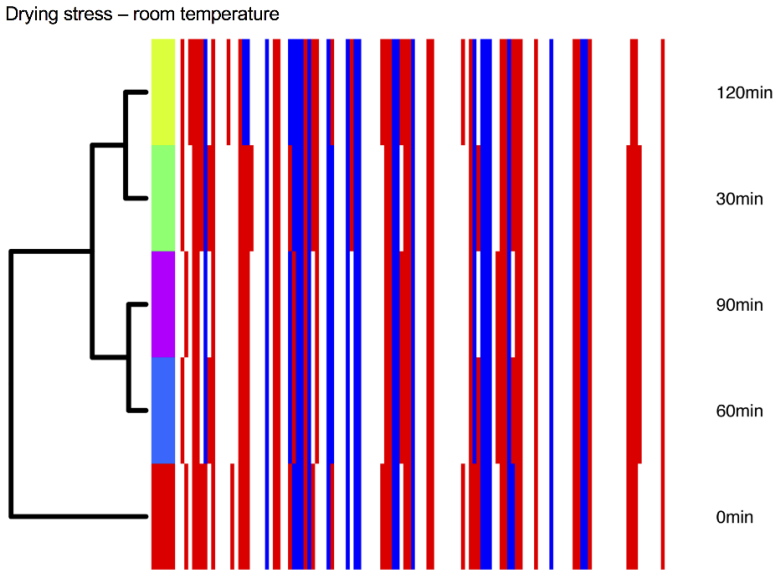


Figure S 29: Peak-based cluster analysis of stress response kinetics of drying stress (desiccation at room temperature) of Lb. paracasei subsp. paracasei F19. Cluster analysis is displayed as dendrogram with varying stress application times from 0 min (control) to 120 min in 30 min intervals.

#### 10.2.2.2 Stress response grouping

Besides analysing stress response kinetics, the differentiation of these stress responses in groups based on protein expression profiles was additionally performed using Discriminant Analysis (DA) along with Principal Component Analysis (PCA).

All data were centered before calculation. Applying ‘find.clusters’ from the R package ‘adegenet’, 3 optimal clusters were identified using the first two PCs explaining 80 % of the cumulative variance, followed by DAPC based on these 3 clusters (Figure S 30A.1). The same data were additionally stress labelled (Figure S 30A.2). A scatterplot was provided by plotting the first two discriminant functions of a DAPC that enabled a graphical estimation of the distance or proximity between groups.

The comparison of the optimal clusters with the stress labelled data revealed that cluster 1 corresponds to the stress response to high hydrostatic pressure stress (HHP), cluster 3 harbors stress responses to alkaline pH stress (pH9) and cluster 2 covers the remaining stress responses (45 °C, 15 °C, D, glu10, H2O2, KCl, lac, NaCl, pH4, suc). One outlier of the grouped stress response to pH9 stress (cluster 3) overlapped with the ellipse of the grouped stress response in cluster 2. Looking at the stress labelled data, stress responses to alkaline pH and HHP stress clearly differed from each other and also to any other stress conditions.

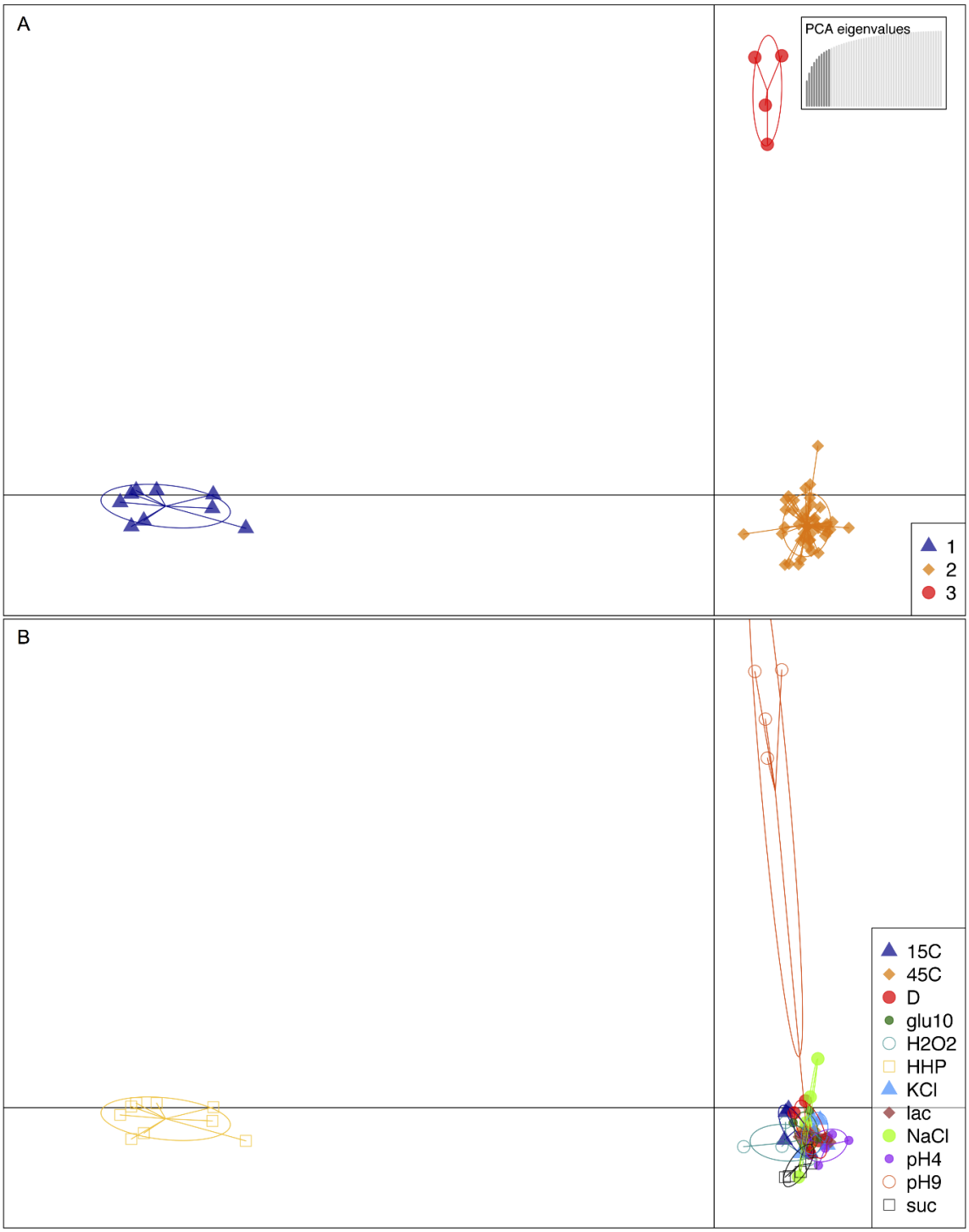


Figure S 30: DAPC of stress responses of *Lb. paracasei* subsp. *paracasei* F19 – scatterplots of first 2 principle components of the discriminant analysis of principle components (DAPC). DAPC was done including all data based on protein expression profiles. Each point represents a single stress application time, while coloration varies between the different panels. (A.1) Optimal clusters defined by *find.clusters*; also shown a scheme of the PCA eigenvalues contribution to cumulative variance. The figure illustrates that three optimal clusters are formed. (A.2) Data labelled according to sublethal stress conditions.

# 11 Supplementary Part III - Results

## 11.1 Proteome analysis

### 11.1.1 General proteomic analysis

Table S 5: Biological functions based on SEED categories of *in silico* proteome, identified, quantified and differentially expressed (DE) proteins. Number and percentage are listed.

| SEED category | *In silico* proteome | | Proteins identified | | Proteins quantified | | DE proteins | |
|---|---|---|---|---|---|---|---|---|
| **Carbohydrates** | 270 | 23.0 % | 228 | 21.6 % | 207 | 20.9 % | 53 | 26.6 % |
| **Protein Metabolism** | 139 | 11.8 % | 135 | 12.8 % | 133 | 13.4 % | 22 | 11.1 % |
| **Cell Wall and Capsule** | 87 | 7.4% | 80 | 7.6% | 75 | 7.6% | 8 | 4.0% |
| **Cofactors Vitamins Prosthetic Groups Pigments** | 77 | 6.6% | 65 | 6.2% | 61 | 6.2% | 7 | 3.5% |
| **Amino Acids and Derivatives** | 77 | 6.6% | 72 | 6.8% | 67 | 6.8% | 11 | 5.5% |
| **Nucleosides and Nucleotides** | 68 | 5.8% | 67 | 6.3% | 61 | 6.2% | 19 | 9.5% |
| **DNA Metabolism** | 68 | 5.8% | 63 | 6.0% | 60 | 6.1% | 6 | 3.0% |
| **RNA Metabolism** | 67 | 5.7% | 64 | 6.1% | 62 | 6.3% | 8 | 4.0% |
| **Virulence Disease and Defense** | 58 | 4.9% | 49 | 4.6% | 41 | 4.1% | 10 | 5.0% |
| **Membrane Transport** | 54 | 4.6% | 42 | 4.0% | 40 | 4.0% | 14 | 7.0% |
| **Fatty Acids Lipids and Isoprenoids** | 38 | 3.2% | 37 | 3.5% | 35 | 3.5% | 12 | 6.0% |
| **Stress Response** | 32 | 2.7% | 27 | 2.6% | 26 | 2.6% | 10 | 5.0% |
| **Other SEED categories** | 32 | 11.8 % | 32 | 12.0 % | 32 | 12.3 % | 3 | 9.5% |

## 11.1.2 Proteomic analysis of stress responses

### 11.1.2.1 Acid stress

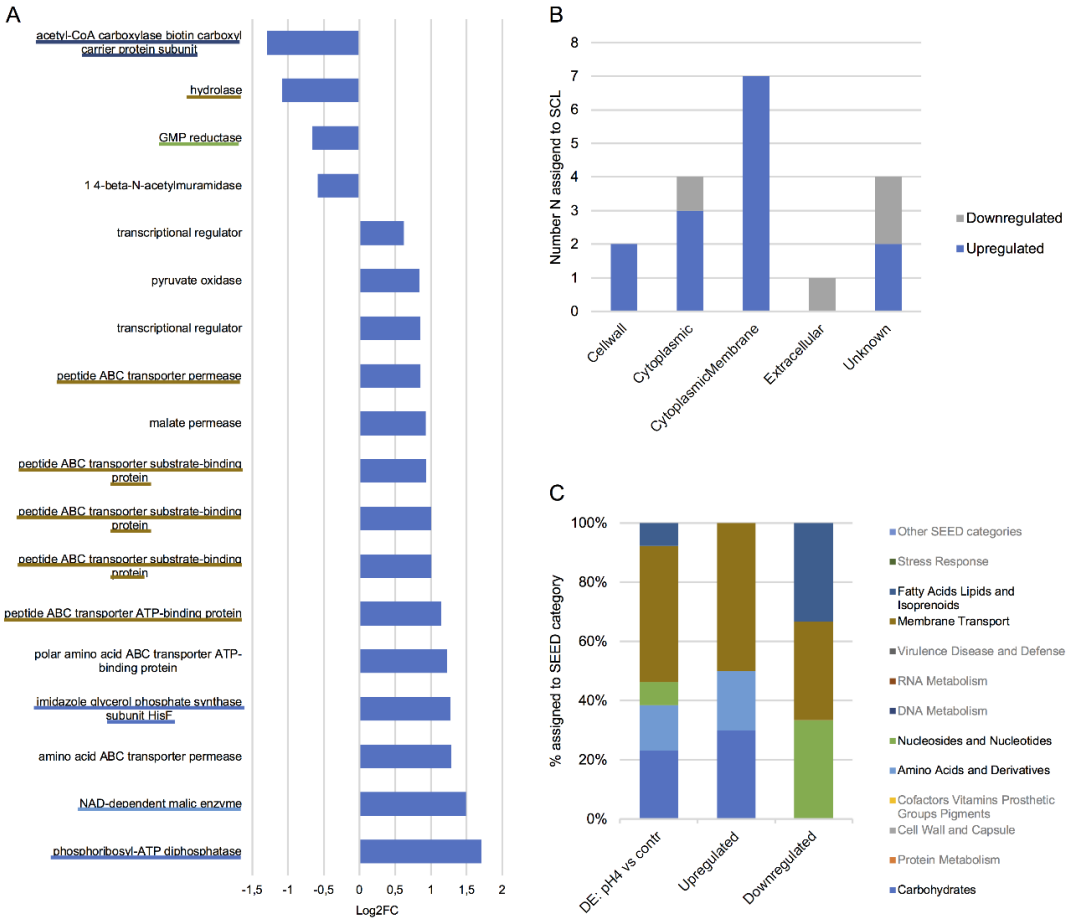


Figure S 31: Differential protein expression of *Lb. paracasei* subsp. *paracasei* F19 upon acid stress with respect to control condition (DE: pH4 vs contr). (A) Differentially expressed (DE) proteins with respective Log2FoldChange (Log2FC) are illustrated. Based on SEED subsystem analysis, assigned SEED category of respective protein is emphasized using a colored underscore (where applicable), whereby color legend of SEED category can be obtained from C. (B) Subcellular localization prediction of DE proteins. (C) Functional analysis of DE proteins based on SEED subsystem analysis. Percentage (%) of assigned proteins are shown with respect to functional SEED category of total DE proteins (DE: pH4 vs contr), up regulated and down regulated proteins.

Table S 6: Differential protein expression of *Lb. paracasei* subsp. *paracasei* F19 upon acid stress with respect to control condition. Listed are DE proteins with respect to NCBI-annotation, Log2FoldChange (Log2FC), log10 p-value (log10.p), SEED category, subcellular localization prediction (SCL) and KO/EC number.

| protein_ID | NCBI-annotation | Log2FC | log10.p | SEED category | SCL | KO number | EC number |
|---|---|---|---|---|---|---|---|
| BBD24_07445 | phosphoribosyl-ATP diphosphatase | 1.71 | 1.43 | Amino Acids and Derivatives | Cytoplasmic | K01523 | EC 3.6.1.31 |
| BBD24_04015 | NAD-dependent malic enzyme | 1.49 | 3.07 | Carbohydrates | Unknown | K00027 | EC 1.-.-.- |
| BBD24_06625 | amino acid ABC transporter permease | 1.28 | 5.73 | | CytoplasmicMembrane | K02029 | |
| BBD24_07455 | imidazole glycerol phosphate synthase subunit HisF | 1.28 | 4.10 | Amino Acids and Derivatives | Cytoplasmic | K02500 | EC 4.1.3.- |
| BBD24_06630 | polar amino acid ABC transporter ATP-binding protein | 1.23 | 7.40 | | CytoplasmicMembrane | K02028 | |
| BBD24_10265 | peptide ABC transporter ATP-binding protein | 1.15 | 4.03 | Membrane Transport | CytoplasmicMembrane | K15583 | |
| BBD24_10280 | peptide ABC transporter substrate-binding protein | 1.01 | 4.20 | Membrane Transport | Cellwall | K15580 | |
| BBD24_00895 | peptide ABC transporter substrate-binding protein | 1.00 | 2.54 | Membrane Transport | Cellwall | K15580 | |

| | | | | | | | |
|---|---|---|---|---|---|---|---|
| BBD24_10260 | peptide ABC transporter substrate-binding protein | 0.94 | 1.98 | Membrane Transport | CytoplasmicMembrane | K10823 | |
| BBD24_04020 | malate permease | 0.92 | 1.46 | Carbohydrates | CytoplasmicMembrane | K07088 | |
| BBD24_10270 | peptide ABC transporter permease | 0.86 | 2.17 | Membrane Transport | CytoplasmicMembrane | K15582 | |
| BBD24_09600 | transcriptional regulator | 0.84 | 4.55 | | Unknown | K09017 | |
| BBD24_02545 | pyruvate oxidase | 0.84 | 3.29 | Carbohydrates | CytoplasmicMembrane | K00158 | EC 1.2.2.2 |
| BBD24_00645 | transcriptional regulator | 0.62 | 1.47 | | Cytoplasmic | | |
| BBD24_09905 | 1 4-beta-N-acetylmuramidase | -0.58 | 1.31 | | Extracellular | | |
| BBD24_04815 | GMP reductase | -0.66 | 1.32 | Nucleosides and Nucleotides | Cytoplasmic | K00364 | EC 1.7.1.7 |
| BBD24_11030 | hydrolase | -1.08 | 2.07 | Membrane Transport | Unknown | | |
| BBD24_09540 | acetyl-CoA carboxylase biotin carboxyl carrier protein subunit | -1.29 | 1.61 | Fatty Acids Lipids and Isoprenoids | Unknown | | |

### 11.1.2.2 Alkaline stress

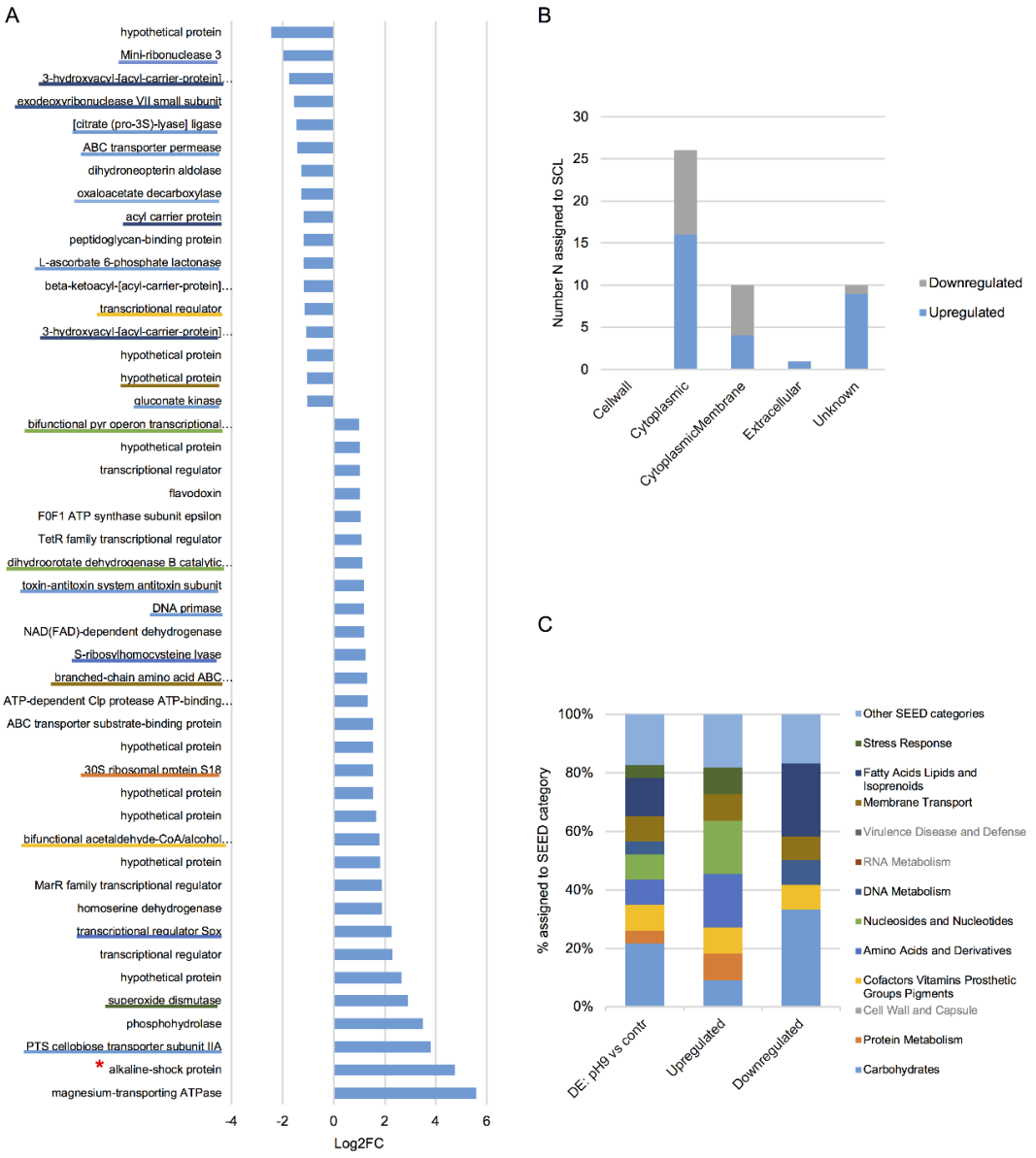


Figure S 32: Differential protein expression of *Lb. paracasei* subsp. *paracasei* F19 upon alkaline stress in reference to control condition (DE: pH9 vs contr). (A) Differentially expressed (DE) proteins with respective Log2FoldChange (Log2FC) are illustrated. Based on SEED subsystem analysis, assigned SEED category of respective protein is emphasized using a colored underscore (where applicable), whereby color legend of SEED category can be obtained from C. (B) Subcellular localization prediction of DE proteins. (C) Functional analysis of DE proteins based on SEED subsystem analysis. Percentage (%) of assigned proteins are shown with respect to functional SEED category of total DE proteins (DE: pH9 vs contr), up regulated and down regulated proteins.

Table S 7: Differential protein expression of *Lb. paracasei* subsp. *paracasei* F19 upon alkaline stress in reference to control condition. Listed are DE proteins with respect to NCBI-annotation, Log2FoldChange (Log2FC), log10 p-value (log10.p), SEED category, subcellular localization prediction (SCL) and KO/EC number.

| protein_ID | NCBI-annotation | Log2FC | log10.p | SEED category | SCL | KO number | EC number |
|---|---|---|---|---|---|---|---|
| BBD24_03845 | magnesium-transporting ATPase | 5.57 | 4.78 | | CytoplasmicMembrane | | |
| BBD24_01020 | alkaline-shock protein | 4.76 | 5.03 | | Cytoplasmic | | |
| BBD24_10320 | PTS cellobiose transporter subunit IIA | 3.81 | 11.34 | Carbohydrates | Cytoplasmic | K02759 | EC 2.7.1.69 |
| BBD24_04740 | phosphohydrolase | 3.50 | 3.27 | | Unknown | | |
| BBD24_09465 | superoxide dismutase | 2.91 | 4.54 | Stress Response | Extracellular | K04564 | EC 1.15.1.1 |
| BBD24_00715 | hypothetical protein | 2.66 | 7.78 | | Unknown | | |
| BBD24_03135 | transcriptional regulator | 2.30 | 7.75 | | Unknown | | |
| BBD24_08930 | transcriptional regulator Spx | 2.27 | 5.25 | | CytoplasmicMembrane | K16509 | |
| BBD24_10685 | homoserine dehydrogenase | 1.91 | 8.54 | Amino Acids and Derivatives | Cytoplasmic | K00003 | EC 1.1.1.3 |
| BBD24_12960 | MarR family transcriptional regulator | 1.88 | 3.86 | | Unknown | | |
| BBD24_08495 | hypothetical protein | 1.81 | 2.76 | | Unknown | | |

| | | | | | | | |
|---|---|---|---|---|---|---|---|
| BBD24_04170 | bifunctional acetaldehyde-CoA/alcohol dehydrogenase | 1.78 | 6.71 | Cofactors Vitamins Prosthetic Groups Pigments | Cytoplasmic | K04072 | EC 1.1.1.1 |
| BBD24_15055 | hypothetical protein | 1.65 | 2.10 | | CytoplasmicMembrane | | |
| BBD24_11450 | hypothetical protein | 1.55 | 2.97 | | Unknown | | |
| BBD24_00060 | 30S ribosomal protein S18 | 1.55 | 3.43 | Protein Metabolism | Cytoplasmic | K02963 | |
| BBD24_00915 | hypothetical protein | 1.55 | 7.82 | | Cytoplasmic | | |
| BBD24_03820 | ABC transporter substrate-binding protein | 1.54 | 3.79 | | Unknown | K01989 | |
| BBD24_10105 | ATP-dependent Clp protease ATP-binding subunit | 1.33 | 2.46 | | Cytoplasmic | K04086 | |
| BBD24_01340 | branched-chain amino acid ABC transporter substrate-binding protein | 1.32 | 2.84 | Membrane Transport | Unknown | K01999 | |
| BBD24_04135 | S-ribosylhomocysteine lyase | 1.25 | 1.65 | Amino Acids and Derivatives | Cytoplasmic | K07173 | EC 4.4.1.21 |
| BBD24_02360 | NAD(FAD)-dependent dehydrogenase | 1.20 | 3.71 | | Cytoplasmic | K05910 | |
| BBD24_07820 | DNA primase | 1.19 | 1.72 | Cell Division and Cell Cycle | Cytoplasmic | K02316 | EC 2.7.7.- |
| BBD24_03210 | toxin-antitoxin system antitoxin subunit | 1.17 | 12.44 | Regulation and Cell signaling | Cytoplasmic | | |
| BBD24_07565 | dihydroorotate dehydrogenase B catalytic subunit | 1.13 | 1.40 | Nucleosides and Nucleotides | Cytoplasmic | K17828 | EC 1.3.3.1 |

| | | | | | | | |
|---|---|---|---|---|---|---|---|
| BBD24_06025 | TetR family transcriptional regulator | 1.08 | 1.76 | | Unknown | | |
| BBD24_06125 | F0F1 ATP synthase subunit epsilon | 1.06 | 2.40 | | Cytoplasmic | K02114 | |
| BBD24_04030 | flavodoxin | 1.03 | 2.43 | | CytoplasmicMembrane | | |
| BBD24_00625 | transcriptional regulator | 1.03 | 4.88 | | Cytoplasmic | | |
| BBD24_03750 | hypothetical protein | 1.02 | 2.37 | | Cytoplasmic | | |
| BBD24_07595 | bifunctional pyr operon transcriptional regulator/uracil phosphoribosyltransferase | 1.00 | 1.78 | Nucleosides and Nucleotides | Cytoplasmic | K02825 | EC 2.4.2.9 |
| BBD24_01210 | gluconate kinase | -1.04 | 2.58 | Carbohydrates | Cytoplasmic | K00851 | EC 2.7.1.12 |
| BBD24_10235 | hypothetical protein | -1.05 | 1.80 | Membrane Transport | CytoplasmicMembrane | | |
| BBD24_01275 | hypothetical protein | -1.05 | 1.53 | | CytoplasmicMembrane | | |
| BBD24_10500 | 3-hydroxyacyl-[acyl-carrier-protein] dehydratase FabZ | -1.09 | 2.77 | Fatty Acids Lipids and Isoprenoids | Cytoplasmic | K02372 | EC 4.2.1.59 |
| BBD24_05405 | transcriptional regulator | -1.14 | 2.39 | Cofactors Vitamins Prosthetic Groups Pigments | Cytoplasmic | | |
| BBD24_10510 | beta-ketoacyl-[acyl-carrier-protein] synthase II | -1.15 | 1.66 | | CytoplasmicMembrane | K09458 | |
| BBD24_13535 | L-ascorbate 6-phosphate lactonase | -1.19 | 1.84 | Carbohydrates | Cytoplasmic | K03476 | EC 3.1.1.- |

| | | | | | | | |
|---|---|---|---|---|---|---|---|
| BBD24_10865 | peptidoglycan-binding protein | -1.19 | 4.26 | | Unknown | | |
| BBD24_10530 | acyl carrier protein | -1.19 | 1.60 | Fatty Acids Lipids and Isoprenoids | Cytoplasmic | K02078 | |
| BBD24_09500 | oxaloacetate decarboxylase | -1.27 | 2.93 | Respiration | Cytoplasmic | K01571 | EC 4.1.1.3 |
| BBD24_02500 | dihydroneopterin aldolase | -1.28 | 3.36 | | Cytoplasmic | | |
| BBD24_05245 | ABC transporter permease | -1.43 | 3.52 | Carbohydrates | CytoplasmicMembrane | K02026 | |
| BBD24_09525 | [citrate (pro-3S)-lyase] ligase | -1.47 | 2.29 | Carbohydrates | CytoplasmicMembrane | K01910 | EC 6.2.1.22 |
| BBD24_08440 | exodeoxyribonuclease VII small subunit | -1.55 | 1.79 | DNA Metabolism | Cytoplasmic | K03602 | EC 3.1.11.6 |
| BBD24_10545 | 3-hydroxyacyl-[acyl-carrier-protein] dehydratase FabZ | -1.76 | 4.41 | Fatty Acids Lipids and Isoprenoids | Cytoplasmic | K02372 | EC 4.2.1.59 |
| BBD24_11435 | Mini-ribonuclease 3 | -1.97 | 1.69 | Miscellaneous | Cytoplasmic | K11145 | |
| BBD24_06095 | hypothetical protein | -2.47 | 2.18 | | CytoplasmicMembrane | K02110 | |

### 11.1.2.3 Starvation stress – Lack of glucose

There were no proteins DE upon starvation stress.

### 11.1.2.4 Cold stress

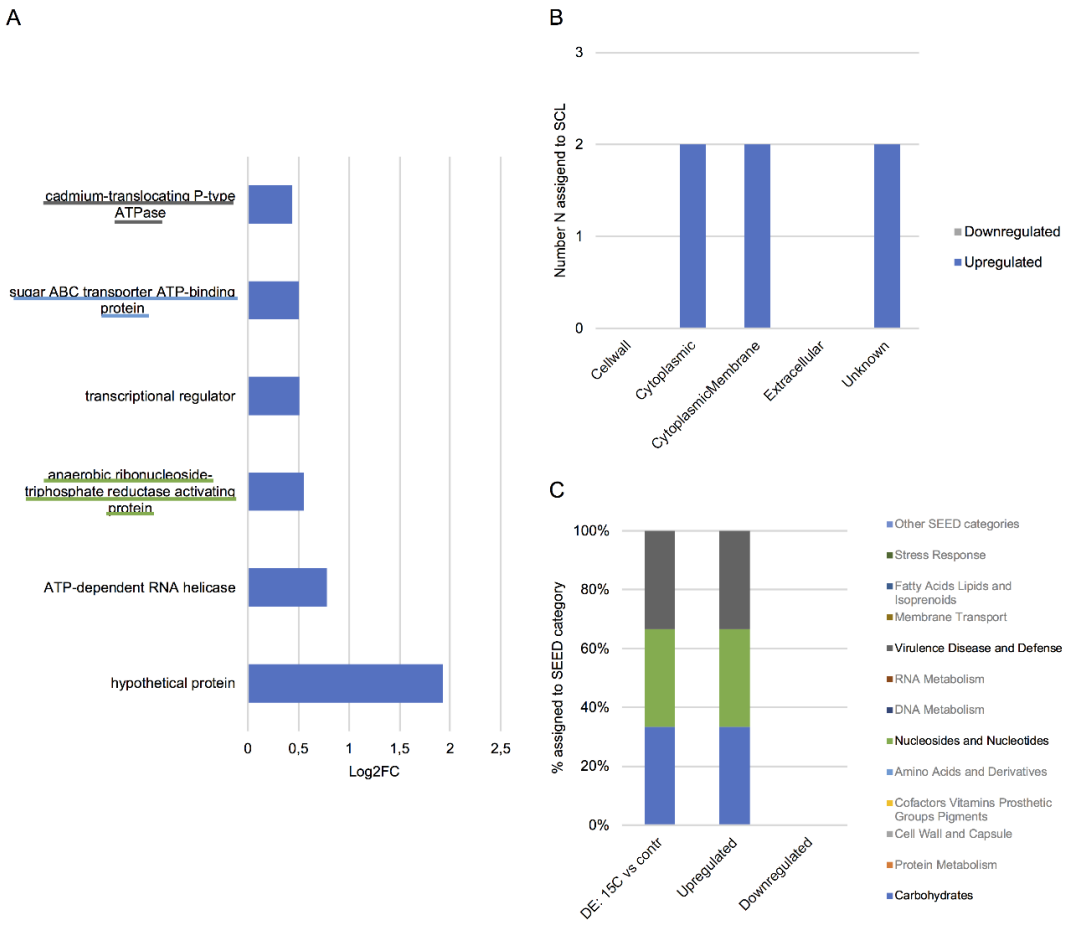


Figure S 33: Differential protein expression of *Lb. paracasei* subsp. *paracasei* F19 upon cold stress with respect to control condition (DE: 15C vs contr). (A) Differentially expressed (DE) proteins with respective Log2FoldChange (Log2FC) are illustrated. Based on SEED subsystem analysis, assigned SEED category of respective protein is emphasized using a colored underscore (where applicable), whereby color legend of SEED category can be obtained from C. (B) Subcellular localization prediction of DE proteins. (C) Functional analysis of DE proteins based on SEED subsystem analysis. Percentage (%) of assigned proteins are shown with respect to functional SEED category of total DE proteins (DE: 15C vs contr), up regulated and down regulated proteins.

Table S 8: Differential protein expression of *Lb. paracasei* subsp. *paracasei* F19 upon cold stress with respect to control condition. Listed are DE proteins with respect to NCBI-annotation, Log2FoldChange (Log2FC), log10 p-value (log10.p), SEED category, subcellular localization prediction (SCL) and KO/EC number

| protein_ID | NCBI-annotation | Log2FC | log10.p | SEED category | SCL | KO number | EC number |
|---|---|---|---|---|---|---|---|
| BBD24_08495 | hypothetical protein | 1.93 | 3.11 | | Unknown | | |
| BBD24_12595 | ATP-dependent RNA helicase | 0.78 | 2.61 | | Cytoplasmic | K05592 | |
| BBD24_08965 | anaerobic ribonucleoside-triphosphate reductase activating protein | 0.55 | 2.85 | Nucleosides and Nucleotides | Cytoplasmic | K04068 | EC 1.97.1.4 |
| BBD24_09600 | transcriptional regulator | 0.51 | 1.67 | | Unknown | K09017 | |
| BBD24_05200 | sugar ABC transporter ATP-binding protein | 0.51 | 1.64 | Carbohydrates | CytoplasmicMembrane | K10112 | |
| BBD24_13985 | cadmium-translocating P-type ATPase | 0.44 | 1.41 | Virulence Disease and Defense | CytoplasmicMembrane | | EC 3.6.3.4 |

### 11.1.2.5 Sodium chloride stress

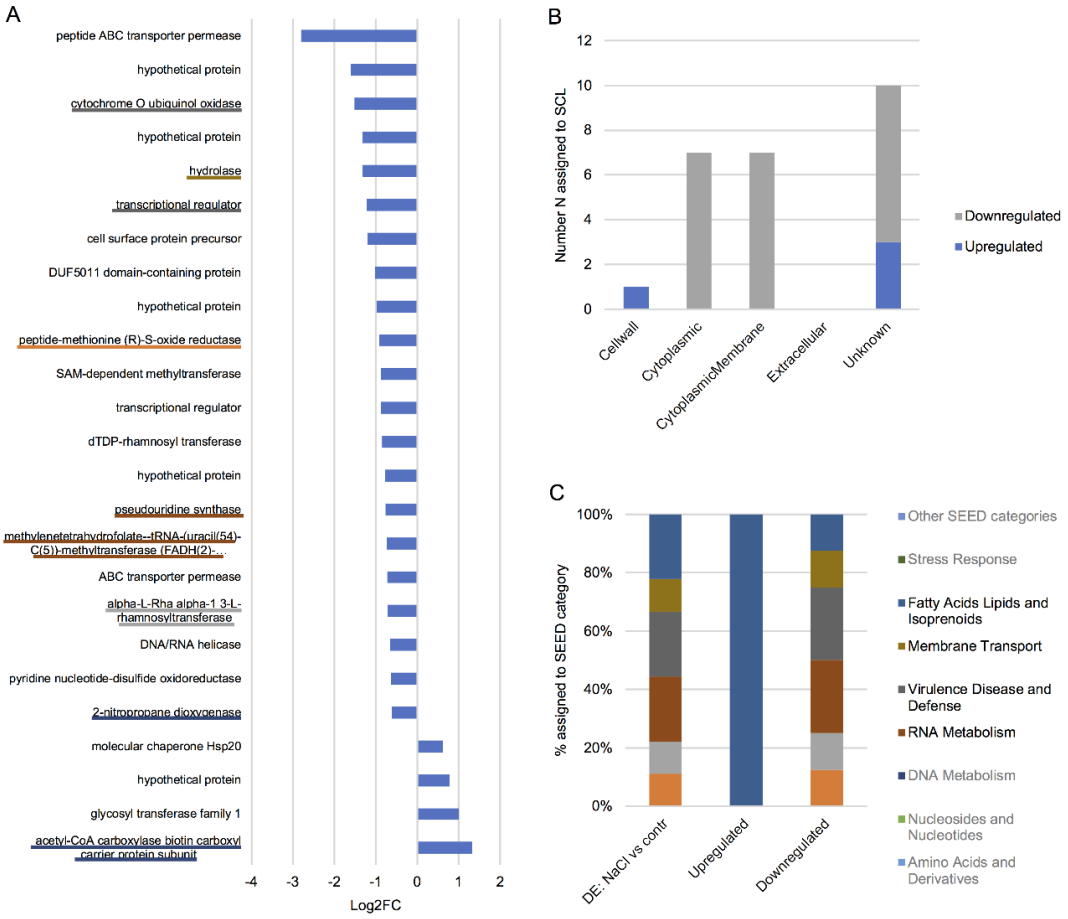


Figure S 34: Differential protein expression of *Lb. paracasei* subsp. *paracasei* F19 upon sodium chloride stress with respect to control condition (DE: NaCl vs contr). (A) Differentially expressed (DE) proteins with respective Log2FoldChange (Log2FC) are illustrated. Based on SEED subsystem analysis, assigned SEED category of respective protein is emphasized using a colored underscore (where applicable), whereby color legend of SEED category can be obtained from C. (B) Subcellular localization prediction of DE proteins. (C) Functional analysis of DE proteins based on SEED subsystem analysis. Percentage (%) of assigned proteins are shown with respect to functional SEED category of total DE proteins (DE: NaCl vs contr), up regulated and down regulated proteins.

Table S 9: Differential protein expression of *Lb. paracasei* subsp. *paracasei* F19 upon sodium chloride stress with respect to control condition. Listed are DE proteins with respect to NCBI-annotation, Log2FoldChange (Log2FC), log10 p-value (log10.p), SEED category, subcellular localization prediction (SCL) and KO/EC number.

| protein_ID | NCBI-annotation | Log2FC | log10.p | SEED category | SCL | KO number | EC number |
|---|---|---|---|---|---|---|---|
| BBD24_09540 | acetyl-CoA carboxylase biotin carboxyl carrier protein subunit | 1.33 | 1.72 | Fatty Acids Lipids and Isoprenoids | Unknown | | |
| BBD24_14275 | glycosyl transferase family 1 | 1.00 | 2.85 | | Unknown | | |
| BBD24_12740 | hypothetical protein | 0.77 | 3.16 | | Unknown | | |
| BBD24_13995 | molecular chaperone Hsp20 | 0.62 | 1.46 | | Cellwall | K13993 | |
| BBD24_10525 | 2-nitropropane dioxygenase | -0.62 | 2.00 | Fatty Acids Lipids and Isoprenoids | Cytoplasmic | K02371 | EC 1.3.1.9 |
| BBD24_01415 | pyridine nucleotide-disulfide oxidoreductase | -0.65 | 1.72 | | Cytoplasmic | K17869 | |
| BBD24_07280 | DNA/RNA helicase | -0.66 | 1.90 | | Unknown | | |
| BBD24_10185 | alpha-L-Rha alpha-1 3-L-rhamnosyltransferase | -0.71 | 1.66 | Cell Wall and Capsule | Cytoplasmic | | EC 2.4.1.- |
| BBD24_09830 | ABC transporter permease | -0.72 | 5.21 | | CytoplasmicMembrane | K02004 | |

| | | | | | | | |
|---|---|---|---|---|---|---|---|
| BBD24_07330 | methylenetetrahydrofolate--tRNA-(uracil(54)- C(5))-methyltransferase (FADH(2)-oxidizing) TrmFO | -0.74 | 3.34 | RNA Metabolism | Cytoplasmic | K04094 | |
| BBD24_07145 | pseudouridine synthase | -0.76 | 4.54 | RNA Metabolism | Cytoplasmic | K06178 | EC 4.2.1.70 |
| BBD24_05525 | hypothetical protein | -0.79 | 1.78 | | CytoplasmicMembrane | | |
| BBD24_10190 | dTDP-rhamnosyl transferase | -0.85 | 4.77 | | CytoplasmicMembrane | | |
| BBD24_06235 | transcriptional regulator | -0.87 | 1.54 | | CytoplasmicMembrane | | |
| BBD24_07790 | SAM-dependent methyltransferase | -0.88 | 3.17 | | Unknown | | |
| BBD24_07900 | peptide-methionine (R)-S-oxide reductase | -0.92 | 3.97 | Protein Metabolism | Unknown | K07305 | EC 1.8.4.12 |
| BBD24_00205 | hypothetical protein | -0.97 | 2.68 | | Cytoplasmic | | |
| BBD24_02975 | DUF5011 domain-containing protein | -1.01 | 1.65 | | Unknown | | |
| BBD24_05795 | cell surface protein precursor | -1.19 | 4.22 | | Unknown | | |
| BBD24_10995 | transcriptional regulator | -1.22 | 2.00 | Virulence Disease and Defense | Cytoplasmic | | |
| BBD24_11030 | hydrolase | -1.32 | 3.11 | Membrane Transport | Unknown | | |

| | | | | | | |
|---|---|---|---|---|---|---|
| BBD24_03220 | hypothetical protein | -1.32 | 6.73 | Unknown | | |
| BBD24_04405 | cytochrome O ubiquinol oxidase | -1.52 | 3.63 | Virulence Disease and Defense | CytoplasmicMembrane | K03975 |
| BBD24_09375 | hypothetical protein | -1.60 | 2.10 | | CytoplasmicMembrane | |
| BBD24_08945 | peptide ABC transporter permease | -2.80 | 1.57 | | CytoplasmicMembrane | K02004 |

### 11.1.2.6 Lactose stress

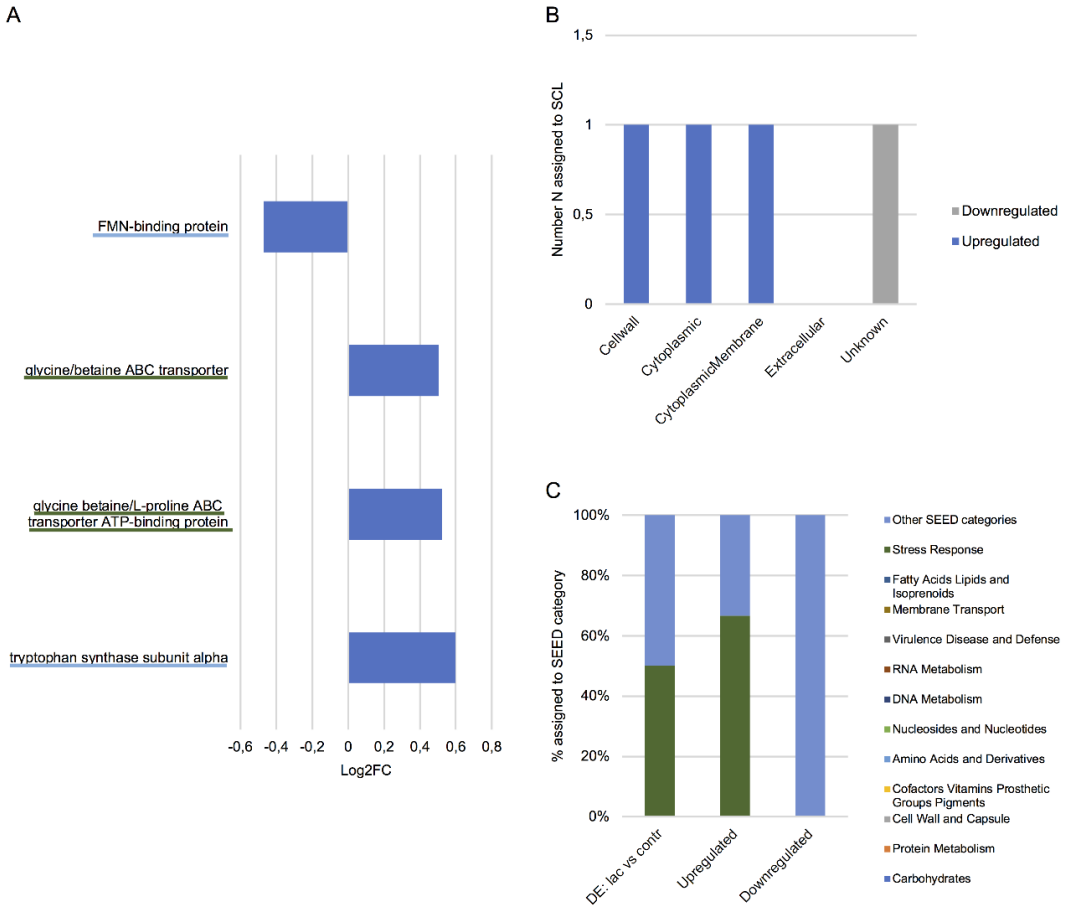


Figure S 35: Differential protein expression of *Lb. paracasei* subsp. *paracasei* F19 upon lactose stress with respect to control condition (DE: lac vs contr). (A) Differentially expressed (DE) proteins with respective Log2FoldChange (Log2FC) are illustrated. Based on SEED subsystem analysis, assigned SEED category of respective protein is emphasized using a colored underscore (where applicable), whereby color legend of SEED category can be obtained from C. (B) Subcellular localization prediction of DE proteins. (C) Functional analysis of DE proteins based on SEED subsystem analysis. Percentage (%) of assigned proteins are shown with respect to functional SEED category of total DE proteins (DE: lac vs contr), up regulated and down regulated proteins.

Table S 10: Differential protein expression of *Lb. paracasei* subsp. *paracasei* F19 upon lactose stress with respect to control condition. Listed are DE proteins with respect to NCBI-annotation, Log2FoldChange (Log2FC), log10 p-value (log10.p), SEED category, subcellular localization prediction (SCL) and KO/EC number.

| protein_ID | NCBI-annotation | Log2FC | log10.p | SEED category | SCL | KO number | EC number |
|---|---|---|---|---|---|---|---|
| BBD24_00380 | tryptophan synthase subunit alpha | 0.60 | 2.17 | Secondary Metabolism | Cytoplasmic | K01695 | EC 4.2.1.20 |
| BBD24_10645 | glycine betaine/L-proline ABC transporter ATP-binding protein | 0.52 | 1.69 | Stress Response | CytoplasmicMembrane | K02000 | EC 3.6.3.32 |
| BBD24_10655 | glycine/betaine ABC transporter | 0.51 | 1.81 | Stress Response | Cellwall | K02002 | |
| BBD24_11380 | FMN-binding protein | -0.47 | 2.38 | Regulation and Cell signaling | Unknown | | |

### 11.1.2.7 Sucrose stress

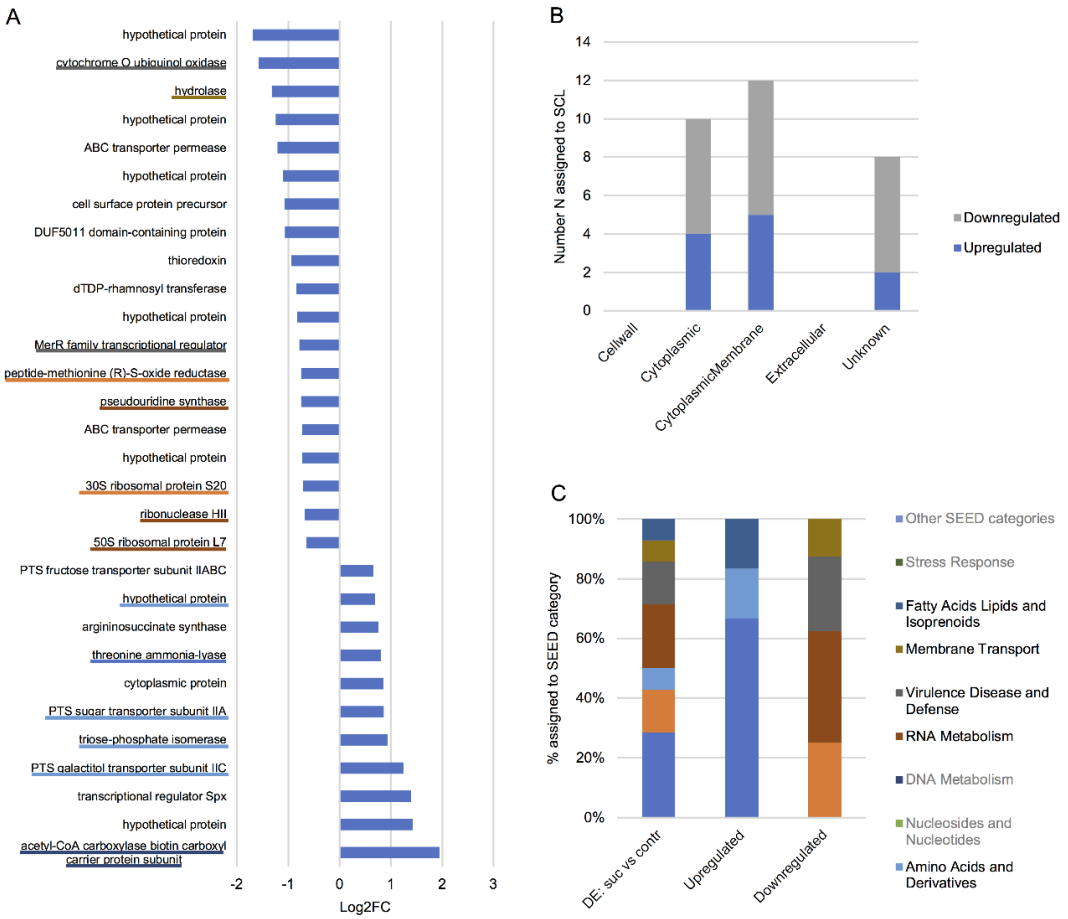


Figure S 36: Differential protein expression of *Lb. paracasei* subsp. *paracasei* F19 upon sucrose stress with respect to control condition (DE: suc vs contr). (A) Differentially expressed (DE) proteins with respective Log2FoldChange (Log2FC) are illustrated. Based on SEED subsystem analysis, assigned SEED category of respective protein is emphasized using a colored underscore (where applicable), whereby color legend of SEED category can be obtained from C. (B) Subcellular localization prediction of DE proteins. (C) Functional analysis of DE proteins based on SEED subsystem analysis. Percentage (%) of assigned proteins are shown with respect to functional SEED category of total DE proteins (DE: suc vs contr), up regulated and down regulated proteins.

Table S 11: Differential protein expression of *Lb. paracasei* subsp. *paracasei* F19 upon sucrose stress with respect to control condition. Listed are DE proteins with respect to NCBI-annotation, Log2FoldChange (Log2FC), log10 p-value (log10.p), SEED category, subcellular localization prediction (SCL) and KO/EC number.

| protein_ID | NCBI-annotation | Log2FC | log10.p | SEED category | SCL | KO number | EC number |
|---|---|---|---|---|---|---|---|
| BBD24_09540 | acetyl-CoA carboxylase biotin carboxyl carrier protein subunit | 1.95 | 3.77 | Fatty Acids Lipids and Isoprenoids | Unknown | | |
| BBD24_15055 | hypothetical protein | 1.42 | 1.46 | | CytoplasmicMembrane | | |
| BBD24_08930 | transcriptional regulator Spx | 1.39 | 2.19 | | CytoplasmicMembrane | K16509 | |
| BBD24_13335 | PTS galactitol transporter subunit IIC | 1.24 | 1.35 | Carbohydrates | CytoplasmicMembrane | K02775 | EC 2.7.1.69 |
| BBD24_13320 | triose-phosphate isomerase | 0.94 | 1.75 | Carbohydrates | Cytoplasmic | K01803 | EC 5.3.1.1 |
| BBD24_13340 | PTS sugar transporter subunit IIA | 0.87 | 1.75 | Carbohydrates | Cytoplasmic | K02773 | EC 2.7.1.69 |
| BBD24_13440 | cytoplasmic protein | 0.85 | 1.96 | | Unknown | | |
| BBD24_10800 | threonine ammonia-lyase | 0.80 | 2.19 | Amino Acids and Derivatives | Cytoplasmic | K01754 | EC 4.3.1.19 |
| BBD24_14050 | argininosuccinate synthase | 0.76 | 4.02 | | Cytoplasmic | K01940 | |

| | | | | | | | |
|---|---|---|---|---|---|---|---|
| BBD24_10310 | hypothetical protein | 0.69 | 3.66 | Carbohydrates | CytoplasmicMembrane | K18928 | |
| BBD24_13040 | PTS fructose transporter subunit IIABC | 0.66 | 1.68 | | CytoplasmicMembrane | | |
| BBD24_08130 | 50S ribosomal protein L7 | -0.64 | 4.89 | RNA Metabolism | Cytoplasmic | | |
| BBD24_07315 | ribonuclease HII | -0.69 | 1.93 | RNA Metabolism | Cytoplasmic | K03470 | EC 3.1.26.4 |
| BBD24_06930 | 30S ribosomal protein S20 | -0.72 | 1.73 | Protein Metabolism | Cytoplasmic | K02968 | |
| BBD24_05525 | hypothetical protein | -0.72 | 1.46 | | CytoplasmicMembrane | | |
| BBD24_09830 | ABC transporter permease | -0.73 | 5.33 | | CytoplasmicMembrane | K02004 | |
| BBD24_07145 | pseudouridine synthase | -0.75 | 4.41 | RNA Metabolism | Cytoplasmic | K06178 | EC 4.2.1.70 |
| BBD24_07900 | peptide-methionine (R)-S-oxide reductase | -0.75 | 2.76 | Protein Metabolism | Unknown | K07305 | EC 1.8.4.12 |
| BBD24_02585 | MerR family transcriptional regulator | -0.79 | 2.62 | Virulence Disease and Defense | Unknown | | |
| BBD24_04120 | hypothetical protein | -0.83 | 3.61 | | CytoplasmicMembrane | | |

| | | | | | | |
|---|---|---|---|---|---|---|
| BBD24_10190 | dTDP-rhamnosyl transferase | -0.84 | 4.69 | | CytoplasmicMembrane | |
| BBD24_04250 | thioredoxin | -0.94 | 1.38 | | Cytoplasmic | K03671 |
| BBD24_02975 | DUF5011 domain-containing protein | -1.07 | 1.88 | | Unknown | |
| BBD24_05795 | cell surface protein precursor | -1.08 | 3.55 | | Unknown | |
| BBD24_03220 | hypothetical protein | -1.09 | 5.22 | | Unknown | |
| BBD24_02350 | ABC transporter permease | -1.21 | 1.98 | | CytoplasmicMembrane | K02004 |
| BBD24_00205 | hypothetical protein | -1.24 | 4.17 | | Cytoplasmic | |
| BBD24_11030 | hydrolase | -1.32 | 3.12 | Membrane Transport | Unknown | |
| BBD24_04405 | cytochrome O ubiquinol oxidase | -1.58 | 3.88 | Virulence Disease and Defense | CytoplasmicMembrane | K03975 |
| BBD24_09375 | hypothetical protein | -1.69 | 2.38 | | CytoplasmicMembrane | |

### 11.1.2.8 Oxidative stress

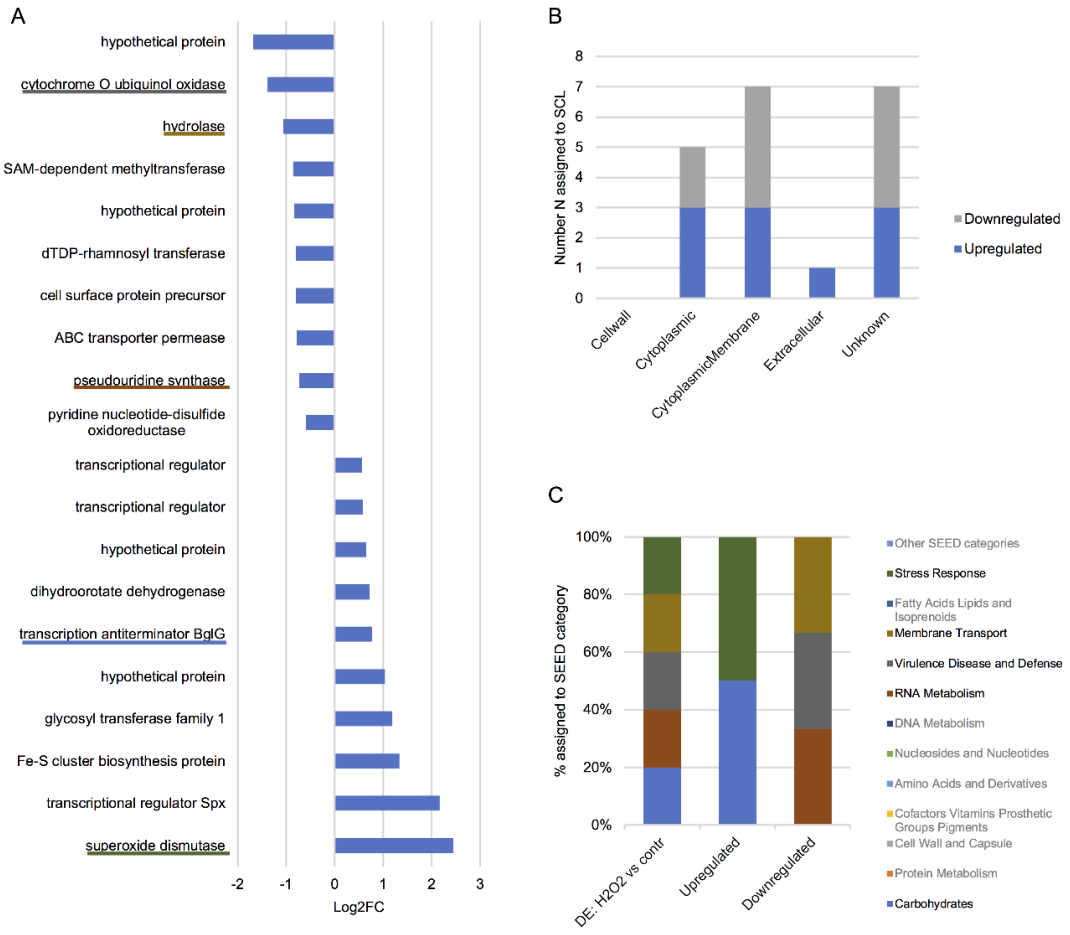


Figure S 37: Differential protein expression of *Lb. paracasei* subsp. *paracasei* F19 upon oxidative stress with respect to control condition (DE: H2O2 vs contr). (A) Differentially expressed (DE) proteins with respective Log2FoldChange (Log2FC) are illustrated. Based on SEED subsystem analysis, assigned SEED category of respective protein is emphasized using a colored underscore (where applicable), whereby color legend of SEED category can be obtained from C. (B) Subcellular localization prediction of DE proteins. (C) Functional analysis of DE proteins based on SEED subsystem analysis. Percentage (%) of assigned proteins are shown with respect to functional SEED category of total DE proteins (DE: H2O2 vs contr), up regulated and down regulated proteins.

Table S 12: Differential protein expression of *Lb. paracasei* subsp. *paracasei* F19 upon oxidative stress with respect to control condition. Listed are DE proteins with respect to NCBI-annotation, Log2FoldChange (Log2FC), log10 p-value (log10.p), SEED category, subcellular localization prediction (SCL) and KO/EC number.

| protein_ID | NCBI-annotation | Log2FC | log10.p | SEED category | SCL | KO number | EC number |
|---|---|---|---|---|---|---|---|
| BBD24_09465 | superoxide dismutase | 2.45 | 3.39 | Stress Response | Extracellular | EC 1.15.1.1 | K04564 |
| BBD24_08930 | transcriptional regulator Spx | 2.16 | 4.90 | | CytoplasmicMembrane | | K16509 |
| BBD24_09710 | Fe-S cluster biosynthesis protein | 1.34 | 2.92 | | Unknown | | |
| BBD24_14275 | glycosyl transferase family 1 | 1.19 | 3.90 | | Unknown | | |
| BBD24_14000 | hypothetical protein | 1.03 | 2.16 | | Unknown | | |
| BBD24_10845 | transcription antiterminator BglG | 0.78 | 1.69 | Carbohydrates | CytoplasmicMembrane | | K03488 |
| BBD24_04760 | dihydroorotate dehydrogenase | 0.71 | 1.80 | | Cytoplasmic | | |
| BBD24_00915 | hypothetical protein | 0.65 | 1.84 | | Cytoplasmic | | |
| BBD24_07290 | transcriptional regulator | 0.57 | 1.36 | | Cytoplasmic | | |

| | | | | | | | |
|---|---|---|---|---|---|---|---|
| BBD24_07640 | transcriptional regulator | 0.56 | 1.48 | | CytoplasmicMembrane | | |
| BBD24_01415 | pyridine nucleotide-disulfide oxidoreductase | -0.60 | 1.41 | | Cytoplasmic | | K17869 |
| BBD24_07145 | pseudouridine synthase | -0.73 | 4.23 | RNA Metabolism | Cytoplasmic | EC 4.2.1.70 | K06178 |
| BBD24_09830 | ABC transporter permease | -0.79 | 5.91 | | CytoplasmicMembrane | | K02004 |
| BBD24_05795 | cell surface protein precursor | -0.80 | 1.93 | | Unknown | | |
| BBD24_10190 | dTDP-rhamnosyl transferase | -0.80 | 4.38 | | CytoplasmicMembrane | | |
| BBD24_03220 | hypothetical protein | -0.84 | 3.38 | | Unknown | | |
| BBD24_07790 | SAM-dependent methyltransferase | -0.86 | 3.02 | | Unknown | | |
| BBD24_11030 | hydrolase | -1.06 | 1.99 | Membrane Transport | Unknown | | |
| BBD24_04405 | cytochrome O ubiquinol oxidase | -1.40 | 3.12 | Virulence Disease and Defense | CytoplasmicMembrane | | K03975 |
| BBD24_09375 | hypothetical protein | -1.67 | 2.34 | | CytoplasmicMembrane | | |

### 11.1.2.9 High hydrostatic pressure stress

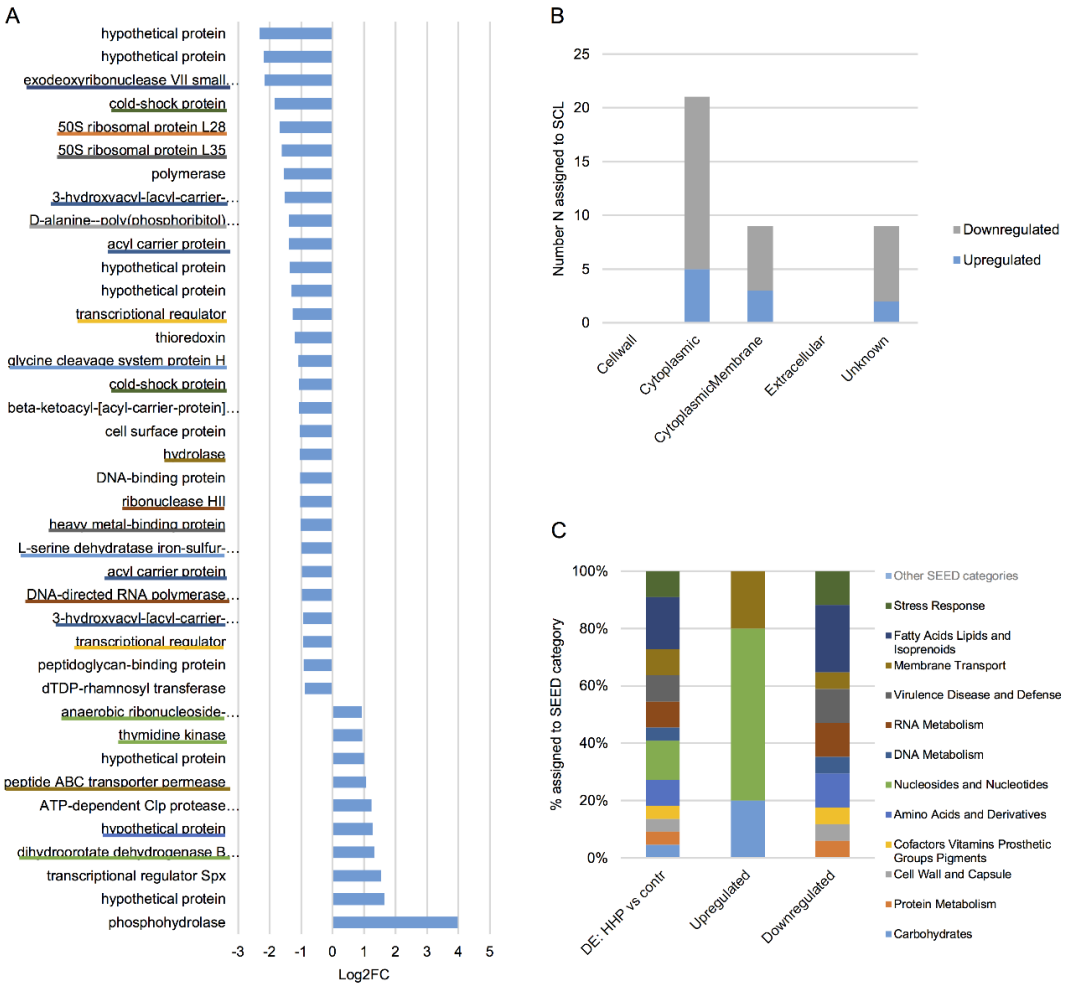


Figure S 38: Differential protein expression of *Lb. paracasei* subsp. *paracasei* F19 upon high hydrostatic pressure stress in reference to control condition (DE: HHP vs contr). (A) Differentially expressed (DE) proteins with respective Log2FoldChange (Log2FC) are illustrated. Based on SEED subsystem analysis, assigned SEED category of respective protein is emphasized using a colored underscore (where applicable), whereby color legend of SEED category can be obtained from C. (B) Subcellular localization prediction of DE proteins. (C) Functional analysis of DE proteins based on SEED subsystem analysis. Percentage (%) of assigned proteins are shown with respect to functional SEED category of total DE proteins (DE: HHP vs contr), up regulated and down regulated proteins.

Table S 13: Differential protein expression of *Lb. paracasei* subsp. *paracasei* F19 upon high hydrostatic pressure stress in reference to control condition. Listed are DE proteins with respect to NCBI-annotation, Log2FoldChange (Log2FC), log10 p-value (log10.p), SEED category, subcellular localization prediction (SCL) and KO/EC number.

| protein_ID | NCBI-annotation | Log2FC | log10.p | SEED category | SCL | KO number | EC number |
|---|---|---|---|---|---|---|---|
| BBD24_04740 | phosphohydrolase | 3.97 | 4.08 | | Unknown | | |
| BBD24_15055 | hypothetical protein | 1.66 | 2.12 | | CytoplasmicMembrane | | |
| BBD24_08930 | transcriptional regulator Spx | 1.54 | 2.72 | | CytoplasmicMembrane | K16509 | |
| BBD24_07565 | dihydroorotate dehydrogenase B catalytic subunit | 1.33 | 2.10 | Nucleosides and Nucleotides | Cytoplasmic | K17828 | EC 1.3.3.1 |
| BBD24_02055 | hypothetical protein | 1.27 | 1.50 | Carbohydrates | Cytoplasmic | K01624 | EC 4.1.2.40 |
| BBD24_10105 | ATP-dependent Clp protease ATP-binding subunit | 1.24 | 2.14 | | Cytoplasmic | K04086 | |
| BBD24_08310 | peptide ABC transporter permease | 1.07 | 2.43 | Membrane Transport | CytoplasmicMembrane | K02033 | |
| BBD24_14000 | hypothetical protein | 0.99 | 1.97 | | Unknown | | |
| BBD24_06060 | thymidine kinase | 0.94 | 1.60 | Nucleosides and Nucleotides | Cytoplasmic | K00857 | EC 2.7.1.21 |

| | | | | | | | |
|---|---|---|---|---|---|---|---|
| BBD24_08965 | anaerobic ribonucleoside-triphosphate reductase activating protein | 0.93 | 6.49 | Nucleosides and Nucleotides | Cytoplasmic | K04068 | EC 1.97.1.4 |
| BBD24_10190 | dTDP-rhamnosyl transferase | -0.88 | 5.02 | | CytoplasmicMembrane | | |
| BBD24_10865 | peptidoglycan-binding protein | -0.91 | 2.63 | | Unknown | | |
| BBD24_07240 | transcriptional regulator | -0.95 | 2.23 | Cofactors, Vitamins, Prosthetic Groups, Pigments | Cytoplasmic | | |
| BBD24_10500 | 3-hydroxyacyl-[acyl-carrier-protein] dehydratase FabZ | -0.95 | 2.08 | Fatty Acids Lipids and Isoprenoids | Cytoplasmic | K02372 | EC 4.2.1.59 |
| BBD24_08400 | DNA-directed RNA polymerase subunit omega | -0.97 | 3.33 | RNA Metabolism | Cytoplasmic | K03060 | EC 2.7.7.6 |
| BBD24_08325 | acyl carrier protein | -0.98 | 2.13 | Fatty Acids Lipids and Isoprenoids | Cytoplasmic | K02078 | |
| BBD24_06270 | L-serine dehydratase iron-sulfur-dependent subunit beta | -1.00 | 2.93 | Amino Acids and Derivatives | Cytoplasmic | K01752 | EC 4.3.1.17 |
| BBD24_14900 | heavy metal-binding protein | -1.02 | 1.37 | Virulence Disease and Defense | Cytoplasmic | | |
| BBD24_07315 | ribonuclease HII | -1.03 | 4.22 | RNA Metabolism | Cytoplasmic | K03470 | EC 3.1.26.4 |
| BBD24_04700 | DNA-binding protein | -1.03 | 2.63 | | Unknown | K07069 | |
| BBD24_11030 | hydrolase | -1.05 | 1.94 | Membrane Transport | Unknown | | |

| | | | | | | | |
|---|---|---|---|---|---|---|---|
| BBD24_00795 | cell surface protein | -1.06 | 3.43 | | Unknown | | |
| BBD24_10510 | beta-ketoacyl-[acyl-carrier-protein] synthase II | -1.06 | 1.33 | | CytoplasmicMembrane | K09458 | |
| BBD24_05860 | cold-shock protein | -1.06 | 1.78 | Stress Response | Cytoplasmic | K03704 | |
| BBD24_06160 | glycine cleavage system protein H | -1.08 | 2.42 | Amino Acids and Derivatives | Unknown | K02437 | |
| BBD24_04250 | thioredoxin | -1.19 | 2.40 | | Cytoplasmic | K03671 | |
| BBD24_05405 | transcriptional regulator | -1.28 | 3.01 | Cofactors, Vitamins, Prosthetic Groups, Pigments | Cytoplasmic | | |
| BBD24_07255 | hypothetical protein | -1.31 | 5.21 | | Unknown | | |
| BBD24_09375 | hypothetical protein | -1.37 | 1.46 | | CytoplasmicMembrane | | |
| BBD24_10530 | acyl carrier protein | -1.39 | 2.28 | Fatty Acids Lipids and Isoprenoids | Cytoplasmic | K02078 | |
| BBD24_04270 | D-alanine--poly(phosphoribitol) ligase subunit 2 | -1.40 | 2.44 | Cell Wall and Capsule | Unknown | K14188 | EC 6.1.1.13 |
| BBD24_10545 | 3-hydroxyacyl-[acyl-carrier-protein] dehydratase FabZ | -1.52 | 3.45 | Fatty Acids Lipids and Isoprenoids | Cytoplasmic | K02372 | EC 4.2.1.59 |
| BBD24_10195 | polymerase | -1.54 | 1.36 | | CytoplasmicMembrane | | |

| | | | | | | | |
|---|---|---|---|---|---|---|---|
| BBD24_08740 | 50S ribosomal protein L35 | -1.62 | 1.95 | Virulence Disease and Defense | Cytoplasmic | K02916 | |
| BBD24_08350 | 50S ribosomal protein L28 | -1.69 | 1.78 | Protein Metabolism | Cytoplasmic | K02902 | |
| BBD24_03480 | cold-shock protein | -1.84 | 3.54 | Stress Response | Cytoplasmic | K03704 | |
| BBD24_08440 | exodeoxyribonuclease VII small subunit | -2.17 | 3.58 | DNA Metabolism | Cytoplasmic | K03602 | EC 3.1.11.6 |
| BBD24_06095 | hypothetical protein | -2.19 | 1.65 | | CytoplasmicMembrane | K02110 | |
| BBD24_09545 | hypothetical protein | -2.33 | 1.45 | | CytoplasmicMembrane | | |

## 11.1.3 Comparative analysis of stress responses

### 11.1.3.1 Unique and shared differentially expressed proteins

Table S 14: Unique and shared DE proteins among stress conditions. Listed are DE proteins in reference to control condition with respect to NCBI-annotation and NCBI-ID upon various stress conditions. If protein is DE upon one specific stress condition, it will be marked in the respective field with “1”. Color indicate whether DE are shared (blue) or unique (orange).

| NCBI-ID | NCBI-annotation | D | pH9 | HPP | suc | NaCl | KCl | $H_2O_2$ | pH4 | 45C | 15C | lac |
|---|---|---|---|---|---|---|---|---|---|---|---|---|
| BBD24_08930 | transcriptional regulator Spx | 1 | 1 | 1 | 1 | 0 | 0 | 1 | 0 | 0 | 0 | 0 |
| BBD24_10190 | dTDP-rhamnosyl transferase | 0 | 0 | 1 | 1 | 1 | 1 | 1 | 0 | 0 | 0 | 0 |
| BBD24_11030 | hydrolase | 0 | 0 | 1 | 1 | 1 | 0 | 1 | 1 | 0 | 0 | 0 |
| BBD24_04405 | cytochrome O ubiquinol oxidase | 1 | 0 | 0 | 1 | 1 | 0 | 1 | 0 | 0 | 0 | 0 |
| BBD24_09375 | hypothetical protein | 0 | 0 | 1 | 1 | 1 | 0 | 1 | 0 | 0 | 0 | 0 |
| BBD24_03220 | hypothetical protein | 0 | 0 | 0 | 1 | 1 | 1 | 1 | 0 | 0 | 0 | 0 |
| BBD24_05795 | cell surface protein precursor | 0 | 0 | 0 | 1 | 1 | 1 | 1 | 0 | 0 | 0 | 0 |
| BBD24_07145 | pseudouridine synthase | 0 | 0 | 0 | 1 | 1 | 1 | 1 | 0 | 0 | 0 | 0 |
| BBD24_07900 | peptide-methionine (R)-S-oxide reductase | 0 | 0 | 0 | 1 | 1 | 1 | 0 | 0 | 1 | 0 | 0 |
| BBD24_09540 | acetyl-CoA carboxylase biotin carboxyl carrier protein subunit | 0 | 0 | 0 | 1 | 1 | 0 | 0 | 1 | 1 | 0 | 0 |

| | | | | | | | | | | | | |
|---|---|---|---|---|---|---|---|---|---|---|---|---|
| BBD24_05405 | transcriptional regulator | 1 | 1 | 1 | 0 | 0 | 0 | 0 | 0 | 0 | 0 | 0 |
| BBD24_06095 | hypothetical protein | 1 | 1 | 1 | 0 | 0 | 0 | 0 | 0 | 0 | 0 | 0 |
| BBD24_07565 | dihydroorotate dehydrogenase B catalytic subunit | 1 | 1 | 1 | 0 | 0 | 0 | 0 | 0 | 0 | 0 | 0 |
| BBD24_08440 | exodeoxyribonuclease VII small subunit | 1 | 1 | 1 | 0 | 0 | 0 | 0 | 0 | 0 | 0 | 0 |
| BBD24_10865 | peptidoglycan-binding protein | 1 | 1 | 1 | 0 | 0 | 0 | 0 | 0 | 0 | 0 | 0 |
| BBD24_07315 | ribonuclease HII | 1 | 0 | 1 | 1 | 0 | 0 | 0 | 0 | 0 | 0 | 0 |
| BBD24_15055 | hypothetical protein | 0 | 1 | 1 | 1 | 0 | 0 | 0 | 0 | 0 | 0 | 0 |
| BBD24_00915 | hypothetical protein | 0 | 1 | 0 | 0 | 0 | 1 | 1 | 0 | 0 | 0 | 0 |
| BBD24_02975 | DUF5011 domain-containing protein | 0 | 0 | 0 | 1 | 1 | 1 | 0 | 0 | 0 | 0 | 0 |
| BBD24_09830 | ABC transporter permease | 0 | 0 | 0 | 1 | 1 | 0 | 1 | 0 | 0 | 0 | 0 |
| BBD24_07790 | SAM-dependent methyltransferase | 0 | 0 | 0 | 0 | 1 | 1 | 1 | 0 | 0 | 0 | 0 |
| BBD24_14275 | glycosyl transferase family 1 | 0 | 0 | 0 | 0 | 1 | 1 | 1 | 0 | 0 | 0 | 0 |
| BBD24_03750 | hypothetical protein | 1 | 1 | 0 | 0 | 0 | 0 | 0 | 0 | 0 | 0 | 0 |
| BBD24_07595 | bifunctional pyr operon transcriptional regulator/uracil phosphoribosyltransferase | 1 | 1 | 0 | 0 | 0 | 0 | 0 | 0 | 0 | 0 | 0 |

| | | | | | | | | | | | | |
|---|---|---|---|---|---|---|---|---|---|---|---|---|
| BBD24_09500 | oxaloacetate decarboxylase | 1 | 1 | 0 | 0 | 0 | 0 | 0 | 0 | 0 | 0 | 0 |
| BBD24_10235 | hypothetical protein | 1 | 1 | 0 | 0 | 0 | 0 | 0 | 0 | 0 | 0 | 0 |
| BBD24_10320 | PTS cellobiose transporter subunit IIA | 1 | 1 | 0 | 0 | 0 | 0 | 0 | 0 | 0 | 0 | 0 |
| BBD24_00795 | cell surface protein | 1 | 0 | 1 | 0 | 0 | 0 | 0 | 0 | 0 | 0 | 0 |
| BBD24_07240 | transcriptional regulator | 1 | 0 | 1 | 0 | 0 | 0 | 0 | 0 | 0 | 0 | 0 |
| BBD24_08350 | 50S ribosomal protein L28 | 1 | 0 | 1 | 0 | 0 | 0 | 0 | 0 | 0 | 0 | 0 |
| BBD24_08740 | 50S ribosomal protein L35 | 1 | 0 | 1 | 0 | 0 | 0 | 0 | 0 | 0 | 0 | 0 |
| BBD24_10195 | polymerase | 1 | 0 | 1 | 0 | 0 | 0 | 0 | 0 | 0 | 0 | 0 |
| BBD24_02350 | ABC transporter permease | 1 | 0 | 0 | 1 | 0 | 0 | 0 | 0 | 0 | 0 | 0 |
| BBD24_09025 | 5-(carboxyamino)imidazole ribonucleotide synthase | 1 | 0 | 0 | 0 | 0 | 0 | 0 | 0 | 1 | 0 | 0 |
| BBD24_04740 | phosphohydrolase | 0 | 1 | 1 | 0 | 0 | 0 | 0 | 0 | 0 | 0 | 0 |
| BBD24_10105 | ATP-dependent Clp protease ATP-binding subunit | 0 | 1 | 1 | 0 | 0 | 0 | 0 | 0 | 0 | 0 | 0 |
| BBD24_10500 | 3-hydroxyacyl-[acyl-carrier-protein] dehydratase FabZ | 0 | 1 | 1 | 0 | 0 | 0 | 0 | 0 | 0 | 0 | 0 |
| BBD24_10510 | beta-ketoacyl-[acyl-carrier-protein] synthase II | 0 | 1 | 1 | 0 | 0 | 0 | 0 | 0 | 0 | 0 | 0 |
| BBD24_10530 | acyl carrier protein | 0 | 1 | 1 | 0 | 0 | 0 | 0 | 0 | 0 | 0 | 0 |

| | | | | | | | | | | | | |
|---|---|---|---|---|---|---|---|---|---|---|---|---|
| BBD24_10545 | 3-hydroxyacyl-[acyl-carrier-protein] dehydratase FabZ | 0 | 1 | 1 | 0 | 0 | 0 | 0 | 0 | 0 | 0 | 0 |
| BBD24_09465 | superoxide dismutase | 0 | 1 | 0 | 0 | 0 | 0 | 1 | 0 | 0 | 0 | 0 |
| BBD24_08495 | hypothetical protein | 0 | 1 | 0 | 0 | 0 | 0 | 0 | 0 | 0 | 1 | 0 |
| BBD24_04250 | thioredoxin | 0 | 0 | 1 | 1 | 0 | 0 | 0 | 0 | 0 | 0 | 0 |
| BBD24_14000 | hypothetical protein | 0 | 0 | 1 | 0 | 0 | 0 | 1 | 0 | 0 | 0 | 0 |
| BBD24_08965 | anaerobic ribonucleoside-triphosphate reductase activating protein | 0 | 0 | 1 | 0 | 0 | 0 | 0 | 0 | 0 | 1 | 0 |
| BBD24_00205 | hypothetical protein | 0 | 0 | 0 | 1 | 1 | 0 | 0 | 0 | 0 | 0 | 0 |
| BBD24_05525 | hypothetical protein | 0 | 0 | 0 | 1 | 1 | 0 | 0 | 0 | 0 | 0 | 0 |
| BBD24_07330 | methylenetetrahydrofolate--tRNA-(uracil(54)- C(5))-methyltransferase (FADH(2)-oxidizing) TrmFO | 0 | 0 | 0 | 0 | 1 | 1 | 0 | 0 | 0 | 0 | 0 |
| BBD24_12740 | hypothetical protein | 0 | 0 | 0 | 0 | 1 | 1 | 0 | 0 | 0 | 0 | 0 |
| BBD24_01415 | pyridine nucleotide-disulfide oxidoreductase | 0 | 0 | 0 | 0 | 1 | 0 | 1 | 0 | 0 | 0 | 0 |
| BBD24_00895 | peptide ABC transporter substrate-binding protein | 0 | 0 | 0 | 0 | 0 | 1 | 0 | 1 | 0 | 0 | 0 |
| BBD24_10645 | glycine/betaine ABC transporter | 0 | 0 | 0 | 0 | 0 | 1 | 0 | 0 | 0 | 0 | 1 |
| BBD24_10655 | glycine betaine/L-proline ABC transporter ATP-binding protein | 0 | 0 | 0 | 0 | 0 | 1 | 0 | 0 | 0 | 0 | 1 |

| | | | | | | | | | | | | |
|---|---|---|---|---|---|---|---|---|---|---|---|---|
| BBD24_00645 | transcriptional regulator | 0 | 0 | 0 | 0 | 0 | 0 | 0 | 1 | 1 | 0 | 0 |
| BBD24_09600 | transcriptional regulator | 0 | 0 | 0 | 0 | 0 | 0 | 0 | 1 | 0 | 1 | 0 |
| BBD24_00380 | tryptophan synthase subunit alpha | 0 | 0 | 0 | 0 | 0 | 0 | 0 | 0 | 1 | 0 | 1 |
| BBD24_00220 | Gar-IM | 1 | 0 | 0 | 0 | 0 | 0 | 0 | 0 | 0 | 0 | 0 |
| BBD24_00480 | hypothetical protein | 1 | 0 | 0 | 0 | 0 | 0 | 0 | 0 | 0 | 0 | 0 |
| BBD24_00820 | hypothetical protein | 1 | 0 | 0 | 0 | 0 | 0 | 0 | 0 | 0 | 0 | 0 |
| BBD24_00870 | phage infection protein | 1 | 0 | 0 | 0 | 0 | 0 | 0 | 0 | 0 | 0 | 0 |
| BBD24_01235 | phosphoesterase | 1 | 0 | 0 | 0 | 0 | 0 | 0 | 0 | 0 | 0 | 0 |
| BBD24_03045 | prevent-host-death family protein | 1 | 0 | 0 | 0 | 0 | 0 | 0 | 0 | 0 | 0 | 0 |
| BBD24_04165 | preprotein translocase subunit YajC | 1 | 0 | 0 | 0 | 0 | 0 | 0 | 0 | 0 | 0 | 0 |
| BBD24_04390 | transcriptional regulator | 1 | 0 | 0 | 0 | 0 | 0 | 0 | 0 | 0 | 0 | 0 |
| BBD24_04670 | multidrug transporter | 1 | 0 | 0 | 0 | 0 | 0 | 0 | 0 | 0 | 0 | 0 |
| BBD24_04810 | 30S ribosomal protein S14 | 1 | 0 | 0 | 0 | 0 | 0 | 0 | 0 | 0 | 0 | 0 |
| BBD24_04865 | CDP-diacylglycerol--glycerol-3-phosphate 3-phosphatidyltransferase | 1 | 0 | 0 | 0 | 0 | 0 | 0 | 0 | 0 | 0 | 0 |

| | | | | | | | | | | | | |
|---|---|---|---|---|---|---|---|---|---|---|---|---|
| BBD24_05140 | preprotein translocase subunit SecG | 1 | 0 | 0 | 0 | 0 | 0 | 0 | 0 | 0 | 0 | 0 |
| BBD24_05400 | hypothetical protein | 1 | 0 | 0 | 0 | 0 | 0 | 0 | 0 | 0 | 0 | 0 |
| BBD24_07555 | transcriptional regulator | 1 | 0 | 0 | 0 | 0 | 0 | 0 | 0 | 0 | 0 | 0 |
| BBD24_07570 | orotate phosphoribosyltransferase | 1 | 0 | 0 | 0 | 0 | 0 | 0 | 0 | 0 | 0 | 0 |
| BBD24_07575 | carbamoyl phosphate synthase large subunit | 1 | 0 | 0 | 0 | 0 | 0 | 0 | 0 | 0 | 0 | 0 |
| BBD24_08265 | carbamoyl phosphate synthase small subunit | 1 | 0 | 0 | 0 | 0 | 0 | 0 | 0 | 0 | 0 | 0 |
| BBD24_08425 | 30S ribosomal protein S16 | 1 | 0 | 0 | 0 | 0 | 0 | 0 | 0 | 0 | 0 | 0 |
| BBD24_08980 | ArgR family transcriptional regulator | 1 | 0 | 0 | 0 | 0 | 0 | 0 | 0 | 0 | 0 | 0 |
| BBD24_08985 | phosphoribosylamine--glycine ligase | 1 | 0 | 0 | 0 | 0 | 0 | 0 | 0 | 0 | 0 | 0 |
| BBD24_08995 | bifunctional phosphoribosylaminoimidazolecarboxamide formyltransferase/IMP cyclohydrolase | 1 | 0 | 0 | 0 | 0 | 0 | 0 | 0 | 0 | 0 | 0 |
| BBD24_09000 | phosphoribosylformylglycinamidine cyclo-ligase | 1 | 0 | 0 | 0 | 0 | 0 | 0 | 0 | 0 | 0 | 0 |
| BBD24_09020 | amidophosphoribosyltransferase | 1 | 0 | 0 | 0 | 0 | 0 | 0 | 0 | 0 | 0 | 0 |
| BBD24_09050 | phosphoribosylaminoimidazolesuccinocarboxamide synthase | 1 | 0 | 0 | 0 | 0 | 0 | 0 | 0 | 0 | 0 | 0 |
| BBD24_10375 | phosphocarrier protein HPr | 1 | 0 | 0 | 0 | 0 | 0 | 0 | 0 | 0 | 0 | 0 |

| | | | | | | | | | | | | |
|---|---|---|---|---|---|---|---|---|---|---|---|---|
| BBD24_10425 | hypothetical protein | 1 | 0 | 0 | 0 | 0 | 0 | 0 | 0 | 0 | 0 | 0 |
| BBD24_10485 | integrase | 1 | 0 | 0 | 0 | 0 | 0 | 0 | 0 | 0 | 0 | 0 |
| BBD24_10835 | acetyl-CoA carboxylase carboxyl transferase subunit alpha | 1 | 0 | 0 | 0 | 0 | 0 | 0 | 0 | 0 | 0 | 0 |
| BBD24_11955 | 6-phospho-beta-glucosidase | 1 | 0 | 0 | 0 | 0 | 0 | 0 | 0 | 0 | 0 | 0 |
| BBD24_12575 | hypothetical protein | 1 | 0 | 0 | 0 | 0 | 0 | 0 | 0 | 0 | 0 | 0 |
| BBD24_12980 | PemK family transcriptional regulator | 1 | 0 | 0 | 0 | 0 | 0 | 0 | 0 | 0 | 0 | 0 |
| BBD24_13110 | hypothetical protein | 1 | 0 | 0 | 0 | 0 | 0 | 0 | 0 | 0 | 0 | 0 |
| BBD24_13350 | PTS cellobiose transporter subunit IIA | 1 | 0 | 0 | 0 | 0 | 0 | 0 | 0 | 0 | 0 | 0 |
| BBD24_13580 | transcriptional antiterminator | 1 | 0 | 0 | 0 | 0 | 0 | 0 | 0 | 0 | 0 | 0 |
| BBD24_13980 | dehydrogenase | 1 | 0 | 0 | 0 | 0 | 0 | 0 | 0 | 0 | 0 | 0 |
| BBD24_14895 | FliK family flagellar hook-length control protein | 1 | 0 | 0 | 0 | 0 | 0 | 0 | 0 | 0 | 0 | 0 |
| BBD24_15000 | DNA starvation/stationary phase protection protein | 1 | 0 | 0 | 0 | 0 | 0 | 0 | 0 | 0 | 0 | 0 |
| BBD24_15015 | hypothetical protein | 1 | 0 | 0 | 0 | 0 | 0 | 0 | 0 | 0 | 0 | 0 |
| BBD24_00060 | 30S ribosomal protein S18 | 0 | 1 | 0 | 0 | 0 | 0 | 0 | 0 | 0 | 0 | 0 |
| BBD24_00625 | transcriptional regulator | 0 | 1 | 0 | 0 | 0 | 0 | 0 | 0 | 0 | 0 | 0 |

| | | | | | | | | | | | | |
|---|---|---|---|---|---|---|---|---|---|---|---|---|
| BBD24_00715 | hypothetical protein | 0 | 1 | 0 | 0 | 0 | 0 | 0 | 0 | 0 | 0 | 0 |
| BBD24_01020 | alkaline-shock protein | 0 | 1 | 0 | 0 | 0 | 0 | 0 | 0 | 0 | 0 | 0 |
| BBD24_01210 | gluconate kinase | 0 | 1 | 0 | 0 | 0 | 0 | 0 | 0 | 0 | 0 | 0 |
| BBD24_01275 | hypothetical protein | 0 | 1 | 0 | 0 | 0 | 0 | 0 | 0 | 0 | 0 | 0 |
| BBD24_01340 | branched-chain amino acid ABC transporter substrate-binding protein | 0 | 1 | 0 | 0 | 0 | 0 | 0 | 0 | 0 | 0 | 0 |
| BBD24_02360 | NAD(FAD)-dependent dehydrogenase | 0 | 1 | 0 | 0 | 0 | 0 | 0 | 0 | 0 | 0 | 0 |
| BBD24_02500 | dihydroneopterin aldolase | 0 | 1 | 0 | 0 | 0 | 0 | 0 | 0 | 0 | 0 | 0 |
| BBD24_03135 | transcriptional regulator | 0 | 1 | 0 | 0 | 0 | 0 | 0 | 0 | 0 | 0 | 0 |
| BBD24_03210 | toxin-antitoxin system antitoxin subunit | 0 | 1 | 0 | 0 | 0 | 0 | 0 | 0 | 0 | 0 | 0 |
| BBD24_03820 | ABC transporter substrate-binding protein | 0 | 1 | 0 | 0 | 0 | 0 | 0 | 0 | 0 | 0 | 0 |
| BBD24_03845 | magnesium-transporting ATPase | 0 | 1 | 0 | 0 | 0 | 0 | 0 | 0 | 0 | 0 | 0 |
| BBD24_04030 | flavodoxin | 0 | 1 | 0 | 0 | 0 | 0 | 0 | 0 | 0 | 0 | 0 |
| BBD24_04135 | S-ribosylhomocysteine lyase | 0 | 1 | 0 | 0 | 0 | 0 | 0 | 0 | 0 | 0 | 0 |
| BBD24_04170 | bifunctional acetaldehyde-CoA/alcohol dehydrogenase | 0 | 1 | 0 | 0 | 0 | 0 | 0 | 0 | 0 | 0 | 0 |

| | | | | | | | | | | | | |
|---|---|---|---|---|---|---|---|---|---|---|---|---|
| BBD24_05245 | ABC transporter permease | 0 | 1 | 0 | 0 | 0 | 0 | 0 | 0 | 0 | 0 | 0 |
| BBD24_06025 | TetR family transcriptional regulator | 0 | 1 | 0 | 0 | 0 | 0 | 0 | 0 | 0 | 0 | 0 |
| BBD24_06125 | F0F1 ATP synthase subunit epsilon | 0 | 1 | 0 | 0 | 0 | 0 | 0 | 0 | 0 | 0 | 0 |
| BBD24_07820 | DNA primase | 0 | 1 | 0 | 0 | 0 | 0 | 0 | 0 | 0 | 0 | 0 |
| BBD24_09525 | [citrate (pro-3S)-lyase] ligase | 0 | 1 | 0 | 0 | 0 | 0 | 0 | 0 | 0 | 0 | 0 |
| BBD24_10685 | homoserine dehydrogenase | 0 | 1 | 0 | 0 | 0 | 0 | 0 | 0 | 0 | 0 | 0 |
| BBD24_11435 | Mini-ribonuclease 3 | 0 | 1 | 0 | 0 | 0 | 0 | 0 | 0 | 0 | 0 | 0 |
| BBD24_11450 | hypothetical protein | 0 | 1 | 0 | 0 | 0 | 0 | 0 | 0 | 0 | 0 | 0 |
| BBD24_12960 | MarR family transcriptional regulator | 0 | 1 | 0 | 0 | 0 | 0 | 0 | 0 | 0 | 0 | 0 |
| BBD24_13535 | L-ascorbate 6-phosphate lactonase | 0 | 1 | 0 | 0 | 0 | 0 | 0 | 0 | 0 | 0 | 0 |
| BBD24_02055 | hypothetical protein | 0 | 0 | 1 | 0 | 0 | 0 | 0 | 0 | 0 | 0 | 0 |
| BBD24_03480 | cold-shock protein | 0 | 0 | 1 | 0 | 0 | 0 | 0 | 0 | 0 | 0 | 0 |
| BBD24_04270 | D-alanine--poly(phosphoribitol) ligase subunit 2 | 0 | 0 | 1 | 0 | 0 | 0 | 0 | 0 | 0 | 0 | 0 |
| BBD24_04700 | DNA-binding protein | 0 | 0 | 1 | 0 | 0 | 0 | 0 | 0 | 0 | 0 | 0 |
| BBD24_05860 | cold-shock protein | 0 | 0 | 1 | 0 | 0 | 0 | 0 | 0 | 0 | 0 | 0 |

| | | | | | | | | | | | | |
|---|---|---|---|---|---|---|---|---|---|---|---|---|
| BBD24_06060 | thymidine kinase | 0 | 0 | 1 | 0 | 0 | 0 | 0 | 0 | 0 | 0 | 0 |
| BBD24_06160 | glycine cleavage system protein H | 0 | 0 | 1 | 0 | 0 | 0 | 0 | 0 | 0 | 0 | 0 |
| BBD24_06270 | L-serine dehydratase iron-sulfur-dependent subunit beta | 0 | 0 | 1 | 0 | 0 | 0 | 0 | 0 | 0 | 0 | 0 |
| BBD24_07255 | hypothetical protein | 0 | 0 | 1 | 0 | 0 | 0 | 0 | 0 | 0 | 0 | 0 |
| BBD24_08310 | peptide ABC transporter permease | 0 | 0 | 1 | 0 | 0 | 0 | 0 | 0 | 0 | 0 | 0 |
| BBD24_08325 | acyl carrier protein | 0 | 0 | 1 | 0 | 0 | 0 | 0 | 0 | 0 | 0 | 0 |
| BBD24_08400 | DNA-directed RNA polymerase subunit omega | 0 | 0 | 1 | 0 | 0 | 0 | 0 | 0 | 0 | 0 | 0 |
| BBD24_09545 | hypothetical protein | 0 | 0 | 1 | 0 | 0 | 0 | 0 | 0 | 0 | 0 | 0 |
| BBD24_14900 | heavy metal-binding protein | 0 | 0 | 1 | 0 | 0 | 0 | 0 | 0 | 0 | 0 | 0 |
| BBD24_02585 | MerR family transcriptional regulator | 0 | 0 | 0 | 1 | 0 | 0 | 0 | 0 | 0 | 0 | 0 |
| BBD24_04120 | hypothetical protein | 0 | 0 | 0 | 1 | 0 | 0 | 0 | 0 | 0 | 0 | 0 |
| BBD24_06930 | 30S ribosomal protein S20 | 0 | 0 | 0 | 1 | 0 | 0 | 0 | 0 | 0 | 0 | 0 |
| BBD24_08130 | 50S ribosomal protein L7 | 0 | 0 | 0 | 1 | 0 | 0 | 0 | 0 | 0 | 0 | 0 |
| BBD24_10310 | hypothetical protein | 0 | 0 | 0 | 1 | 0 | 0 | 0 | 0 | 0 | 0 | 0 |
| BBD24_10800 | threonine ammonia-lyase | 0 | 0 | 0 | 1 | 0 | 0 | 0 | 0 | 0 | 0 | 0 |

| | | | | | | | | | | | | |
|---|---|---|---|---|---|---|---|---|---|---|---|---|
| BBD24_13040 | PTS fructose transporter subunit IIABC | 0 | 0 | 0 | 1 | 0 | 0 | 0 | 0 | 0 | 0 | 0 |
| BBD24_13320 | triose-phosphate isomerase | 0 | 0 | 0 | 1 | 0 | 0 | 0 | 0 | 0 | 0 | 0 |
| BBD24_13335 | PTS galactitol transporter subunit IIC | 0 | 0 | 0 | 1 | 0 | 0 | 0 | 0 | 0 | 0 | 0 |
| BBD24_13340 | PTS sugar transporter subunit IIA | 0 | 0 | 0 | 1 | 0 | 0 | 0 | 0 | 0 | 0 | 0 |
| BBD24_13440 | cytoplasmic protein | 0 | 0 | 0 | 1 | 0 | 0 | 0 | 0 | 0 | 0 | 0 |
| BBD24_14050 | argininosuccinate synthase | 0 | 0 | 0 | 1 | 0 | 0 | 0 | 0 | 0 | 0 | 0 |
| BBD24_06235 | transcriptional regulator | 0 | 0 | 0 | 0 | 1 | 0 | 0 | 0 | 0 | 0 | 0 |
| BBD24_07280 | DNA/RNA helicase | 0 | 0 | 0 | 0 | 1 | 0 | 0 | 0 | 0 | 0 | 0 |
| BBD24_08945 | peptide ABC transporter permease | 0 | 0 | 0 | 0 | 1 | 0 | 0 | 0 | 0 | 0 | 0 |
| BBD24_10185 | alpha-L-Rha alpha-1 3-L-rhamnosyltransferase | 0 | 0 | 0 | 0 | 1 | 0 | 0 | 0 | 0 | 0 | 0 |
| BBD24_10525 | 2-nitropropane dioxygenase | 0 | 0 | 0 | 0 | 1 | 0 | 0 | 0 | 0 | 0 | 0 |
| BBD24_10995 | transcriptional regulator | 0 | 0 | 0 | 0 | 1 | 0 | 0 | 0 | 0 | 0 | 0 |
| BBD24_13995 | molecular chaperone Hsp20 | 0 | 0 | 0 | 0 | 1 | 0 | 0 | 0 | 0 | 0 | 0 |
| BBD24_01535 | peptidase T | 0 | 0 | 0 | 0 | 0 | 1 | 0 | 0 | 0 | 0 | 0 |
| BBD24_03475 | glutamate dehydrogenase | 0 | 0 | 0 | 0 | 0 | 1 | 0 | 0 | 0 | 0 | 0 |

| | | | | | | | | | | | | |
|---|---|---|---|---|---|---|---|---|---|---|---|---|
| BBD24_05875 | xanthine phosphoribosyltransferase | 0 | 0 | 0 | 0 | 0 | 1 | 0 | 0 | 0 | 0 | 0 |
| BBD24_07940 | ABC transporter ATP-binding protein | 0 | 0 | 0 | 0 | 0 | 1 | 0 | 0 | 0 | 0 | 0 |
| BBD24_10180 | glycosyl transferase | 0 | 0 | 0 | 0 | 0 | 1 | 0 | 0 | 0 | 0 | 0 |
| BBD24_10650 | glycine/betaine ABC transporter | 0 | 0 | 0 | 0 | 0 | 1 | 0 | 0 | 0 | 0 | 0 |
| BBD24_11260 | peptidylprolyl isomerase | 0 | 0 | 0 | 0 | 0 | 1 | 0 | 0 | 0 | 0 | 0 |
| BBD24_14485 | alcohol dehydrogenase | 0 | 0 | 0 | 0 | 0 | 1 | 0 | 0 | 0 | 0 | 0 |
| BBD24_04760 | dihydroorotate dehydrogenase | 0 | 0 | 0 | 0 | 0 | 0 | 1 | 0 | 0 | 0 | 0 |
| BBD24_07290 | transcriptional regulator | 0 | 0 | 0 | 0 | 0 | 0 | 1 | 0 | 0 | 0 | 0 |
| BBD24_07640 | transcriptional regulator | 0 | 0 | 0 | 0 | 0 | 0 | 1 | 0 | 0 | 0 | 0 |
| BBD24_09710 | Fe-S cluster biosynthesis protein | 0 | 0 | 0 | 0 | 0 | 0 | 1 | 0 | 0 | 0 | 0 |
| BBD24_10845 | transcription antiterminator BglG | 0 | 0 | 0 | 0 | 0 | 0 | 1 | 0 | 0 | 0 | 0 |
| BBD24_02545 | pyruvate oxidase | 0 | 0 | 0 | 0 | 0 | 0 | 0 | 1 | 0 | 0 | 0 |
| BBD24_04015 | NAD-dependent malic enzyme | 0 | 0 | 0 | 0 | 0 | 0 | 0 | 1 | 0 | 0 | 0 |
| BBD24_04020 | malate permease | 0 | 0 | 0 | 0 | 0 | 0 | 0 | 1 | 0 | 0 | 0 |
| BBD24_04815 | GMP reductase | 0 | 0 | 0 | 0 | 0 | 0 | 0 | 1 | 0 | 0 | 0 |

| | | | | | | | | | | | | |
|---|---|---|---|---|---|---|---|---|---|---|---|---|
| BBD24_06625 | amino acid ABC transporter permease | 0 | 0 | 0 | 0 | 0 | 0 | 0 | 1 | 0 | 0 | 0 |
| BBD24_06630 | polar amino acid ABC transporter ATP-binding protein | 0 | 0 | 0 | 0 | 0 | 0 | 0 | 1 | 0 | 0 | 0 |
| BBD24_07445 | phosphoribosyl-ATP diphosphatase | 0 | 0 | 0 | 0 | 0 | 0 | 0 | 1 | 0 | 0 | 0 |
| BBD24_07455 | imidazole glycerol phosphate synthase subunit HisF | 0 | 0 | 0 | 0 | 0 | 0 | 0 | 1 | 0 | 0 | 0 |
| BBD24_09905 | 1 4-beta-N-acetylmuramidase | 0 | 0 | 0 | 0 | 0 | 0 | 0 | 1 | 0 | 0 | 0 |
| BBD24_10260 | peptide ABC transporter substrate-binding protein | 0 | 0 | 0 | 0 | 0 | 0 | 0 | 1 | 0 | 0 | 0 |
| BBD24_10265 | peptide ABC transporter ATP-binding protein | 0 | 0 | 0 | 0 | 0 | 0 | 0 | 1 | 0 | 0 | 0 |
| BBD24_10270 | peptide ABC transporter permease | 0 | 0 | 0 | 0 | 0 | 0 | 0 | 1 | 0 | 0 | 0 |
| BBD24_10280 | peptide ABC transporter substrate-binding protein | 0 | 0 | 0 | 0 | 0 | 0 | 0 | 1 | 0 | 0 | 0 |
| BBD24_01885 | gamma-glutamyl-gamma-aminobutyrate hydrolase | 0 | 0 | 0 | 0 | 0 | 0 | 0 | 0 | 1 | 0 | 0 |
| BBD24_02565 | peptide-methionine (R)-S-oxide reductase | 0 | 0 | 0 | 0 | 0 | 0 | 0 | 0 | 1 | 0 | 0 |
| BBD24_09720 | peptidoglycan-binding protein LysM | 0 | 0 | 0 | 0 | 0 | 0 | 0 | 0 | 1 | 0 | 0 |
| BBD24_10245 | hypothetical protein | 0 | 0 | 0 | 0 | 0 | 0 | 0 | 0 | 1 | 0 | 0 |
| BBD24_14215 | hypothetical protein | 0 | 0 | 0 | 0 | 0 | 0 | 0 | 0 | 1 | 0 | 0 |
| BBD24_05200 | sugar ABC transporter ATP-binding protein | 0 | 0 | 0 | 0 | 0 | 0 | 0 | 0 | 0 | 1 | 0 |

| | | | | | | | | | | | | |
|---|---|---|---|---|---|---|---|---|---|---|---|---|
| BBD24_12595 | ATP-dependent RNA helicase | 0 | 0 | 0 | 0 | 0 | 0 | 0 | 0 | 0 | 1 | 0 |
| BBD24_13985 | cadmium-translocating P-type ATPase | 0 | 0 | 0 | 0 | 0 | 0 | 0 | 0 | 0 | 1 | 0 |
| BBD24_11380 | FMN-binding protein | 0 | 0 | 0 | 0 | 0 | 0 | 0 | 0 | 0 | 0 | 1 |

# 12 List of Publications and Student Theses

### Peer-reviewed journals

Schott, A.S., et al., MALDI-TOF Mass Spectrometry Enables a Comprehensive and Fast Analysis of Dynamics and Qualities of Stress Responses of *Lactobacillus paracasei* subsp. *paracasei* F19. PLoS One, 2016. 11(10): p. e0165504.

Schott, A.S., et al., Quantitative Proteomics for the Comprehensive Analysis of Stress Responses of *Lactobacillus paracasei* subsp. *paracasei* F19. J Proteome Res, 2017. 16(10): p. 3816-3829.

### Student theses

The following student theses were supervised. The resulting raw data were partially incorporated into this thesis with written permission by the respective students.

Franziska Weisbart, Bachelor Thesis 2014. Kinetik und Qualitäten der Stressantwort von *Lactobacillus sanfranciscensis* analysiert mit MALDI-TOFMS.

Jennifer E. Quinn, Research Internship 2016. Identifikation deregulierter Proteine von *L. paracasei* ssp. *paracasei* TMW 1.1434 (F19) infolge 60 minutiger Applikation osmotischen Stress mittels 2D-GE.

Melanie Kittner, Research Internship 2016. Untersuchung des Metabolismus von *Lb. paracasei* subsp. *paracasei* TMW 1.1434 (F19).

### Oral presentations

Ann-Sophie Schott, Rudi F. Vogel, Jürgen Behr. Kinetics and stress response of *Lactobacillus paracasei* ssp. *paracasei* analyzed by MALDI-TOF MS. Oral presentation at the 11th International Symposium on Lactic Acid Bacteria (LAB11), Egmond an Zee, Netherlands, 31.08.- 04.09.2014.

### Poster presentation

Ann-Sophie Schott, Rudi F. Vogel, Jürgen Behr. Kinetics and stress response of *Lactobacillus paracasei* ssp. *paracasei* analyzed by MALDI-TOF MS. Poster presentation at the 11th International Symposium on Lactic Acid Bacteria (LAB11), Egmond an Zee, Netherlands, 31.08.- 04.09.2014.

Ann-Sophie Schott, Benjamin C. Schurr, Rudi F. Vogel, Jürgen Behr. Detection of stress responses in lactic acid bacteria *Lactobacillus paracasei* ssp. *paracasei* and Lactobacillus brevis by MALDI-TOF mass spectrometry. Poster presentation at the Proteomic Forum 2015 of the Deutschen Gesellschaft für Proteomforschung (DGPF, German Society of Proteome Research), Berlin, Deutschland. 22.03.-25.03.2015.

Ann-Sophie Schott, Benjamin C. Schurr, Rudi F. Vogel, Jürgen Behr. Detection of stress responses in probiotic lactic acid bacteria *Lactobacillus paracasei* ssp. *paracasei* by MALDI-TOF mass spectrometry. Poster presentation at the 9th International Scientific Conference on Probiotics and Prebiotics (IPC 2015), Budapest, Hungary. 23.06.-25.06.2015